APPENDIX H

GROUND INVESTIGATION AND ENGINEERING GEOLOGICAL STUDY

CONTENTS

H.1 INTRODUCTION

A comprehensive ground investigation and engineering geological study were carried out by the Geotechnical Engineering Office (GEO) shortly after the landslide. The main objectives were :

(a) to examine the engineering geological conditions at the site after the landslide,

(b) to obtain soil samples for laboratory testing, and

(c) to deduce the engineering geological conditions at the site before the failure.

The findings are presented in this Appendix.

H.2 ENGINEERING GEOLOGICAL STUDY

H.2.1 Scope

The scope of the engineering geological study included :

(a) a review of published geological maps and documents,

(b) a search of previous ground investigation data, and

(c) an interpretation of aerial photographs.

H.2.2 Published Maps and Documents

The relevant information available directly from published geological maps and documents can be summarised as follows :

(a) The Hong Kong Geological Survey previously mapped the site at 1:20000 scale and identified the dominant rock to be volcanic rock belonging to the Tai Mo Shan Formation of the Repulse Bay Group (GCO, 1986; Strange & Shaw, 1986). A more recent study (Strange et al, 1994) re-classified the volcanic rock at the site as part of the Mount Davis Formation of the Repulse Bay Group. Stratigraphic relationships indicate that this formation is Jurassic - Cretaceous in age.

(b) The Geotechnical Area Study Programme for Hong Kong and Kowloon (GCO, 1987a) classified this site as having high geotechnical limitations to development. The classification was based on terrain evaluation data, including

slope gradient, morphology and erosion and instability features.

H.2.3 Ground Investigation Data

There are no records of ground investigations having been carried out within the area of the landslide prior to the 23 July 1994 failure. However, extensive ground investigation works had been carried out previously in the vicinity for building developments and slope studies.

At the time of the present study, a ground investigation was being carried out at Kwun Lung Lau under the direction of Mott Connell Ltd, consultant to the Hong Kong Housing Society, and preliminary information on the ground conditions encountered was made available to the GEO.

The sources of the ground investigation data reviewed for the post-failure landslide investigation are given in Table H1. The key information is summarised in Table H2.

The above information confirms that the area is underlain by partially weathered volcanic rocks. In addition, the available piezometer records indicate that the main groundwater table is generally well below the ground surface.

From the available data, an assessment was made of the likely amount of fill in the area. It was found that the landslide site was located in a spur, and extensive filling was unlikely. However, the terrain at Kwun Lung Lau had been greatly modified by site formation works at different times over the years, which could result in local variations in fill thickness. The available information does not cover the landslide area directly, and the actual fill thickness at the site cannot therefore be interpreted reliably from the data.

H.2.4 Aerial Photograph Interpretation

H.2.4.1 Site History

Aerial photographs taken between 1924 and 1992 were studied to determine the development history of the landslide site. The following observations were made :

(a) The footpath on the north side of Kwun Lung Lau is visible in the 1924 aerial photographs. No significant changes to the alignment of the footpath can be observed in the subsequent photographs.

(b) The 1924 aerial photographs indicate the presence of very steep ground on the upslope side of the footpath. The face of the very steep ground cannot be seen in the photographs taken prior to 1974. The masonry wall at this location can be recognised in the 1974 photographs. Between 1924 and 1974, there is no evidence of realignment or reconstruction

work in this locality. This is consistent with the deduction made from old topographic maps that the masonry wall had been constructed by 1901.

(c) Between 1924 and 1963, a platform that was about 6 m wide can be seen upslope of where the wall was located. Just behind and upslope of this platform, a small steep cut slope appeared to have been excavated in the natural slope. The observations that can be made from the aerial photographs taken between 1924 and 1963 are shown in Figure H1.

(d) The platform and the crest area of the small cut slope were partly occupied by squatters between 1945 and 1963 (Figure H2).

(e) In 1964, some squatters on the platform above the wall at the location of the 23 July 1994 landslide were cleared. There are no signs of fill having been placed on the platform. Kwun Lung Lau had not yet been constructed.

(f) Fill was placed on the platform between 1964 and 1969. (Results of the post-failure ground investigations suggest that the cut slope on the upslope side of the platform was partly covered by fill and partly removed.)

(g) Not much could be observed in the aerial photographs taken after 1969, as the area where the landslide occurred in 1994 was usually in the shadow of Kwun Lung Lau when the photographs were taken.

H.2.4.2 Photogrammetric Survey

A photogrammetric survey was carried out to assess the topography of the area prior to the site formation work for Kwun Lung Lau carried out between 1965 and 1968. The high quality 1963 aerial photographs were used for this survey.

The approximate topography of the area in 1963 is shown in Figure H3. The accuracy that could be achieved in the photogrammetric survey was about ± 2 m.

A cross-section (Section B-B) through the landslide area is shown in Figure H4. The photogrammetric survey could not identify the full details of the ground behind the wall at the location of the section, partly because of the presence of squatters on the platform in 1963, and partly because of the limited accuracy of the survey. The information shown in Figure H4 was supplemented by observations made from the 1963 aerial photographs, and from the 1924 aerial photographs (in which the platform was not occupied).

It can be seen from Figure H4 that the landslide site is well below the projected natural

slope profile. This suggests that the wall and the platform were formed by excavation into the natural hillside.

H.2.5 Engineering Geological Mapping of the Landslide Scar

Surface geological mapping was carried out between 25 and 29 July 1994 during the removal of the landslide debris and prior to shotcreting. The landslide scar could not be mapped in full because of the presence of landslide debris, the difficult accessibility to the scar and the threat of further failures. The rescue operation, debris removal and emergency repair works also impeded the mapping. As a result, only isolated exposures could be examined.

A total of 17 field observations were made on the landslide scar. The locations of the field observations are shown on Figure H5, and the findings are summarised in Table H3.

H.3 GROUND INVESTIGATION

Ground investigation was carried out after the completion of the emergency repair works in early August 1994 to determine the subsurface conditions at the site. The ground investigation was carried out by Vibro (HK) Ltd, under full-time supervision by GEO's professional and technical staff.

The ground investigation comprised 18 drillholes, 15 trial pits, three surface strippings and ten coreholes through the unfailed part of the masonry wall (Figure H6). In addition, 24 pits were also dug underneath Block D and in the yard area to the south of the block for the inspection of the building substructure, the drainage systems, and water seepages (Appendices J & K).

During the ground investigations, disturbed and undisturbed soil and rock samples were retrieved for visual inspection and laboratory testing. Field tests were carried out to determine the insitu properties of the soil.

The techniques used for soil and rock sampling were :

(a) undisturbed Mazier or HMLC sampling in soil and HMLC or TNW sampling in rock (GCO, 1984), combined with foam flush drilling,

(b) undisturbed block samples, driven U100 and U76 tube samples and large bulk samples in trial pits, and

(c) open-tube drillhole samples from drilling through masonry wall using dry or water-flush drilling.

The field tests carried out were :

(a) standard penetration tests (SPT) with liner samples in

drillholes,

(b) falling head permeability tests in drillholes in soil,

(c) sand replacement tests in trial pits, and

(d) GCO-probing along the line of each stripped surface.

The logging of samples and exposures was carried out by GEO geologists in conjunction with the Contractor's geologist. Some simple index tests, including consistency, slake and hand penetrometer strength tests, were also carried out where possible in accordance with the recommendations by Martin (1985). These index tests were adopted to assess the strength of the soil and to assist in the classification of weathering grades for the volcanics. The results of the index tests are summarised in Table H4.

The geological logs and the results of the field tests are contained in the ground investigation report (Vibro, 1994).

H.4 GEOLOGICAL PROFILES OF THE LANDSLIDE SITE

H.4.1 Geological Profiles after the Landslide

The geology of the landslide site was determined using the information obtained from the desk and field studies. Three representative cross-sections have been constructed at the locations shown in Figures H7 to H9.

Section B-B is through the higher part of the post-failure ground, and Sections A-A & C-C are through two depressions on either side of Section B-B.

The geological profiles along the three cross-sections after the landslide are also shown in Figures H7 to H9. The geological sequence is :

(a) rock fill,

(b) landslide debris,

(c) fill, and

(d) volcanic bedrock, including residual soil, saprolite and volcanic rock.

H.4.2 Geological Profiles before the Landslide

On the basis of the information collected, a geological model of the site before the landslide was constructed. This comprised a fill slope overlying a retained cut platform and a cut slope at the landslide site. Shown in Figures H10 to H12 are the assessed geological profiles along Sections A-A, B-B & C-C before the landslide.

The geological model is based on the following :

(a) It was observed from old aerial photographs that the wall originally retained a platform and a cut slope further back. The platform and parts of the cut slope were covered by fill during the construction of Kwun Lung Lau in the mid 1960s.

(b) Part of the buried platform was exposed in trial pit No. TP19, and partially weathered volcanics were found below the platform.

(c) Along Section D-D (Figure H13) to the immediate west of the landslide area, the presence of the buried platform was inferred by correlating information from drillholes No. BH9 & BH9A and from field observation point No. 10 (Table H3).

(d) The buried cut slope was uncovered in trial pits No. TP7, TP8 & TP9, where the interface of the fill and insitu soil dipped at 30° to 45° towards the former wall.

(e) A flat channel was found in trial pit No. TP19, which was thought to be part of the channel along the toe of the buried cut slope.

(f) When the base elevations of the fill behind the landslide scar were plotted, they were found to fall on an inclined plane (Figure H14) that agreed with the profile of the cut slope established from the aerial photographs.

The results of the coreholes through the adjacent unfailed portion of the masonry wall were inconclusive because of the difficulties in properly retrieving rubble set in soil or mortar matrix. Better results were achieved by a horizontal drillhole which was sunk into the section of the wall to the west of the landslide area using foam as flushing medium. The horizontal drillhole showed that the wall thickness was about 0.8 m to 1 m at that location.

H.4.3 Field Properties of Geological Materials

H.4.3.1 General

The field properties of the different geological materials identified during the ground investigation are as follows :

H.4.3.2 Landslide Debris

Landslide debris was widespread over the slip scar, as is evident in Figure H5. This

deposit was generally thin, as the bulk of the debris had been removed, the thickest encountered being 1.5 m in drillhole No. BH2. The debris was loose, reddish brown, silty fine sand containing angular to subrounded gravel of moderately decomposed volcanics and occasional subangular cobbles.

H.4.3.3 Fill

Fill was found at the south-eastern part of the landslide site (Figure H14). Trial pit No. TP2 at the crest of the slope revealed fill with a vertical thickness of more than 3 m. The fill was generally less than 2 m thick in the other trial pits downslope of trial pit No. TP2.

The fill was generally derived from weathered volcanics, which were pinkish, orangish, and yellowish brown in colour. It comprises very loose to loose silty gravelly fine sand and soft to firm sandy clay and silt with some cobbles and fragments of brick, concrete, plastic sheet and other man-made materials.

The hand penetrometer strength of the fill varied from 10 kPa to 150 kPa. This shows that the fill was variable, and could be locally very loose or very soft. The dry density as determined in sand replacement tests varied from 1.42 to 1.70 Mg/m^3. The bulk density varied from 1.69 to 2.07 Mg/m^3, and the moisture content was between about 19% to 22%. The fill was generally moist.

In trial pit No. TP7 located near the crest of the landslide scar, two layers of fill of different ages could be recognised. The lower, and older, fill was probably placed by cut and fill methods in connection with the squatter activities in the area prior to the construction of Kwun Lung Lau. A squatter platform, characterised by thin concrete slabs and red floor tiles, was found at the top of the lower fill layer. The younger and more major filling was placed on the squatter areas, forming the slope to approximately the original level before the landslide.

The boundary between the fill and the underlying soil is generally sharp and dips from subhorizontal in trial pit No. TP20 to 45° downslope in trial pit No. TP8.

H.4.3.4 Residual Soil

Residual soil was identified at limited exposures in trial pits No. TP6, TP7 & TP9. It was soft, moist, orangish brown gravelly silt and clay. The gravel is believed to be the remnant of the more weathering-resistant lithic lapilli in the original lapilli-bearing volcanic rock. The residual soil was derived from insitu weathering. The contact between the residual soil and the underlying saprolite was often gradual. The hand penetrometer strength of the residual soil was between 35 kPa and 50 kPa. This showed that the material was fairly uniform.

H.4.3.5 Volcanic Saprolite

The volcanic saprolite at the landslide site comprised completely decomposed and some highly decomposed volcanics. It was generally extremely weak to weak, mottled grey, reddish brown and yellow, with relict rock texture. However, the relict joints were not persistent, and were not adversely orientated with respect to the profile of the landslide surface.

The volcanic saprolite could disintegrate into slightly gravelly, fine sandy silt or silty fine sand when crumbled by hand, depending on the degree of decomposition.

No adversely orientated relict joints within the volcanic saprolite could be identified.

The bulk density of the completely decomposed volcanics, as determined in sand replacement tests, ranged from 1.62 to 1.96 Mg/m^3, with the dry density ranging from 1.35 to 1.70 Mg/m^3. The moisture content was generally between 16% and 20%.

The Standard Penetration Test (SPT) N values for the volcanic saprolite within a depth of 2 m below the landslide scar generally varied between 5 and 14. The N value of the volcanic saprolite near the toe of the landslide scar was higher (about 40).

H.4.3.6 Volcanic Rock

The volcanic rock comprised moderately to slightly decomposed, fine to coarse ash tuff containing some lithic lapilli. The strength of the rock varied from moderately weak to very strong. The fresher rock was grey, with close to medium-spaced joints. The more weathered rock tended to have discoloured to light grey and to have closer joints.

The volcanic rock was only found well below the toe of the landslide scar, except for occasional corestones found within the saprolite.

H.5 GROUNDWATER MONITORING

Twenty-one piezometers and a standpipe were installed by Vibro (HK) Ltd to monitor the groundwater levels at the site of the landslide. Information from previous ground investigations in the Kwun Lung Lau area was examined, but the available data was limited and was not relevant to the landslide site. The purpose of the post-failure set of piezometers and standpipe was to obtain information about the groundwater level specifically at the landslide site.

Table H5 lists the levels of the piezometers and standpipe, the drillholes in which they were installed, the period for which monitoring data is available, and the maximum and minimum water levels measured during the monitoring period. Groundwater level readings were initially taken by Vibro (HK) Ltd shortly after the completion of each drillhole. The GEO began to take readings in early September 1994. The summary of the data shown in Table H5 takes account of the measurements obtained by both parties. The data obtained by Vibro (HK) Ltd up to 10 September 1994 was used in conjunction with readings taken by the

GEO after this date.

The highest recorded water levels are shown in Table H5, and contours of the highest recorded water levels have been constructed from this data (Figure H15). The results show a gradual rise in the groundwater level from about 10 mPD near the toe of the wall to about 13 mPD under the slope behind the wall.

The contours in Figure H15 indicate that the highest recorded groundwater level was about 3 m below the toe of the landslide scar, and about 9 m below the crest of the landslide scar.

The above data, which was obtained during August, September and October, indicates that the groundwater level was well below the landslide scar shortly after the landslide, and remained low. This is consistent with the field observations made immediately after the failure on 23 July 1994, i.e. there was no trace of significant flow or seepage of water from the landslide scar indicative of a groundwater table or perched water table having risen above the slip surface at the time of the landslide.

H.6 FIELD PERMEABILITY TESTS

H.6.1 General

The permeability values of the fill and partially weathered volcanics were assessed by field tests carried out during the landslide investigation. These included permeability tests in drillholes, water tests in trial pits dug in the ground underneath Block D, and infiltration tests in the yard area to the south of Block D.

The soil permeability tests in drillholes are described in the following sections. The results of the water tests and infiltration tests carried out by the GEO are given in Appendix K.

H.6.2 Tests in Fill

Four falling-head permeability tests in the fill stratum were attempted in drillholes. One test was carried out in drillhole No. BH6B at 1 m to 2 m depth. The other tests were carried out in drillhole No. BH12 at 3 m to 4 m depth, 5.5 m to 6 m depth and 7.7 m to 8 m depth respectively. At 7.7 m to 8 m in drillhole No. BH12, the permeability of the fill was found to be about 10^{-4} m/s. In the other tests, the water introduced into the drillholes flowed into the ground so rapidly that the tests could not be carried out properly. This indicates that the fill at these test locations was very permeable.

Response tests were also carried out in standpipes and piezometers to confirm there were no blockages. In two of the response tests (drillholes No. BH6 & BH10), in which the test sections were partly within the fill stratum, the pipes could not be filled as a result of water flowing rapidly into the ground.

H.6.3 Tests in Volcanic Saprolite

Falling-head permeability tests were carried out in four drillholes at different depths within the partially weathered volcanics stratum. The test locations are given in Table H6.

The test results were analysed using the method recommended in BS 5930 (BSI, 1981). The interpreted permeability values (k) are summarised in Table H6. The results have also been analysed using the alternative methods proposed by Hvorslev (1951) and by Schmid (1966), and it was found that the calculated k values were not sensitive to the method of analysis.

The k values at different elevations are shown in Figure H16. It can be seen that the values were of the order of 10^{-6} m/s.

During a response test carried out in a piezometer installed in drillhole No. BH12, the pipes could not be filled as a result of water flowing rapidly into the ground. This suggests that either the PWV was locally very permeable or that the response zone of the piezometer had not been sealed properly.

H.7 REFERENCES

Bachy (1990). Ground Investigation : Stage 2 Study - Slope No. 11SW-A/C3, C4, R323 at Kwun Loong Lau Estate. Bachy Solentanche Group, Hong Kong, 105 p.

Binnie (1979a). Slope No. 11SW-A/C1 Between Blocks A & F, Kwun Loong Lau Estate. Landslide Study Phase IID, Binnie & Partners (Hong Kong) for Geotechnical Control Office, Hong Kong, 58 p.

Binnie (1979b). Slope No. 11SW-A/C5 South of Block A, Kwun Loong Lau Estate. Landslide Study Phase IID, Binnie & Partners (Hong Kong) for Geotechnical Control Office, Hong Kong, 28 p.

Binnie (1979c). Slope No. 11SW-A/C129 North-east of Blocks B and C, Kwun Loong Lau Estate. Landslide Study Phase IID, Binnie & Partners (Hong Kong) for Geotechnical Control Office, Hong Kong, 28 p.

Binnie (1979d). Slope No. 11SW-A/C3 West of Block F, Kwun Loong Lau Estate. Landslide Study Phase IID, Binnie & Partners (Hong Kong) for Geotechnical Control Office, Hong Kong, 39 p.

Binnie (1979e). Slope No. 11SW-A/C4 South of Block G, Kwun Loong Lau Estate. Landslide Study Phase IID, Binnie & Partners (Hong Kong) for Geotechnical Control Office, Hong Kong, 35 p.

Binnie (1979f). Slope No. 11SW-A/C2 South of Block A, Kwun Loong Lau Estate. Landslide Study Phase IID, Binnie & Partners (Hong Kong) for Geotechnical Control Office, Hong Kong, 26 p.

Binnie (1980). Slope No. 11SW-A/C115 North of Block C and D, Kwun Loong Lau Estate. Landslide Study Phase IID, Binnie & Partners (Hong Kong) for Geotechnical Control Office, Hong Kong, 40 p.

BSI (1981). Code of Practice for Site Investigations (BS 5930:1981). British Standards Institution, London, 148 p.

Enpack (1979a). Landslide Study Site Investigation for Slope No. 11SW-A/C115, Kwoon Lung Lau. Enpack (HK) Ltd, 18 p.

Enpack (1979b). Landslide Study Site Investigation for Slope No. 11SW-A/C118, Kwoon Lung Lau. Enpack (HK) Ltd, 3 p.

Enpack (1979c). Landslide Study Site Investigation for Slope No. 11SW-A/C129, Kwoon Lung Lau. Enpack (HK) Ltd, 3 p.

Enpack (1979d). Landslide Study Site Investigation for Slope No. 11SW-A/FR20, Kennedy Town Service Reservoir. Enpack (HK) Ltd, 46 p.

Freeman Fox (1981). Geotechnical Report Proposed Development at I.L. 8450, Smithfield Road, Hong Kong, Freeman Fox & Partners, 21 p. plus Figures and Appendices.

Fugro (1983). Geotechnical Report for Slope Nos. 11SW-A/C1, C2 and C5, Kwun Loong Lau Estate, Kennedy Town. Fugro (Hong Kong) Ltd for Hong Kong Housing Society, 11 p. plus Figures and Appendices.

GCO (1984). Geotechnical Manual for Slopes. (Second edition). Geotechnical Control Office, Hong Kong, 295 p.

GCO (1986). Hong Kong and Kowloon : solid and superficial geology. Hong Kong Geological Survey, Map Series HGM20, sheet 11, 1:20 000. Geotechnical Control Office, Hong Kong.

GCO (1987a). Geotechnical Area Studies Programme - Hong Kong and Kowloon. Geotechnical Control Office, Hong Kong, GASP Report no. 1, 170 p. plus 4 maps.

GCO (1987b). Retaining Wall 11SW-A/R309 Below Block D Kwun Loong Lau Estate. Geotechnical Control Office, Hong Kong, Stage 1 Report no. S1R 97/87, 29 p. (Unpublished).

Hvorslev, M.J. (1951). Time lag and permeability in groundwater observations. US Army Waterways Experiment Station, Bulletin no. 36, 50 p.

Martin, R.P. (1985). An Investigation of the Influence of Moisture Content on Some Soil Field Index Tests. Geotechnical Control Office, Hong Kong, Technical Note no. TN 5/85, Hong Kong, 64 p. (Unpublished).

Schmid, W.E. (1966). Field determination of permeability by the infiltration test. Permeability and Capillarity of Soils, American Society for Testing and Materials,

Special Technical Publication no. 417, pp 142-159.

Strange, P.J. & Shaw, R. (1986). Geology of Hong Kong Island and Kowloon. Geotechnical Control Office, Hong Kong, 134 p. (Hong Kong Geological Survey Memoir No. 2).

Strange, P.J., Langford, R.L., Lai, K.W., Addison, R., & Sewell, R.J. (1994). Upper Jurassic to Lower Cretaceous Stratigraphy of the Repulse Bay Volcanic Group, Hong Kong. Geotechnical Engineering Office, Hong Kong (Draft Report).

Vibro (1994). Ground Investigation Report for Landslide at Kwun Lung Lau, Smithfield Road, Kennedy Town. Vibro (Hong Kong) Ltd, 10 p. plus Appendices.

LIST OF TABLES

Table H1 - Sources of Available Gound Investigation Data at Kwun Lung Lau

Year	Source of Information	Reference
1977	Construction of Canopy to the Entrance Steps to Kwun Lung Lau, Kennedy Town.	BOO file No. 2-3/2121/77
1979	Landslide Study Phase II D : Slope 11SW-A/C1.	Binnie (1979a)
1979	Landslide Study Phase II D : Slope 11SW-A/C5.	Binnie (1979b)
1979	Landslide Study Phase II D : Slope 11SW-A/C129.	Binnie (1979c)
1979	Landslide Study Phase II D : Slope 11SW-A/C3.	Binnie (1979d)
1979	Landslide Study Phase II D : Slope 11SW-A/C4.	Binnie (1979e)
1979	Landslide Study Phase II D : Slope 11SW-A/C2.	Binnie (1979f)
1980	Landslide Study Phase II D : Slope 11SW-A/C115.	Binnie (1980)
1979	Landslide Study Site Investigation : Slope 11SW-A/C115.	Enpack (1979a)
1979	Landslide Study Site Investigation : Slope 11SW-A/C118.	Enpack (1979b)
1979	Landslide Study Site Investigation : Slope 11SW-A/C129.	Enpack (1979c)
1979	Landslide Study Site Investigation : Slope 11SW-A/FR20.	Enpack (1979d)
1990	Ground Investigation : Stage 2 Study Slope 11SW-A/C3, C4, R323 at Kwun Lung Lau.	Bachy (1990)
1981	Geotechnical Report : Proposed Development at I.L. 8450 Smithfield Road, Hong Kong	Freeman Fox (1981)
1983	Geotechnical Report for Slope No. 11SW-A/C1, C2 and C5.	Fugro (1983)
1987	Stage 1 Study Report : Retaining Wall 11SW-A/R309 below Block D, Kwun Lung Lau Estate.	GCO (1987b)
1994	Preliminary Drillhole and Trial Pit Logs for Slope 11SW-A/FR21.	(Draft Logs from Mott Connell)

Table H2 - Summary of Relevant Ground Investigation Data at Kwun Lung Lau (Sheet 1 of 8)

Source of Information	GI Station No.	Type of GI	Co-ordinates		Elevation (mPD)	Depth of Investi-gation (m)	Base of Fill (mPD)	Thickness of Fill (m)	Base of Superficial Deposits (mPD)	Top of PW90/100 (mPD)	Reliability of Data
			Easting	Northing							
BOO file No. 2-3/2121/77 (1977)	BH1	DH	31190	15771	23.4	6.4	-	0.0	-	-	Low
	BH2	DH	31168	15767	21.3	11.0	20.4	1.0	-	10.3	Low
Binnie (1979a)	KLL5	DH	31255	15680	83.4	40.0	80.9	2.5	-	46.0	High
	KLL7	DH	31206	15678	62.5	20.0	-	0.0	-	47.5	High
	KLL9	DH	31239	15686	62.6	30.0	62.1	0.5	-	30.4(?)	High
	KLL10	DH	31227	15646	80.5	33.7	78.5	2.0	-	47.9	High
	KTSR1	DH	31166	15627	92.3	37.6	87.5	4.8	-	59.7	High
Binnie (1979b)	KLL6	DH	31265	15635	69.3	30.0	-	0.0	65.1	41.0	Moderate
	KLL11	DH	31286	15657	49.7	19.9	49.2	0.5	-	34.7	High
Binnie (1979c)	TP1	TP	31274	15743	≈ 31.0	2.9	28.0	3.0	-	-	Moderate
	KLL8	DH	31530	16010	32.5	28.8	29.5	3.0	-	4.8(?)	High
Binnie (1979d)	KLL3	DH	31155	15665	53.5	16.0	-	0.0	-	40.0	High
	KLL4	DH	31152	15663	73.2	32.7	-	0.0	-	56.2(?)	High
Binnie (1979e)	KLL1	DH	31127	15760	25.2	29.9	20.2	5.0	-	-	High
	KLL2	DH	31126	15750	33.0	27.1	25.2	7.8	-	8.5	High

Table H2 - Summary of Relevant Ground Investigation Data at Kwun Lung Lau (Sheet 2 of 8)

Source of Information	GI Station No.	Type of GI	Co-ordinates		Elevation (mPD)	Depth of Investi-gation (m)	Base of Fill (mPD)	Thickness of Fill (m)	Base of Superficial Deposits (mPD)	Top of PW90/100 (mPD)	Reliability of Data
			Easting	Northing							
Enpack (1979a)	TP1	TP	31237	15772	19.3	2.2	< 17.1	> 2.2	-	-	Low
	TP2	TP	31257	15750	31.9	1.8	< 30.1	> 1.8	-	-	Moderate
Enpack (1979b)	TP1	TP	31099	15704	55.8	1.5	-	0.0	-	-	Moderate
	TP2	TP	31081	15689	70.0	3.0	-	0.0	-	-	Moderate
Enpack (1979c)	TP1	TP	31270	15740	32.5	-	< 29.5	> 3.0	-	-	Moderate
Enpack (1979d)	NKTSR1	DH	31155	15632	92.1	8.4	89.1	2.9	-	< 83.7	High
	NKTSR2	DH	31140	15628	89.5	9.2	86.3	3.2	-	< 80.4	High
	NKSTR3	DH	31134	15625	88.1	9.7	83.6	4.5	-	< 78.5	High
	TP2	TP	31169	15623	93.3	3.0	< 90.3	> 3.0	-	-	Low
	TP3	TP	31166	15633	89.7	2.1	< 87.6	> 2.1	-	-	Low
	TP4	TP	31137	15621	91.2	3.6	< 87.7	> 3.5	-	-	Low
	TP5	TP	31164	15644	83.0	1.5	< 81.5	> 1.5	-	-	Low
	TP6	TP	31152	15643	84.1	1.8	-	0.0	-	-	Low
	TP7	TP	31145	15637	85.8	1.8	-	0.0	-	-	Low
	TP8	TP	31128	15614	92.8	3.0	-	0.0	-	-	Low
	TP11	TP	31151	15636	89.2	1.2	< 88.0	> 1.2	-	-	Low

Table H2 - Summary of Relevant Ground Investigation Data at Kwun Lung Lau (Sheet 3 of 8)

Source of Information	GI Station No.	Type of GI	Co-ordinates		Elevation (mPD)	Depth of Investi-gation (m)	Base of Fill (mPD)	Thickness of Fill (m)	Base of Superficial Deposits (mPD)	Top of PW90/100 (mPD)	Reliability of Data
			Easting	Northing							
Enpack (1979d)	TP12	TP	31160	15645	84.3	2.0	< 82.3	> 2.0	-	-	Low
	TP13	TP	31173	15635	86.8	1.7	< 85.1	> 1.7	-	-	Low
Bachy (1990)	DH1	DH	31134	15764	24.5	15.0	20.5	4.0	< 9.5	-	High
	DH2	DH	31134	15750	32.8	15.0	24.8	8.0	< 17.8	-	High
	DH3	DH	31154	15690	53.3	15.0	-	0.0	< 38.3	-	High
	DH4	DH	31159	15680	64.5	16.0	-	0.0	< 48.5	-	High
	TP1	TP	31132	15771	17.5	0.4	< 17.1	> 0.4	-	-	High
	TP2	TP	31111	15767	17.6	0.6	< 17.0	> 0.6	-	-	High
	TP3	TP	31121	15763	23.9	3.2	< 20.7	> 3.2	-	-	High
	TP4	TP	31140	15769	21.5	3.2	< 18.3	> 3.2	-	-	High
	TP5	TP	31114	15750	31.5	1.4	< 30.1	> 1.4	-	-	High
	TP6	TP	31129	15757	28.0	3.0	< 25.0	> 3.0	-	-	High
	TP7	TP	31142	15758	26.8	0.8	< 26.0	> 0.8	-	-	High
	CS-1	SS	31161 31158	15684 15702	63.2 43.9	-	59.2	3.3	-	-	High
	CS-2	SS	31152 31145	15679 15696	64.4 43.7	-	-	0.0	-	-	High

Table H2 - Summary of Relevant Ground Investigation Data at Kwun Lung Lau (Sheet 4 of 8)

Source of Information	GI Station No.	Type of GI	Co-ordinates		Elevation (mPD)	Depth of Investi-gation (m)	Base of Fill (mPD)	Thickness of Fill (m)	Base of Superficial Deposits (mPD)	Top of PW90/100 (mPD)	Reliability of Data
			Easting	Northing							
Freeman Fox (1981)	BH1	DH	31341	15682	29.7	40.9	21.6	8.1	-	9.3	High
	BH2	DH	31318	15700	31.5	5.4	< 26.1	5.4	-	-	High
	BH3	DH	31293	15691	38.3	17.8	35.3	3.0	-	25.5	High
	BH4	DH	31312	15719	26.7	32.4	-	0.0	-	8.7	High
	BH5	DH	31291	15710	36.6	25.8	34.1	2.5	32.1(C)	8.9	High
	BH6	DH	31287	15725	35.6	20.8	32.6	3.0	-	-	Low
	BH6A	DH	31331	15716	20.5	29.7	-	0.0	16.5(C)	11.1	Moderate
	BH7	DH	31299	15742	24.6	33.0	11.1(?)	13.5(?)	-	- 0.9	Moderate
	BH8	DH	31267	15735	34.5	16.1	30.0	4.5	-	23.6	High
	BH9	DH	31280	15754	24.2	36.3	16.7(?)	7.5(?)	-	- 2.9	Moderate
	BH10	DH	31289	15763	14.5	44.6	10.0	4.5	-0.3(A)	- 15.1	Moderate
	BH11	DH	31328	15738	19.9	30.3	16.6	3.4	-	12.4	High
	BH12	DH	31307	15753	16.5	52.8	-	0.0	-	- 11.8	
	BH13	DH	31315	15767	16.2	30.0	6.7(?)	9.4(?)	-	2.5	Moderate
	BH14	DH	31326	15755	18.2	24.6	14.7	3.5	-	- 6.1	Moderate
	BH15	DH	31335	15729	19.9	18.0	16.9	3.0	-	> 1.9	Moderate

Table H2 - Summary of Relevant Ground Investigation Data at Kwun Lung Lau (Sheet 5 of 8)

Source of Information	GI Station No.	Type of GI	Co-ordinates		Elevation (mPD)	Depth of Investi-gation (m)	Base of Fill (mPD)	Thickness of Fill (m)	Base of Superficial Deposits (mPD)	Top of PW90/100 (mPD)	Reliability of Data
			Easting	Northing							
Freeman Fox (1981)	BH16	DH	31338	15731	19.9	32.1	15.9	4.0	-	11.0	Moderate
	BH17	DH	31335	15705	22.9	31.0	-	0.0	-	- 7.2(?)	Low
	BH18	DH	31348	15715	22.8	13.9	16.0	6.8	-	7.9	High
	BH19	DH	31323	15681	33.9	31.1	-	0.0	30.85(C)	13.0	Moderate
	BH21	DH	31313	15700	33.3	-	-	0.0	29.25(C)	6.7(?)	Low
	AH1	DH	31355	15693	20.7	21.5	13.2	7.5	-	14.7	High
	AH2	DH	31322	15726	19.9	60.6	17.4	2.6	-	- 3.4	High
	AH3	DH	31315	15740	18.3	30.1	17.7	0.6	-	- 0.1	High
	AH4	DH	31296	15760	15.4	50.9	9.4(?)	6.0(?)	-	- 17.5	Moderate
	AH5	DH	31335	15697	22.9	60.0	-	0.0	-	2.5	High
	AH6	DH	31331	15716	22.8	35.5	-	0.0	-	3.4	Moderate
	TP1	TP	31343	15686	-	1.5	-	0.0	-	-	High
	TP2	TP	31325	15701	-	1.5	-	0.4	-	-	High
	TP3	TP	31319	15703	-	1.5	-	> 1.5	-	-	High
	TP4	TP	31328	15687	-	1.5	-	0.0	-	-	High
Fugro (1983)	BH1	DH	31218	15688	62.5	25.3	-	0.0	-	41.5	High

Table H2 - Summary of Relevant Ground Investigation Data at Kwun Lung Lau (Sheet 6 of 8)

Source of Information	GI Station No.	Type of GI	Co-ordinates		Elevation (mPD)	Depth of Investi-gation (m)	Base of Fill (mPD)	Thickness of Fill (m)	Base of Superficial Deposits (mPD)	Top of PW90/100 (mPD)	Reliability of Data
			Easting	Northing							
Furgo (1983)	BH2	DH	31210	15706	44.2	12.1	42.7	1.5	-	32.9(?)	Moderate
	BH3	DH	31225	15671	62.6	35.0	-	0.0	77.1(C)	> 43.6(?)	Moderate
	BH4	DH	31234	15692	62.5	23.0	-	0.0	-	> 39.5(?)	Moderate
	BH5	DH	31243	15717	44.2	10.1	42.2	1.9	-	-	High
	BH6	DH	31235	15640	82.9	45.1	81.0	1.9	78.9(C)(?)	40.1	Moderate
	BH7	DH	31254	15639	62.1	27.7	-	0.0	-	> 34.5(?)	Moderate
	BH8	DH	31285	15666	44.9	9.9	43.4	1.5	-	-	High
	BH9	DH	31307	15637	47.8	12.0	47.3	1.5	-	-	High
	BH10	DH	31272	15638	65.8	31.6	-	0.0	61.8(C)(?)	39.7	Moderate
	BH11	DH	31272	15757	25.0	15.2	23.0	2.0	-	> 5.0(?)	Moderate
	BH12	DH	31251	15754	32.7	25.0	31.2	1.5	29.7(C)	> 7.7(?)	Moderate
	TP1	TP	31242	15775	-	1.8	-	0.2-1.8	-	-	High
	TP2	TP	31245	15764	-	1.9	-	0.0-0.5	1 m thick(C)	-	High
	TP3	TP	31203	15660	-	1.5	-	0.4	1.1 m thick(C)	-	High
	TP4	TP	31285	15655	-	1.8	-	0.0	-	-	High

Table H2 - Summary of Relevant Ground Investigation Data at Kwun Lung Lau (Sheet 7 of 8)

Source of Information	GI Station No.	Type of GI	Co-ordinates		Elevation (mPD)	Depth of Investi-gation (m)	Base of Fill (mPD)	Thickness of Fill (m)	Base of Superficial Deposits (mPD)	Top of PW90/100 (mPD)	Reliability of Data
			Easting	Northing							
Fugro (1983)	TP5	TP	31300	15619	-	2.0	-	0.6-0.1	-	-	High
	A1	SS	31235 31240	15761 15771	-	-	-	0.9	6.4 m thick	-	Low
	A2	SS	31250 31256	15687 15693	-	-	-	0.0	-	-	High
	A3	SS	31225 31242	15664 15665	-	-	-	0.0	-	-	High
	A4	SS	31282 31291	15641 15649	-	-	-	0.0	-	-	High
GCO (1987)	D1	DH	31205	15774	22.6	26.2	0.0	-	-	-	Low
	No. 4	DH	31211	15763	34.2	11.0	0.0	-	-	-	Low
Draft Logs from Mott Connell (1994)	KS1-1	DH	31188	15750	31.3	21.2	29.8	1.5	-	16.6	High
	KS1-2	DH	31161	15740	33.2	24.2	31.7	1.5	-	14.6	High
	KS1-3	DH	31177	15755	27.5	16.0	-	0.0	-	14.5	High
	KS1-4	DH	31162	15754	24.9	16.0	-	0.0	-	-	High
	KS1-5	DH	31167	15762	23.0	10.0	19.5(?)	3.5(?)	19.51(?)	-	Moderate
	KS1-8	DH	31212	15748	42.4	45.9	37.4	5.0	-	11.8	High
	KS1-10	DH	31213	15738	42.6	33.4	41.1	1.5	-	15.2	High

Table H2 - Summary of Relevant Ground Investigation Data at Kwun Lung Lau (Sheet 8 of 8)

Source of Information	GI Station No.	Type of GI	Co-ordinates		Elevation (mPD)	Depth of Investi-gation (m)	Base of Fill (mPD)	Thickness of Fill (m)	Base of Superficial Deposits (mPD)	Top of PW90/100 (mPD)	Reliability of Data
			Easting	Northing							
Draft Logs from Mott Connell (1994)	KS1-11	DH	31207	15742	42.4	28.5	37.4	5.0	-	19.1	High
	KS1-6H	DH	31185	15776	18.9	-	-	3.0	-	-	Horizontal Hole
	KS1-7H	DH	31155	15766	17.8	-	-	4.9	-	-	Horizontal Hole-Low
	KS1-P1	TP	31182	15773	23.0	2.0	22.0	1.0	-	-	High
	KS1-P2	TP	31181	15777	15.8	0.7	15.5	0.3	-	-	High
	KS1-P3	TP	31165	15766	21.1	0.7	< 20.1	> 1.0	-	-	High
	KS1-P3A	TP	31164	15766	21.1	1.7	19.9	1.2	-	-	Moderate

Legend :

DH Drill hole
TP Trial pit
SS Surface stripping
(A) Alluvium
(C) Colluvium
(?) Data is questionable
- Not encountered
GI Ground investigation
PW90/100 Partially weathered rock mass (90% - 100% rock)

Note : The GI data in Binnie (1979f & 1980) are contained in Binnie (1979a to 1979e) and therefore not listed in this Table.

Table H3 - Observations Made on the Failure Scar between 25 July and 29 July 1994

Observation Point	Description
1	FILL. Loose, moist, light brown, gravelly, silty fine SAND, structureless.
2	Sewage flowing from the underground pipe in a manhole.
3	10 mm to 50 mm wide cracks in the chunam surface. The slope of the adjacent intact surface dips at 30°
4	FILL. Loose, moist, gravelly, silty fine SAND with boulders and concrete fragments.
5	Boundary of FILL(Qf) and COMPLETELY DECOMPOSED VOLCANICS(CDV). The CDV is weak, mottled reddish brown, gravelly, silty fine SAND with relict texture. Based on the 1:20 000 geological map and drillcore examination the parent rock is a lapilli coarse to fine ash TUFF belonging to the Mount Davis Formation (JMD).
6	The column footing is mainly founded on CDV. A thin layer of compacted fill varying from 0 to 50 mm thick occurs between the column footing and CDV.
7	HIGHLY DECOMPOSED VOLCANICS(HDV). Moderately weak, light grey with yellowish brown patches. The parent rock is a lapilli coarse to fine ash TUFF belonging to the Mount Davis Formation(JMD). The exposure is partially weathered rock mass with rock less than 50 % (PW 30/50). Relict joints with dip directions and dip angles of 040/80, 035/78, 045/80 and 347/56 are exposed.
8	HDV. Relict joints could be clearly seen.
9	Boundary between FILL and CDV. The fill is loose, moist, yellowish brown, gravelly, silty fine SAND with concrete fragments and building debris. The interface between FILL and CDV is at about 1.2 m to 1.5 m below the base of the pile cap.
10	FILL. Loose, dry, yellowish brown, silty fine SAND with boulders, concrete fragments and rubbish. The thickness of the fill is 2.4 m. The slope surface dips at 50°, and is protected by chunam. Behind the masonry wall a layer of fill 0.5 m to 0.8 m thick overlies the CDV. The average thickness of the wall at this location is 700 mm, varying from 500 mm to 750 mm. The height of the wall at this location is 8.46 m, inclining at 73° to the horizontal.
11	Joints between the coping stones wedged open by vegetation roots. The width of the cracks varies from 30 mm to 80 mm. A coping stone of the remaining masonry wall was observed to have been dislocated by 150mm.
12	HDV exposed behind the remaining masonry wall. Relict joints could be seen in the HDV. The dip direction and dip angle of a relict joint are 040/85.
13	CDV, covered by a thin layer of landslide debris.
14	HDV. Relict joints could be seen on the lower landslide surface.
15	VOLCANIC RESIDUAL SOIL (Grade VI), covered by a thin layer of landslide debris.
16	A 1.1 m diameter hole infilled by boulders of volcanic rocks. The depth of the hole is greater than 2 m.
17	HDV, showing evident relict joints.
Note :	The observation points are shown in Figure H5

Table H4 - Measured Index Properties

Material	Composition	Consistency	Hand Penetrometer Strength (kPa)		Slake Test
			Range	Mean	
Fill	Varies from silty gravelly fine sand to sandy clay and silt	Very loose to loose, soft to firm	10 to 150	50	N/A
CDV	Silty fine sand	Extremely weak	100 to 200	100	Slake readily
C/HDV	Silty fine sand with some gravel	Extremely weak to weak	130 to 240	190	Slake on agitation
HDV	Gravelly silty fine sand	Weak to moderately weak	> 300	> 300	Not slake

Legend :

CDV	Completely decomposed volcanics
C/HDV	Completely to highly decomposed volcanics
HDV	Highly decomposed volcanics

Table H5 - Summary of Groundwater Level Readings

Drillhole No.	Piezometer Tip Level (mPD)	Monitoring Period	Maximum Level (mPD)	Minimum Level (mPD)
BH 1	+8.83	6 Sep 94 - 1 Nov 94	+12.83	+10.23
	+3.63	6 Sep 94 - 1 Nov 94	+10.93	+9.98
BH 1A	+8.87	6 Sep 94 - 1 Nov 94	+11.77	+10.27
BH 2	+3.67	24 Aug 94 - 1 Nov 94	+11.37	+4.32(2)
BH 2A	+7.56	24 Aug 94 - 1 Nov 94	+11.91	+7.91
BH 3	+14.51	17 Aug 94 - 1 Nov 94	Dry	Dry
	+1.91	17 Aug 94 - 1 Nov 94	+10.11	+4.21(3)
BH 4	+6.15	19 Aug 94 - 1 Nov 94	+11.75	+10.55
	-2.97	19 Aug 94 - 1 Nov 94	+10.74	+9.74
BH 5	+4.77	13 Aug 94 - 7 Oct 94	+10.92	+10.37
BH 5A	+12.62	18 Aug 94 - 7 Oct 94	+14.02	+12.52
BH 6	+24.05	24 Aug 94 - 1 Nov 94	Dry	Dry
	+10.80	24 Aug 94 - 1 Nov 94	+12.30	+11.10
BH 7	+5.75	26 Aug 94 - 1 Nov 94	+9.65	Dry
	+2.44	26 Aug 94 - 1 Nov 94	+9.64	+9.14
BH 8	+7.77	25 Aug 94 - 1 Nov 94	+10.92	+10.12
	-3.75	25 Aug 94 - 1 Nov 94	+10.75	+9.75
BH 9	+11.63	12 Sep 94 - 1 Nov 94	Dry	Dry
	+3.23	12 Sep 94 - 1 Nov 94	+11.13	+10.23
BH 9A	+12.32	12 Sep 94 - 1 Nov 94	Dry	Dry
BH 10	+16.57(1)	27 Sep 94 - 18 Oct 94	Dry	Dry
	+13.77	27 Sep 94 - 18 Oct 94	Dry	Dry

Notes : (1) This is a standpipe.
(2) The water level in BH2 was consistently low at around +4.5 mPD during the period 24 August 1994 to 15 September 1994 but rose to +11.0 mPD after 15 September 1994.
(3) The ambient groundwater level prior to the response test in the deeper piezometer of BH3 was about +10.5 mPD. After the response test, this level fell gradually to +4.2 mPD on 16 September 1994 and then rose to about +10 mPD on 20 September 1994.

Table H6 - Summary of Falling-head Permeability Test Results

Drillhole No.	Depth	Material	Permeability (m/s)
BH1A	2.5 m - 3.5 m	CDV	4.52×10^{-7}
	5.5 m - 6.5 m	CDV	2.34×10^{-6}
	8.5 m - 9.5 m	C/HDV	3.02×10^{-6}
	11.5 m - 12.5 m	C/HDV	9.37×10^{-7}
	14.5 m - 15.5 m	C/HDV	2.34×10^{-6}
BH2A	3.5 m - 4.5 m	CDV	9.80×10^{-8}
	7.0 m - 8.0 m	CDV	1.92×10^{-6}
	10.0 m - 11.0 m	H/MDV	3.46×10^{-6}
	13.0 m - 14.0 m	HDV	2.97×10^{-6}
BH51	3.8 m - 4.8 m	CDV	1.09×10^{-7}
	6.8 m - 7.8 m	CDV	1.13×10^{-7}
	9.8 m - 10.8 m	CDV	6.69×10^{-7}
BH9A	2.0 m - 3.0 m	CDV	4.46×10^{-7}
	5.0 m - 6.0 m	C/HDV	3.12×10^{-7}
	8.0 m - 9.0 m	CDV	1.56×10^{-7}
	11.0 m - 12.0 m	C/HDV	2.92×10^{-7}

Legend :

CDV	Completely decomposed volcanics
C/HDV	Completely to highly decomposed volcanics
HDV	Highly decomposed volcanics
H/MDV	Highly to moderately decomposed volcanics

LIST OF FIGURES

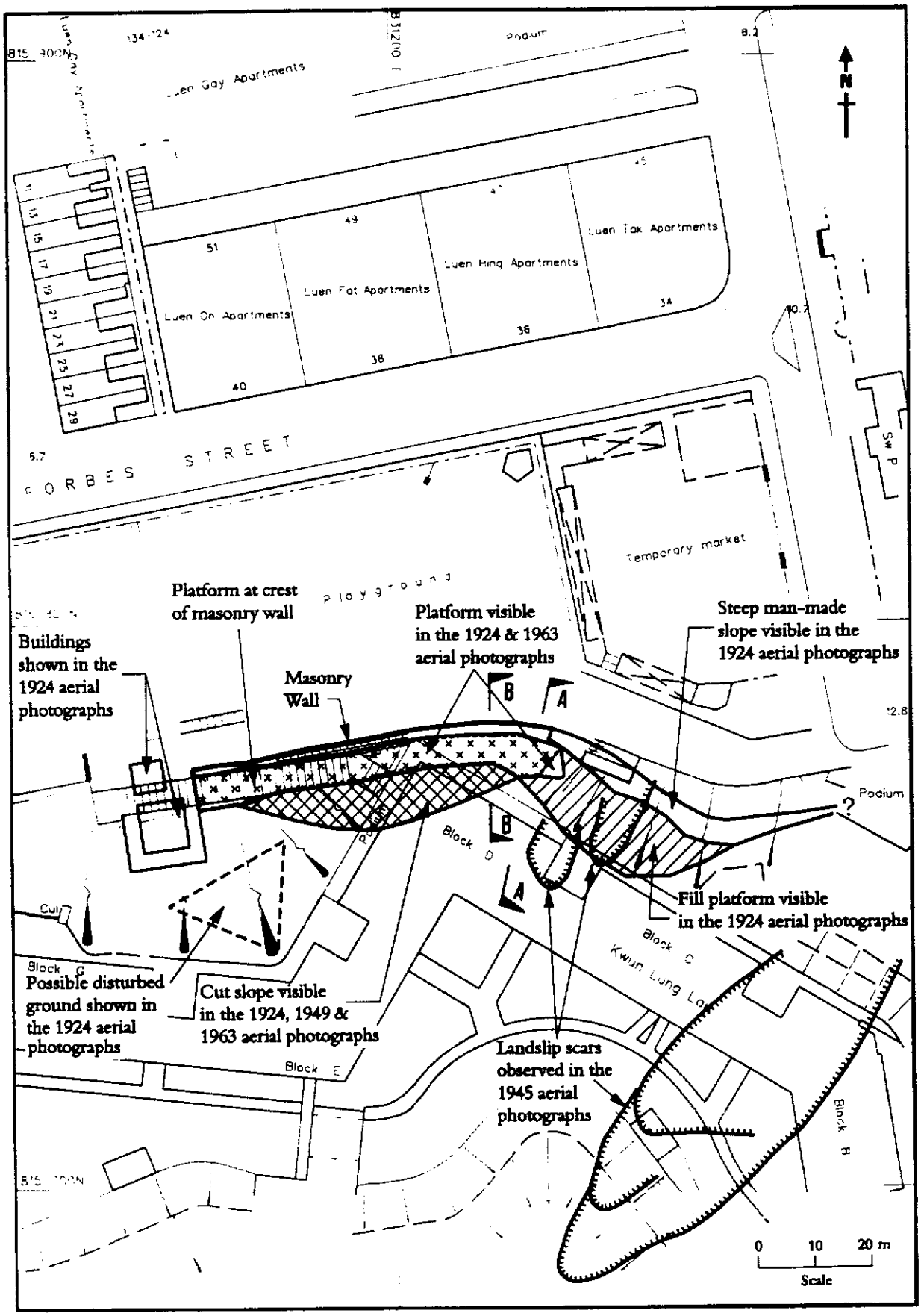

Figure H1 - Observations from Aerial Photographs Taken between Years 1924 & 1963

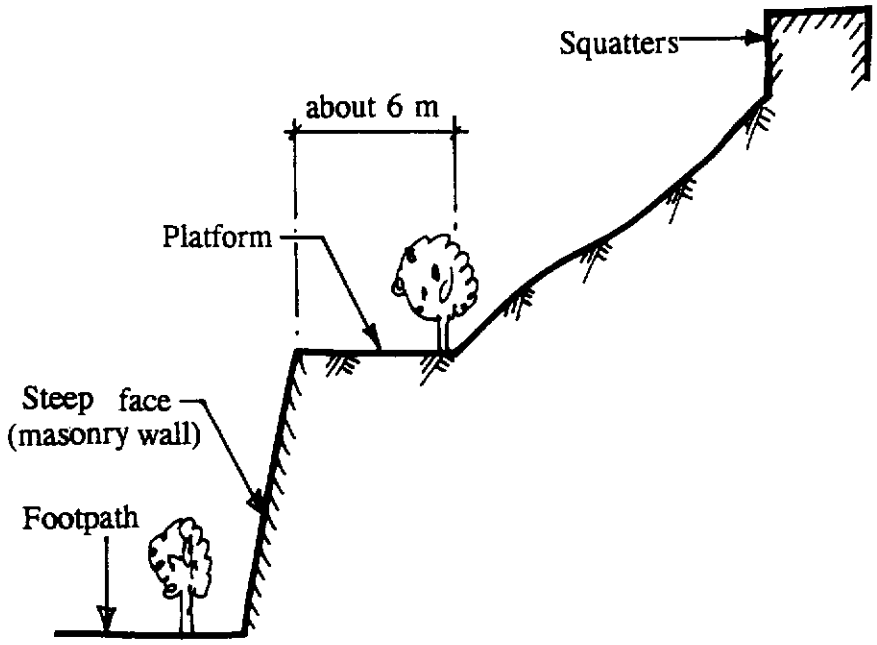

(a) Section A - A

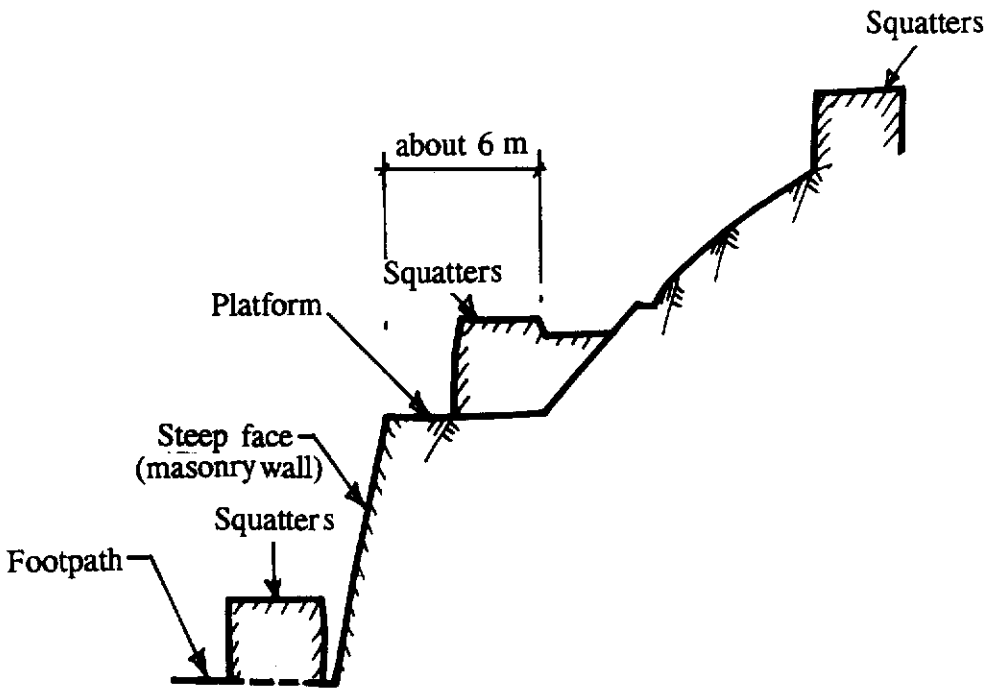

(b) Section B - B

Notes : (1) For locations of Sections A-A & B-B, see Figure H1.
(2) Information shown in this Figure is based on observations made from the 1963 aerial photographs.

Figure H2 - Diagrammatic Sections through the Site in 1963

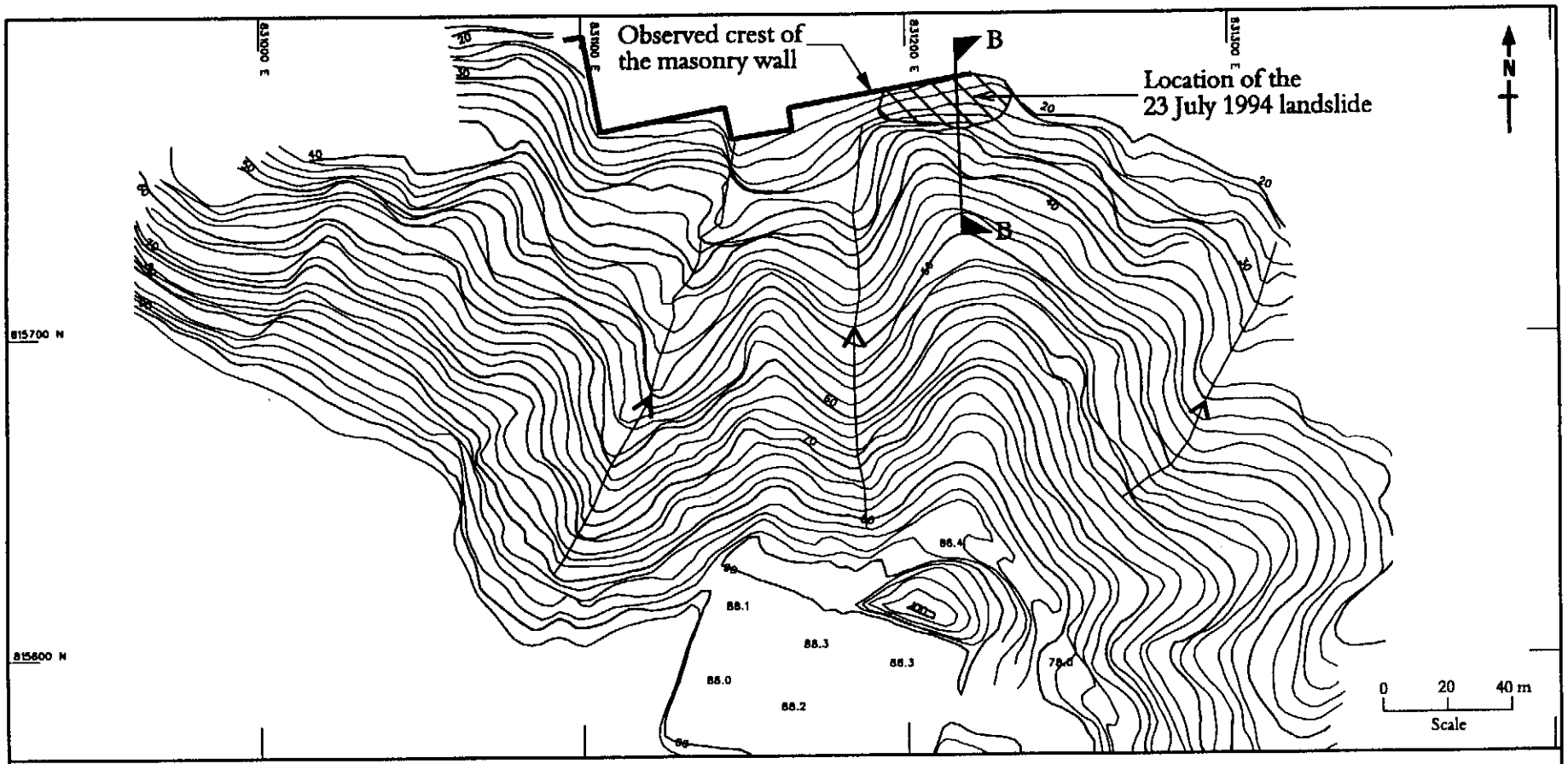

Legend :

Natural drainage line showing direction of flow

Notes :

1) This is a machine plot produced by photogrammetry and has not been field checked. Some contours have been adjusted based on an interpretation of the 1963 aerial photographs.
2) The photogrammetric survey was produced by Photogrammetric Unit, Lands Department. (Folder Number 453 (part 2))
3) Minor contour adjustments were carried out by the Civil Engineering Department.
4) Contour Interval : 2 meters
5) Accuracy : ± 2 meters
6) Section B-B is shown in Figure H4

Figure H3 - Topographic Plan of the Area in 1963

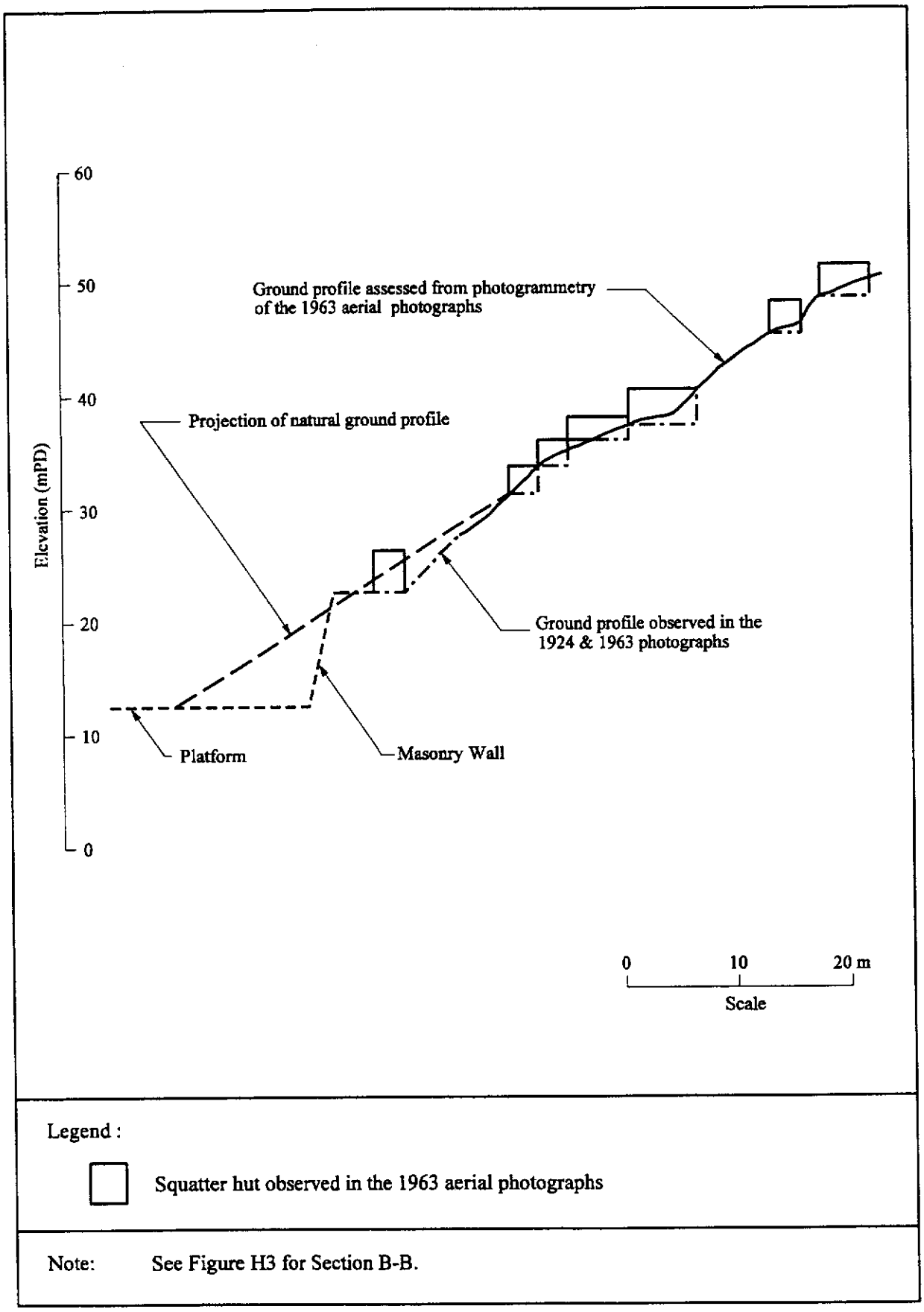

Figure H4 - Ground Profile in 1963

Figure H5 - Photograph of the Failure Scar Showing the Field Observation Points Described in Table H3

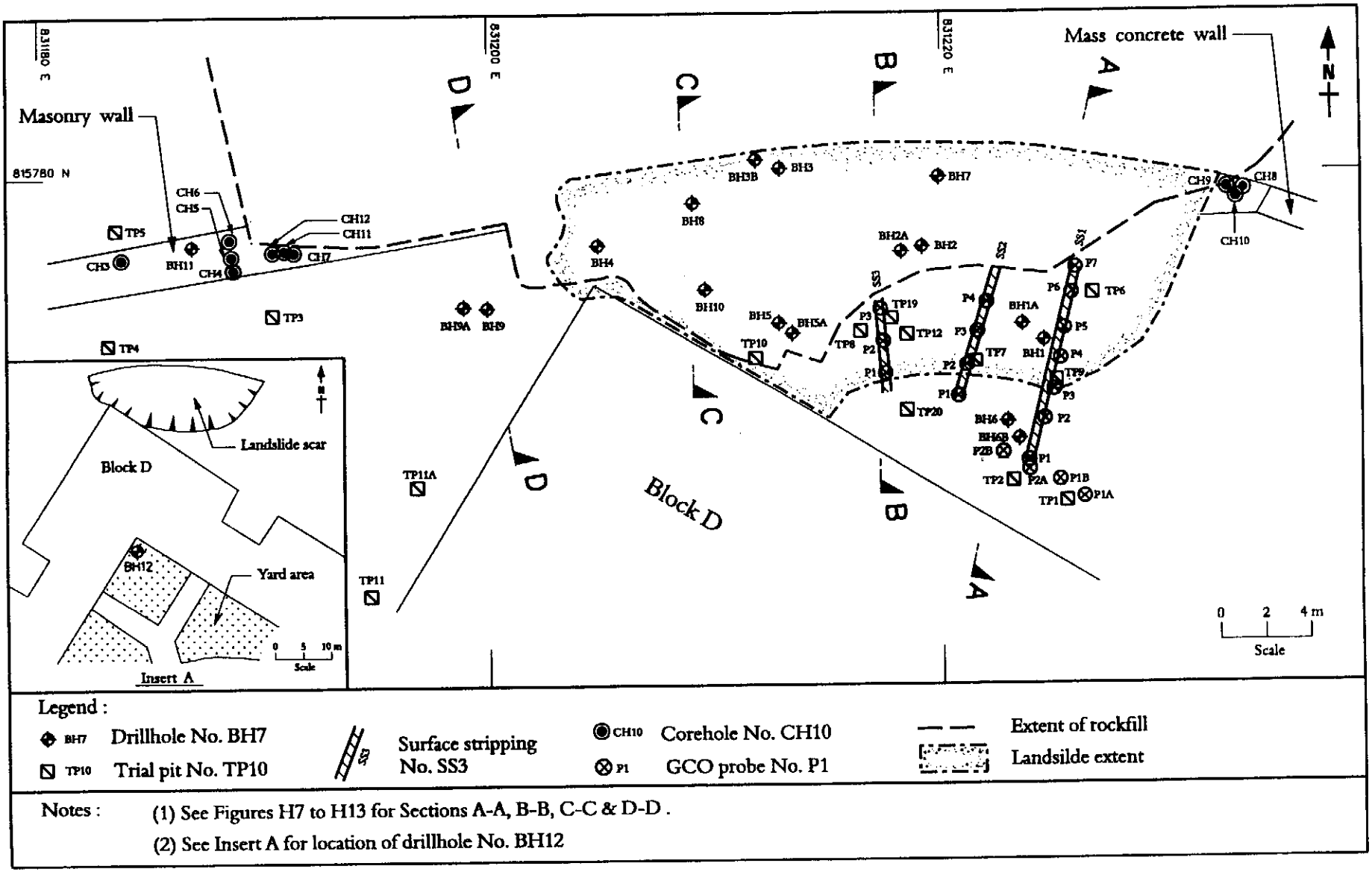

Figure H6 - Location Plan of the Ground Investigation Work

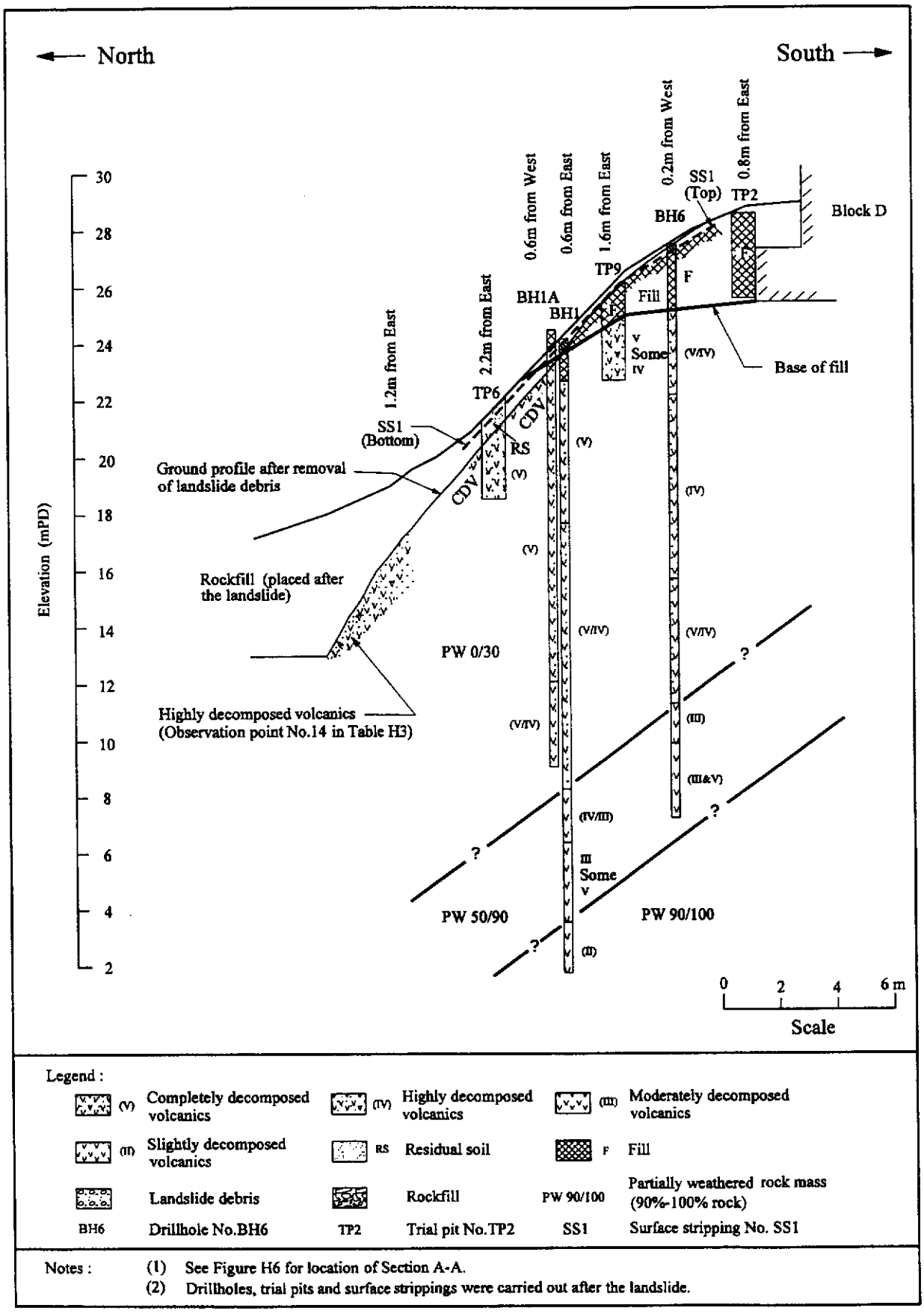

Figure H7 - Section A-A Showing the Geological Profile after the Landslide

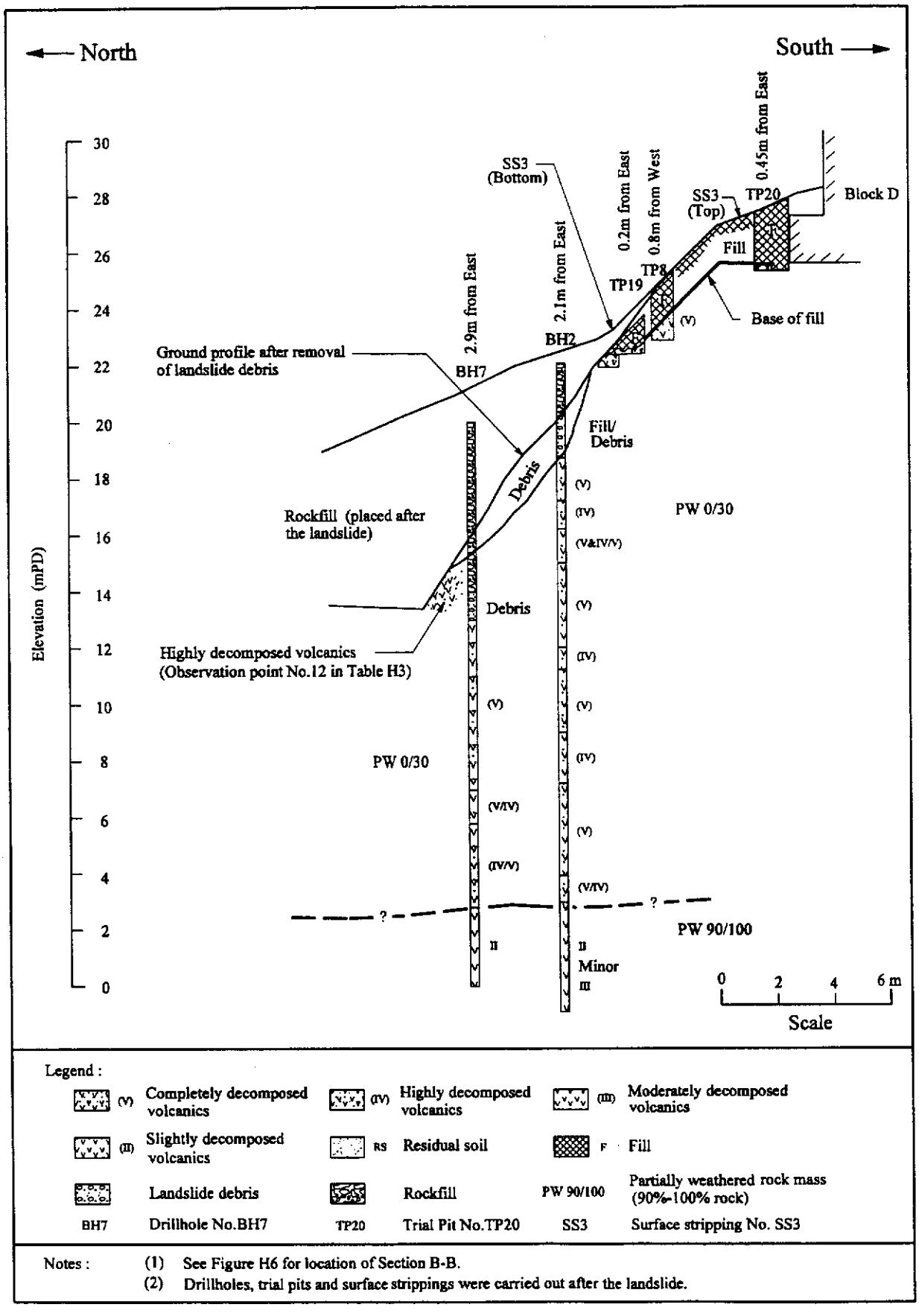

Figure H8 - Section B-B Showing the Geological Profile after the Landslide

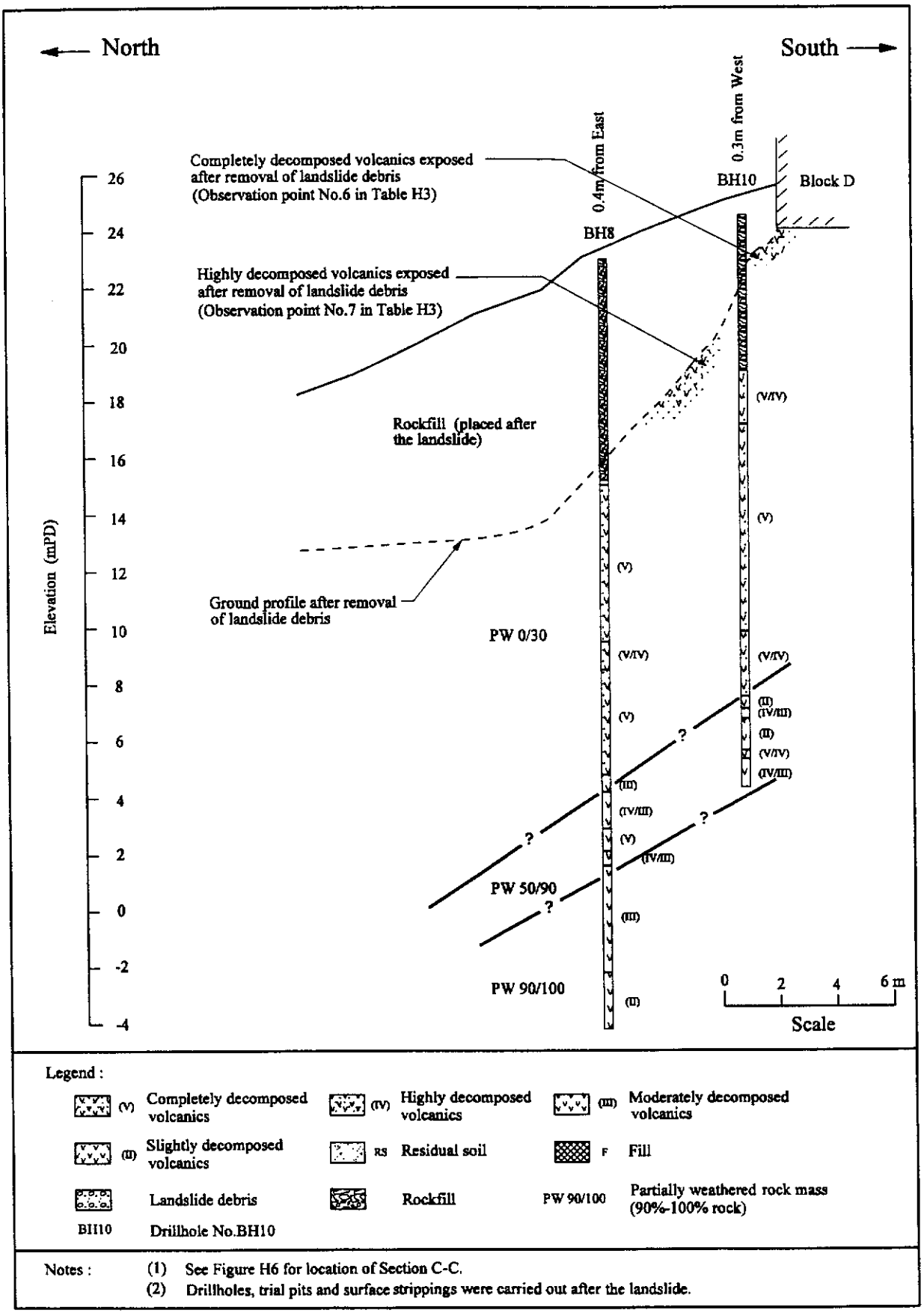

Figure H9 - Section C-C Showing the Geological Profile after the Landslide

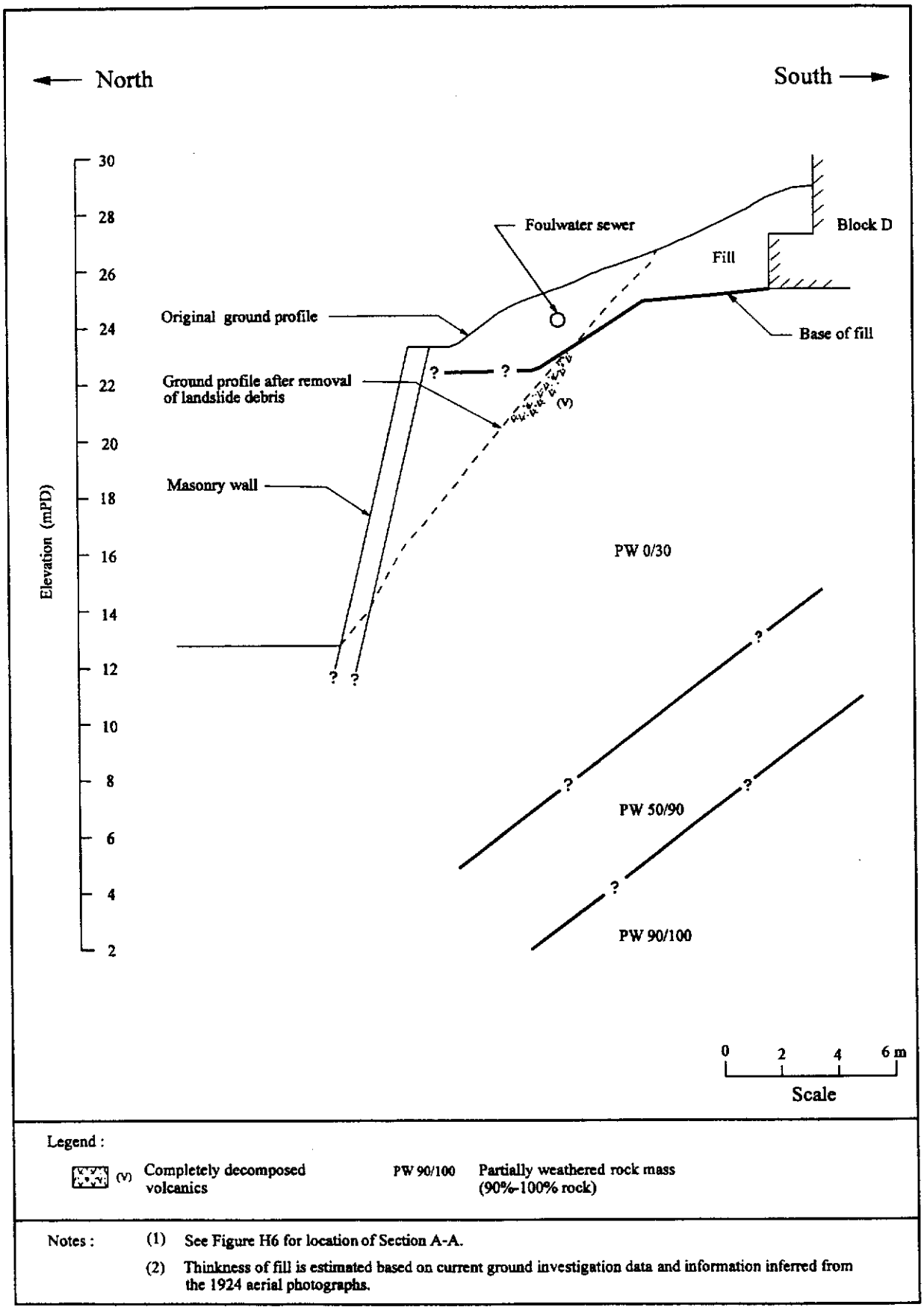

Figure H10 - Section A-A Showing the Interpreted Geological Profile before the Landslide

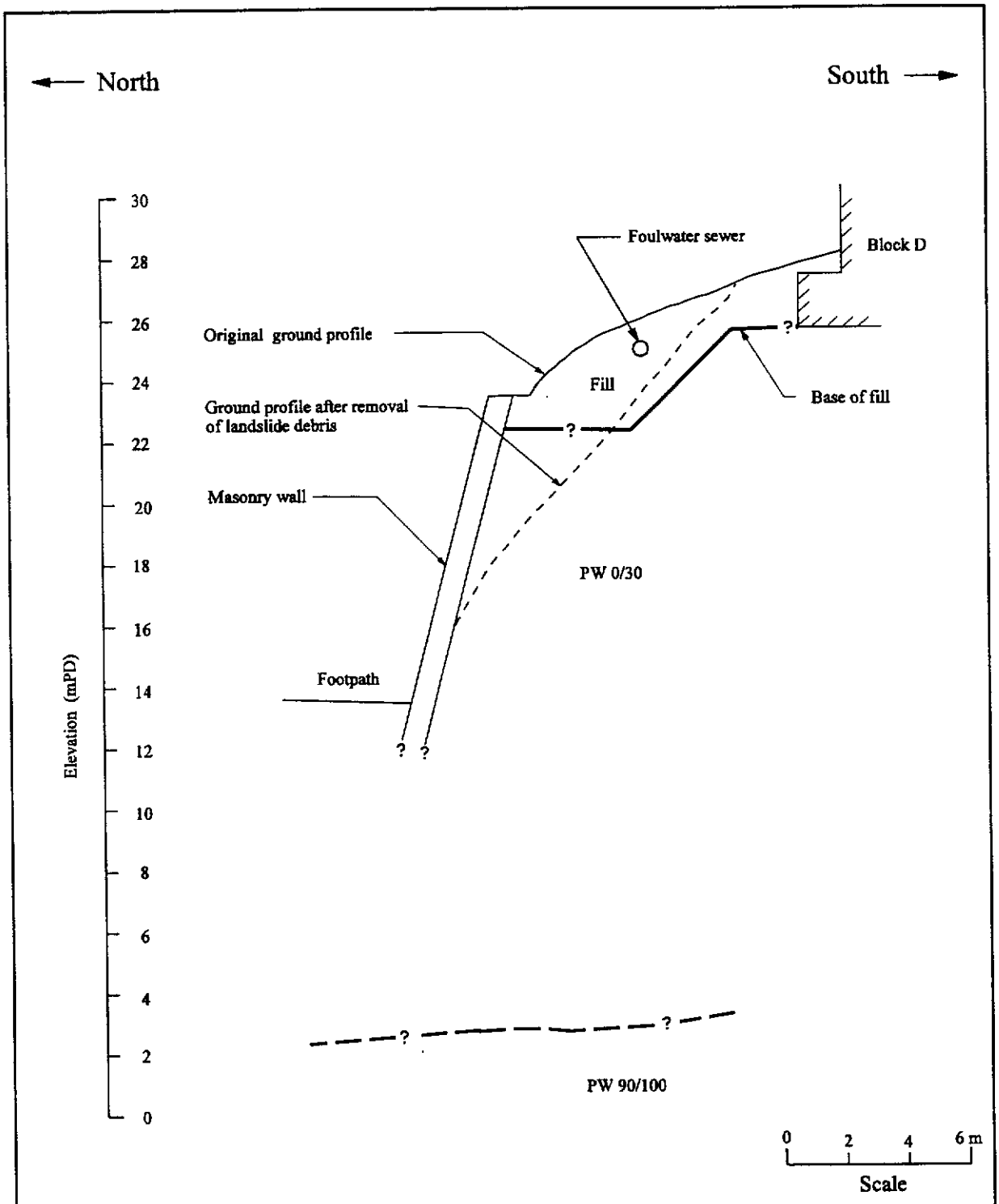

Legend :

PW 90/100 Partially weathered rock mass (90%-100% rock)

Notes :

(1) See Figure H6 for location of Section B-B.

(2) Thinkness of fill is estimated based on current ground investigation data and information inferred from the 1924 aerial photographs.

Figure H11 - Section B-B Showing the Interpreted Geological Profile before the Landslide

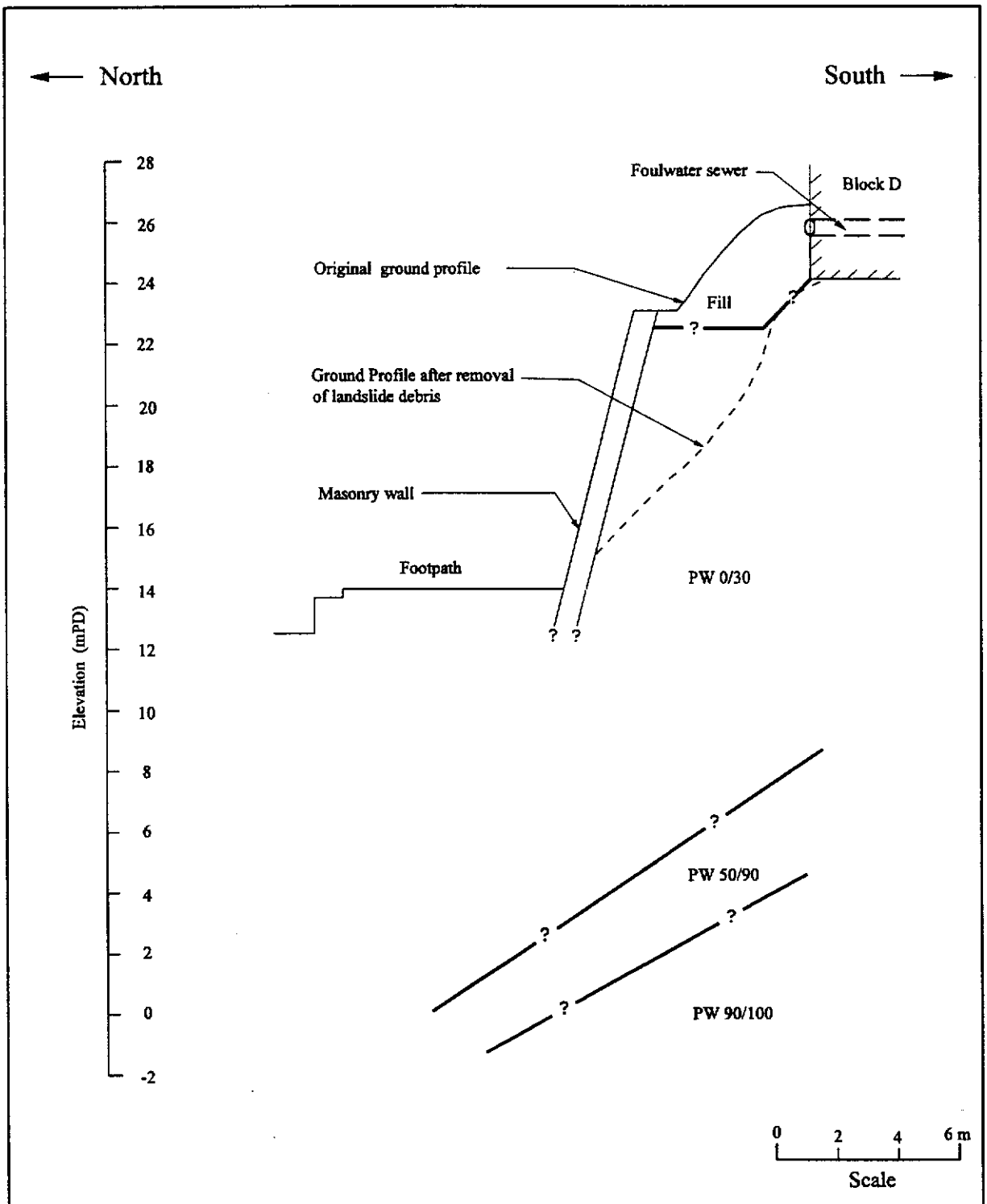

Legend :

PW 90/100 Partially weathered rock mass (90%-100% rock)

Notes :

(1) See Figure H6 for location of Section C-C.

(2) Thickness of fill is estimated based on current ground investigation data and information inferred from the 1924 aerial photographs.

Figure H12 - Section C-C Showing the Interpreted Geological Profile before the Landslide

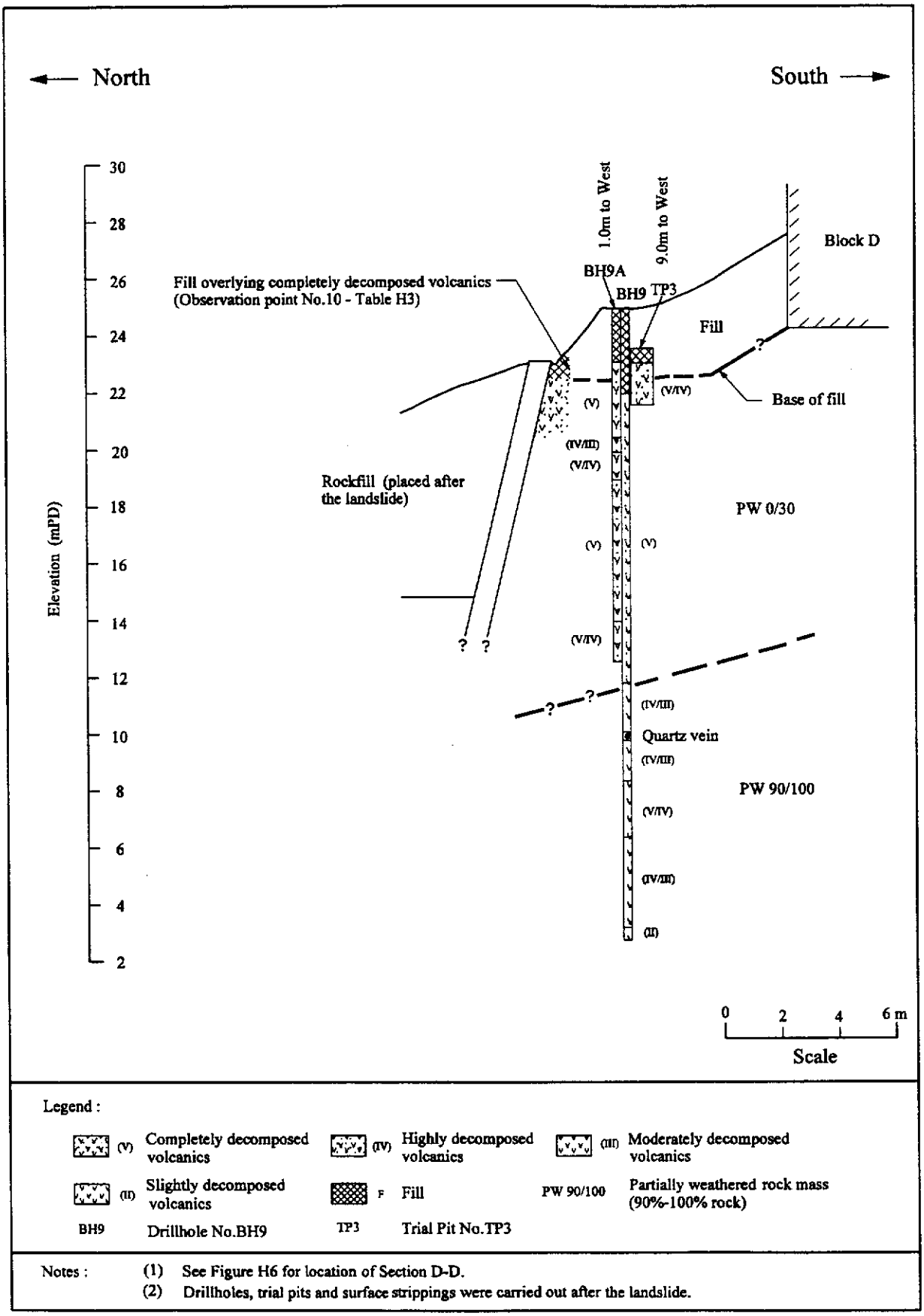

Figure H13 - Section D-D Showing the Geological Profile behind the Remaining Masonry wall

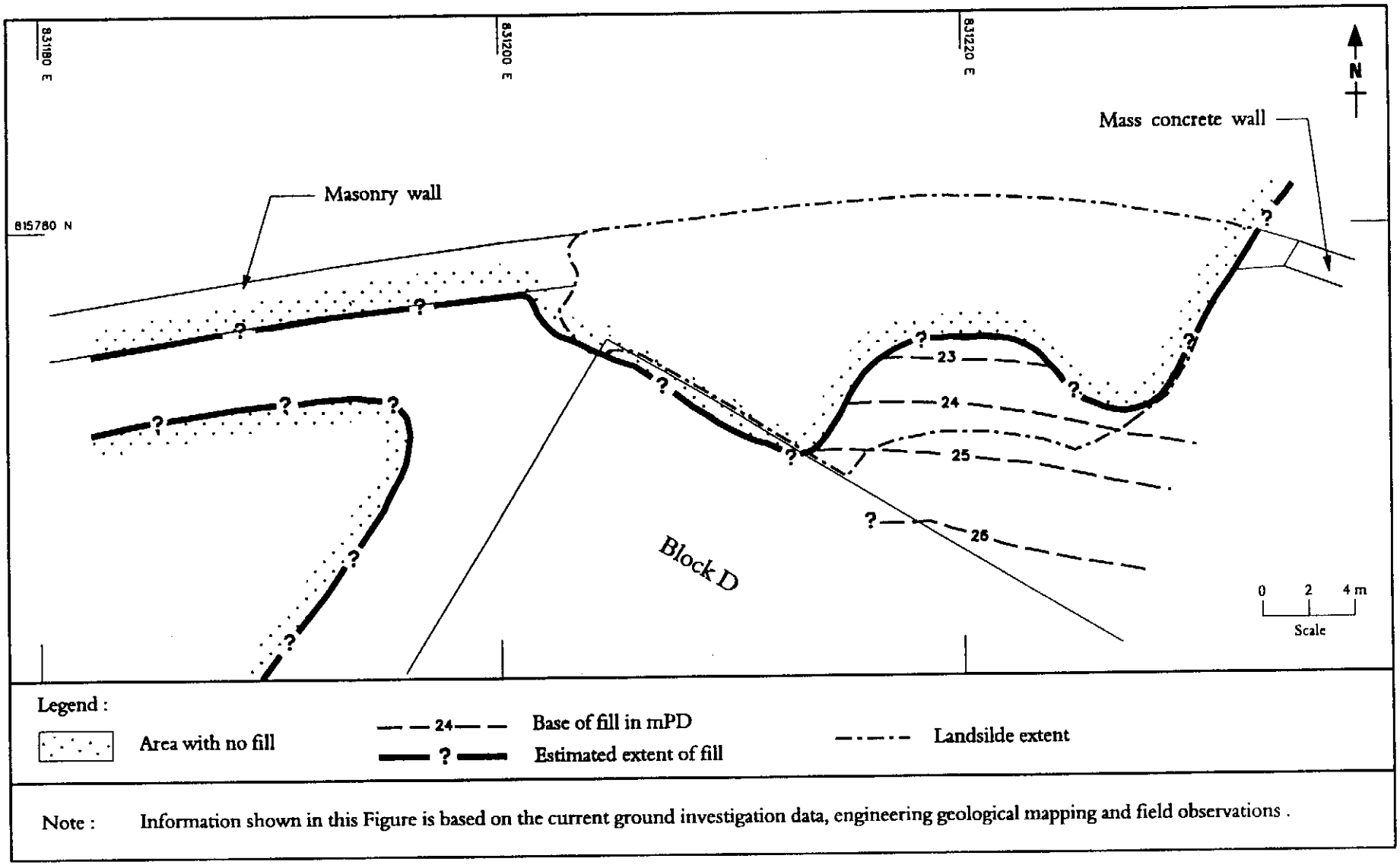

Figure H14 - Plan Showing Contours of the Base of the Fill at the Site after the Landslide

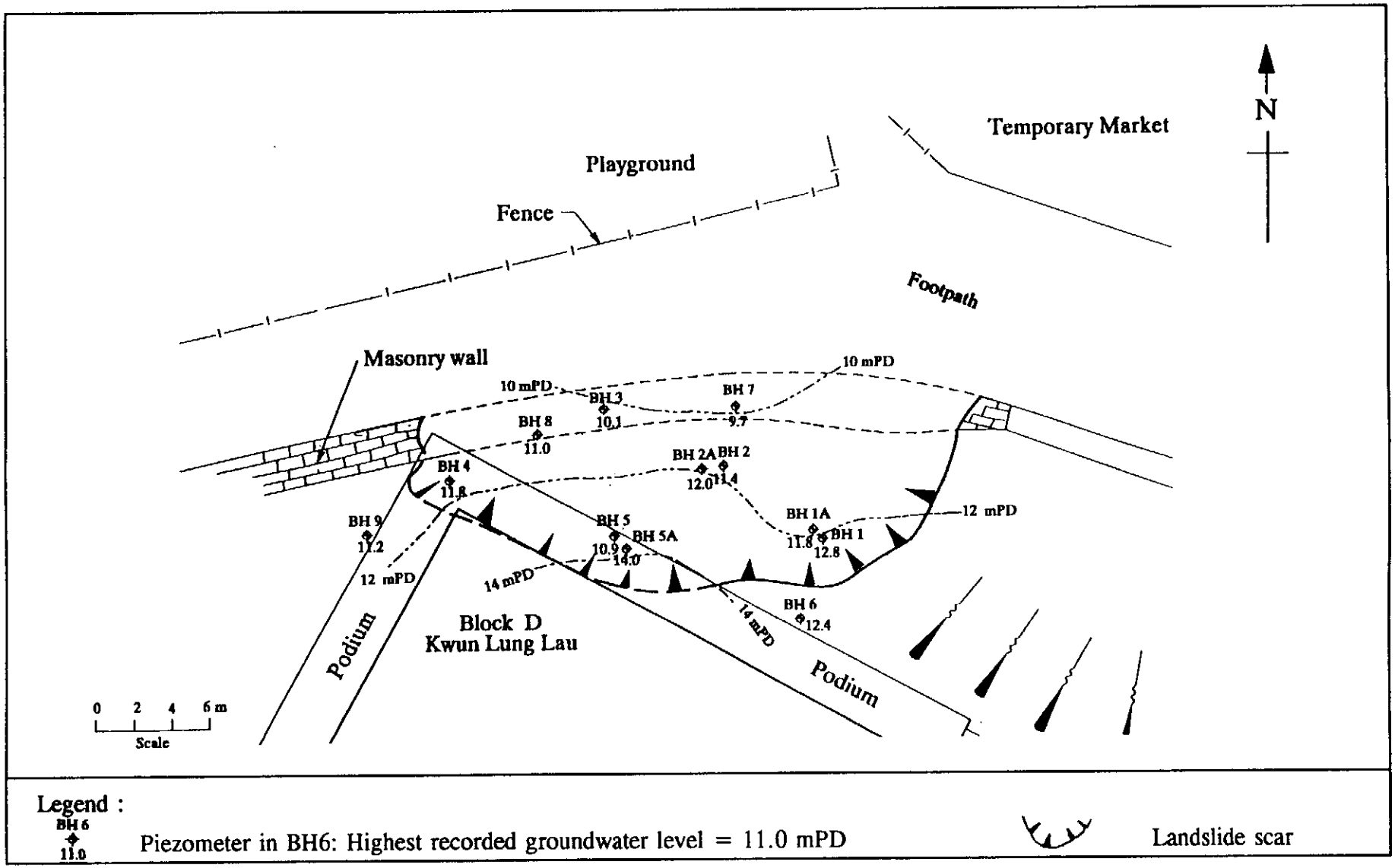

Figure H15 - Contours of the Highest Recorded Groundwater Levels (13 August 1994 to 1 September 1994)

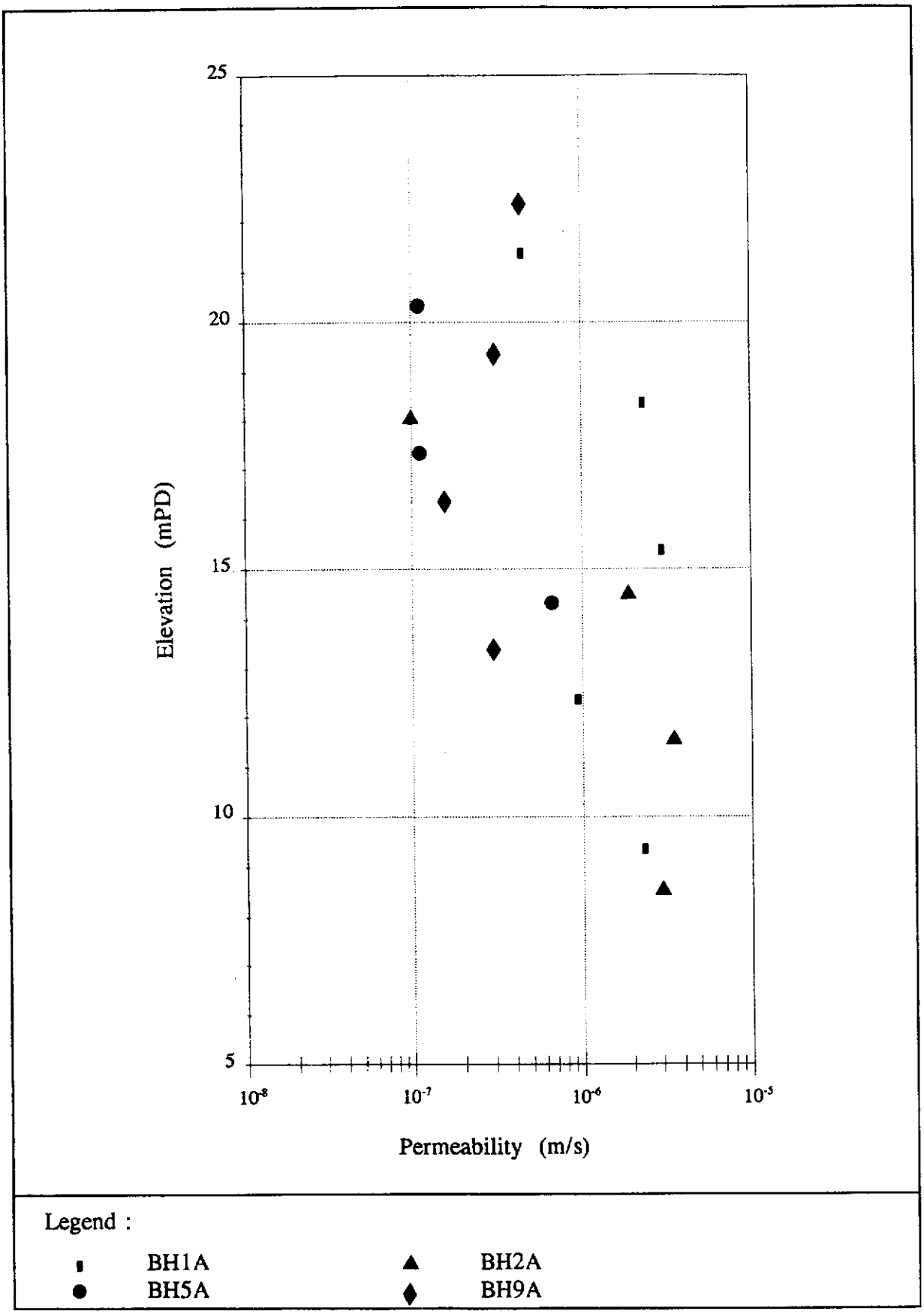

Figure H16 - Results of Falling-head Permeability Tests in Drillholes

APPENDIX I

LABORATORY TESTING

CONTENTS

I.1 INTRODUCTION

After the landslide, a comprehensive series of laboratory tests were conducted on samples retrieved during the ground investigation undertaken at the landslide site. The tests carried out included classification and index tests, compaction tests, shear box tests, conventional triaxial compression tests, and special triaxial tests. These tests were aimed at determining the geotechnical properties of the materials at the landslide site. Point-load tests were also carried out on samples of mortar taken from between the masonry blocks recovered from the landslide debris. In addition, chemical analyses were undertaken on soil and water samples to help assess the likely sources of the water that existed in the ground behind the masonry wall.

The majority of the laboratory tests were carried out at the Public Works Central Laboratory (PWCL). For the special triaxial tests, dead-load tests were carried out at the PWCL, stress-path tests were conducted at the University of Hong Kong and at the Hong Kong University of Science & Technology, and tests on unsaturated samples were undertaken at Nanyang Technological University in Singapore. Chemical analyses were carried out jointly by the PWCL, the Hong Kong Government Laboratory and the Drainage Services Department.

A summary of the results of the laboratory tests, together with discussion on the findings, are given in this Appendix.

I.2 CLASSIFICATION AND INDEX TESTS

I.2.1 Method of Testing

A range of classification and index tests was carried out, including determination of particle size distribution, Atterberg limits, moisture content, degree of saturation and specific gravity.

The methods of testing generally followed the procedures recommended by Chen (1994).

I.2.2 Test Results

The results of the grading analyses, together with measurements of the Atterberg limits and specific gravity, are summarised in Table I1.

The fill is heterogeneous, with a fines (i.e. silt and clay) content varying from 19% to 63%, a sand content varying from 24% to 50% and a gravel content varying from 1% to 55% (Figure I1).

The completely decomposed volcanics (CDV) has a mean grading of 40% fines, 42% sand and 18% gravel, whilst the mean grading for the completely to highly decomposed volcanics (C/HDV) is 35% fines, 42% sand and 23% gravel. The CDV and C/HDV samples were obtained from the partially weathered volcanics (PWV) stratum.

The fill has a liquid limit varying from 27% to 47%, and a plastic limit varying from 16% to 25%. The CDV has a liquid limit varying from 29% to 40%, and a plastic limit generally between 19% and 29%. The C/HDV has a liquid limit varying from 31% to 38%, and a plastic limit varying from 22% to 27%. The water content of each specimen was generally less than the plastic limit.

The specific gravity of all the materials is reasonably consistent, with a value generally in the range of 2.63 to 2.66.

Apart from measurements of the water contents of isolated triaxial test specimens, continuous profiles of water content and degree of saturation were determined using samples from four drillholes (Table I2). The profiles are plotted in Figure I2. It can be seen that material throughout the upper 6 to 10 m (or about 7 to 11 m of the pre-failure profile) in Drillhole No. 5A was wetter and more saturated than the deeper material. The pattern of wetting, however, was more erratic and less clearly defined in Drillholes No. 2A & 10. Samples from Drillhole No. 3B, which was located further away from the foulwater sewer than Drillholes No. 2A, 5A and 10, had a degree of saturation that varied between about 75% and 85% at depths ranging from 10 m to 19 m.

I.3 COMPACTION TESTS

I.3.1 Method of Testing

Two standard Proctor compaction tests were carried out on fill samples in accordance with the procedures recommended by Chen (1994).

I.3.2 Test Results

The results of the tests are shown in Figures I3 & I4 in terms of dry density versus moisture content. Also shown in the figures are the corresponding particle size distribution curves of the samples.

The maximum dry densities of the two fill samples were 1.78 Mg/m^3 and 1.89 Mg/m^3 respectively, with the corresponding optimum moisture content being 16% and 13%. The insitu dry densities of the fill were determined from sand replacement tests and ranged from 1.42 Mg/m^3 to 1.70 Mg/m^3. The average insitu dry density was about 1.57 Mg/m^3, which corresponds to about 85% of the maximum dry density, suggesting that the fill is generally loose. The scatter in the results indicates that the fill at the landslide site was variable and locally could be in a very loose state.

I.4 SHEAR BOX TESTS

I.4.1 Method of Testing

The method of shear box testing was based on that recommended by Head (1986). Tests were carried out only on compacted fill material. The specimens were compacted in

three layers into a 100 mm x 100 mm x 40.5 mm deep shear box at a range of dry densities varying between 1.285 and 1.70 Mg/m^3. The specimens were soaked in water for 24 hours under a vertical stress of approximately 1.4 kPa, which corresponded to that resulting from the weight of the top plate.

After compaction, each specimen was consolidated under the specified vertical stress, which ranged from 15 kPa to 60 kPa. When there was no further vertical displacement, the shearing stage was commenced. Each specimen was sheared at a rate of 0.08 mm/min until the horizontal displacement reached about 15 mm, which was the limit of travel of the shear box apparatus.

A total of 12 single-stage tests were carried out. Shear failure was considered to occur at the point of peak shear stress.

I.4.2 Test Results

The test results are summarised in Table I3. The typical behaviour of the fill material during shearing is shown in Figure I5.

It was possible to prepare three of the test specimens at a very loose state, with a dry density down to 1.285 Mg/m^3. However, the dry density of these specimens increased to 1.45 Mg/m^3 upon soaking and further to 1.780 Mg/m^3 upon consolidation (Table I3). This indicates that the fill material at such low densities was prone to collapse upon wetting.

The test results are summarised in Figure I6 in terms of shear stress versus normal effective stress. A least-squares fit through the results gives shear strength parameters of $c' = 1.3$ kPa and $\phi' = 35.7°$.

I.5 CONVENTIONAL TRIAXIAL TESTS

I.5.1 Method of Testing

Consolidated undrained triaxial compression tests with pore water pressure measurement were carried out on 74 mm diameter specimens prepared from either Mazier samples or block samples. The specimens were saturated under an effective confining stress of 5 kPa by elevating the back pressure. Saturation was deemed to have been completed when the value of pore pressure parameter B (Skempton, 1954) was equal to or greater than 0.97. The specimens were then consolidated isotropically at the specified effective stresses and subsequently sheared at the same confining pressure at a constant rate of 0.03 mm/min to an axial strain of about 15%.

Tests were carried on undisturbed CDV and C/HDV specimens, together with fill samples which had been recompacted to a range of dry densities. Both single-stage and multi-stage tests were conducted.

The recompacted fill specimens were prepared at dry densities ranging from 1.30 to 1.70 Mg/m^3. However, it should be noted that the very loose specimens experienced

significant collapse upon saturation and further densification took place during the consolidation stage. As a result, the minimum dry density of the specimen prior to shearing was 1.68 Mg/m^3 (Table I4).

Shear failure was considered to occur at the point of maximum stress obliquity, i.e. maximum stress ratio, σ_1'/σ_3', where σ_1' and σ_3' are the major and minor principal effective stresses respectively.

I.5.2 Test Results

The test results are summarised in Tables I4 to I6. The typical behaviour of CDV and C/HDV during shearing is shown in Figure I7. An example of a typical effective stress path is shown in Figure I8.

It should be noted that two of the C/HDV specimens were not included in the analysis because of their apparently unusual behaviour. An example of the shear behaviour of a specimen for which the results have been excluded from the analyses is shown in Figure I9. It can be seen that the initial stress-strain behaviour was very stiff, and the stress state of the sample reached an atypically high stress ratio before brittle failure. Such material characteristics may reflect the influence of large inclusions or bonding. The test procedure adopted and the stress paths involved in conventional undrained triaxial compression tests are such that the strength parameters of the more weathered material can reasonably be obtained. However, the effect of any remnant bonding, which may give rise to increased peak strength and stiffness with a brittle response upon failure, may not be fully recovered because of possible disturbance during sampling and specimen preparation.

It may be noted from Tables I5 & I6 that practically all the specimens of CDV and C/HDV dilated during shearing. This is reflected by the values of the pore pressure parameter at failure, A_f (Skempton, 1954), which ranged generally from zero to 0.3. On the other hand, all the recompacted fill specimens compressed upon shearing, with A_f values ranging from 0.82 to 1.86 (Table I4).

The CDV and C/HDV specimens failed at an axial strain of about 2% to 3.5%, whereas the fill specimens generally failed at an axial strain of between 5% and 15%.

The test results for the weathered volcanics and fill are shown in Figure I10 & Figure I11 respectively in terms of $q' = \frac{1}{2}(\sigma_1'-\sigma_3')$ versus $p' = \frac{1}{2}(\sigma_1'+\sigma_3')$, i.e. half the deviator stress versus mean effective stress. In view of the small depth of the landslide failure surface, only the results with a mean effective stress level of less than or equal to 200 kPa at failure for CDV and C/HDV were considered. Also, it is noted that the test results on CDV and C/HDV are comparable and the ranges of dry densities are broadly similar (Tables I5 & I6). Therefore, it is considered that the two types of material may be taken to have common shear strength parameters for the present purposes.

Least-squares fit lines through the test results summarised in Figures I10 & I11 give the shear strength parameters of $c' = 1.7$ kPa and $\phi' = 32°$ for the fill, and $c' = 2$ kPa and $\phi' = 38.5°$ for the CDV & C/HDV.

Taking into account the results of the shear box and triaxial test results, and assuming the c' of fill is zero, the ϕ' of fill may be taken as 35°.

I.6 SPECIAL TRIAXIAL TESTS

I.6.1 Method of Testing

Three sets of special triaxial tests were conducted on specimens of CDV and one specimen of HDV. These tests were :

(a) dead-load tests,

(b) stress-path tests, and

(c) unsaturated tests.

Dead-load triaxial tests undertaken in the PWCL were generally based on the method used by Bishop & Henkel (1962). In this series of tests, each specimen was saturated by means of back pressure, followed by anisotropic consolidation to specified stresses. Shearing of the specimen involved an increase of the pore pressure by controlled injection of water at such a rate that the difference in pore pressures across the specimen did not exceed 1 kPa. The increase in pore pressure resulted in a reduction in the mean effective stress, whilst the shear stress remained constant up to the point of failure.

Similar tests were carried out in hydraulic stress-path cells at the University of Hong Kong and at the Hong Kong University of Science & Technology. The stress paths followed were similar to those in the PWCL tests, the difference being in the methods of controlling the pore pressures and stresses. For instance, in the case of the University of Hong Kong tests, the pore pressure was increased at a constant rate of 2 kPa/hour.

The unsaturated triaxial tests were in accordance with the procedures given by Fredlund & Rahardjo (1993). The test involved consolidation of the specimen isotropically under a constant net confining pressure and matric suction. The pore air pressure was controlled by a low air-entry disk at the top of the specimen, whilst the pore water pressure was controlled through a high air-entry disk at the bottom of the specimen. After reaching equilibrium, the specimen was sheared by increasing the deviator stress (σ_1' - σ_3') under drained conditions at a rate of 0.0009 mm/min. The net confining pressure and the matric suction were maintained constant during shearing. Multi-stage tests were carried out at different combinations of net confining pressure and matric suction.

I.6.2 Test Results

I.6.2.1 Dead-load Tests and Stress-path Tests

Typical results of dead-load tests and stress-path tests are shown in Figure I12 & Figure I13 respectively. The results of the tests, that involved a stress path corresponding to the reduction of the mean effective stress at constant shear stress, are summarised in

Figure I14 in terms of $\frac{1}{2}(\sigma_1'-\sigma_3')$ and $\frac{1}{2}(\sigma_1'+\sigma_3')$. Superimposed on Figure I14 is the mean line through the results of the conventional triaxial compression tests discussed in Section I5.2.

The results indicate that the stress-strain relationship obtained from such a stress path, which is considered to best simulate the process of gradual increase in pore pressure in a slope due to water infiltration, exhibits a stiffer and more brittle behaviour than that obtained from conventional triaxial compression tests. The specimens generally failed at an axial strain of 0.5% to 1%. The strength envelope given by the dead-load and stress-path tests is generally slightly higher than that determined in conventional triaxial compression tests, and the post-peak strength is comparable.

I.6.2.2 Unsaturated Tests

Typical results of the tests on unsaturated CDV specimens are shown in Figure I15.

Fredlund & Rahardjo (1993) suggested that the shear strength of an unsaturated soil can be expressed as follows :

$$\tau_f = c' + (\sigma_f - u_a)_f \tan \phi' + (u_a - u_w)_f \tan \phi^b$$

where τ_f = shear stress on the failure plane at failure

c' = apparent cohesion in terms of effective stress

$(\sigma_f - u_a)_f$ = net confining pressure on the failure plane at failure

σ_f = total normal stress on the failure plane at failure

u_a = pore air pressure

ϕ' = angle of shearing resistance associated with the net normal stress state variable $(\sigma_f - u_a)_f$

$(u_a - u_w)_f$ = matric suction at failure

u_w = pore water pressure

ϕ^b = angle indicating the rate of change in shear strength relative to changes in matric suction

The results of the tests show that ϕ^b varies with matric suction, as follows :

Matric Suction, $u_a - u_w$ (kPa)	ϕ^b (degrees)
0 - 25	39
25 - 50	31
50 - 100	22

I.7 POINT-LOAD TESTS

I.7.1 Method of Testing

Point-load tests were carried out on mortar samples taken from between the masonry blocks recovered from the landslide debris. The tests were based on the procedure recommended by ISRM (1985).

The tests were conducted on samples in their natural state, and on samples soaked in water for seven days.

I.7.2 Test Results

The test results are summarised in Table I7. There is some scatter in the results, with the point load indices varying between 0.08 MPa and 0.26 MPa for samples in their natural state, with a mean of 0.18 MPa. The corresponding indices for samples soaked in water for seven days varied between 0.07 MPa and 0.48 MPa, with a mean of 0.22 MPa.

The results show that there is no reduction in the mortar strength upon soaking.

I.8 CHEMICAL TESTS

I.8.1 Method of Testing

Chemical analyses of both soil and water samples were carried out. For the soil samples, the analyses comprised the determination of organic matter content (BSI, 1990).

Water samples were either taken directly from the landslide site or prepared by squeezing the soil samples with the use of an oedometer. For the water samples, the analyses included determination of chloride, ammoniacal nitrogen, nitrate and nitrite, as well as chemical oxygen demand (COD) and total organic carbon (TOC). Chloride, TOC, ammoniacal nitrogen, nitrate and nitrite were determined in accordance with the procedure of the American Public Health Association (1992), and COD was determined in accordance with the procedure of the American Society for Testing and Materials (1993).

I.8.2 Test Results

The results of the analyses of soil and water samples are shown in Tables I8 to I10.

The purpose of organic matter analyses was to assess if the black-stained soil in close vicinity of the foulwater sewer was affected by leakage of foulwater. Samples H, I & J provided a control in that these samples were not affected by foulwater, and the corresponding organic content was low, being in the range of 0.1 to 0.3 % by mass. The sample of deposit recovered from the inside surface of the foulwater sewer had a organic matter content of 21.6%, whilst samples of black-stained soil recovered from the outside surface of the foulwater sewer or from manholes with signs of leakage had an organic matter

content of between 2.9% and 4.5%. It can therefore be concluded that the black-stained soil taken from the outside of the foulwater sewer or from manholes were likely to have been affected by leakage from the foulwater sewer.

Salt water is used for toilet flushing at Kwun Lung Lau. Accordingly, the results of the water sample analyses in terms of chloride content can be used with reasonable confidence to help delineate the source of the water. Thus, where the ground mass had been subjected to seepage flow arising from leakage of the foulwater sewer, the chloride content could be expected to be higher than that if the source of the water were stormwater or groundwater. Although the process of the aqueous flow of chemicals through an unsaturated soil involving sorption and filtering phenomena is highly complex, the results of the chemical analyses nevertheless indicate a reasonable pattern of chloride content which is consistent with the position of the foulwater sewer.

Sample W9 (rainwater) and samples F1A15, F3A17 & TP37AH4 (water squeezed from soil samples taken underneath Block D that are away from the influence of the defective foulwater sewer) provided a control on the chloride content. This varied between 36 mg/litre and 146 mg/litre in the control samples. Samples of the foam used for advancing the drillholes were also tested, and the results confirmed that the chloride content of the soil would not have been affected by the foam.

Drillholes No. 1A & 2A were in close proximity to the foulwater sewer that became severed during the landslide. Samples from these drillholes showed a chloride content much higher than that of the control samples (generally by about two orders of magnitude) down to a depth of about 11 m. Drillhole No. 7, which is more than 5 m away from the reconstructed alignment of the foulwater sewer on its downslope side, also exhibited high chloride content down to about 11 m. Overall, the test results suggest that the source of the water was foulwater from the sewer.

After the landslide, foulwater was discharged from the severed sewer onto the landslide scar until about 6 p.m. on 24 July 1994. However, the point of discharge was near the northwest corner of Block D and was far away from the locations of the drillholes. The high chloride content measured therefore cannot be due to the discharge of foulwater subsequent to the landslide.

Reference to the results of the analyses of samples retrieved from depths of 1.8 m and 3.25 m in Drillhole No. 5A shows that the chloride contents of 75 mg/litre to 150 mg/litre are comparable to those of the control samples. These results are consistent with the fact that the samples were located above the position of the foulwater sewer. Furthermore, the moisture contents reported in Table I2 indicate that samples down to 3.75 m in Drillhole No. 5A were much wetter than those at greater depths. This is evidence that there was a source of 'fresh' water in addition to the foulwater sewer that was responsible for wetting the soil.

I.9 REFERENCES

American Public Health Association (1992). Standard Methods for the Examination of Water and Wastewater. (18th edition). Section 4 : Inorganic non-metallic constituents. American Public Health Association, 135 p.

American Society for Testing and Materials (1993). Standard Test Methods for Chemical Oxygen Demand (Dichromate Oxygen Demand) of Water. ASTM Test Designation : D1252-88 Test Method A, American Society for Testing and Materials, pp 68-71.

Bishop, A.W. & Henkel, D.J. (1962). The Measurement of Soil Properties in the Triaxial Test. (Second edition). Edward Arnold, London, 227 p.

BSI (1990). Methods of Test for Soils for Civil Engineering Purposes. (BS1377 : 1990). Part 3 : Chemical and Electro-chemical Tests. British Standards Institution, London, 44 p.

Chen, P.Y.M. (1994). Methods of Test for Soils in Hong Kong for Civil Engineering Purposes (Phase 1 Tests). Geotechnical Engineering Office, Hong Kong, 91 p. (GEO Report No. 36).

Fredlund, D.G. & Rahardjo, H. (1993). Soil Mechanics for Unsaturated Soils. John Wiley & Sons, New York, 517 p.

Head, K.H. (1986). Manual of Soil Laboratory Testing. Volume 2 : Permeability, Shear Strength and Compressibility Tests. Halsted Press, New York, 413 p.

ISRM (1985). Suggested method for determining point load strength. International Journal of Rock Mechanics and Mining Sciences & Geomechanics Abstracts, vol. 22, no. 2, pp 51-60.

Skempton, A.W. (1954). The pore pressure coefficients A and B. Géotechnique, vol. 4, pp 143-147.

LIST OF TABLES

Table I1 - Summary of Classification and Index Test Results (Sheet 1 of 4)

Material Type	Sample Location	Depth (m)	Sample Type	Particle Size Distribution				LL (%)	PL (%)	PI (%)	Moisture Content (%)	Specific Gravity	Remarks
				Gravel (%)	Sand (%)	Silt (%)	Clay (%)						
Fill	TP1	2.8	Bulk	18	32	25	25	47	22	25		2.63	
Fill	BH6	1.3 - 2.3	Mazier	23	29	31	17	39	19	20	16.7 (1.47 m - 2.29 m)		*
Fill	TP4	0.73 - 1.03	Bulk	1	42	57		32	25	7			
Fill	TP9	0 - 1.5	Bulk	20	34	46		29	16	13			
Fill	RM1/V		Remoulded	20	34	46							
Fill	RM1/X		Remoulded	7	38	30	25						
Fill	RM1/W		Remoulded	8	37	31	24						
Fill	RM1/AD		Remoulded	9	44	36	21	30	16	14			
Fill	RM1/AE		Remoulded	6	35	38	21						
Fill	TP11	0.5	Bulk	27	37	36		27	21	6			
Fill	TP37	0.5	Bulk	36	30	34					11.2		
Fill	TP12	0.5	Bulk	22	26	52		35	19	16	22.6		
Fill	BH12	0 - 0.5	Bulk	55	26	19					9.7		
Fill	TP8	1 - 1.13	Bulk	39	24	37					16.7		
Fill	Underneath Block D	0.5	Bulk	6	35	59							*
Fill	Underneath Block D	1.0	Bulk	27	29	44							*
Fill	Underneath Block D	Near ground surface	Bulk	32	31	37							*
Fill	Underneath Block D	1.2	Bulk	50	28	22							*
Fill	Underneath Block D	0.8	Bulk	18	29	53							*
Fill	Underneath Block D	0.8	Bulk	37	30	33							*

Table I1 - Summary of Classification and Index Test Results (Sheet 2 of 4)

Material Type	Sample Location	Depth (m)	Sample Type	Particle Size Distribution				LL (%)	PL (%)	PI (%)	Moisture Content (%)	Specific Gravity	Remarks
				Gravel (%)	Sand (%)	Silt (%)	Clay (%)						
Fill	Underneath Block D	Near ground surface	Bulk	24	36	40							*
Fill	Underneath Block D	1.4	Bulk	35	30	35							*
Fill	Underneath Block D	0.5	Bulk	26	50	24							
Fill	Underneath Block D		Bulk	2	37	51	10						
Fill	Underneath Block D		Bulk	2	35	53	10						
CDV	TP2	2.6	Bulk	46	27	22	6	28	22	6		2.65	
CDV	TP3	1.6	Bulk	48	23	20	9	40	26	14		2.68	
CDV	TP6	1 - 1.3	Block	9	46	37	8	36	NP	NP	23.0	2.65	*
CDV	TP7	1.5	Bulk	41	25	34							
CDV	TP8	2.5 - 2.95	U100	5	42	45	8	29	19	10	24.3		*
CDV	BH1	1.5 - 2.5	Mazier	14	52	24	10	37	25	12	22.8 (1.88 m - 2.08 m) 24.4 (2.28 m - 2.48 m)	2.64	
CDV	BH1	3.5 - 4.5	Mazier	30	42	23	5	39	29	10	19.1 (3.70 m - 3.90 m) 22.3 (4.1 m - 4.3 m) 21.3 (4.3 m - 4.5 m)	2.65	
CDV	BH1	4.5 - 5.5	Mazier	16	48	30	6	35	25	10	24.6 (5.09 m - 5.29 m) 26.9 (5.29 m - 5.49 m)	2.64	
CDV	BH1	5.5 - 6.5	Mazier	20	34	41	5	35	25	10	14.7 (5.69 m - 5.89 m) 25.1 (5.89 m - 6.09 m) 24.2 (6.09 m - 6.29 m) 21.2 (6.29 m - 6.49 m)	2.65	
CDV	BH1	6.5 - 7.5	Mazier	33	28	37	2	36	27	9	19.8 (6.76 m - 6.96 m)	2.62	

Table I1 - Summary of Classification and Index Test Results (Sheet 3 of 4)

Material Type	Sample Location	Depth (m)	Sample Type	Particle Size Distribution				LL (%)	PL (%)	PI (%)	Moisture Content (%)	Specific Gravity	Remarks
				Gravel (%)	Sand (%)	Silt (%)	Clay (%)						
CDV	BH3	8 - 9	Mazier	4	45	42	10	33	22	11			
CDV	BH3	10 - 11	Mazier	12	47	36	5	32	20	12	17.5 (10.19 m - 10.39 m) 16.9 (10.39 m - 10.59 m) 15.0 (10.79 m - 10.99 m)	2.66	
CDV	BH7	10 - 11	Mazier	11	70	17	2	32	NP	NP	18.2 (10.18 m - 10.38 m) 19.2 (10.38 m - 10.58 m) 18.1 (10.58 m - 10.98 m)	2.63	*
CDV	BH8	9.5 - 10.5	Mazier	5 1	47 43	43 48	5 8				26.2 (9.6 m - 9.88 m) 22.7 (9.88 m - 10.08 m) 23.7 (10.08 m - 10.28 m) 22.4 (10.28 m - 10.48 m)	2.63	*
CDV	BH8	11 - 12	Mazier	6 10	48 50	38 36	8 4				19.2 (11.19 m - 11.39 m) 16.9 (11.39 m - 11.59 m) 18.4 (11.59 m - 11.79 m) 19.8 (11.79 m - 11.99 m)		*
CDV	BH9	5.3 - 6.4	Mazier	24	37	29	10						
CDV	F2	(≈30 mPD)	Bulk	17	48	35					12.5		*
CDV	F5	1.4	Bulk	29	38	33					14.1		*
C/HDV	TP4	1.5	Bulk	13	39	41	7	34	25	9		2.65	
C/HDV	BH1	2.5 - 3.5	Mazier	24	51	20	6	38	27	11	19.7 (3.09 m - 3.29 m) 22.8 (3.29 m - 3.49 m)	2.62	
C/HDV	BH2	3.5 - 4.5	Mazier	30	46	18	6	37	25	12	22.9 (4.08 m - 4.28 m) 24.2 (4.28 m - 4.48 m)	2.63	
C/HDV	BH2	8.2 - 9.2	Mazier	20	55	22	3	31	22	9	12.9 (8.98 m - 9.18 m)	2.62	
C/HDV	BH3	11.5 - 12.5	Mazier	7	48	41	4	33	24	9	16.1 (11.77 m - 12.48 m)		*

Table I1 - Summary of Classification and Index Test Results (Sheet 4 of 4)

Material Type	Sample Location	Depth (m)	Sample Type	Particle Size Distribution				LL (%)	PL (%)	PI (%)	Moisture Content (%)	Specific Gravity	Remarks
				Gravel (%)	Sand (%)	Silt (%)	Clay (%)						
C/HDV	BH4	6.5 - 7.5	Mazier	48	32	18	2	33	22	11	10.4 (6.74 m - 7.49 m)		*
C/HDV	BH6	2.3 - 3.3	Mazier					36	23	13	24.2 (2.68 m - 2.88 m) 24.0 (2.88 m - 3.08 m)	2.65	*
C/HDV	BH7	7 - 8	Mazier	36	35	26	3	33	24	9			
C/HDV	BH7	11.5 - 12.5	Mazier	10	41	43	6				19.9 (11.51 m - 11.89 m) 18.1 (11.89 m - 12.09 m) 18.2 (12.09 m - 12.29 m) 15.6 (12.29 m - 12.49 m)	2.67	*
C/HDV	BH9	6.4 - 7.5	Mazier	10	32	50	8				17.6 (7.19 m - 7.39 m)	2.66	

Legend :

LL	Liquid Limite	CDV	Completely decomposed volcanics	*	Tests carried out by MateriaLab Limited
PL	Plastic Limit	HDV	Highly decomposed volcanics	BH6	Drillhole No. 6
PI	Plasticity Index	NP	Not plastic	TP11	Trial pit No. 11

Notes : (1) Samples of the RM1 series were mixed using the following sources : Trial pit No. TP7 (bulk samples at 0.5 m & 1 m, block sample at 0.5 m - 0.8 m)
Trial pit No. TP9 (bulk samples at 0.5 m, 1 m & 1.5 m)

(2) See Figure H6 for locations of drillholes and trial pits.

Table I2 - Profiles of Moisture Content and Degree of Saturation

Borehole No.	Depth (m)	Material Type	Sample Type	Moisture Content (%)	Dry Density (Mg/m^3)	Bulk Density (Mg/m^3)	Degree of Saturation (%)	Saturation Moisture Content (%)
BH2A	2.00 - 2.45	CDV	SPT liner	18.0	1.709	2.017	86.7	20.8
BH2A	3.00 - 3.45	CDV	SPT liner	17.2	1.758	2.060	89.8	19.2
BH2A	4.00 - 4.45	CDV	SPT liner	13.3	1.889	2.140	87.5	15.2
BH2A	5.00 - 5.45	CDV	SPT liner	15.0	1.831	2.106	88.9	16.9
BH5A	2.30 - 2.75	CDV	SPT liner	24.2	1.564	1.942	92.3	26.2
BH5A	3.30 - 3.75	CDV	SPT liner	24.1	1.600	1.985	97.2	24.8
BH5A	4.30 - 4.75	CDV	SPT liner	16.3	1.705	1.983	77.9	20.9
BH5A	5.30 - 5.75	CDV	SPT liner	22.8	1.657	2.035	100.8	22.6
BH5A	10.30 - 10.68	CDV	SPT liner	13.1	1.894	2.142	87.0	15.1
BH10	6.09 - 6.29	C/HDV	Mazier	22.7	1.573	1.930	87.9	25.8
BH10	6.29 - 6.49	C/HDV	Mazier	22.3	1.594	1.950	89.3	25.0
BH10	6.89 - 7.09	C/HDV	Mazier	19.8	1.678	2.010	90.6	21.9
BH10	7.09 - 7.29	C/HDV	Mazier	20.8	1.647	1.990	90.6	23.0
BH10	8.16 - 8.34	CDV	Mazier	21.0	1.570	1.900	80.9	25.9
BH10	9.26 - 9.44	CDV	Mazier	18.9	1.640	1.950	81.3	23.2
BH10	10.06 - 10.24	CDV	Mazier	19.3	1.685	2.010	89.3	21.6
BH10	11.16 - 11.34	CDV	Mazier	20.8	1.639	1.980	89.4	23.3
BH10	12.26 - 12.44	CDV	Mazier	23.9	1.525	1.890	85.9	27.8
BH10	13.36 - 13.54	CDV	Mazier	20.7	1.624	1.960	86.8	23.8
BH10	14.45 - 14.63	CDV	Mazier	21.9	1.608	1.960	89.5	24.5
BH10	15.14 - 15.32	C/HDV	Mazier	14.6	1.850	2.120	89.5	16.3
BH10	16.19 - 16.39	C/HDV	Mazier	15.1	1.833	2.110	89.8	16.8
BH10	16.39 - 16.59	C/HDV	Mazier	13.7	1.900	2.160	91.9	14.9
BH3B	10.06 - 10.24	C/HDV	Mazier	11.7	1.880	2.100	75.7	15.5
BH3B	11.01 - 11.19	C/HDV	Mazier	9.9	1.929	2.120	70.2	14.1
BH3B	12.46 - 12.64	C/HDV	Mazier	9.7	1.969	2.160	74.3	13.1
BH3B	13.71 - 13.89	C/HDV	Mazier	9.0	2.028	2.210	77.7	11.6
BH3B	15.24 - 15.44	CDV	Mazier	11.4	1.957	2.180	85.3	13.4
BH3B	16.86 - 17.04	CDV	Mazier	9.6	2.007	2.200	79.5	12.1
BH3B	17.15 - 17.34	CDV	Mazier	12.1	1.891	2.120	79.9	15.1
BH3B	18.71 - 18.89	C/HDV	Mazier	8.4	2.057	2.230	77.2	10.9

Note : Specific gravity of the soil is taken to be 2.65.

Table I3 - Summary of Shear Box Test Results for Recompacted Fill

Sample No.	Moisture Content before Soaking (%)	Degree of Saturation before Soaking (%)	Void Ratio before Soaking	Dry Density before Soaking (Mg/m^3)	Vertical Displacement upon Soaking (mm)	Dry Density after Soaking (Mg/m^3)	Vertical Stress (kPa)	Vertical Displacement upon Consolidation (mm)	Dry Density before Shearing (Mg/m^3)	Maximun Shear Stress (kPa)	Horizontal Displacement at Maximum Shear Stress (mm)	Vertical Displacement at Maximum Shear Stress (mm)	Vertical Strain at Maximum Shear Stress (%)
RM1/AG	16.7	41.9	1.054	1.285	4.600	1.450	25	6.564	1.774	19.9	14.73	0.938	2.32
RM1/AH	16.1	40.8	1.044	1.292	3.462	1.413	40	8.045	1.805	28.3	13.42	0.823	2.03
RM1/AI	16.1	40.8	1.043	1.292	3.717	1.423	60	8.600	1.857	44.9	9.01	0.681	1.68
RM1/AP	15.5	53.8	0.762	1.499	-0.028	1.498	15	2.921	1.614	12.0	14.84	1.994	4.92
RM1/AJ	15.9	54.6	0.766	1.493	-0.018	1.492	25	4.589	1.683	20.4	14.48	1.372	3.39
RM1/AQ	15.9	54.7	0.767	1.494	-0.011	1.493	32	4.184	1.665	23.6	14.49	1.551	3.83
RM1/AK	16.3	55.6	0.772	1.488	-0.030	1.486	40	2.092	1.567	29.7	14.31	1.578	3.90
RM1/AR	15.6	53.9	0.762	1.497	-0.064	1.495	50	4.588	1.686	38.6	14.55	1.375	3.40
RM1/AL	14.8	52.0	0.750	1.507	0.047	1.509	60	5.997	1.771	42.3	14.51	1.293	3.19
RM1/AM	15.4	73.6	0.554	1.700	0.067	1.703	25	0.892	1.741	18.6	14.80	0.809	2.00
RM1/AN	15.4	73.5	0.553	1.700	-0.049	1.698	40	0.675	1.727	30.3	13.31	0.783	1.93
RM1/AO	15.5	73.9	0.555	1.699	-0.012	1.698	60	1.301	1.755	45.8	12.84	1.112	2.75

Notes : (1) The size of the shear box was 100 mm x 100 mm x 40.5 mm.
(2) All samples were soaked under a pressure of about 1.4 kPa for 24 hours.
(3) The shearing rate was 0.08 mm/min.
(4) The samples were mixed using the following sources : Trial pit No.TP7 : 0.5 m, 1.0 m (bulk sample)
Trial pit No.TP7 : 0.5 m - 0.8 m (block sample)
Trial pit No.TP9 : 0.5 m, 1.0 m & 1.5 m (bulk sample)
(5) The typical range of grading of the remoulded fill is as follows : gravel (6 % - 20 %), sand (35 % - 44 %), silt + clay (46 % - 59 %)
(6) A negative vertical displacement denotes swelling or dilation.

Table I4 - Summary of Triaxial Test Results for Recompacted Fill

Sample No.	Material Type	Moisture Content before Testing (%)	Dry Density before Testing (Mg/m^3)	Dry Density after Saturation (Mg/m^3)	Dry Density after Consolidation (Mg/m^3)	Specific Gravity	Type of Test	Consolidation and Confining Pressure (kPa)	Maximum Stress Ratio (q'/p')	Axial Strain at Maximum Stress Ratio (%)	p' at Maximum Stress Ratio (kPa)	q' at Maximum Stress Ratio (kPa)	Pore Pressure Parameter A_f at Maximum Stress Ratio
RM1 P	Remoulded Fill	15.4	1.700	1.720	1.750	2.64	CUS	25	4.52	2.72	17.7	11.3	0.82
RM1 Q	Remoulded Fill	15.5	1.700	1.740	1.780	2.64	CUS	40	3.19	1.81	29.5	15.4	0.84
RM1 R	Remoulded Fill	15.3	1.700	1.730	1.800	2.64	CUS	60	3.74	11.06	41.5	24.0	0.89
RM1 S	Remoulded Fill	15.9	1.490	1.620	1.680	2.64	CUS	25	4.3	15.83	14.0	8.7	1.13
RM1 T	Remoulded Fill	15.9	1.490	1.650	1.710	2.64	CUS	40	4.16	10.84	21.2	13.0	1.22
RM1 U	Remoulded Fill	15.3	1.500	1.640	1.770	2.64	CUS	60	3.73	15.96	30.0	17.3	1.36
RM1 Z	Remoulded Fill	15.5	1.300	1.580	1.680	2.64	CUS	25	4.85	15.91	9.0	5.9	1.86
RM1 AA	Remoulded Fill	15.2	1.300	1.600	1.730	2.64	CUS	40	4.52	5.27	19.3	12.3	1.34
RM1 AB	Remoulded Fill	14.9	1.300	1.600	1.780	2.64	CUS	60	3.73	15.99	33.9	19.5	1.17

Legend :

q'	$\frac{1}{2}(\sigma_1' - \sigma_3')$	σ_1'	Major principal effective stress	CUS	Consolidated undrained test (single-stage)
p'	$\frac{1}{2}(\sigma_1' + \sigma_3')$	σ_3'	Minor principal effective stress	A_f	Ratio of pore pressure response to change of deviator stress

Notes : (1) Samples were mixed using the following sources : Trial pit No. TP7 : 0.5 m, 1.0 m (bulk sample)
Trial pit No. TP7 : 0.5 m - 0.8 m (block sample)
Trial pit No. TP9 : 0.5 m, 1.0 m & 1.5 m (bulk sample)

(2) The range of grading of the recompacted fill is as follows : gravel (6 % - 20 %), sand (35 % - 44 %), silt + clay (46 % - 59 %).

Table I5 - Summary of Triaxial Test Results for CDV (Sheet 1 of 2)

Sample Location	Depth (m)	Material Type	Moisture Content before Testing (%)	Dry Density before Testing (Mg/m^3)	Atterberg Limits		Specific Gravity	Particle Size Distribution				Type of Test	Consolidation and Confining Pressure (kPa)	Maximum Stress Ratio (q'/p')	Axial Strain at Maximum Stress Ratio (%)	p' at Maximum Stress Ratio (kPa)	q' at Maximum Stress Ratio (kPa)	Pore Pressure Parameter A_f at Maximum Stress Ratio
					PL (%)	LL (%)		Gravel (%)	Sand (%)	Silt (%)	Clay (%)							
BH1	3.29 - 3.49	CDV	22.8	1.440	27	38	2.63					CUM	50 100 150	4.24 4.17 3.91	2.68 5.38 8.64	128 204 291	79 125 172	0.01 0.07 0.09
BH1	4.1 - 4.3	CDV	20.8	1.440			2.65					CUS	60	4.65	3.42	93	60	0.22
BH1	5.29 - 5.49	CDV	26.4	1.470			2.64					CUS	90	4.03	2.21	147	88	0.18
BH1	5.89 - 6.09	CDV	23.5	1.430			2.65					CUS	50	3.94	3.64	59	35	0.37
BH1	6.09 - 6.29	CDV	22.8	1.500			2.65					CUS	100	4.31	3.44	153	95	0.22
BH1	6.29 - 6.49	CDV	21.3	1.590			2.65					CUS	150	4.74	3.00	233	152	0.23
BH1	6.76 - 6.96	CDV	16.6	1.570	27	36	2.62	33	28	37	2	CUS	150	4.08	6.11	141	85	0.55
BH2	4.28 - 4.48	CDV	23.5	1.520			2.63					CUM	50 100 150	5.39 4.5 4.35	2.50 5.03 7.22	101 163 231	70 104 145	0.13 0.20 0.22
BH3	10.19 - 10.39	CDV	15.8	1.690			2.66	12	47	36	5	CUS	50	4.86	3.92	110	73	0.09
BH3	10.39 - 10.59	CDV	17.1	1.720			2.66					CUM	50 100 150	5.72 5.32 4.95	2.87 5.38 7.43	130 247 354	91 169 235	0.06 0.06 0.07
BH7	10.18 - 10.38	CDV	17.3	1.580			2.63					CUS	70	3.62	4.03	88	50	0.32
BH7	10.38 - 10.58	CDV	17.8	1.570			2.63					CUM	50 100 150	5.08 4.62 4.35	5.28 9.18 12.27	105 224 351	70 144 220	0.11 0.07 0.04
BH7	11.89 - 12.09	CDV	17.2	1.690			2.67					CUS	50	5.71	2.81	137	96	0.05
BH8	9.88 - 10.08	CDV	24.3	1.620			2.63	1	43	48	8	CUS	40	4.44	2.63	67	42	0.18
BH8	10.08 - 10.28	CDV	24	1.570			2.63					CUS	70	4.26	4.01	144	89	0.09
BH8	10.28 - 10.48	CDV	22.9	1.590			2.63					CUM	50 100 150	3.74 3.49 3.31	1.76 3.95 5.48	77 151 214	44 84 115	0.20

Table I5 - Summary of Triaxial Test Results for CDV (Sheet 2 of 2)

Sample Location	Depth (m)	Material Type	Moisture Content before Testing (%)	Dry Density before Testing (Mg/m^3)	Atterberg Limits		Specific Gravity	Particle Size Distribution				Type of Test	Consolidation and Confining Pressure (kPa)	Maximum Stress Ratio (q'/p')	Axial Strain at Maximum Stress Ratio (%)	p' at Maximum Stress Ratio (kPa)	q' at Maximum Stress Ratio (kPa)	Pore Pressure Parameter A_f at Maximum Stress Ratio
					PL (%)	LL (%)		Gravel (%)	Sand (%)	Silt (%)	Clay (%)							
BH8	11.19 - 11.39	CDV	17.2	1.660			2.65	6	48	38	8	CUS	50	3.5	4.17	122	68	-0.03
BH8	11.39 - 11.59	CDV	17	1.740			2.65					CUS	150	3.86	3.05	218	128.3	0.24
BH8	11.79 - 11.99	CDV	19.2	1.670			2.65					CUS	100	3.77	2.03	138	80	0.26
BH9	5.69 - 5.89	CDV	16.2	1.750			2.66					CUS	40	5.13	2.00	85	57	0.11
BH9	5.89 - 6.09	CDV	13.2	1.780			2.66					CUS	70	4.69	2.76	127	82	0.16
BH9	6.09 - 6.29	CDV	15.3	1.770			2.66	24	37	39		CUM	50 100 150	5.63 5.15 4.73	2.10 4.49 6.69	173 287 400	121 194 260	0.02 0.02 0.02
BH9	6.99 - 7.19	CDV	18	1.680			2.66					CUS	50	4.59	2.42	109	70	0.08
BH9	7.19 - 7.39	CDV	16.9	1.750			2.66					CUS	150	5.05	3.18	316	212	0.11
TP8	2.7 - 3.0	CDV	24.3	1.320	19	29	2.64	5	42	45	8	CUS	40	3.7	4.89	54	31	0.28
BH10	6.29 - 6.49	CDV	22.3	1.590			2.63					CUM	30 60 90	5.79 4.83 4.61	1.95 5.02 7.50	93 185 257	66 122 165	0.02 -0.01 -0.01
BH10	7.09 - 7.29	CDV	20.8	1.640			2.64					CUM	50 80 110	4.48 4.04 3.88	2.21 4.02 5.50	105 165 219	67 100 129	0.09 0.07 0.08

Legend :

q' $\frac{1}{2}(\sigma_1' - \sigma_3')$ σ_1' Major principal effective stress PL Plastic Limit CUS Consolidated undrained test (single-stage)

p' $\frac{1}{2}(\sigma_1' + \sigma_3')$ σ_3' Minor principal effective stress LL Liquid Limit CUM Consolidated undrained test (multi-stage)

A_f Ratio of pore pressure response to change of deviator stress

CDV Completely decomposed volcanics

C/HDV Completely to highly decomposed volcanics

Note : All test specimens were prepared from Mazier samples except for that from trial pit No. TP8 which was prepared from a block sample.

Table I6 - Summary of Triaxial Test Results for C/HDV (Sheet 1 of 2)

Sample Location	Depth (m)	Material Type	Moisture Content before Testing (%)	Dry Density before Testing (Mg/m^3)	Atterberg Limits		Specific Gravity	Particle Size Distribution				Type of Test	Consolidation and Confining Pressure (kPa)	Maximum Stress Ratio (q'/p')	Axial Strain at Maximum Stress Ratio (%)	p' at Maximum Stress Ratio (kPa)	q' at Maximum Stress Ratio (kPa)	Pore Pressure Parameter A_f at Maximum Stress Ratio
					PL (%)	LL (%)		Gravel (%)	Sand (%)	Silt (%)	Clay (%)							
BH1	2.28-2.48	C/HDV	23	1.450			2.64					CUS	60	5.86	2.84	155	110	0.07
BH1	3.09-3.29*	C/HDV	19.7	1.580	27	38	2.62	24	51	20	6	CUS	30	30.2	0.91	80	75	0.17
BH1	4.295-4.495	C/HDV	21.2	1.520			2.65					CUS	90	4.65	3.34	150	97	0.19
BH1	5.09-5.29	C/HDV	23	1.480			2.64	16	48	30	6	CUS	60	4.61	2.03	107	69	0.16
BH2	4.08-4.28	C/HDV	20.8	1.540			2.63	30	46	18	6	CUS	70	4.49	2.09	103	66	0.25
BH2	8.98-9.18*	C/HDV	12.8	1.910			2.62	20	55	22	3	CUS	60	9.98	1.99	177	145	0.10
BH3	10.79-10.99	C/HDV	13.6	1.790			2.66					CUS	100	4.29	1.99	189	118	0.12
BH7	12.09-12.29	C/HDV	17.4	1.690								CUS	150	4.07	3.17	231	140	0.21
BH7	12.29-12.49	C/HDV	15.2	1.790			2.67					CUS	100	6.66	2.95	259	191	0.08
BH7	13.39-13.59	C/HDV	14.1	1.800			2.65					CUM	30 60 90	4.5 4.13 3.97	3.87 6.50 8.58	64 120 195	41 73 116	0.08 0.09 0.05
BH7	13.79-13.99	C/HDV	10.4	1.940			2.65					CUM	50 100 150	7.41 5.96 5.32	1.46 2.99 4.37	114 230 353	87 164 241	0.13 0.10 0.08
BH9	6.79-6.99	C/HDV	16.2	1.700			2.66					CUM	50 100 150	3.66 3.22 3.08	1.48 2.80 3.80	64 123 180	37 65 92	0.30 0.32 0.34
BH10	6.09-6.29	C/HDV	22.7	1.570			2.63					CUM	25 50 75	5.98 5.12 4.68	1.25 3.36 5.41	63 120 175	45 81 113	0.08 0.07 0.06
BH10	6.89-7.09	C/HDV	19.8	1.680			2.64					CUS	60	4.26	2.65	103	64	0.16
BH10	16.19-16.39	C/HDV	15.1	1.830			2.63					CUM	50 100 150	5.55 4.67 4.35	3.16 5.70 7.34	96 196 281	67 127 176	0.16 0.12 0.13

Table I6 - Summary of Triaxial Test Results for C/HDV (Sheet 2 of 2)

Sample Location	Depth (m)	Material Type	Moisture Content before Testing (%)	Dry Density before Testing (Mg/m^3)	Atterberg Limits		Specific Gravity	Particle Size Distribution				Type of Test	Consolidation and Confining Pressure (kPa)	Maximum Stress Ratio (q'/p')	Axial Strain at Maximum Stress Ratio (%)	p' at Maximum Stress Ratio (kPa)	q' at Maximum Stress Ratio (kPa)	Pore Pressure Parameter A_f at Maximum Stress Ratio
					PL (%)	LL (%)		Gravel (%)	Sand (%)	Silt (%)	Clay (%)							
BH10	16.39-16.59	C/HDV	13.7	1.900			2.63					CUM	30	6.28	2.13	106	77	0.01
													60	5.27	4.04	186	127	0.00
													90	5.13	5.69	265	179	0.01

Legend :

q'	$\frac{1}{2}(\sigma_1' - \sigma_3')$	σ_1'	Major principal effective stress	PL	Plastic Limit
p'	$\frac{1}{2}(\sigma_1' + \sigma_3')$	σ_3'	Minor principal effective stress	LL	Liquid Limit
*	Test results not included in the analysis.			A_f	Ratio of pore pressure response to change of deviator stress
CDV	Completely decomposed volcanics				
C/HDV	Completely to highly decomposed volcanics				

CUS Consolidated undrained test (single-stage)

CUM Consolidated undrained test (multi-stage)

Table I7 - Summary of Point-load Test Results for Mortar between Masonry Blocks

Specimen No.	Condition	Weight of Test Sample (g)	Size of Sample (mm)			Load at Failure, P (kN)	Equivalent Diameter, De (mm)	P/De^2 (MPa)	Correction Factor, F	Point Load Index, $I_s(50)$ (MPa)
			Width, W	Length, L	Thickness, t					
1	Natural	158.5	54	80	33	0.200	47.63	0.088	0.98	0.086
2	Natural	273.3	60	77	52	0.300	63.03	0.076	1.11	0.084
3	Natural	83.4	48	67	24	0.250	38.30	0.170	0.89	0.151
4	Natural	79.2	50	92	26	0.350	40.68	0.211	0.91	0.193
5	Natural	48.1	46	54	25	0.300	38.27	0.205	0.89	0.182
6	Natural	49.5	40	51	32	0.275	40.37	0.169	0.91	0.153
7	Soaked in water for 7 days	142.5	52	54	43	0.200	53.36	0.070	1.03	0.072
8	Soaked in water for 7 days	176.4	62	68	41	0.325	56.89	0.100	1.06	0.106
9	Soaked in water for 7 days	169.6	47	68	30	0.325	42.37	0.181	0.93	0.168
10	Soaked in water for 7 days	222.9	55	92	28	1.000	44.28	0.510	0.95	0.483
11	Soaked in water for 7 days	101.1	47	48	31	0.300	43.07	0.162	0.94	0.151
12	Soaked in water for 7 days	85.7	42	48	32	0.600	41.37	0.351	0.92	0.322
13	Natural	153.0	65	112	37	0.575	55.34	0.188	1.05	0.197
14	Natural	134.2	50	91	32	0.450	45.14	0.221	0.95	0.211
15	Natural	66.3	35	42	30	0.250	36.56	0.187	0.87	0.162
16	Natural	24.1	28	60	20	0.250	26.70	0.351	0.75	0.264
17	Natural	39.6	31	57	22	0.275	29.47	0.317	0.79	0.250
18	Soaked in water for 7 days	201.4	51	85	32	0.500	45.58	0.241	0.96	0.231
19	Soaked in water for 7 days	96.2	46	75	30	0.550	41.92	0.313	0.92	0.289
20	Soaked in water for 7 days	47.9	40	45	25	0.150	35.68	0.118	0.86	0.101
21	Soaked in water for 7 days	32.9	40	42	20	0.250	31.92	0.245	0.82	0.201
22	Soaked in water for 7 days	36.9	31	45	21	0.325	28.79	0.392	0.78	0.306

Notes :
(1) The largest dimension is designated as 'length', while the smallest dimension is designated as 'thickness'.
(2) De is given by the equation : $De^2 = 4Wt/\pi$.
(3) F is given by the equation : $F = (De/50)^{0.45}$.

Table I8 - Summary of Results of Chemical Analyses of Soil Samples

Item No.	Sampling Location	Remark	Organic Matter (% by mass)
A	Inside surface of a joint of the severed foulwater sewer	Soil/sediment (stained black)	21.6
B	Surface of the concrete bedding of a section of the severed foulwater sewer pipe	Soil (stained black)	4.5
C	Surface of the concrete base of a severed manhole No. 77a, immediately below the inlet of the foulwater sewer	Soil (stained black)	3.4
D	Surface of the concrete base of a severed manhole No. 77a, immediately below the inlet of the foulwater sewer	Soil (stained black)	3.7
E	Surface of the concrete base of a severed manhole No. 77a, immediately below the inlet of the foulwater sewer	Soil (stained black)	7.3
F	Surface of the concrete base of a severed manhole No. 77a, immediately below the inlet of the foulwater sewer	Soil (stained black)	2.9
G	TP11A at 1.5 m depth, immediately next to a joint of the foulwater sewer	Fill (no noticeable sign of sewage leakage and contamination)	0.1
H	Trial pit No. TP1 at 2.8 m depth	Fill	0.3
I	Trial pit No. TP2 at 2.6 m depth	Fill	0.2
Note: See Figure K2 for location of the severed manhole No. 77a			

Table I9 - Summary of Results of Chemical Analyses of Water Samples

Sample No.	Sampling Location	Sample Description	Chloride (mg/l)	Chemical Oxygen Demand (mg/l)	Total Organic Carbon (% by mass)	Ammoniacal Nitrogen (mg/l)	Nitrate (mg/l)	Nitrite (mg/l)
W1	Foulwater manhole No. 77	Foulwater	3800	90				
W2A	Foulwater manhole No. 77	Foulwater	3540	320		24	nil	nil
W2B			4260	330		35	nil	nil
W3	Foulwater manhole No. 38a	Foulwater	3890	450		35	0.11	0.01
W4	Foulwater manhole No. 38	Foulwater	3720	370		27	nil	nil
W5	Surface stripping No. SS3 (4.3 m from strip top)	Soil seepage	1400	48	27			
W6	Trial pit No. TP10	Soil seepage	1600	37	32			
W7	Foulwater manhole No. 38	Foulwater	7110	370	32	26	nil	0.01
W8A	Foulwater manhole No. 38a	Foulwater	6160	140	53	13	nil	nil
W8B			3950	190	67	28	0.02	nil
W9	Roof downpipe south of foulwater manhole No. 38a	Stormwater	36	<10	13	0.7	0.07	nil
W10A	Trial pit No. TP12	Water from trial pit flooded by seepage	3710	120	9	9.9	3.8	0.31
W10B			3730	110	9	11	3.1	0.16
W10C			3840	110	8	7.4	9.3	2.9
W11	Seepage near a joint of a foulwater sewer underneath Block D	Water from pipe leakage?	5620	130	17	34	5.4	3.1
W12	Seepage from masonry wall at Forbes Street		62	90	31	3.8	0.25	0.02
W13	In a trial pit underneath Block D, near foulwater manhole No. 75a		5580			0.7	16	7.8
W14	From an overflowing pipe from pump room at 1/F of Block F	Water for toilet flushing	18400			1.0	nil	0.01
F01		Foam used for borehole drilling	14			2.8	1.4	0.04
F02		Foulwater	18			0.4	0.2	0.03

Notes: (1) See Figure J1 for locations of foulwater manholes.
(2) See Figure H6 for locations of trial pit No. TP12 and surface stripping No. SS3

Table I10 - Summary of Results of Chemical Analyses of Water from Soil Samples

Sample No.	Sampling Location	Sample Description	Chloride (mg/l)	Ammoniacal Nitrogen (mg/l)	Nitrate (mg/l)	Nitrite (mg/l)
BH1AM6-7	Drillhole No. BH1A (0.5 m - 0.95 m)	Water squeezed out of SPT liner sample	240	3.3	0.5	0.02
BH1AM8	Drillhole No. BH1A (1 m - 1.45 m)	Ditto	840	2.4	0.3	0.03
BH1A (01)	Drillhole No. BH1A (2 m - 2.95 m)	Ditto	720	2.8	1.3	0.04
BH1A (02)	Drillhole No. BH1A (3 m - 3.45 m)	Ditto	880	1.9	1.4	1.4
BH1AM10-11	Drillhole No. BH1A (10 m - 11 m)	Ditto	1700	2.3	7.6	0.49
BH2AQ5-Q6	Drillhole No. BH2A (1.5 m - 2.25 m)	Ditto	1630	0.9	0.4	0.07
BH2AQ7-Q8	Drillhole No. BH2A (2.5 m - 3.45 m)	Ditto	3280	7.2	7.0	1.8
BH2AQ9	Drillhole No. BH2A (3.5 m - 4.45 m)	Ditto	4940	0.7	0.4	0.03
BH2AR1	Drillhole No. BH2A (4.5 m - 4.95 m)	Ditto	4770	4.0	0.5	0.09
BH2AR6	Drillhole No. BH2A (7.5 m - 7.95 m)	Ditto	4080	3.7	0.4	0.01
BH5AS8	Drillhole No. BH5A (1.8 m - 2.25 m)	Ditto	150	0.7	0.8	0.07
BH5AS0	Drillhole No. BH5A (2.8 m - 3.25 m)	Ditto	75	0.6	0.6	0.02
BH5AT2	Drillhole No. BH5A (3.8 m - 4.2 m)	Ditto	300	0.5	0.5	0.02
BH5AT5	Drillhole No. BH5A (5.3 m - 5.75 m)	Ditto	87	0.6	0.6	0.02
BH5AU5	Drillhole No. BH5A (10.3 m - 10.68 m)	Ditto	270	0.7	1.3	0.01
BH7Z9	Drillhole No. BH7 (8.0 m - 8.45 m)	Ditto	500	0.8	0.6	0.02
BH7Z0	Drillhole No. BH7 (9.5 m - 9.95 m)	Ditto	1040	1.0	5.6	0.44
BH7AA1	Drillhole No. BH7 (11.0 m - 11.45 m)	Ditto	250	1.0	0.9	0.01
BH12A14	Drillhole No. BH12 (0.5 m - 1 m)	Ditto	295	0.48	70	0.47
F1A15	Trial pit No. TP35 (0.5 m)	Ditto	62	0.49	5.9	0.10
F3A17	Trial pit No. TP36 (0.5 m)	Ditto	146	0.54	11	0.17
TP37AH4	Trial pit No. TP37 (1 m)	Ditto	46	0.46	2.1	0.01

Notes : (1) Samples No. F1A15, F3A17 & TP37AH4 were taken from fill material underneath Block D.
(2) See Figures K3 & K12 for locations of trial pits No. TP35 & TP36 respectively.
(3) Trial pit No. TP37 is in the yard area to the south of Block D.

LIST OF FIGURES

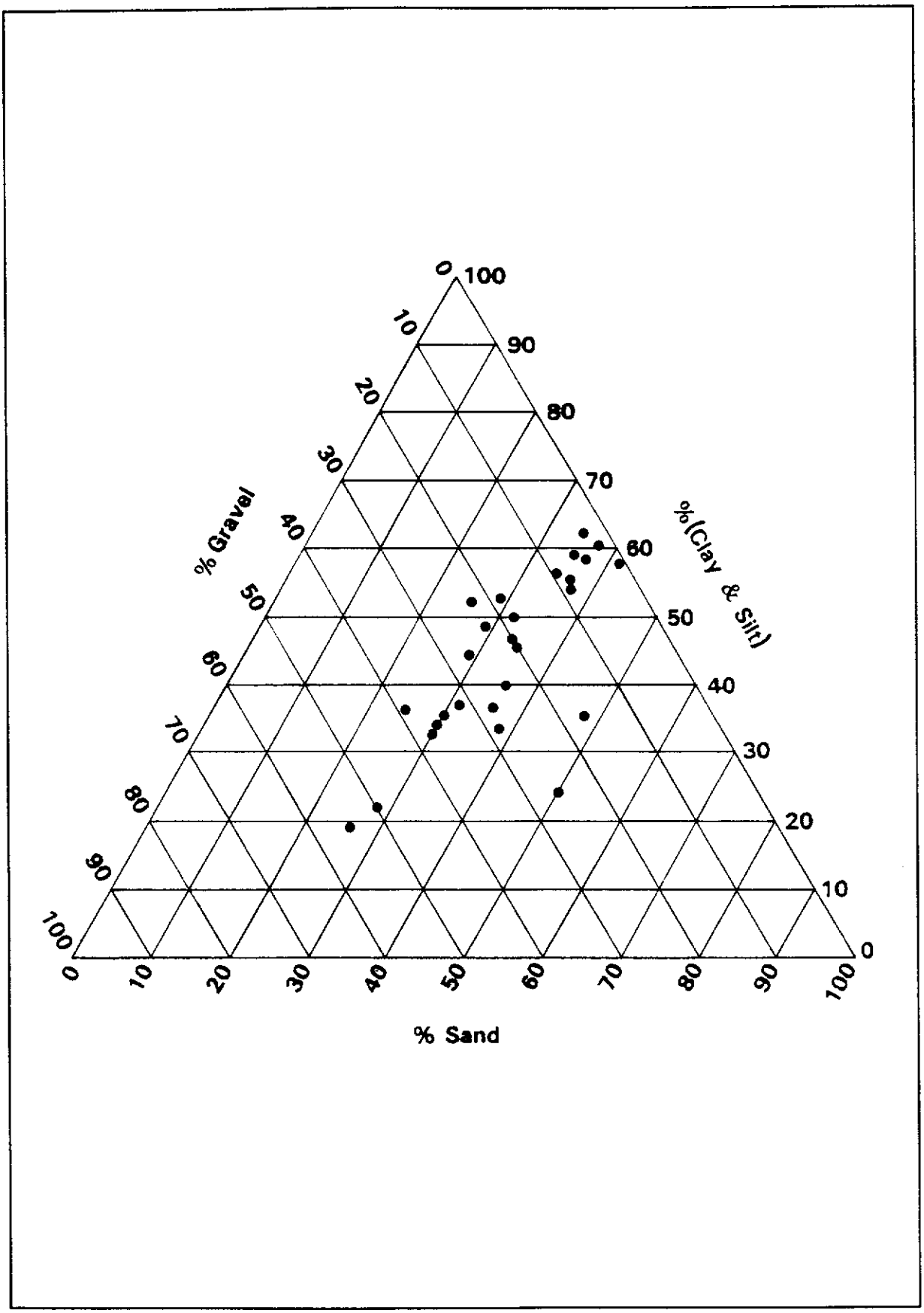

Figure I1 - Particle Size Distribution of the Fill

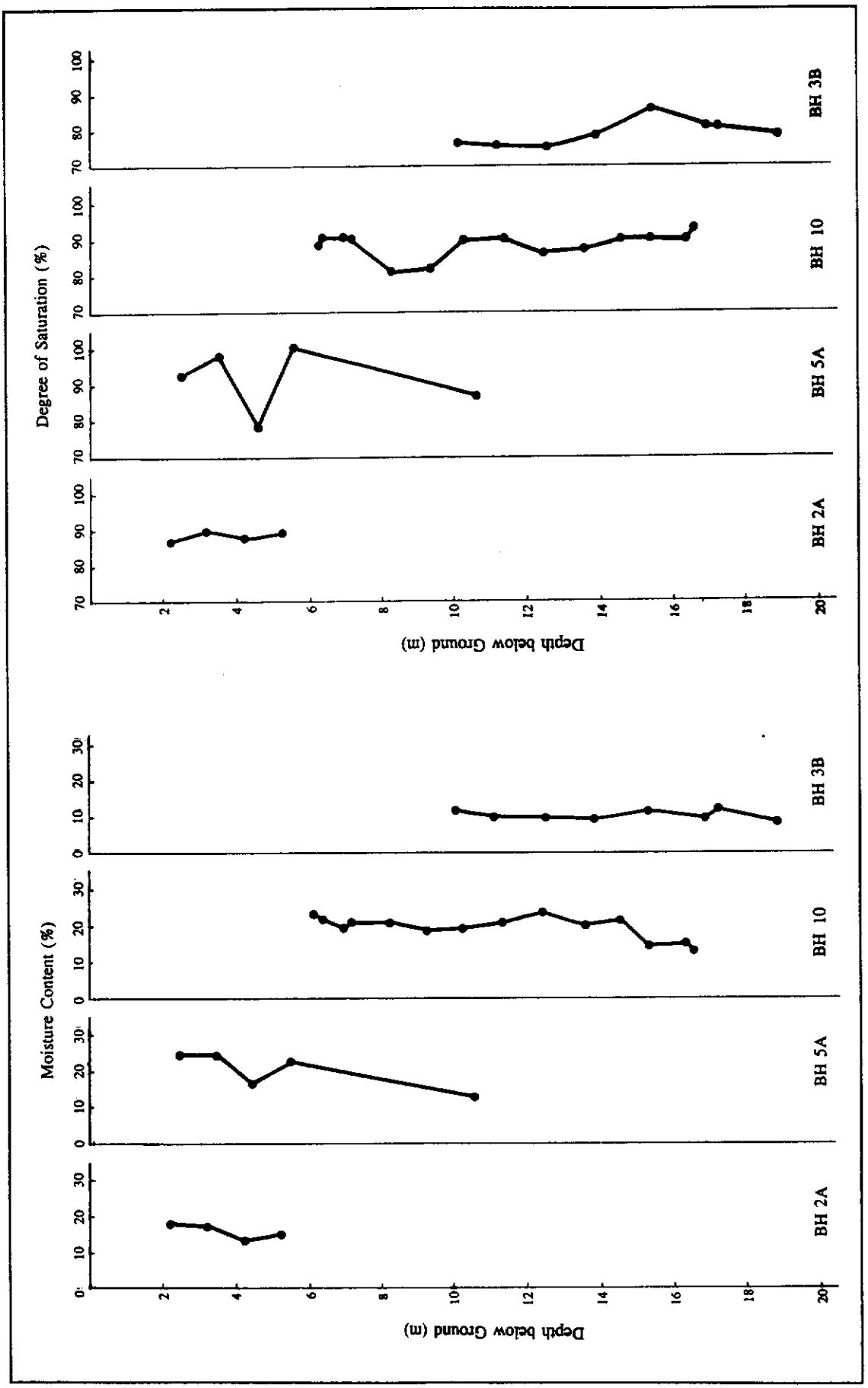

Figure I2 - Profiles of Moisture Content and Degree of Saturation

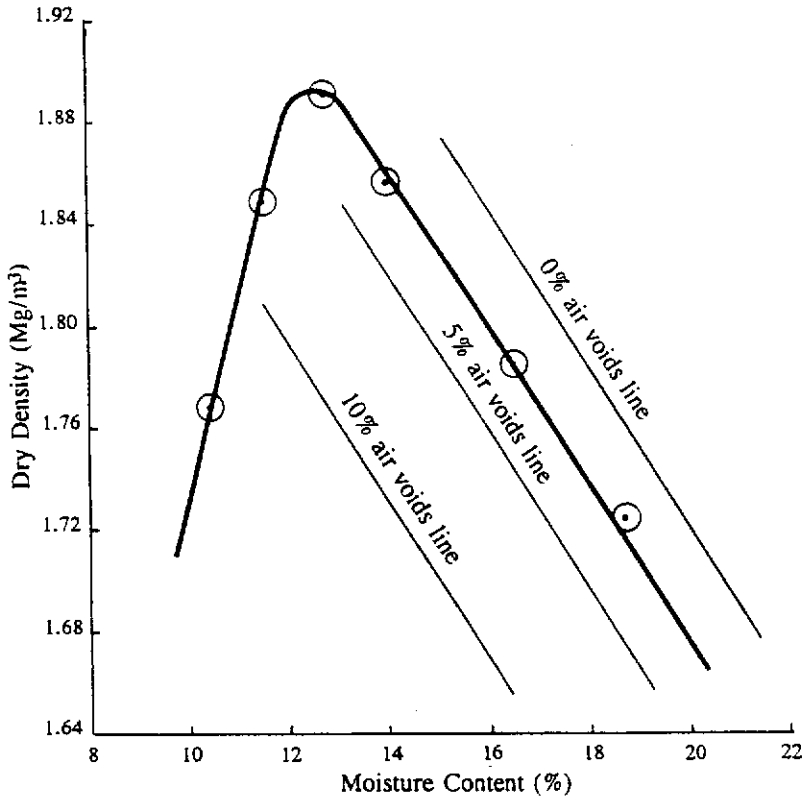

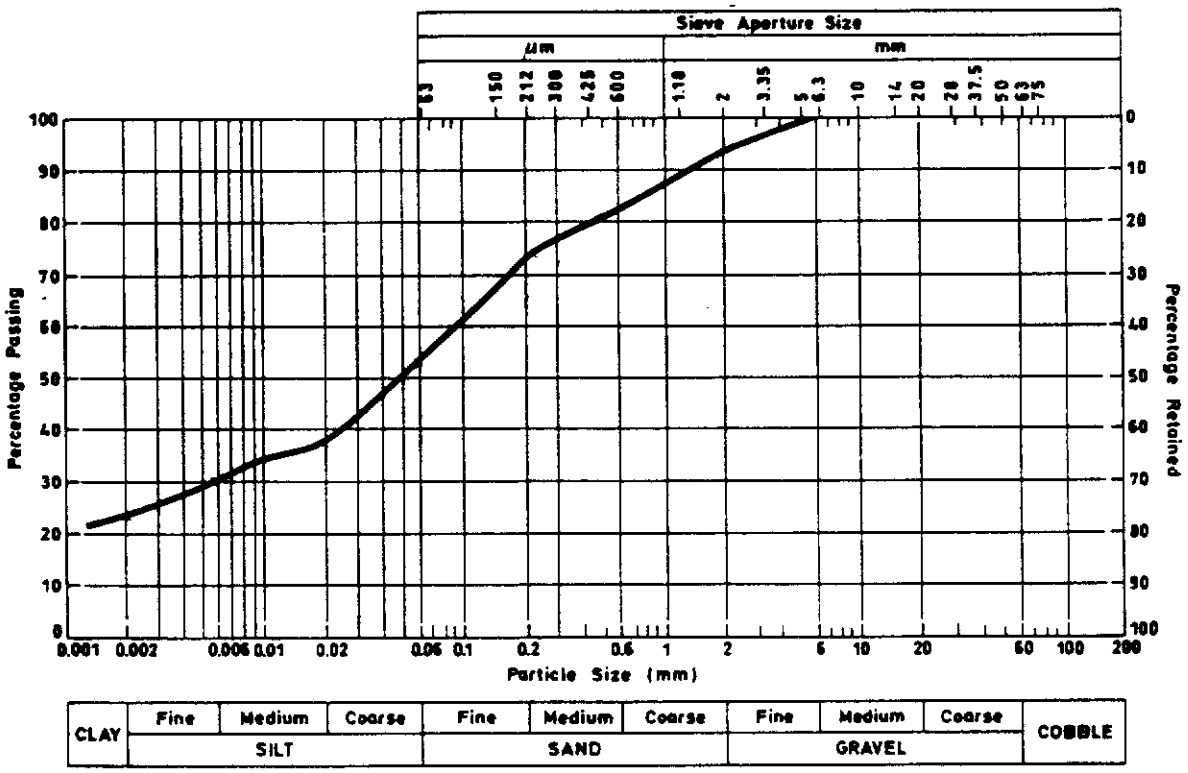

Note : Test results of sample at 2.8 m depth in trial pit No. TP1

Figure 13 - Results of Compaction Tests on Fill from Trial Pit No. TP1

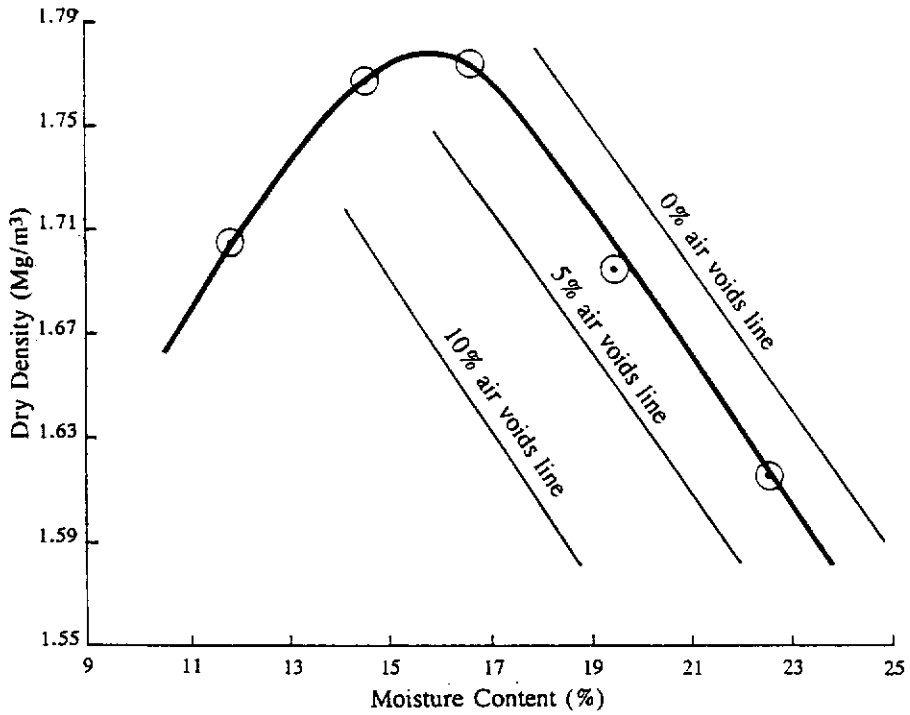

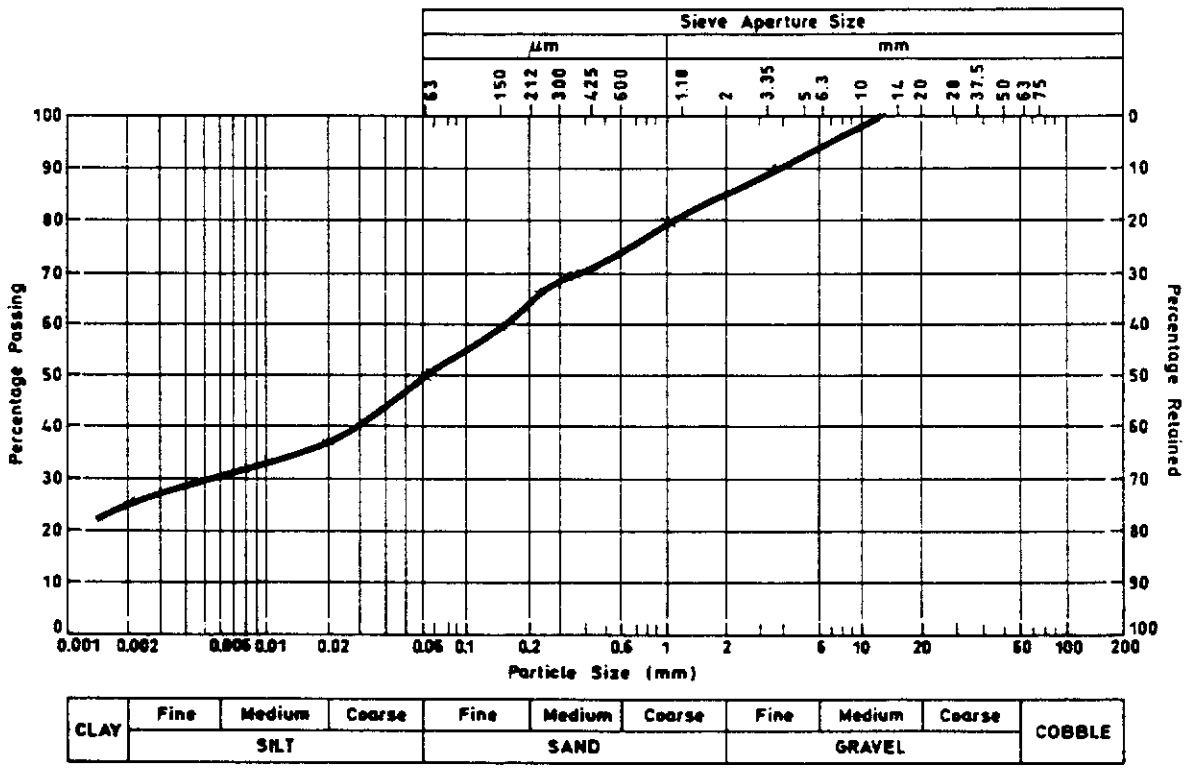

Note : Test results of sample prepared by mixing samples from trial pits No. TP7 & TP9.

Figure I4 - Results of Compaction Tests on Fill from Trial Pits No. TP7 & TP9

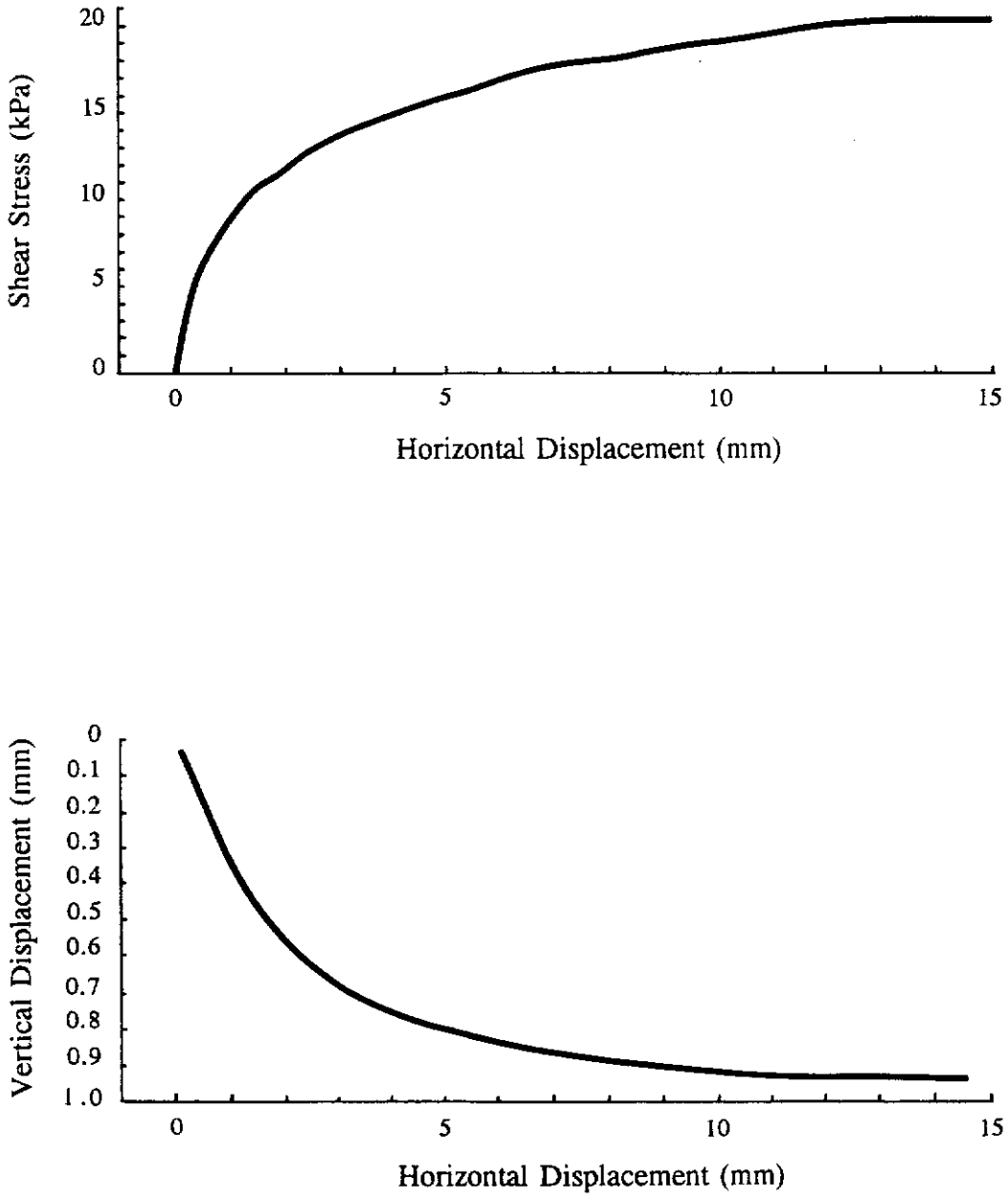

Notes : (1) Test results for sample at 2.8 m depth in trial pit No. TP1.
(2) Positive vertical displacement denotes compression.

Figure 15 - Typical Behaviour of Recompactd Fill in Shear Box Tests

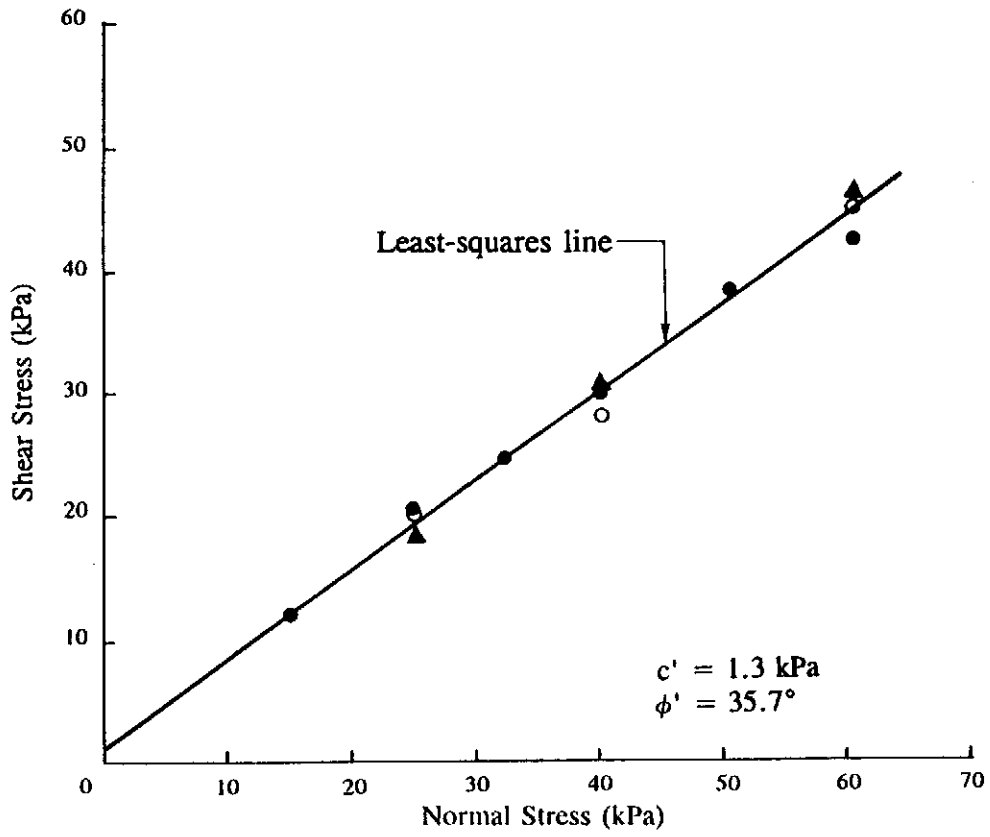

Legend :

○	Compacted dry density = 1.285 - 1.292 Mg/m³ (dry density before shearing = 1.774 - 1.857 Mg/m³)	c'	Apparent cohesion
●	Compacted dry density = 1.488 - 1.507 Mg/m³ (dry density before shearing = 1.567 - 1.771 Mg/m³)	φ'	Angle of shearing resistance
▲	Compacted dry density = 1.700 Mg/m³ (dry density before shearing = 1.727 - 1.755 Mg/m³)		

Figure I6 - Summary of Shear Box Test Results for Recompacted Fill

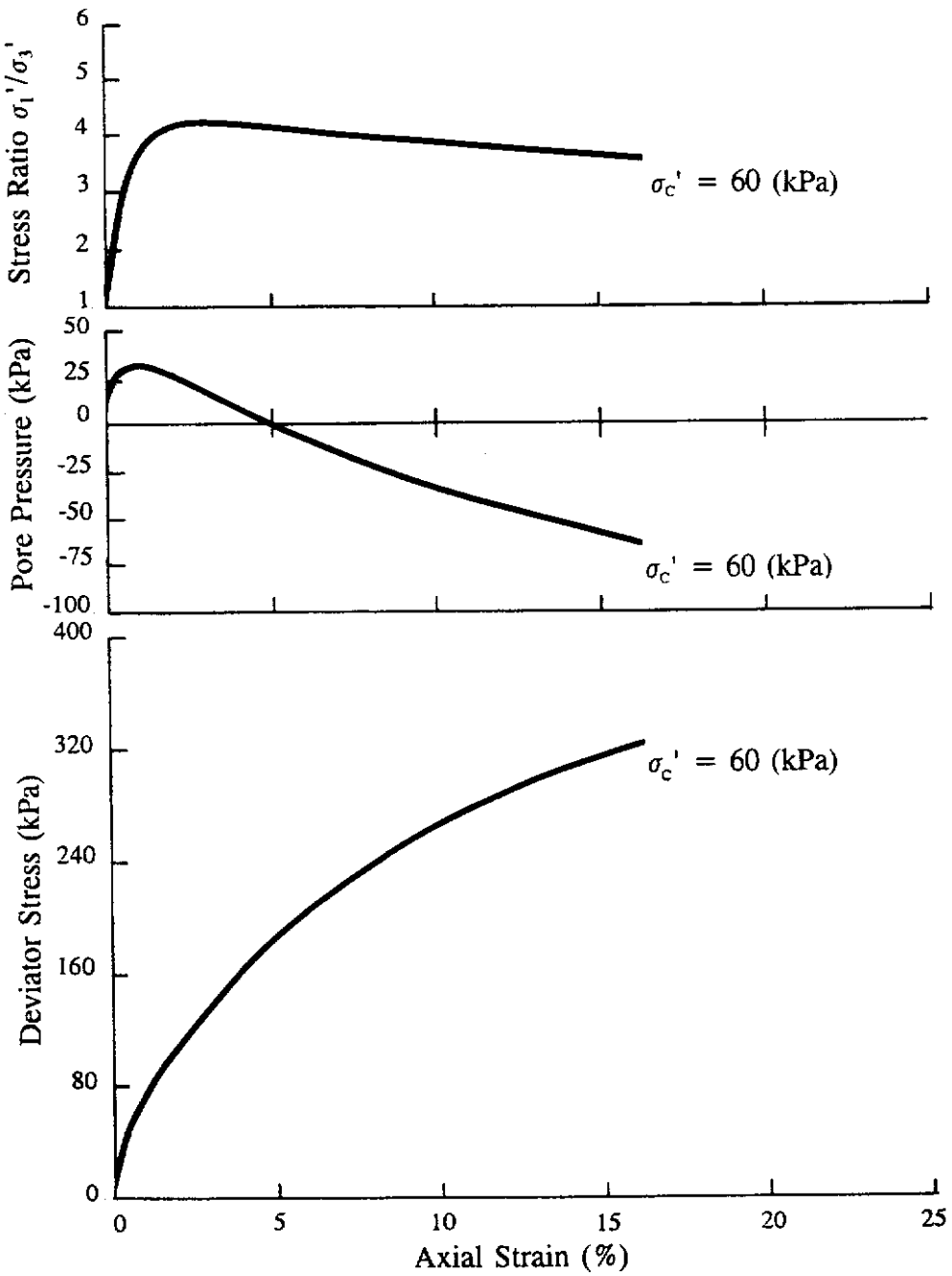

Legend :

σ_c'	Consolidation and confining pressure
σ_1'	Major principal effective stress
σ_3'	Minor principal effective stress

Note : Test results for sample at 6.89 m - 7.09 m depth in drillhole No. BH10.

Figure 17 - Typical Behaviour of CDV and C/HDV in Triaxial Compression Tests

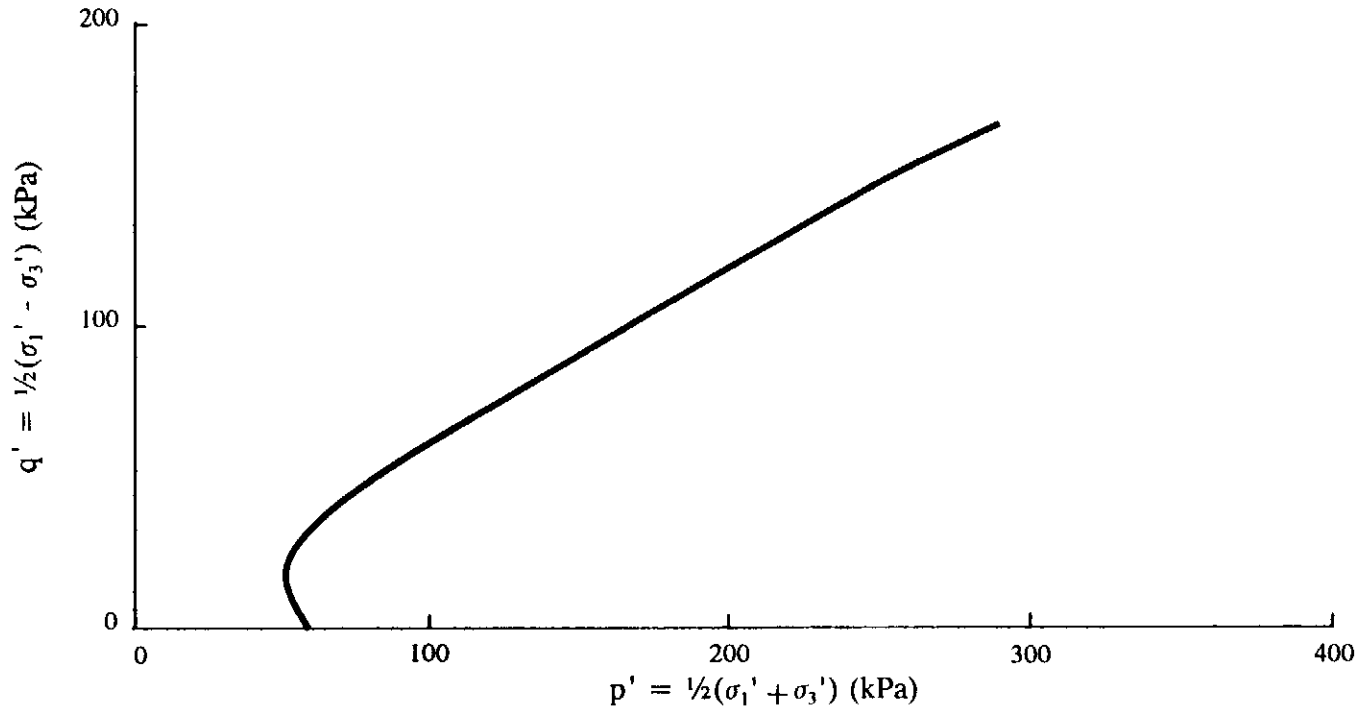

Legend :

σ_1' Major principal effective stress
σ_3' Minor principal effective stress

Note : Test results for sample at 6.89 m - 7.09 m depth in drillhole No. BH 10.

Figure I8 - Typical Stress Path Followed by CDV and C/HDV in Triaxial Compression Tests

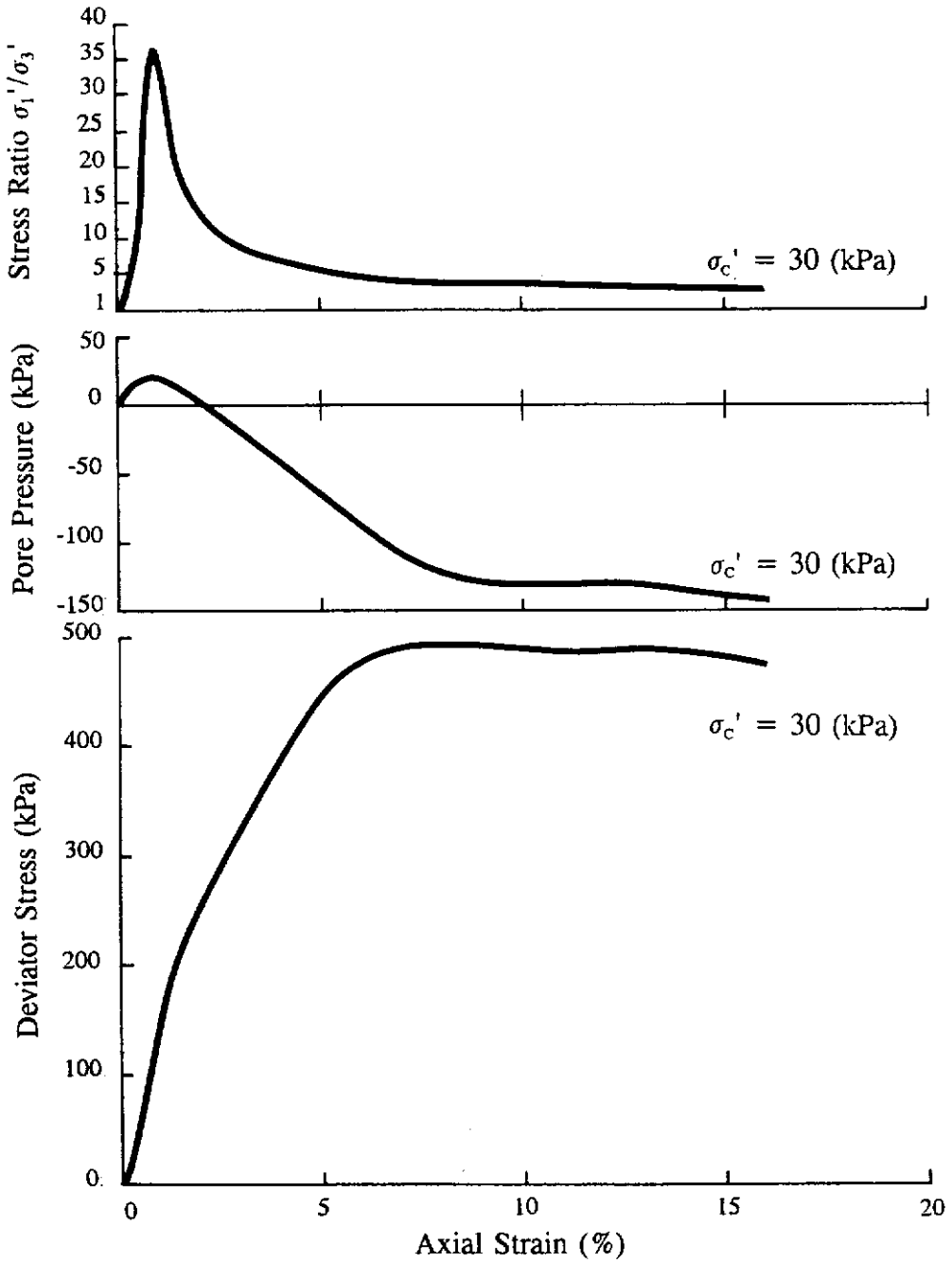

Legend :

σ_C'	Consolidation and confining pressure
σ_1'	Major principal effective stress
σ_3'	Minor principal effective stress

Note : Test results for sample at 3.09 m - 3.29 m borehole in BH1.

Figure I9 - Typical Behaviour of C/HDV in Triaxial Compression Tests Excluded from the Analyses

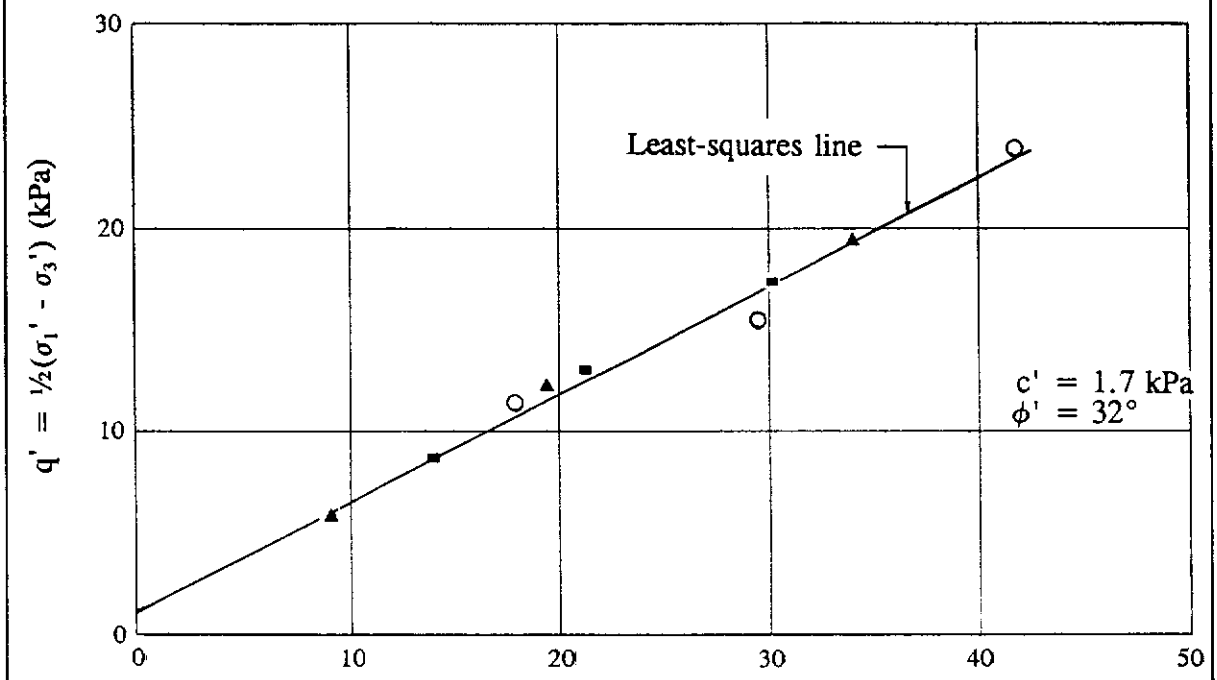

Legend :

σ_1'	Major principal effective stress	c'	Apparent cohesion
σ_3'	Minor principal effective stress	ϕ'	Angle of shearing resistance

▲ Initial dry density = 1.300 Mg/m³ (dry density before shearing = 1.680 - 1.780 Mg/m³)

■ Initial dry density = 1.490 - 1.500 Mg/m³ (dry density before shearing = 1.680 - 1.770 Mg/m³)

○ Initial dry density = 1.700 Mg/m³ (dry density before shearing = 1.750 - 1.800 Mg/m³)

Figure I10 - Summary of Triaxial Compression Test Results for Recompacted Fill

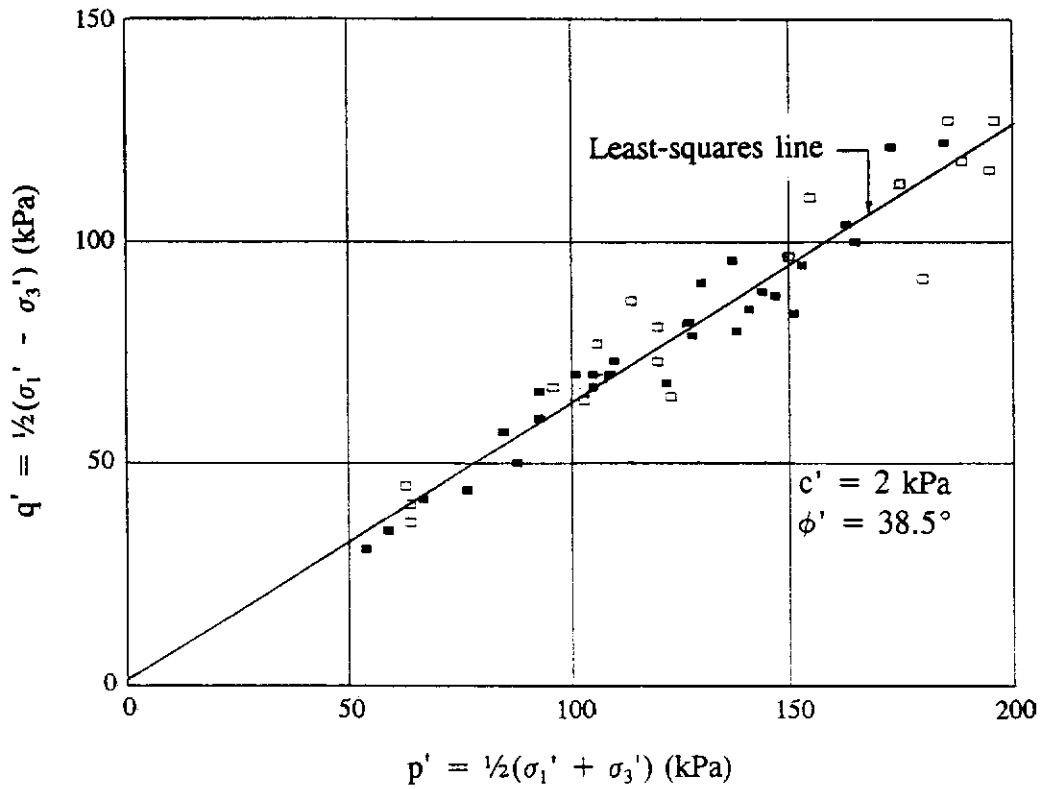

Legend :

σ_1'	Major principal effective stress
σ_3'	Minor principal effective stress
c'	Apparent cohesion
ϕ'	Angle of shearing resistance
▫	Completely to highly decomposed volcanics (C/HDV)
▪	Completely decomposed volcanics (CDV)

Figure I11 - Summary of Triaxial Compression Test Results for CDV and C/HDV for a Mean Effective Stress of Less than 200 kPa

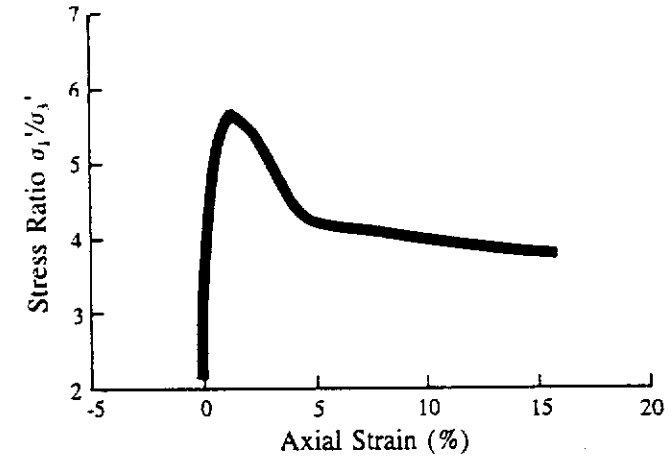

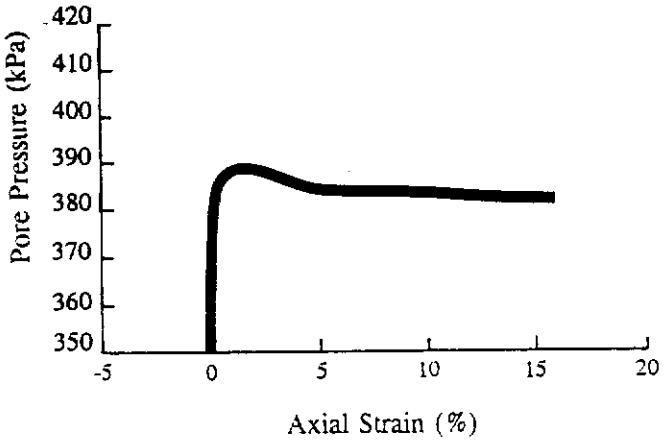

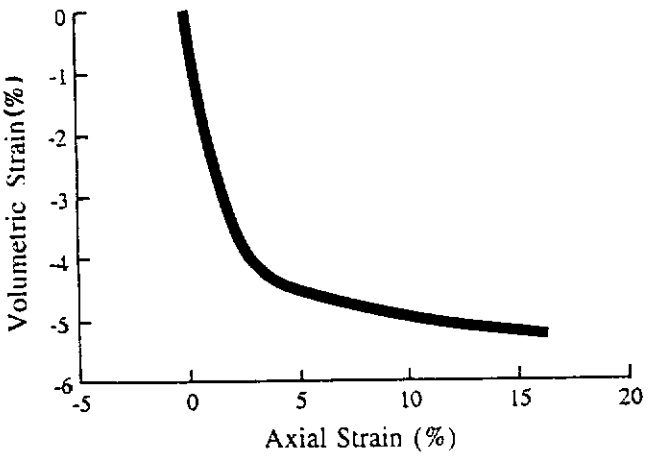

Legend :

σ_1'	Major principal effective stress
σ_3'	Minor principal effective stress

Note : Test results for Sample No. DL1.

Figure I12 - Typical Behaviour of CDV in a Dead-load Triaxial Test

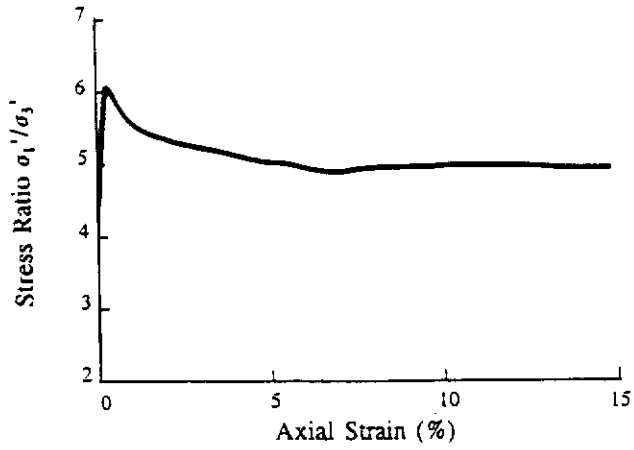

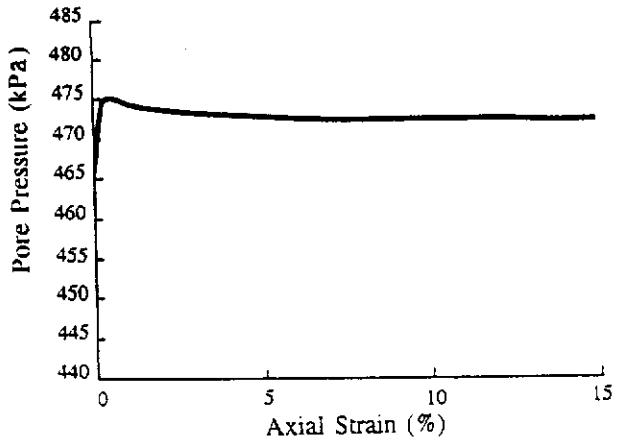

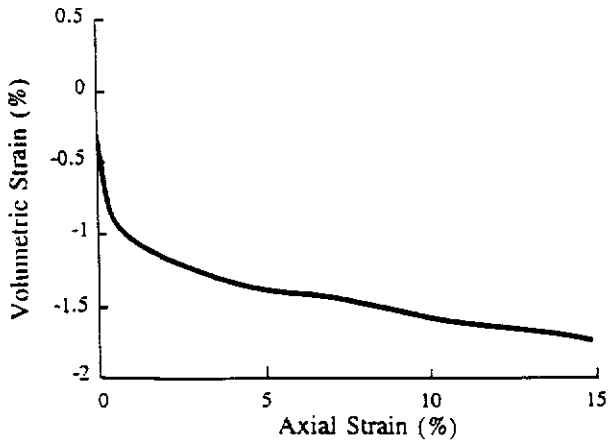

Legend :

σ_1' Major principal effective stress
σ_3' Minor principal effective stress

Note : Results for Sample No. HKU1.

Figure I13 - Typical Behaviour of CDV in a Stress-path Triaxial Test

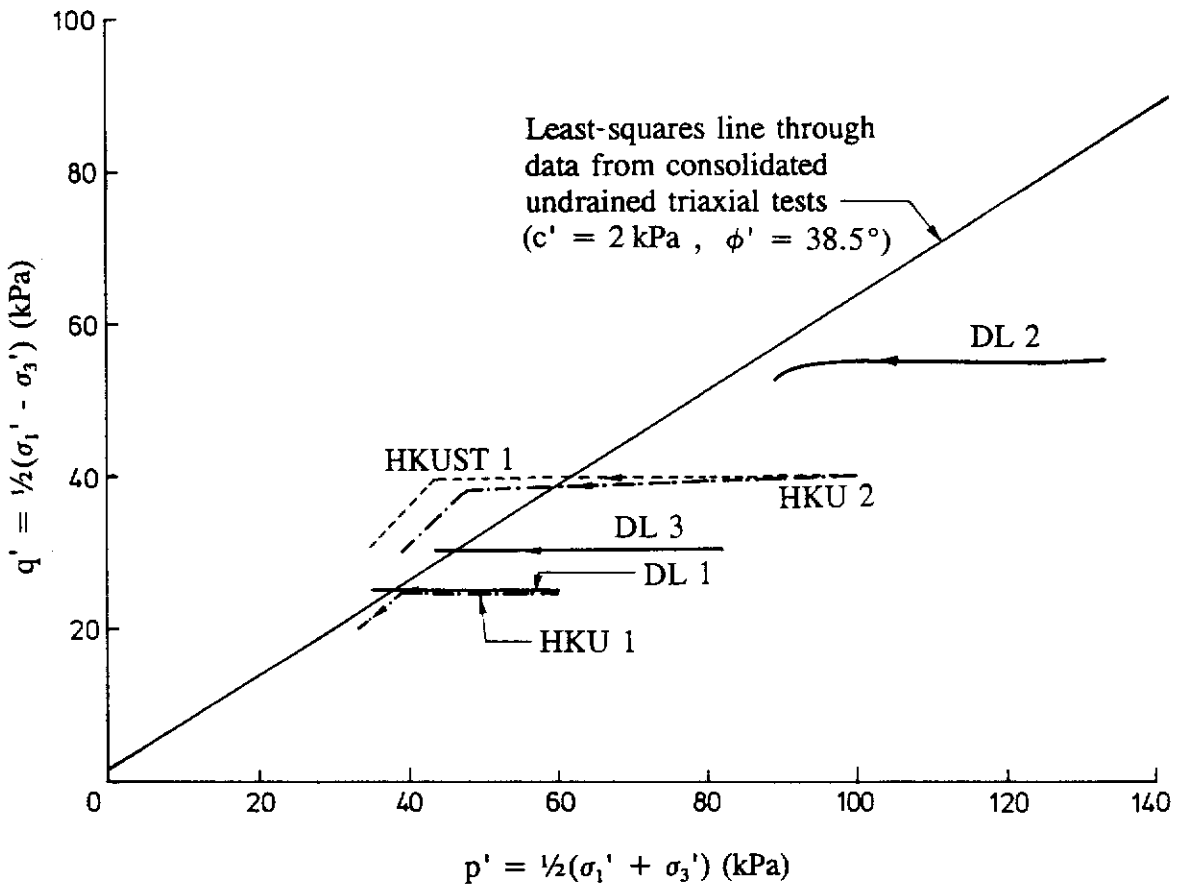

Legend :

σ_1'	Major principal effective stress
σ_3'	Minor principal effective stress
c'	Apparent cohesion
ϕ'	Angle of shearing resistance
$\overleftarrow{\text{DL 2}}$	Stress path for sample No. DL 2
DL	Dead-load tests

Notes :
(1) Test on sample No. DL 2 was not completed, because of malfunctioning of axial displacement transducer.
(2) All samples were CDV except sample No. HKUST 1 which was HDV.

Figure 114 - Summary of Stress Paths Followed in Dead-load and Stress-path Triaxial Tests

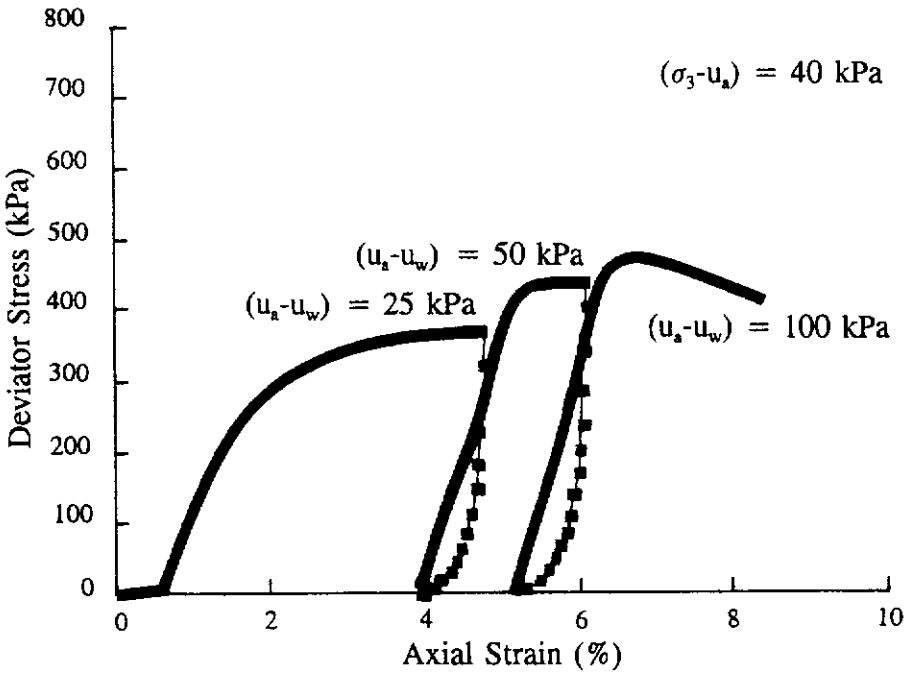

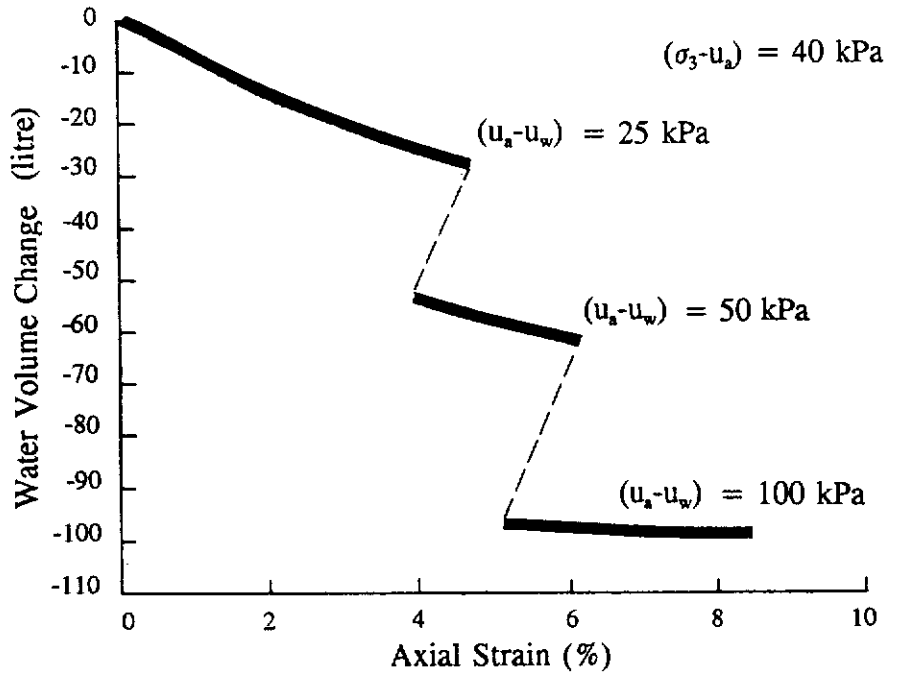

Legend :

σ_3	Cell pressure
u_a	Pore air pressure
u_w	Pore water pressure

Figure 115 - Typical Behaviour of CDV in Unsaturated Triaxial Tests

APPENDIX J

FOULWATER AND STORMWATER DRAINAGE SYSTEMS AT KWUN LUNG LAU

CONTENTS

J.1 INTRODUCTION

A detailed drainage investigation of the Kwun Lung Lau area was carried out after the landslide by the Drainage Unit of the Buildings Department. The objectives of the investigation were :

(a) to identify any connection between the foulwater system and the stormwater system for Blocks D, E, F & G,

(b) to determine whether there was any leakage from the foulwater sewers and stormwater drains in the vicinity of the landslide area, and

(c) to measure the rate of flow from the foulwater sewers serving Blocks D, E, F & G.

The investigation work included :

(a) visual inspection of all foulwater and stormwater manholes in Blocks C, D, E, F & G,

(b) closed-circuit television (CCTV) surveys of the foulwater sewers and stormwater drains, and

(c) 24-hour continuous measurement of the flow rate in the foulwater sewer serving Blocks D, E, F & G.

J.2 FOULWATER DRAINAGE SYSTEM

J.2.1 Background

The foulwater sewers for Kwun Lung Lau are generally located to the south and north sides of each block, with the south side being at a higher level. The foulwater sewers inspected were mainly those for Blocks C, D, E, F & G, as shown in Figure J1. The sewers were made of earthenware and pitch fibre. The sewage from Blocks A, B & C is discharged through a 300 mm diameter pipe into manhole No. 81. The sewage from Blocks D, E, F & G is discharged through another 300 mm diameter pipe into manhole No. 81. The latter pipe, which was made of earthenware, was laid within 2 m of the surface of the failed slope below Block D before connecting into manhole No. 81. The pipe was found to have broken and collapsed after the landslide.

J.2.2 Visual Inspection of Foulwater Manholes

A total of 57 foulwater manholes at Kwun Lung Lau were inspected. They were generally in a dilapidated state. Some had settled and cracked, and leakage from some of these was likely to have occurred in the past.

The defects observed in the manholes are summarised in Table J1.

The inspection also revealed that, apart from minor alterations, the layout of the existing foulwater sewers was generally in agreement with the approved drainage plan. Additional 100 mm diameter drains were found connected into some of the manholes. Dye tests carried out in these additional drains showed that they were part of the foulwater system. No stormwater drains were found to have been connected to the foulwater manholes.

J.2.3 Condition of Foulwater Sewers

J.2.3.1 General

CCTV was employed to survey the condition of the foulwater sewers.

The survey showed that the foulwater sewers were generally in dilapidated condition. Some foulwater sewers were found cracked, fractured, deformed and likely settled. The defects in the foulwater sewers are summarised in Table J2.

In addition to the defects shown in Table J2, open joints and joint displacements were commonly found in many of the foulwater sewers, as shown in Table J3.

Minor leakage would have occurred from some of the defective foulwater sewers, especially those with defects such as cracks, deformation and fracture. The amount of leakage would have depended on the extent of these defects. It is not practicable to examine in detail all the defects in the time available for the investigation. However, some of the foulwater sewers were exposed to check the leakage condition. This showed that there was minor leakage from some of the joints, as evidenced by the staining of the surrounding soil.

Details of the exposures are described in the following sections.

J.2.3.2 Foulwater Sewer between Manholes No. 16a and No. 26 at Block E

The CCTV survey showed that the pipe between the manholes had a circumferential crack. It was also deformed and had probably settled. A section of pipe about 9 m long between the two manholes was exposed in the investigation. The pipes were joined by straight couplings at each end. Three joints were exposed. Two of the joints showed minor leakage, and the other showed no signs of leakage.

J.2.3.3 Foulwater Sewer between Manholes No. 39 and No. 77 at Block D

CCTV survey showed that the pipe had open joints and joint displacements, but the joint openings and displacements were less than the pipe wall thickness. A section of the earthenware pipe was exposed. The length of the pipe between two joints was about 1 m. The exposed joints were of the socket-and-spigot type, and the pipes were connected together rigidly by cement mortar at the joints. Both joints showed no signs of leakage.

J.2.3.4 Foulwater Sewer between Manholes No. 77 and Edge of Landslide Scar

The CCTV survey showed that the pipe had a circumferential crack, open joints and joint displacements, but the joint openings and displacements were less than the pipe wall thickness. Two consecutive pipe joints, at about 1 m spacing and of the socket-and-spigot type, were exposed. The pipe was made of earthenware with a 40 mm to 75 mm thick concrete surround, which was also provided at the pipe joints. The pipes were connected rigidly with cement mortar at the joints. Inspection by the GEO on 10 September 1994 found that one of the joints was leaking at a rate of about 1 litre/hr. Minor leakage at this location was first noted on 5 September 1994. However, no leakage was observed during subsequent inspections on 14 October and 27 October 1994.

J.2.3.5 Foulwater Sewer between Manholes No. 26 and No. 27 at Block E

The CCTV survey showed that the pipe was likely to have settled. Two pipe joints, one each at about 1 m from manholes No. 26 and No. 27 respectively, were exposed. The pipe was made of pitch fibre, and was joined by a straight coupling at each end. The joint near manhole No. 26 showed no signs of leakage, whereas that near manhole No. 27 showed minor leakage.

J.2.3.6 Foulwater Sewer between Manholes No. 33 and No. 34 at Block G

The CCTV survey showed that the pipe was fractured near manhole No. 34. In addition, the pipe had a longitudinal crack and an open joint with a width about one to one-and-a-half times the wall thickness of the pipe. A section of the pipe, about 1 m long and at about 0.5 m from manhole No. 33, was exposed. The pipe was provided with a concrete surround, and there were no signs of leakage from the pipe section.

J.2.4 Flow Monitoring of the Foulwater Sewer

The flow from the 300 mm diameter foulwater sewer taking the sewage from Blocks D, E, F & G was monitored continuously for two weeks between 7 September 1994 and 20 September 1994. This was done with the aid of a rectangular fibreglass tank of 3 m long, 2 m wide and 2 m high erected at the footway below Block D. The tank was separated internally by a 1 m high fibreglass panel, allowing a smaller volume of flow to be measured in a shorter time. The arrangement of the tank is shown in Figure J3.

Measurements of flow were taken at about one-hour and half-hour intervals during dry periods and rainy periods respectively. The times required to fill the two chambers (V1 and V2) were recorded. The flow rates were calculated based on the time to fill the smaller chamber (V1) between water levels of 0.2 m and 0.89 m. The initial water level was taken at 0.2 m so as to eliminate the effect of silting material accumulated at the bottom of the tank. The time taken to fill the larger chamber (V2) was also recorded, and this served as a check on the flow rates obtained from the smaller chamber (V1). In most cases, the time taken to fill the larger chamber was about twice that required to fill the smaller chamber, the volume of which was about half the size of the larger chamber.

The average daily flow rate in the foulwater sewer was about 550 m^3/day throughout the monitoring period. This was in broad agreement with the estimated daily consumption of salt and fresh water at Blocks D, E, F & G by the Water Supplies Department.

There were two periods of peak flow in the foulwater sewer on each day. The maximum flow rates during the morning and evening peaks are shown in Table J4. The morning peak flow from Monday to Saturday was about 0.50 to 0.63 m^3/min and occurred between 6:30 a.m. and 8:30 a.m. On Sundays, the peak flow period shifted to between 9:30 a.m. and 11:30 a.m. A high flow of 1.15 m^3/min was recorded during the dry period at 7:00 a.m. on 9 September 1994. However, the flow rate soon reduced to about 0.6 m^3/min at 7:08 a.m.

In the evenings, the peak flow was about 0.65 to 0.88 m^3/min and was recorded between 6:30 p.m. and 10:30 p.m. On Saturdays, the peak flow reduced to about 0.57 to 0.63 m^3/min.

The minimum flow rate of about 0.07 to 0.10 m^3/min was recorded consistently during the period between 3:00 a.m. and 4:30 a.m.

During the monitoring period, rainfalls were recorded by the GEO automatic raingauge No. H02 at Kwun Lung Lau. Table J5 shows the rainy periods and the recorded maximum five-minute rainfall intensities.

The flow rates in the foulwater sewer recorded during dry periods and rainy periods are plotted in Figures J4 to J10. The flow rates during the rainy periods were generally lower than those in the dry periods. For example, the flow rates recorded during the heavy rain between 8:00 p.m. and 9:00 p.m. on 10 September 1994 (Saturday) were all smaller than the corresponding rates recorded during the dry period on 17 September 1994 (Saturday). This suggests that the rainwater produced no direct response in the foulwater system for Blocks D, E, F & G, which is further evidence of there being no connection between the stormwater system and the foulwater system.

J.3 STORMWATER DRAINAGE SYSTEM

J.3.1 Background

The stormwater system in the vicinity of Blocks C, D, E, F & G was also investigated. The main purpose of this exercise was to check the condition of the underground stormwater drains, including the manholes. The underground drains are generally located in the yard area and in the vehicular access road to the south of the above building blocks. The stormwater drains that were checked mainly lie in the area between Blocks C & G, and in the area south of the landslide area, as shown in Figure J2.

Most of the stormwater drains were made of concrete, with a few being made of cast iron.

J.3.2 Visual Inspection of Manholes

A total of 24 stormwater manholes were inspected. All manholes were found to be in fairly good working condition, with no major cracks or settlement. However, some minor cracks were present in the walls of manholes No. 19 (Block E) and No. 22 (Block G).

The inspection also showed that the layout of the existing stormwater system was at variance with that shown in the approved drainage plan. The main difference occurred in the area of the vehicular turning circle at the west end of Kwun Lung Lau.

J.3.3 Condition of Stormwater Drains

J.3.3.1 General

The CCTV survey showed that some of the stormwater drains were defective, and some were completely blocked with soil. Apart from the defective drains, the other stormwater drains appeared to be in fairly good working condition. The blocked drains, which appeared to have been abandoned, are listed in Table J6.

Minor leakage would have occurred from a number of defective drains (Table J7), the amount of which would have depended on the extent of the defects. As in the case of the foulwater system, an attempt to quantify the leakage from a large number of defects was impracticable because of time constraints.

In addition to the above defects, open joints and joint displacements were found in some of the stormwater drains (Table J8).

Two stormwater drains with serious defects in the yard area to the south of Block D are of particular note, as described in the following sections.

J.3.3.2 Drain between Gully No. GT 15a and Manhole No. 15

The 150 mm diameter concrete pipe, embedded in fill material within 1 m of the ground surface, was found to have broken at a position about 3 m from gully No. GT15a. A dye test was carried out by feeding gully sump No. GT 15a with a continuous supply of water. This showed that all the dyed water leaked through the broken pipe into the subsoil. The dyed water was later found seeping out from the sloping ground underneath Block D. Significant leakage of stormwater from this section of the drain would have occurred in the past.

Subsequent to this test, the drain was replaced by the Hong Kong Housing Society (HKHS) between 22 August and 26 August 1994.

J.3.3.3 Drain between Gully No. GT 16 and Manhole No. 16

A leakage test was carried out by the HKHS in the 150 mm diameter concrete pipe on

6 September 1994. The outlet of the drain was plugged at manhole No. 16, and water drawn from a fire hydrant was used to fill gully No. GT16 for at least 30 minutes. It was found that the gully could not be filled, and significant leakage from the drain was occurring.

The drain was subsequently replaced by the HKHS between 13 September and 16 September 1994.

J.3.4 External Vertical Rainwater Pipes from the Roof

Dye tests were carried out at all the inlets of the rainwater pipes on the roofs of Blocks C, D, E, F & G. The results showed that all the rainwater pipes discharged directly into surface channels or onto the ground. In the latter case, the water was collected by the surface channels before being discharged into the stormwater system.

J.4 CONCLUSIONS

The following conclusions can be drawn from the investigation work undertaken :

(a) There were no mis-connections of stormwater drains to the foulwater system of Blocks D, E, F & G, and the flow in the foulwater system did not respond to rainfall.

(b) Some parts of the foulwater and stormwater systems were found to be in poor condition. Minor leakages would have occurred in the past from some parts of the foulwater system. However, major leakages would have occurred from two defective stormwater drains in the yard area to the south of Block D.

LIST OF TABLES

Table J1 - Defective Foulwater Manholes

Manhole No.	Location	Defects Observed
8	Block F	Top of manhole wall and floor slab separated by about 200 mm; manhole settled and slightly shifted; no signs of leakage.
9	Block F	Top of manhole wall and floor slab separated by about 200 mm; manhole settled and slightly shifted; no signs of leakage.
33	Block G	Cracks, about 1-5 mm wide, near the bottom all around; minor leakage would occur.
34	Block G	Cracks, about 1-8 mm wide, all round at 300 mm from the bottom and near the top; minor leakage would occur.
38	Block D	Erosion of mortar rendering at bottom corner with affected area of about 200 x 75 mm; minor leakage would occur at this erosion area.
65	Block D	A horizontal construction joint of about 1-2 mm wide was found at the walls, located about 350 mm above the bottom of the manhole. Minor leakage would occur.
75a	North of Block D	Manhole wall cracked all around; the width of the crack was about 2-5 mm and at 150 mm from the bottom; minor leakage would occur.
80	North of Block D	Wall rendering slightly peeled off; crack, about 1 mm wide, with seepage mark on wall; erosion at the bottom; minor leakage would occur.
81	North of Block D	As revealed in the CCTV survey, the bottom of the manhole cracked, crack width about 10 mm; leakage would occur.

Table J2 - Defects in Foulwater Sewers

Foulwater Sewer	Location	Defects Observed
MH 61 - MH 62	Block C	Circumferential crack
MH 62 - MH 63	Block C	Longitudinal cracks
MH 63 - MH 64	Block C/D	Longitudinal cracks
MH 72 - MH 73	Block C	Likely pipe settlement
MH 74 - MH 75	Block C/D	Circumferential fracture; circumferential cracks
MH 84 - MH 65	Block D	Deformed pipe
MH 65 - MH 75	Block D	Deformed pipe
MH 77 - Landslide scar	Block D	Circumferential crack
MH 29 - MH 38a	Block D/E	Deformed pipe
MH 16a - MH 26	Block E	Circumferential crack; pipe settlement; deformed pipe
MH 26 - MH 27	Block E	Likely pipe settlement
MH 5 - MH 6	Block G/E	Pipe lying on ground level, with hole about 40 mm diameter at top
MH 7 - MH 16	Block E	Pipe lying on ground level, with hole about 40 mm diameter at top
MH 16 - MH 16a	Block E	Circumferential cracks; deformed pipe
MH 32 - MH 33	Block G	Circumferential cracks; longitudinal crack
MH 33 - MH 34	Block G	Pipe fracture near MH 34; longitudinal crack
MH 34 - MH 35	Block G/E	Circumferential cracks

Legend :

MH Manhole

Table J3 - Open Joints and Joint Displacements in Foulwater Sewers

Foulwater Sewer	Location	Remarks
MH 72 - MH 73	Block C	Open joint (m); joint displacement (s)
MH 73 - MH 74	Block C	Open joint (m); joint displacement (s)
MH 74 - MH 75	Block C/D	Open joint (s); joint displacement (m)
MH 75 - MH 80	Block C	Open joint (m); joint displacement (m)
MH 80 - MH 81	Block D	Open joint (s)
MH 39 - MH 77	Block D	Open joint (s); joint displacement (s)
MH 77 - Landslide scar	Block D	Open joint (s); joint displacement (m)
MH 75a - MH 80	Block D	Open joint (s)
MH 29 - MH 38a	Block D	Open joint (s)
MH 27 - MH 28	Block E/D	Open joint (s)
MH 8 - MH 9	Block F	Open joint (l)
MH 10 - MH 11	Block F	Open joint (m); joint displacement (m)
MH 11 - MH 12	Block F	Open joint (m)
MH 12 - MH 13a	Block F	Joint displacement (m)
MH 14 - MH 15	Block F	Open joint (s)
MH 25 - MH 26	Block F/E	Open Joint (s)
MH 15 - MH 16	Block F/E	Joint displacement (m)
MH 2 - MH 3	Block G	Open joint (s)
MH 4 - MH 5	Block G	Open joint (s)
MH 6 - MH 7	Block E	Open joint (s)
MH 31 - MH 32	Block G	Open joint (s); joint displacement (s)
MH 32 - MH 33	Block G	Open joint (s); joint displacement (s)
MH 33 - MH 34	Block G	Open joint (m); joint displacement (l)
MH 34 - MH 35	Block G/E	Open joint (m); joint displacement (m)
MH 35 - MH 36	Block E	Open joint (m); joint displacement (s)
MH 36 - MH 37	Block E	Open joint (s); joint displacement (s)
MH 37 - MH 38	Block E/D	Open joint (m); joint displacement (s)
MH 38 - MH 39	Block D	Open joint (s)

Legend :

MH	Manhole
s	Joint displacement or opening less than t
m	Joint displacement or opening between t and 1.5 t
l	Joint displacement or opening greater than 1.5 t
t	pipe wall thickness

Table J4 - Peak Flow Rates in the Foulwater Sewer Serving Blocks D, E, F & G

Date	Morning Peak Flow		Evening Peak Flow	
	Peak Flow Rate (m^3 / min)	Time (a.m.)	Peak Flow Rate (m^3 / min)	Time (p.m.)
7 Sep 1994 (Wed)	-	-	0.72	7:00
8 Sep 1994 (Thur)	0.60	7:00	0.79	8:00
9 Sep 1994 (Fri)	1.15*	7:00	0.83	7:30 - 8:30
10 Sep 1994 (Sat)	0.50	7:30	0.63	7:00 & 10:25
11 Sep 1994 (Sun)	0.51	10:30	0.65	6:45 & 9:40
12 Sep 1994 (Mon)	0.52R	7:25	0.80R	7:20 & 9:20
13 Sep 1994 (Tue)	0.53	7:30	0.72	7:00
14 Sep 1994 (Wed)	0.53	7:30	0.88	8:35
15 Sep 1994 (Thur)	0.54	7:30	0.77	10:00
16 Sep 1994 (Fri)	0.59	8:00	0.69	10:30
17 Sep 1994 (Sat)	0.58	7:30	0.57	7:00 - 9:30
18 Sep 1994 (Sun)	0.59	10:30	0.72	10:00
19 Sep 1994 (Mon)	0.63	7:40	0.80	10:30
20 Sep 1994 (Tue)	0.62	7:30	-	-

Legend :

R During rainy period
* Exceptionally high value

Table J5 - Rainy Periods during the Foulwater Sewer Flow Monitoring

Date	Rainy Period	Maximum 5-minute Rainfall Intensity (mm)
10 Sep 1994	12:30 p.m. - 1:00 p.m. 1:00 p.m. - 2:00 p.m. 7:50 p.m. - 8:00 p.m. 8:00 p.m. - 9:00 p.m.	8.5 1.5 2.0 8.0
11 Sep 1994	5:40 a.m. - 6:00 a.m. 6:00 a.m. - 6:45 a.m.	2.0 1.5
12 Sep 1994	1:30 a.m. - 6:00 a.m. 6:15 a.m. - 9:10 a.m. 9:10 a.m. - 9:15 a.m 9:15 a.m. - 11:55 a.m. 12:05 p.m. - 2:00 p.m. 6:00 p.m. - 10:00 p.m.	< 0.5 1.5 3.5 1.0 < 0.5 1.0
13 Sep 1994	1.40 a.m. - 2:55 a.m.	0.5
14 Sep 1994	3:30 a.m. - 4.15 a.m. 2:00 p.m. - 3:00 p.m.	< 0.5 2.0
15 Sep 1994	1:30 a.m. - 2:00 a.m.	< 0.5
17 Sep 1994	11:30 a.m. - 0:00 a.m.	0.5
18 Sep 1994	0:00 a.m. - 1:35 a.m. 1:35 a.m. - 3:15 a.m.	0.5 < 0.5
20 Sep 1994	4:40 a.m. - 7:00 a.m.	2.5

Table J6 - Blocked Stormwater Drains

Connecting Manhole	Location	Diameter of Blocked Drain Pipes
MH 12	South of Block C	150 mm
MH 12	South of Block C	150 mm
MH 13	South of Block C/D	150 mm
MH 19	South of Block E	150 mm
MH 22	South of Block G	300 mm
MH A	South of Block G	600 mm
MH B	South of Block G	300 mm
MH 1b	South of Block G	760 mm
Note : See Figure J2 for locations of the blocked drains.		

Table J7 - Defects in Stormwater Drains

Stormwater Drain	Location	Defects Observed
GT 12(3) - MH 12	South of Block C	Circumferential crack; hole, about 40 mm in diameter, on top of the pipe
GT 12(1) - MH 12	South of Block C	Circumferential fracture
GT 15a - MH 15	South of Block C/D	150 mm diameter concrete pipe found broken; pipe subsequently replaced by HKHS between 22 August and 26 August 1994
GT 16 - MH 16	East of Block E	150 mm diameter concrete pipe was suspected broken; pipe subsequently replaced by HKHS between 13 September and 16 September 1994
GT 20 - MH 20	South of Block E	Circumferential crack
MH 18 - MH 20	South of Block E	Longitudinal crack (estimated to be 5 to 10 mm wide) at the crown of the first 7 m of the pipe from manhole No. 20; ponding at the section from 7.5 m to 11 m and from 17 m to manhole No. 18; likely pipe settlement at these two sections
MH 22 - MH B	South of Block G	Longitudinal and circumferential cracks
GT 22 - MH 22	South of Block G	Circumferential fracture
Legend : GT Gully MH Manhole		

Table J8 - Open Joints and Joint Displacements in Stormwater Drains

Stormwater Drain	Location	Remarks
GT 12(3) - MH 12	South of Block C	Open joint (m); joint displacement (m)
GT 12(1) - MH 12	South of Block C	Open joint (l); joint displacement (m)
MH 14 - MH 12	South of Block C	Joint displacement (s)
MH 13 - MH 5	South of Block C/D	Open joint (l)
GT 5 - MH 5	South of Block C/D	Open joint (s)
GT 13 - MH 13	South of Block C/D	Open joint (l)
GT 15b - MH 15	South of Block C/D	Open joint (m)
GT 12a - MH 12a	South of Block C	Open joint (l)
GT 18 - MH 18	South of Block E	Open joint (l); joint displacement (m)
GT 20 - MH 20	South of Block E	Open joint (s); joint displacement (m)
GT 19 - MH 19	South of Block E	Open joint (m); joint displacement (m)
MH 19 - MH 3	South of Block E	Open joint (m); joint displacement (s)
MH 18 - MH 16	East of Block E	Open joint (s); joint displacement (s)
MH 18b - MH 4	East of Block F	Open joint (l); joint displacement (m)
MH 2 - MH 1	South of Block G	Open joint (s)
MH B - MH 22	South of Block G	Open joint (m)
GT B - MH B	South of Block G	Open joint (m)

Legend :

GT	Gully
MH	Manhole
s	Joint displacement or opening less than t
m	Joint displacement or opening between t and 1.5t
l	Joint displacement or opening greater than 1.5t
t	Pipe wall thickness

LIST OF FIGURES

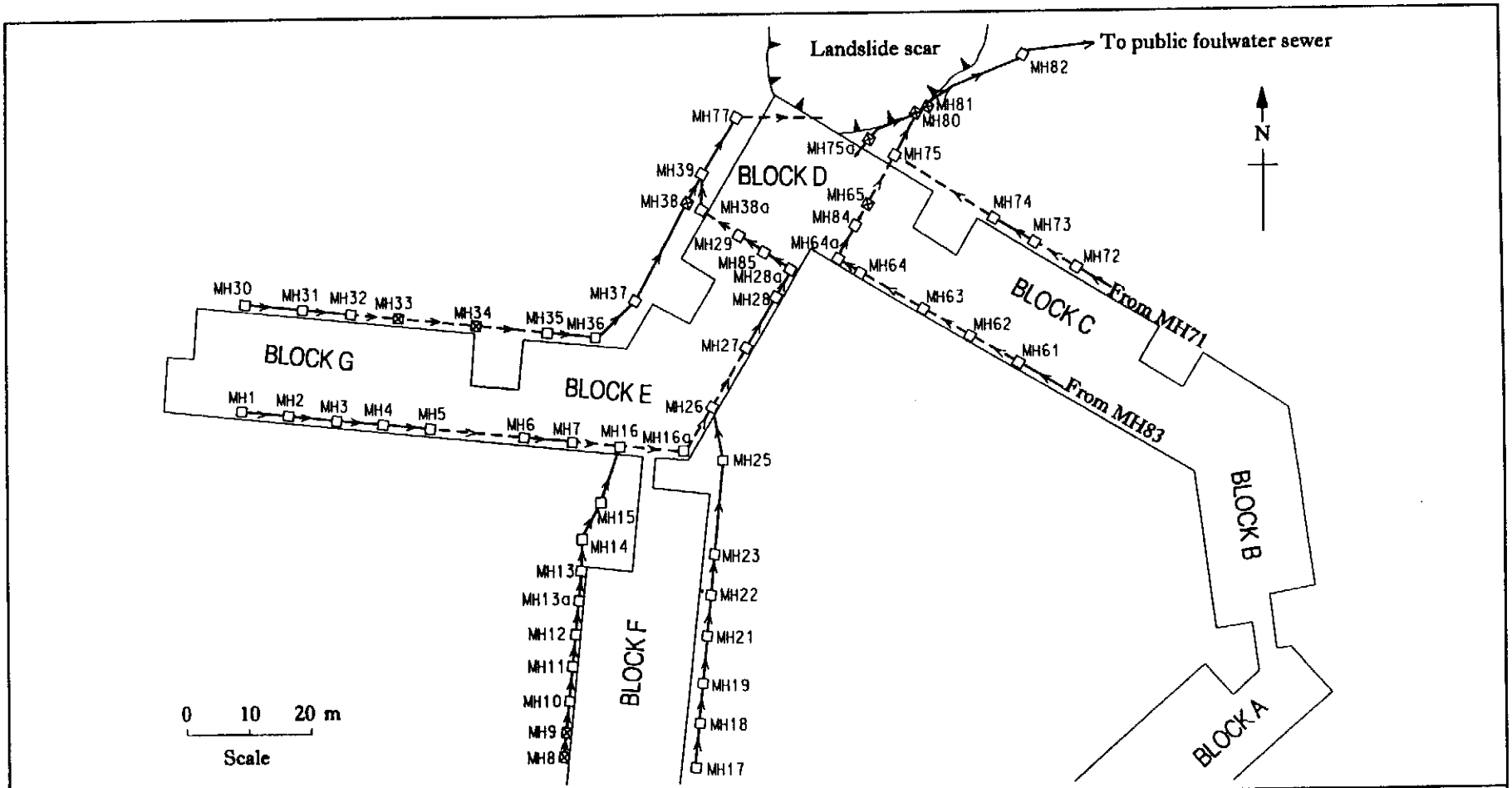

Legend :

— — — Pipe which is cracked, fractured, deformed or settled

□ MH2 Foulwater manhole No.2

⊠ Defective foulwater manhole

Note : Foulwater manhole No.77a was found in the landslide debris. The location of the manhole before the landslide is shown in Figure K2 of Appendix K.

Figure J1 - Layout and Condition of the Foulwater Sewers at the Time of the Post-failure Investigation

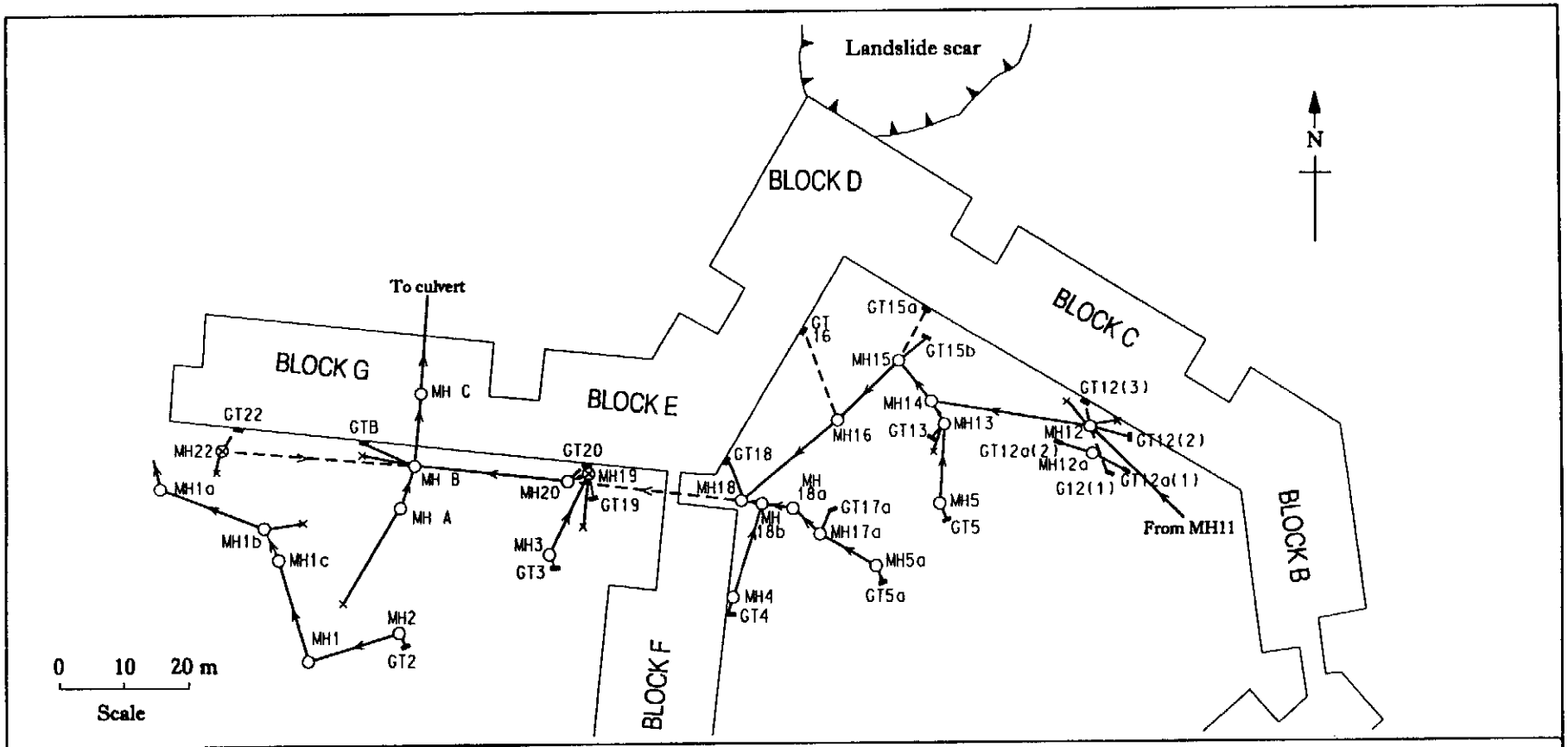

Legend :

– – – Pipe which is cracked, fractured, deformed or settled	GT2 Gully No. GT2
MH2 Stormwater manhole No.2	⊗ Defective stormwater manhole
×—— Blocked drain pipe	

Note : The drains between gully No. GT15a & manhole No.15, and between gully No. GT16 & manhole No.16 were found to suffer from major leakages.

Figure J2 - Layout and Condition of the Stormwater Pipes at the Time of the Post-failure Investigation

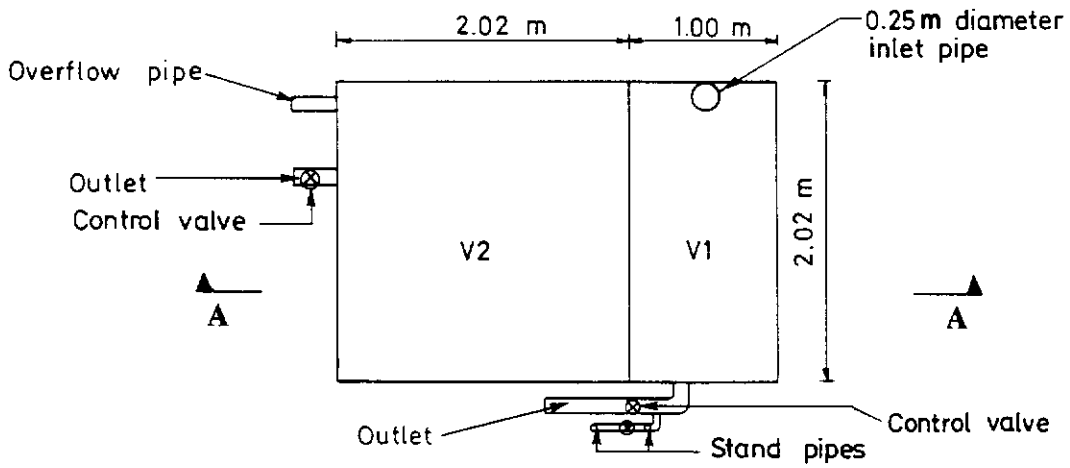

(a) Plan

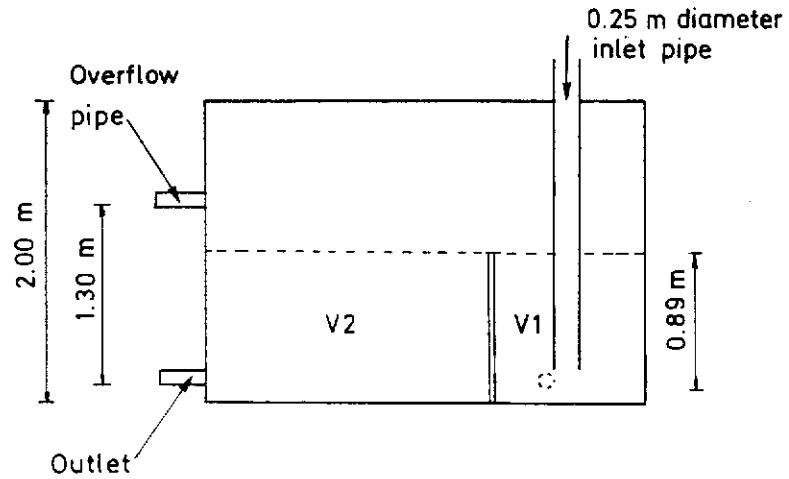

(b) Section A - A

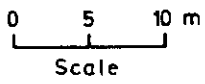

Figure J3 - Tank for Flow Monitoring

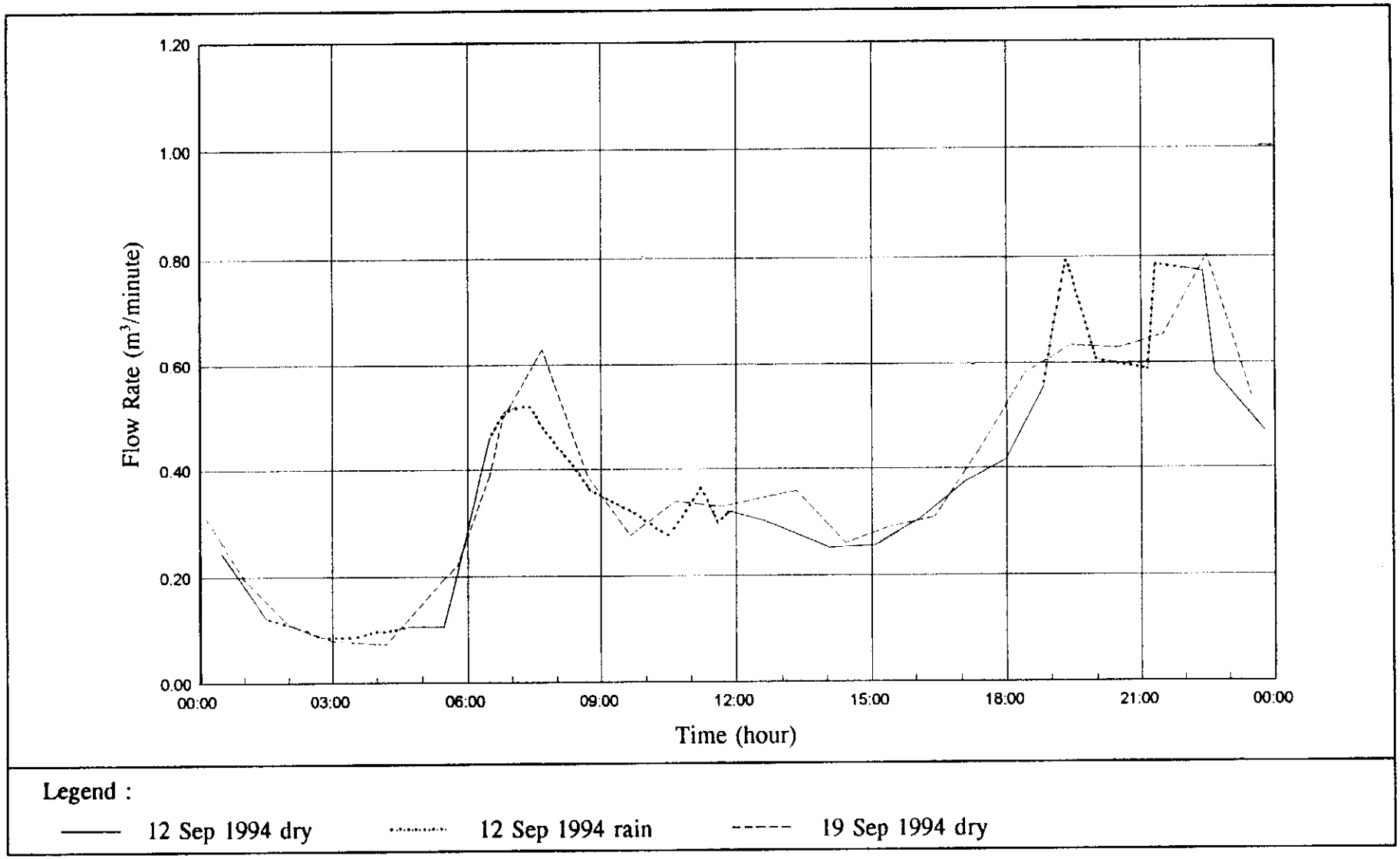

Figure J4 - Results of Flow Monitoring of the Foulwater Sewer (Monday Records)

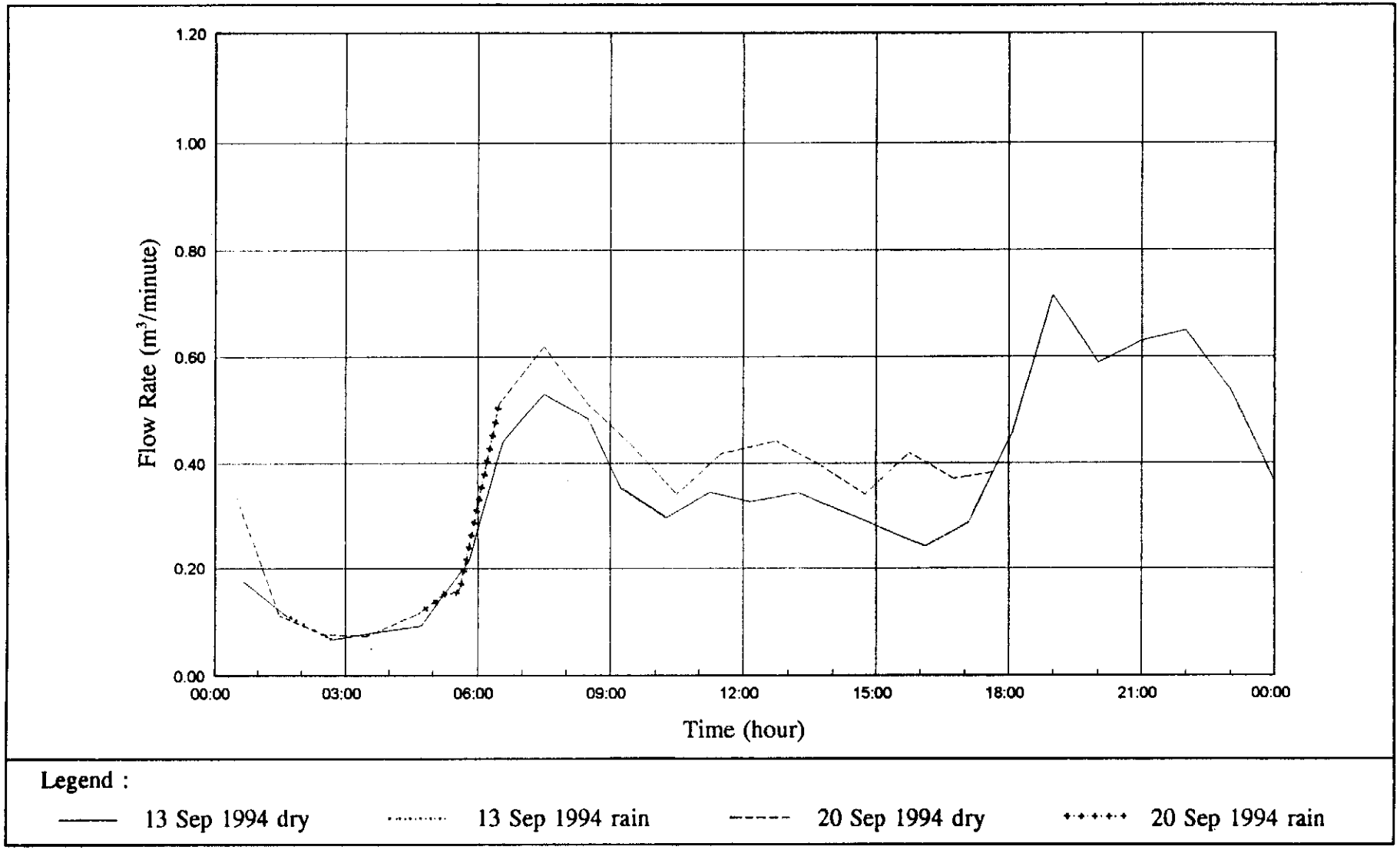

Figure J5 - Results of Flow Monitoring of the Foulwater Sewer (Tuesday Records)

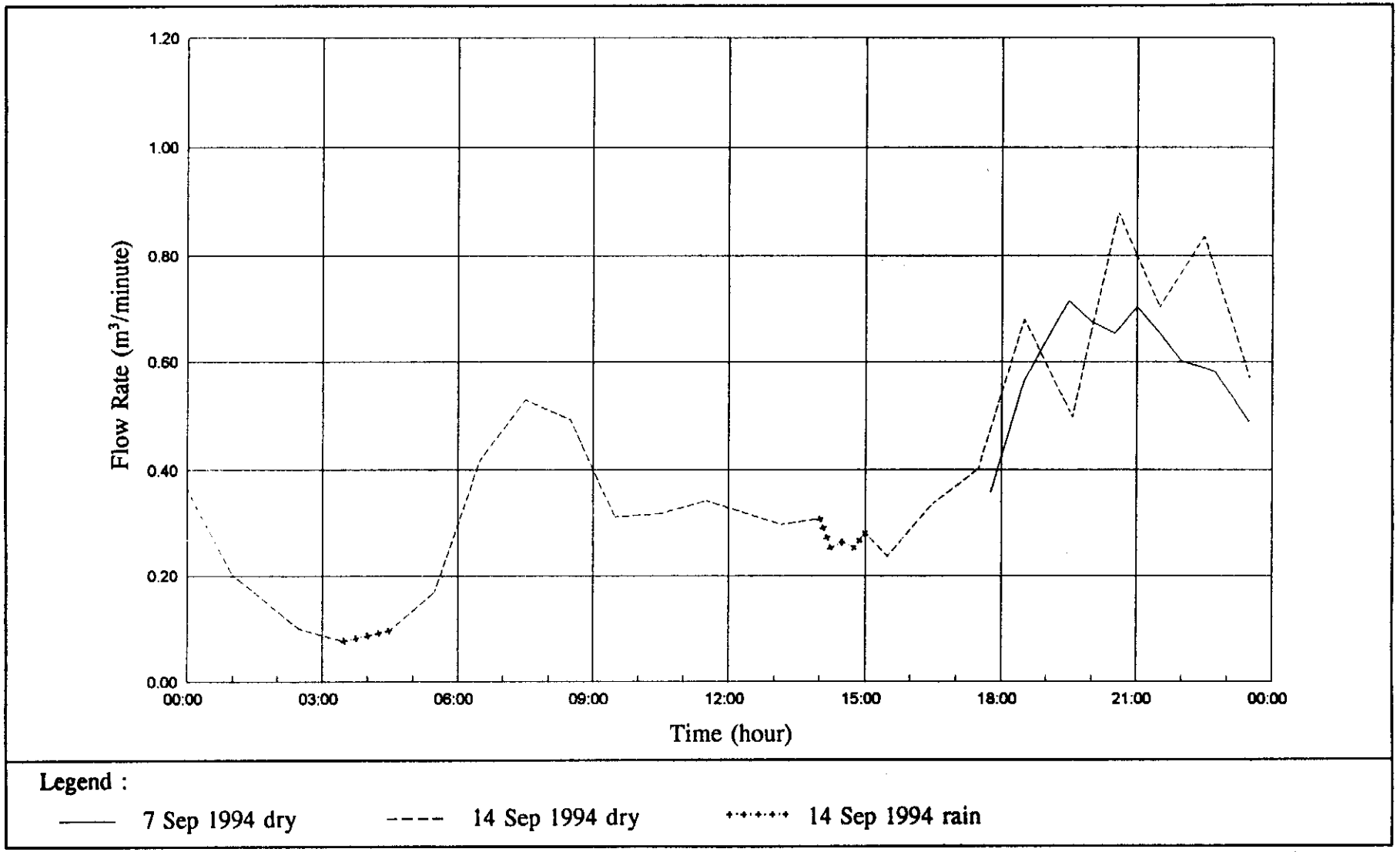

Figure J6 - Results of Flow Monitoring of the Foulwater Sewer (Wednesday Records)

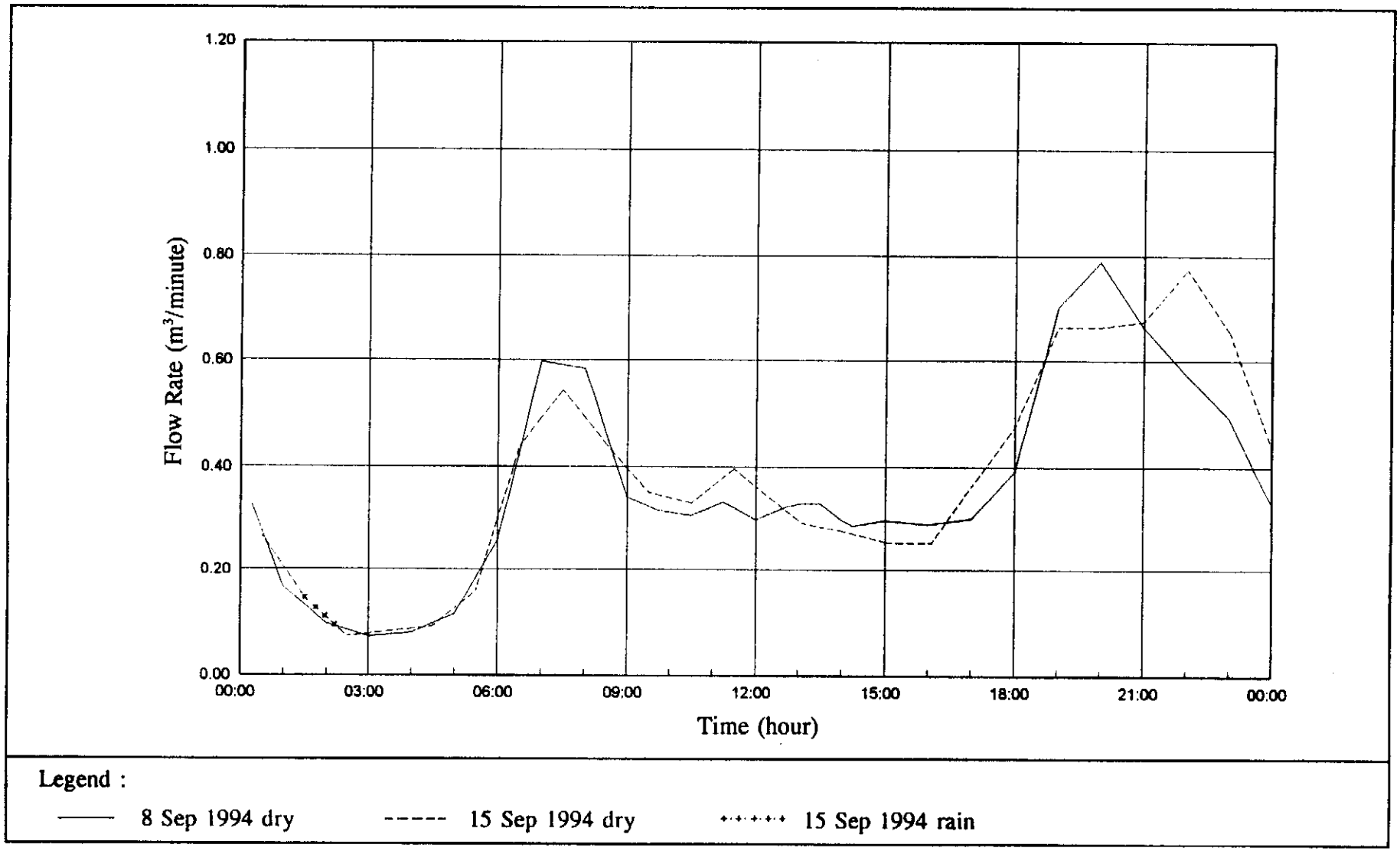

Figure J7 - Results of Flow Monitoring of the Foulwater Sewer (Thursday Records)

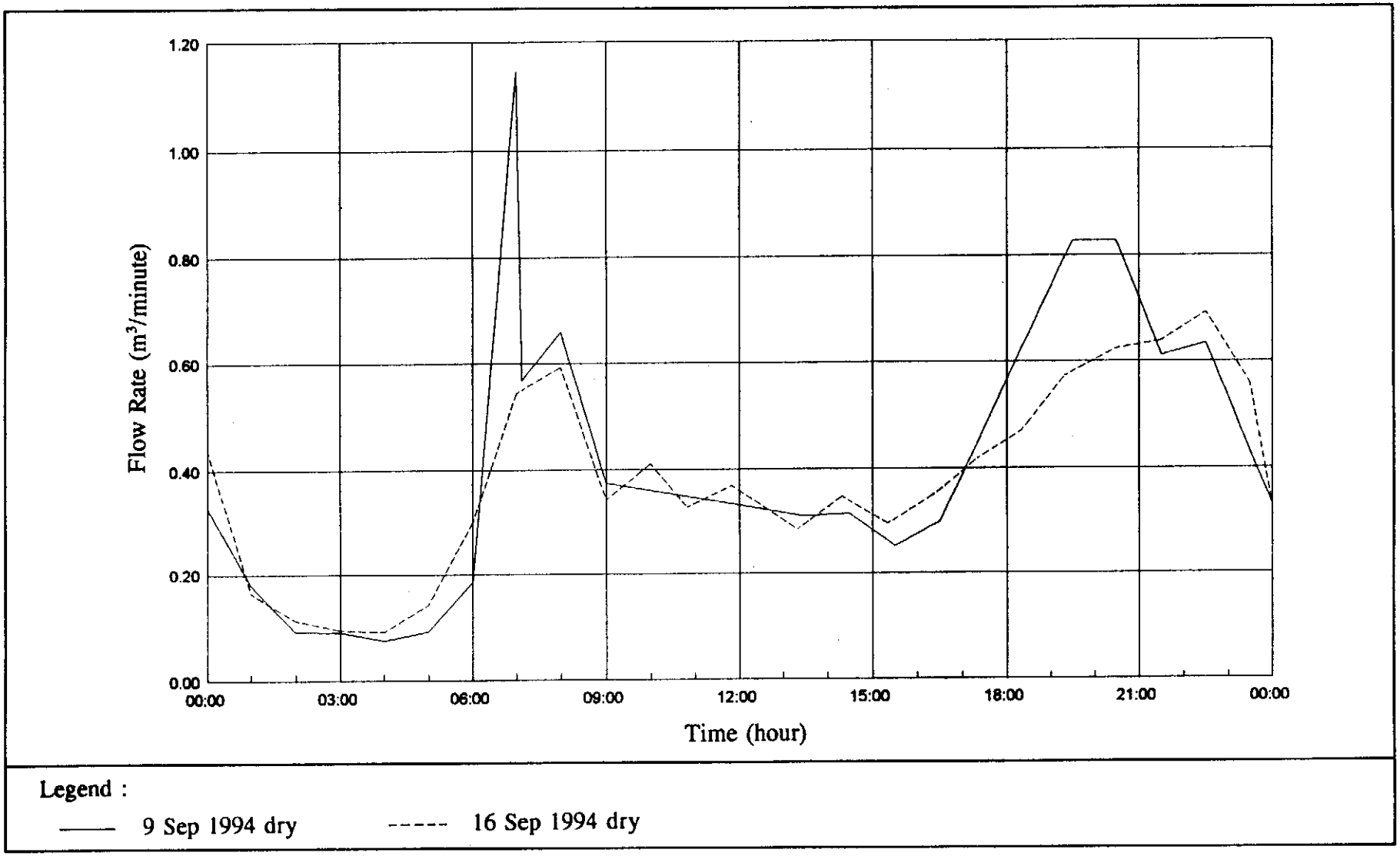

Figure J8 - Results of Flow Monitoring of the Foulwater Sewer (Friday Records)

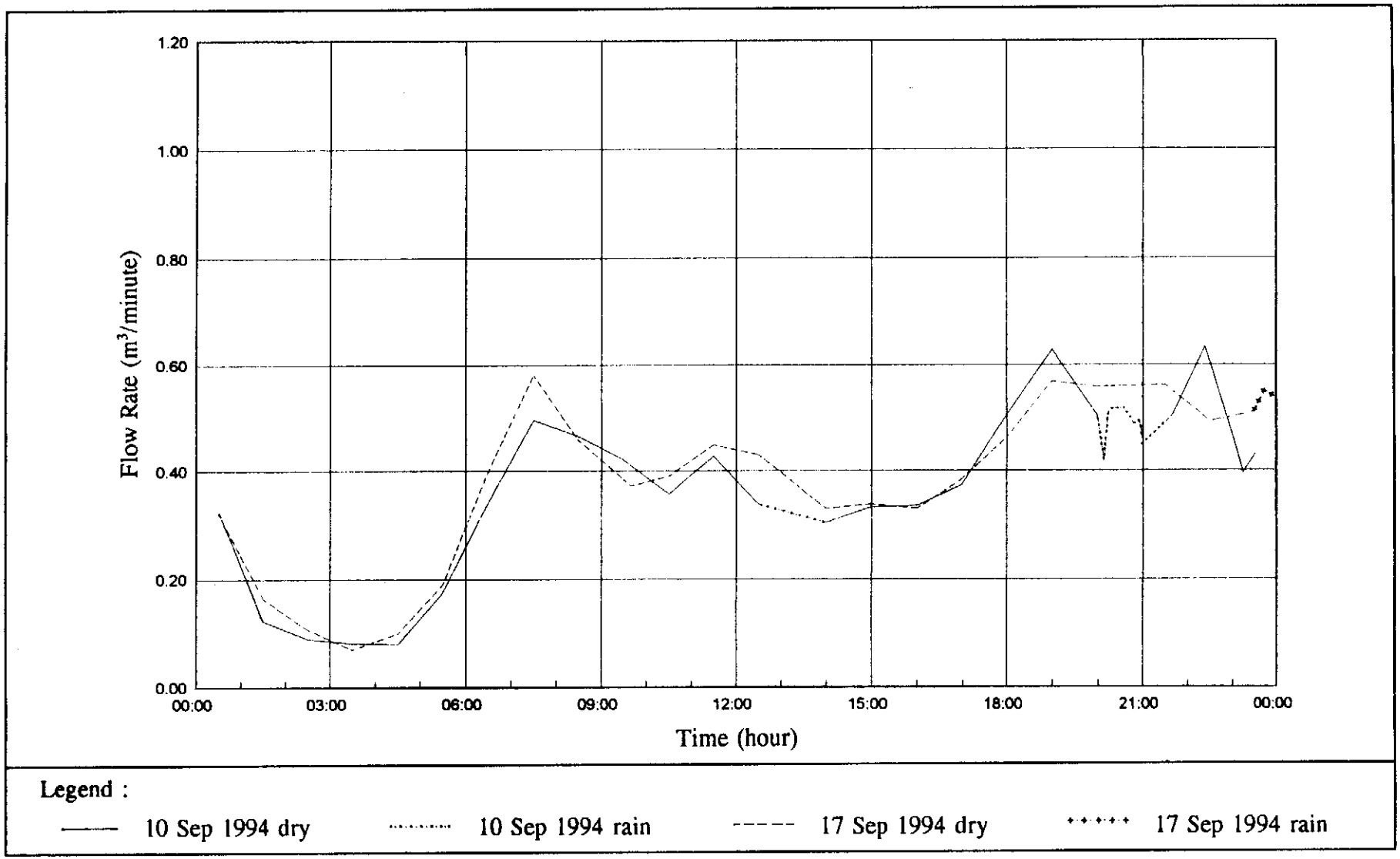

Figure J9 - Results of Flow Monitoring of the Foulwater Sewer (Saturday Records)

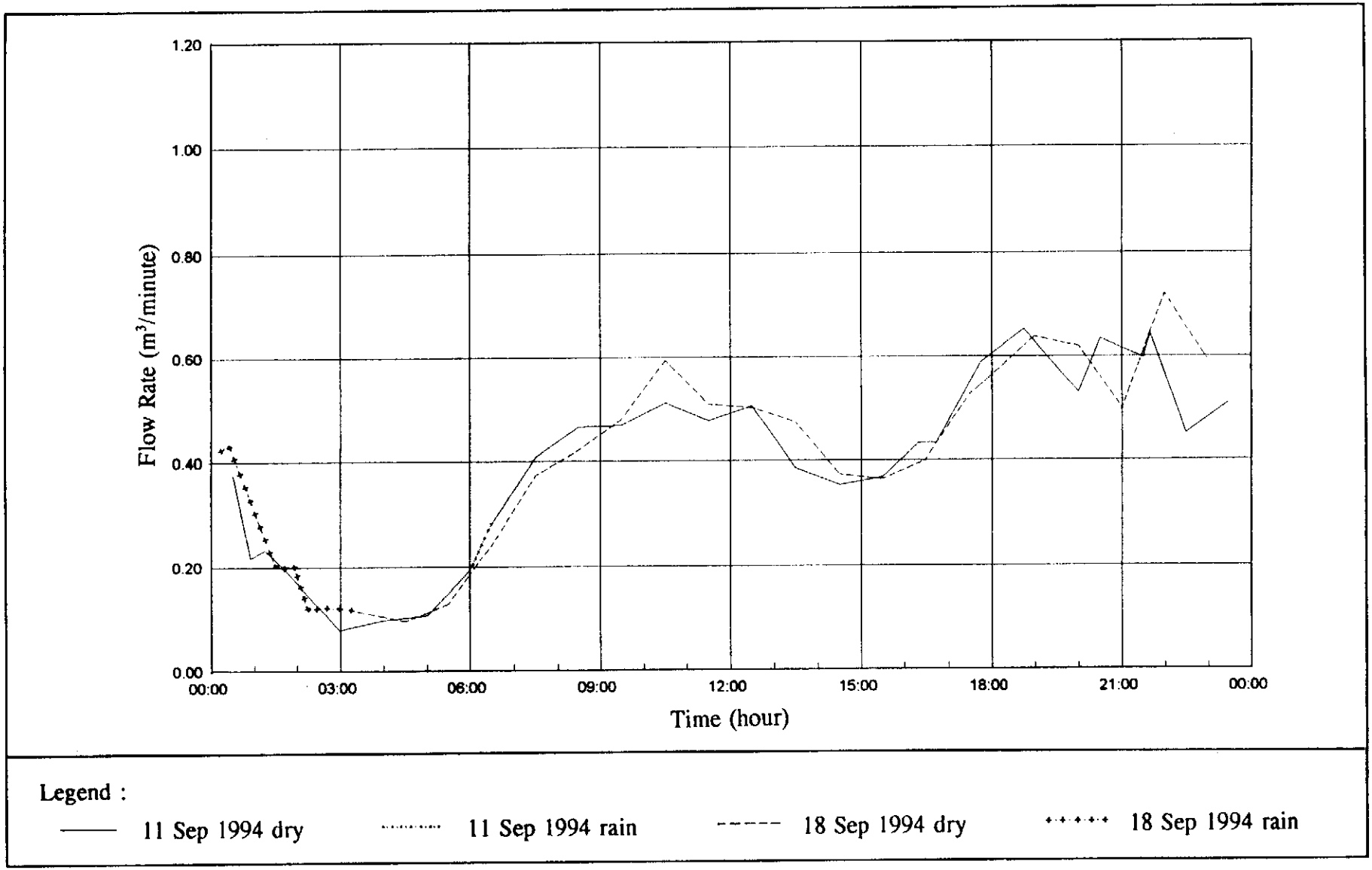

Figure J10 - Results of Flow Monitoring of the Foulwater Sewer (Sunday Records)

APPENDIX K

TOPOGRAPHIC INFORMATION, AND SITE OBSERVATIONS AND MEASUREMENTS

CONTENTS

K.1 INTRODUCTION

As a part of the landslide investigation, the available plans of Kwun Lung Lau and related works were studied. Land surveys and field inspections were carried out. From these, information on the following aspects of the landslide and the site was obtained :

(a) ground profiles before and after the landslide,

(b) surface drainage and site conditions before the landslide,

(c) landslide debris and the alignment of the severed foulwater sewer,

(d) the masonry wall,

(e) seepages on site,

(f) arrangement of the substructure of Block D,

(g) voids in the ground underneath Blocks D & E,

(h) soil suction,

(i) permeability of the ground as determined in water tests conducted underneath Block D, and

(j) infiltration tests carried out in the yard area to the south of Block D.

K.2 GROUND PROFILES BEFORE AND AFTER THE LANDSLIDE

K.2.1 Ground Profile before the Landslide

In 1983, the Hong Kong Housing Society (HKHS) engaged Fugro (Hong Kong) Ltd to design and supervise stabilisation works on slope No. 11SW-A/C115 to the east of the site of the landslide. A survey plan (drawing No. 82118/3A) showing the topography of the slope between the footway and Blocks C & D of Kwun Lung Lau was included in the report by Fugro (1984). After the completion of the stabilisation works, Fugro (Hong Kong) Ltd prepared an as-built drawing (No. 82118/5(AC)) in 1986. On the basis of the information contained in these two drawings and the results of land surveys by the Civil Engineering Department (CED) after the landslide, a plan showing the likely topography and condition of the site before the July 1994 landslide has been compiled in Figure K1.

Before the landslide, the maximum height of the masonry wall was about 10.6 m. The height of the slope between Block D and the masonry wall generally varied between 2.5 m and 6 m, at an angle of between 20° and 50° to the horizontal.

K.2.2 Ground Profile after the Landslide

The extent and profile of the landslide were determined by land surveys carried out by the CED after the landslide. A brief summary of the surveys carried out, the instruments used, the methods adopted, the overall accuracy achieved and the list of survey drawings produced are given in Table K1.

The extent of the landslide and the profile of the debris were surveyed on 24 July 1994, on the morning after the failure. On 28 July 1994, upon completion of the rescue operation and after removal of most of the debris from the landslide location, a land survey was carried out to establish the profile of the exposed landslide scar. Drawing No. GCS 2411/IB was prepared by merging the information obtained from the two surveys. This drawing and Figure K1 form the basis of the plan and cross-sections through the landslide area.

A further topographic survey was carried out by the CED on 7 August 1994 to determine the profile of the landslide site after completion of the emergency repair works.

Land surveys were also carried out to determine the ground profile underneath Blocks C, D & E of Kwun Lung Lau, and to identify potential ponding areas in the yard area to the south of the blocks. The results of the surveys are shown in drawings No. GCS 2411/VI & GCS 2411/VI. The ground surface underneath Blocks D & E was found to be sloping at an angle of between about 20° and 25° to the horizontal.

K.3 SURFACE DRAINAGE AND SITE CONDITIONS BEFORE THE LANDSLIDE

The likely layout of the surface drainage system on the slope between Block D and the masonry wall before the landslide is shown in Figure K1. This has been assessed from the approved drainage plans of Kwun Lung Lau and from drawings No. 82118/3A & 82118/5(AC), supplemented by the information obtained from site inspections after the landslide.

The slope above the masonry wall was covered with chunam. Subsidence and cracks were noted near the slope crest by the HKHS consultant during an inspection on 15 June 1994. Some unplanned vegetation on the slope and a tree at the toe of the slope above the wall are visible in photographs of the site taken during this inspection.

K.4 LANDSLIDE DEBRIS AND THE SEVERED FOULWATER SEWER

The debris of the landslide was found to include mainly soil, fragments of chunam, blocks of masonry and trees. Broken sections of the foulwater sewer, a manhole connecting the severed foulwater sewer, concrete surface drainage channels and two catchpits were recovered from the landslide debris. The total length of severed foulwater sewer pipes recovered from the landslide debris was estimated to be about 20 m.

Results of topographic surveys carried out after the landslide indicate that the volume of the failure was about 1000 m^3. Based on field measurements of the debris removed from

the landslide location, the bulk volume of the debris was estimated to be about 1500 m^3.

The approximate locations of the severed sections of the foulwater sewer in the landslide debris are shown in Figure K2. The foulwater sewer consisted of 300 mm diameter earthenware pipes, each about 1 m long, rigidly connected together by spigot-and-socket joints that were infilled with cement mortar. Some of the pipe sections uncovered from the landslide debris were partly encased in concrete up to about 100 mm thick. On two of the pipe sections (Features E & N in Figure K2) recovered from the debris, there were black stains on the soil that adhered to the outside surface of the pipe junctions and the concrete surrounds.

The portion of the foulwater sewer that was severed by the landslide was assessed to have run across the upper part of the landslide area before the failure (Figure K2). This assessment was based on field observations of the positions of the severed sewer sections in the debris, together with photographs showing the manhole locations. The drainage plan of Kwun Lung Lau approved by the Building Authority on 1 October 1968 also shows a proposed 12-inch diameter foulwater sewer along similar alignments. Based on the drainage plan and field observations, the foulwater sewer was within 2 m of the ground surface before the landslide.

K.5 THE MASONRY WALL

The masonry wall that failed was a pointed squared-rubble wall with ties and weepholes. The ties were elongated strips. The weepholes were about 100 mm in diameter at about 1.5 m spacings. The typical size of the masonry blocks found in the debris was about 300 mm high, 450 wide and 300 mm long.

Coreholes and a horizontal drillhole sunk into the unfailed section of the wall after the landslide (Appendix J) showed that this part of the wall was around 0.8 to 1 m thick. However, measurements of the exposed section of the masonry wall at the western edge of the landslide location indicated that the wall had a uniform thickness of 700 mm to 800 mm.

At the location of the failure, four inspection pits were excavated on 28 July 1994 to expose the remaining part of the wall at the footway level. Field measurements taken in these pits also confirmed that the portion of the wall that collapsed was about 700 mm to 800 mm thick.

The remaining section of the wall to the west of the landslide area was generally in good condition, with no noticeable signs of distress observed immediately after the landslide. Field measurements of the remaining section of the wall showed that its face was inclined at about 75° to the horizontal. Cracks and forward displacement were observed in the wall within a distance of about 4 m from the western edge of the landslide location. The cracks appeared relatively clean, with no trace of vegetation. It is therefore likely that these cracks occurred as a result of the landslide.

K.6 SUBSTRUCTURE OF BLOCK D

The approved plans for the substructures of the Kwun Lung Lau buildings have been examined. The substructure of Block D comprises bored piles, pile caps and structural walls that are partly buried below ground (Figure K3).

A total of seven trial pits (Figure K3) were dug underneath Block D to verify the arrangement of the pile caps and the structural walls, and to examine the condition of the fill material above the pile caps. Trial pit No. TP35 showed that, at this location, the two main pile caps (No. D-F1) are 0.7 m apart. The ground in between the pile caps comprises about 0.5 m of loose fill overlying partially weathered volcanics. The pile caps exposed by trial pit No. TP35 were found to have been cast directly on partially weathered volcanics. Similar observations were made at trial pit No. TP38.

At trial pit No. TP35, a 1.6 m high by 1.4 m wide vertical face of the ground below the yard area was exposed (Figure K3). The ground comprised loose fill. During the sinking of a borehole in the yard area to the south of Block D, heavy seepages were observed in the fill within the top part of the exposed vertical face. This indicated that the ground below the yard area was very permeable.

The approved plans for the substructure of Block D show that the structural walls are connected directly to the pile caps and that there are no openings in the parts of the walls buried below ground. This was confirmed by trial pits No. TP21, TP23 & TP25.

Two trial pits No. TP39 & No. TP41A were dug to examine the ground condition in the area bounded by the structural walls. These were excavated to a depth of about 3 m in the fill, which was found to be very wet below a depth of about 2 m. Water was observed to have ponded to a depth of about 100 mm at the base of trial pit No. TP39.

K.7 SEEPAGE OBSERVATIONS

During the first two weeks after the landslide, when the landslide scar was exposed and inspected, there was no trace of flowing water or heavy seepage from the landslide scar, as would have been expected if there was a high groundwater table or perched water table.

Local and minor seepages were observed, however, at the landslide scar and in the ground underneath Block D during the investigation (Figure K4). The seepages were observed mostly in the fill and appeared to be transient. The probable sources of seepage were traced where possible (Table K2).

K.8 VOIDS IN THE GROUND UNDERNEATH BLOCKS D & E

A number of voids were observed beneath the chunam cover at various locations on the sloping ground underneath Blocks D & E. The chunam cover at some of the void locations was broken. The extent of the voids was assessed by visual inspection and by probing through the weepholes and the broken parts of the chunam. The findings are

summarised in Figures K4 & K5.

Seven voids were found in the ground underneath Block D, and 13 voids were found underneath Block E. The voids were located in loose fill placed above the pile caps (Figures K6 & K7).

The largest void (No. 14 in Figure K4), which measured about 7.5 m by 2.5 m by 1.6 m deep, was found underneath Block E. The chunam cover above had collapsed into the void (Figure K7). Part of the base of a curtain wall was exposed by the void. This wall retains the ground of the yard area to the south. There is an opening (0.9 m by 0.15 m) near the top of the wall directly above the void. Similar openings are present at the top of other parts of the curtain wall below Blocks D & E. It appears that the openings are intended to allow water to overflow onto the ground underneath Blocks D & E in the event of flooding in the yard area.

The topographic survey carried out by the GEO showed that the opening immediately above void No. 14 is at the lowest elevation amongst all the openings in the vicinity. Void No. 14 was probably formed by erosion of the loose fill as a result of water overflowing through the opening.

In the ground underneath Block D, the largest void (No. 4 in Figure K4) was about 1.5 m wide, 3.0 m long and up to a maximum of about 1 m deep. At this location, the chunam cover was in fair condition. The void might have been formed as a result of settlement of the loose fill.

The layout of the substructure of Block D is such that any water present in the ground would have been confined by the pile caps and structural walls, and would not have been able to flow towards the landslide area. The voids are therefore considered to be unrelated to the landslide.

K.9 SOIL SUCTION MEASUREMENTS

A total of 15 jet-fill tensiometers were installed after the landslide to measure the suction in the soil (Figure K8).

Each tensiometer consisted of a 22 mm diameter porous ceramic sensing tip connected to a reservoir at the top via a plastic tube. The soil suction was measured by a dial gauge connected to the tube at a location below the reservoir. The tube and the reservoir were filled with de-aired water during installation. The assembled system was inserted into the ground through a hole formed by probing. The ground surface around the tensiometer was sealed with bentonite to prevent ingress of surface water.

All the tensiometers were installed vertically to depths ranging from 0.5 m to 3.0 m, except for the two tensiometers installed through the masonry wall to the west of the landslide area at about 20° to the horizontal. Seven tensiometers (A1, A2, B1, B2, E1, F1 & G1) were installed into partially weathered volcanics at the landslide scar, while six tensiometers were installed into fill underneath Block D.

The results are summarised in Figures K9 to K11. The soil suction below the landslide scar and in the ground behind the masonry wall generally ranged from 15 kPa to 30 kPa. However, the soil suction underneath the landslide scar dropped to about zero to 10 kPa between 19 September and 22 September 1994, when leakage was occurring from a nearby foulwater sewer that was damaged by drilling. Heavy seepages were observed at the ground surface in the area of the affected tensiometers. The suction recovered in three to four days after diversion of the damaged sewer. This demonstrated that the soil suction could reduce drastically as a result of water ingress into the ground.

In the ground underneath Block D, the recorded soil suction generally ranged from 15 kPa to 65 kPa (Figure K11).

K.10 WATER TESTS

Two water tests were carried out underneath Block D to assess the permeability of the ground. The tests involved filling trial pits with water. During each test, the water level in the pit and the tensiometers installed underneath Block D were monitored, and observations were made of any seepages in other pits.

The tests were carried out in trial pits No. TP36 & No. TP40 (Figure K12). The positions of the tensiometers and of the other inspection pits that were available for inspection of water seepage in the slope are also shown in Figure K12. A cross-section through the test location is shown in Figure K13.

Trial pit No. TP36 was 1 m by 0.7 m by 1.5 m deep, dug in fill and partially weathered volcanics (PWV), as shown in Figure K13. At the location of TP36, the fill within about 1 m of the original ground was previously removed. In the test, water was initially filled to a level that was below the top of the PWV so that infiltration into the ground could only take place through the PWV stratum. After one day, the water level was raised to the top of the trial pit. Water could then flow away through the fill layer.

The results of the water test in trial pit No. TP36 are given in Table K3. No seepages were observed in any of the inspection pits during the test. While the water level in the trial pit was within the PWV stratum, the average rate of drop in water level was about 19 mm/hour. This corresponds to a permeability of about 10^{-6} m/s for the PWV. When the pit was completely filled with water, the rate of drop in water level increased to about 40 mm/hour, and tensiometer No. TS1 showed a rapid reduction in soil suction. The permeability of the fill was estimated to be about 5×10^{-6} m/s.

The second water test was carried out in trial pit No. TP40, which was 1.9 m by 0.7 m by 0.9 m deep, dug in fill. The results of the water test are summarised in Table K4, and the amounts of water outflow from the pit are plotted in Figure K14. The seepage observations are summarised in Table K5.

The rate of outflow increased abruptly after the test in trial pit No. TP40 had been carried out for about one hour. At that time, water was filled to a depth of about 380 mm, and water seepage was observed in trial pit No. A shortly afterwards. About an hour later, water seeped into trial pits No. TP26 & No. TP27, which were at the crest of the landslide

scar. The flow into trial pit No. TP26 was rapid, and the pit was completely filled with water in about 45 minutes. It was observed that the flow into the pits was mainly through some voids at the sides of the pits, which were probably preferential flow channels in the fill.

Throughout the second test, trial pit No. TP40 could not be filled to the top, indicating that the upper part of the fill material in the pit was very permeable. The lack of response in all the tensiometers, except No. TS3S, during the test indicated that the fill material largely remained unsaturated. This suggested that water mainly flowed in the fill along some preferential flow channels rather than through the soil mass.

Based on the second water test, the permeability of the lower part of the fill stratum, where there were no noticeable preferential flow channels, was estimated to be about 10^{-5} m/s. However, the upper part of the fill stratum, with preferential flow channels, was much more permeable. The total cross-sectional area of the flow channels was observed to be about 1% of that of the fill exposed in the pit. The corresponding permeability of the flow channels was calculated to be of the order of 5×10^{-2} m/s.

The average mass permeability of the fill stratum was about 2×10^{-4} m/s.

The mass permeability of the fill determined in the second water test was much higher than that from the first water test. This may be due to the removal of the upper part of the fill stratum consisting of preferential flow channels prior to excavation of trial pit No. TP36, as noted above. The results of the water test carried out in trial pit No. TP40 are considered more representative for the fill.

K.11 INFILTRATION TESTS

Double-ring constant-head field infiltration tests, as described in Geoguide 2 (GCO, 1987), were conducted between 26 October and 28 October 1994. The object of the tests was to assess the likely rate of water infiltration into the unpaved ground in the yard area to the south of Block D. The tests were carried out at three locations (INF1, INF2 & INF3), as shown in Figure K15.

The tests were conducted with the use of a double-ring infiltrometer. This consisted of two metal rings, of 300 mm and 600 mm in diameter respectively, which were driven concentrically into the top soil to a depth of about 300 mm. Water was maintained at a constant depth of 25 mm inside the rings. The test was continued until a constant infiltration rate was attained.

The results of the analysis are shown in Figure K16. The steady-state infiltration capacities ranged between 1.1×10^{-6} m/s and 2.8×10^{-6} m/s.

K.12 REFERENCES

GCO (1987). Guide to Site Investigation (Geoguide 2). Geotechnical Control Office, Hong Kong, 362 p.

Fugro (1984). Supplementary Geotechnical Report for Slope No. 11SW-A/C115, Kwun Loong Lau Estate, Kennedy Town. Fugro (Hong Kong) Ltd, report prepared for Hong Kong Housing Society, 15 p. plus Figures and Appendices.

LIST OF TABLES

Table K1 - Summary of Land Surveys Carried out after the Landslide

Date of Survey	Scope	Instrument Used	Methods	Overall Accuracy	Relevant Drawing No.
24 July 1994	Extent of the landslide	Wild "T1" Wild "Dior"	Traversing and radiation	±100 mm	GCS 2411
24 July 1994	Profile of the debris	Hasselblad MK70 camera with 53 mm x 53 mm format film	Terrestrial photogrammetry	± 200 mm	GCS 2411/III
28 July 1994	Profile of the landslide surface after removal of debris	Topcon GTS	Radiation	± 20 mm	GCS 2411/IA GCS 2411/II
7 August 1994	Ground profile after completion of emergency repair works	Topcon GTS	Radiation	± 20 mm	GCS 2411/IV
3 September 1994 to 30 September 1994	Ground profile beneath Blocks C, D & E	Topcon GTS	Radiation	± 20 mm	GCS 2411/VI
4 October 1994	Ground profile of yard area to the south of Block E	Wild "NA1"	Ordinary levelling and tape measurement	Level ± 10 mm Length ± 35 mm	GCS 2411/V

Notes : (1) Drawing No. GCS 2411/IB was prepared by merging drawings No. GCS 2411/III & No. GCS 2411/IA.
(2) The survey drawings are kept in the GEO.

Table K2 - Locations and Amounts of Seepage Observed at the Landslide Surface and underneath Block D (Sheet 1 of 3)

Seepage Location	Details	Date	Water Source	Remarks
A	Minor seepages observed in partially weathered volcanics at surface stripping No. SS1 after removal of shotcrete cover	8 Aug 1994	Probably from subsurface seepage	
B	Minor seepages observed in fill at 0.5 m depth in trial pit No. TP7	8 Sep 1994	Probably from subsurface seepage	
C	Minor seepages observed in fill at 0.2 m depth in trial pit No. TP12	8 Sep 1994	Probably from subsurface seepage	
D	Minor seepages observed in fill at surface stripping No. SS3 after removal of shotcrete cover	8 Aug 1994	Probably from subsurface seepage	
E	Minor seepages observed in fill at 0.5 m depth in trial pit No. TP8	24 Aug 1994	Probably from subsurface seepage	
F	Minor seepages observed in fill at 1.5 m depth in trial pit No. TP1	3 Aug 1994	Probably from subsurface seepage	
G	Minor seepages observed beneath shotcrete cover near ground level in trial pit No. TP10	23 Aug 1994	Probably from subsurface seepage	
H	Minor seepages observed in fill at 1.3 m depth in trial pit No. TP11A	17 Aug 1994	Probably from subsurface seepage	
I	No seepage was observed, but there were possible signs of seepage near ground level in trial pit No. TP11	-	Unknown	
J	Minor seepages from weepholes in the ground underneath Block D	18 Aug 1994	Possibly from stormwater in the yard area to the south of Block D	

Table K2 - Locations and Amounts of Seepage Observed at the Landslide Surface and underneath Block D (Sheet 2 of 3)

Seepage Location	Details	Date	Water Source	Remarks
J	Drilling foam from weepholes in the ground underneath Block D	10 Sep 1994	Borehole drilling in the yard area to the south of Block D	Drilling advanced to about 11 m depth at the time
K	Relatively heavy seepages through a 200 mm diameter opening in the structural wall	16 Aug 1994	Possibly from stormwater in the yard area to the south of Block D	
K	Minor seepages through a 200 mm diameter opening in the structural wall	5 Sep 1994 15 Sep 1994	Possibly from stormwater and borehole drilling in the yard area to the south of Block D	
L	Relatively heavy seepages through a 200 mm opening in the structural wall	16 Aug 1994	Possibly from stormwater in the yard area to the south of Block D	
L	Minor seepages of dyed water through a 200 mm diameter opening in the structural wall	22 Aug 1994	Leakage from gully No. GT15a (See Figure J1 in Appendix J for the location of the gully)	
M	Minor seepages of dyed water from the ground underneath Block D	22 Aug 1994	Leakage from gully No. GT15a (See Figure J1 in Appendix J for the location of the gully)	Took about 9 minutes for the water to appear, and about 5 minutes for the dyed water to appear.
N	Minor seepages near a joint of a foulwater sewer pipe underneath Block D	5 Sep 1994 to 10 Sep 1994	Leakage from the foulwater sewer; took about 40 minutes to collect 666 ml on 12 September 1994	Seepage turned black and smelly. No seepages were observed at the location on 14 September 1994
O	Seepages through a weephole in the ground underneath Block D	15 Sep 1994 23 Sep 1994	Borehole drilling in the yard area to the south of Block D	Relatively heavy seepage was observed on 15 September 1994, and minor seepage was also observed on 23 September 1994 from 20 mm diameter formwork holes on the curtain wall.

Table K2 - Locations and Amounts of Seepage Observed at the Landslide Surface and underneath Block D (Sheet 3 of 3)

Seepage Location	Details	Date	Water Source	Remarks
P	Minor seepages through a weephole in the ground underneath Block D	15 Sep 1994	Borehole drilling in the yard area to the south of Block D	
Q	Minor seepages of foam through an opening below the structural wall	6 Sep 1994	Borehole drilling in the yard area to the south of Block D	
R & S	Seepages of foam from below the concrete bedding of a foulwater sewer underneath Block D	6 Sep 1994	Borehole drilling in the yard area to the south of Block D	Minor seepages of foam also observed from 20 mm diameter formwork holes on the curtain wall.
T & U	Seepages of foam from two weepholes in the ground underneath Block D	6 Sep 1994	Borehole drilling in the yard area to the south of Block D	
V	Minor leakage near the base of a foulwater sewer manhole	22 Aug 1994	Foulwater sewer	
W	No seepage was observed, but signs of heavy previous seepages were noted from below the curtain wall. A flow channel was formed on the slope surface by erosion	-	Possibly from stormwater in the yard area to the south of Block D	
X	No seepage was observed, but there were signs of previous seepage (i.e. traces of soil deposition on the ground surface were observed)	-	Possibly from stormwater in the yard area to the south of Block D	
Y	Heavy seepages were observed from the ground exposed by trial pit No. TP35 underneath Block D	28 Oct 1994	Borehole drilling in the yard area to the south of Block D	

Note : Seepage locations are shown in Figures K4 & K5.

Table K3 - Results of the Water Test in Trial Pit No. TP36

Date	Time	Suction at Tensiometers (kPa)						Water Depth in Trial Pit (mm)	Cumulative Outflow (litre)	Remarks
		TS1	TS2	TS3L	TS3S	TS4	TS5			
26 Oct 1994	10:34	34	38	33	56	51	62	0	0	Started filling
	11:01	34	38	32	56	52	63	900	86	Stopped filling
	14:30	33.5	37	33	56	52	64	750	191	-
	15:07	33.5	37	33	56	52	64	720	212	Started refilling
	15:14	33.5	37	33	56	52	64	900	230	Stopped refilling
27 Oct 1994	08:15	23.5	38	34	56	52.5	64	580	454	-
	09:30	23.5	38	34	56	52.5	64	570	461	Started refilling
	10:15	0	38	33.5	56	52.5	64	1500	719	Stopped refilling
	13:00	0	38	33.5	56	52.5	64	1390	796	Test terminated

Note : See Figure K12 for location of trial pit No. TP36

Table K4 - Results of the Water Test in Trial Pit No. TP40

Date	Time	Suction at Tensiometers (kPa)					Water Depth in Trial Pit (mm)	Cumulative Outflow (litre)	Remarks
		TS2	TS3L	TS3S	TS4	TS5			
29 Oct 1994	10:39	38.5	34.5	56.5	54	66.5	0	0	Started filling
	11:41	38	35	57	54	66.5	380	750	Filling
	13:00	38	35	56.5	54	66.5	430	4246	Filling
	14:00	38	35	52	54	66.5	580	6130	Stopped filling at 13:55
	14:20	-	-	-	-	-	270	6542	
	14:25	-	-	-	-	-	260	6555	
	14:30	-	-	-	-	-	255	6562	
	14:40	-	-	-	-	-	245	6575	
	14:45	-	-	-	-	-	240	6582	
	14:50	-	-	-	-	-	235	6588	
	15:00	38	34	19	54	66.5	230	6595	
	15:15	-	-	-	-	-	225	6602	
	15:30	-	-	-	-	-	220	6608	
	15:45	-	-	-	-	-	217	6612	
	16:00	38	34	18	54	66.5	215	6615	
	16:30	-	-	-	-	-	210	6622	
	17:00	38	34	18	54	66.5	207	6626	
	17:30	-	-	-	-	-	203	6631	
	18:00	38	34	18	54	66.5	203	6631	

Note : See Figure K12 for location of trial pit No. TP40

Table K5 - Observations Made during the Water Test in Trial Pit No. TP40

Time	Observations
10:39	Started filling trial pit No. TP40 with water.
12:00	Suddenly water flowed into trial pit No. A through a 60 mm diameter erosion hole on the side of the pit, at a level approximately 730 mm below the original ground surface. A pile cap was exposed at the base of the pit. Water ponded in the pit to a depth of about 80 mm. Water depth in trial pit No. TP40 was 440 mm at the time.
12:15	Water in trial pit No. A started to drain away.
12:30	Water started seeping into trial pit No. A rapidly through another erosion hole about 50 mm in diameter on the side of the pit, near the base.
13:15	Water started to seep into trial pit No. TP27 from two locations, one underneath and one above the shotcrete surface, at the face of the pit closest to Block D (see Figure K13). Heavy seepage into trial pit No. TP26 was observed from an erosion hole at the face closest to Block D, at a level of about 1.6 m above the base of the pit (the size of the trial pit was 1.05 m x 0.95 m x 1.8 m deep).
14:00	Trial pit No. TP26 was full of water. Continuous seepage into trial pit No. TP27 was observed from the two locations previously noted. Water continued to flow into trial pit No. A and appeared to be draining away quickly from the pit. No water seepage was observed in other trial pits. Water filling into trial pit No. TP40 was stopped.
14:15	The previously observed seepage at trial pits No. TP26 & No. TP27 diminished quickly and the seepage stopped in about five minutes. There was then no water in trial pit No. A.
Note :	See Figure K12 for locations of trial pits.

LIST OF FIGURES

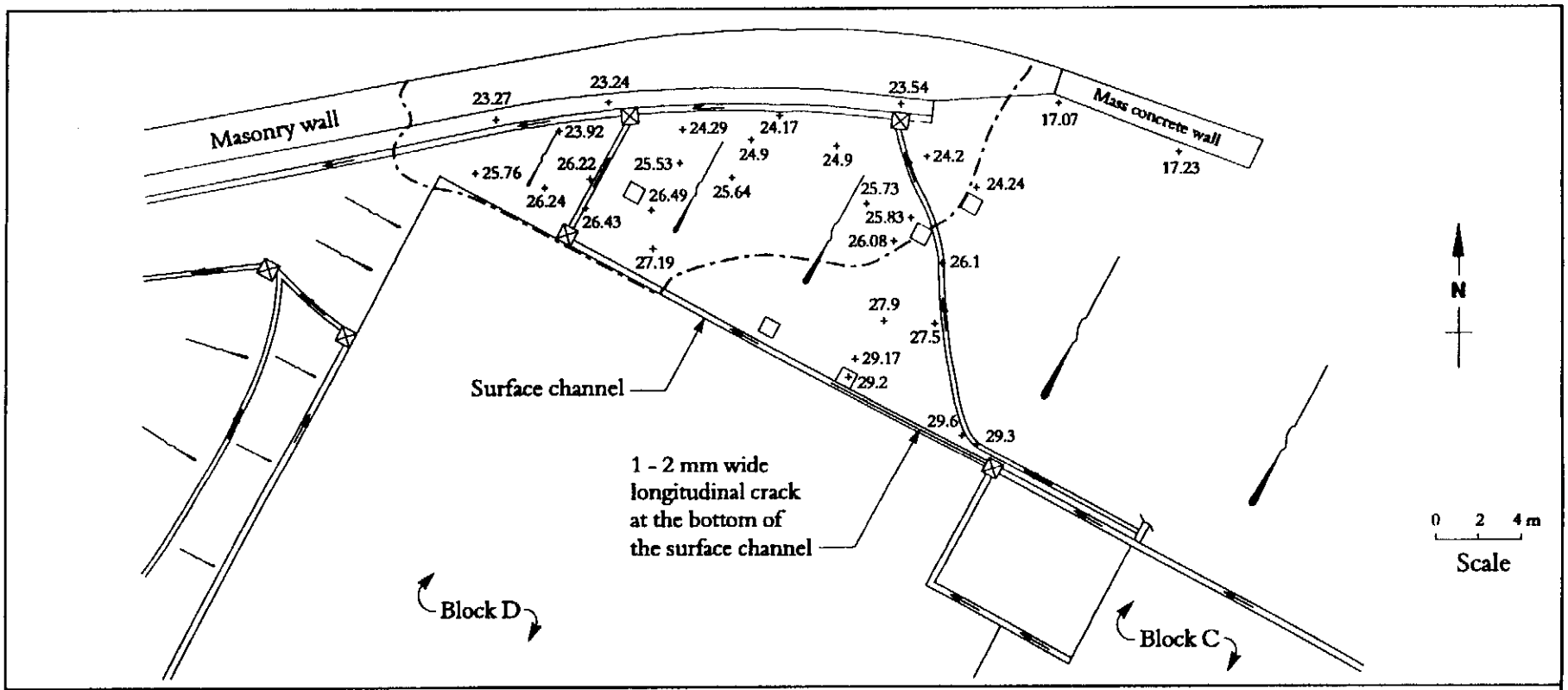

Legend :

— — —	Extent of landslide	□	Manhole	+24.2	Spot level in mPD
⊠	Catchpit	═══	Surface channel		

Notes : Information shown in this Figure is based on :

(a) drawing No. 82118/3A prepared by Fugro (Hong Kong) Ltd in 1984,
(b) as-built drawing No. 82118/5(AC) prepared by Fugro (Hong Kong) Ltd in 1986,
(c) plan No. S12B(4/2233/63) approved by the BOO on 1 October 1968,
(d) drawing No. GCS 2411/VI based on the field survey carried out by the CED after the landslide, and
(e) site observations after the landslide.

Figure K1 - Plan of the Site before the Landslide

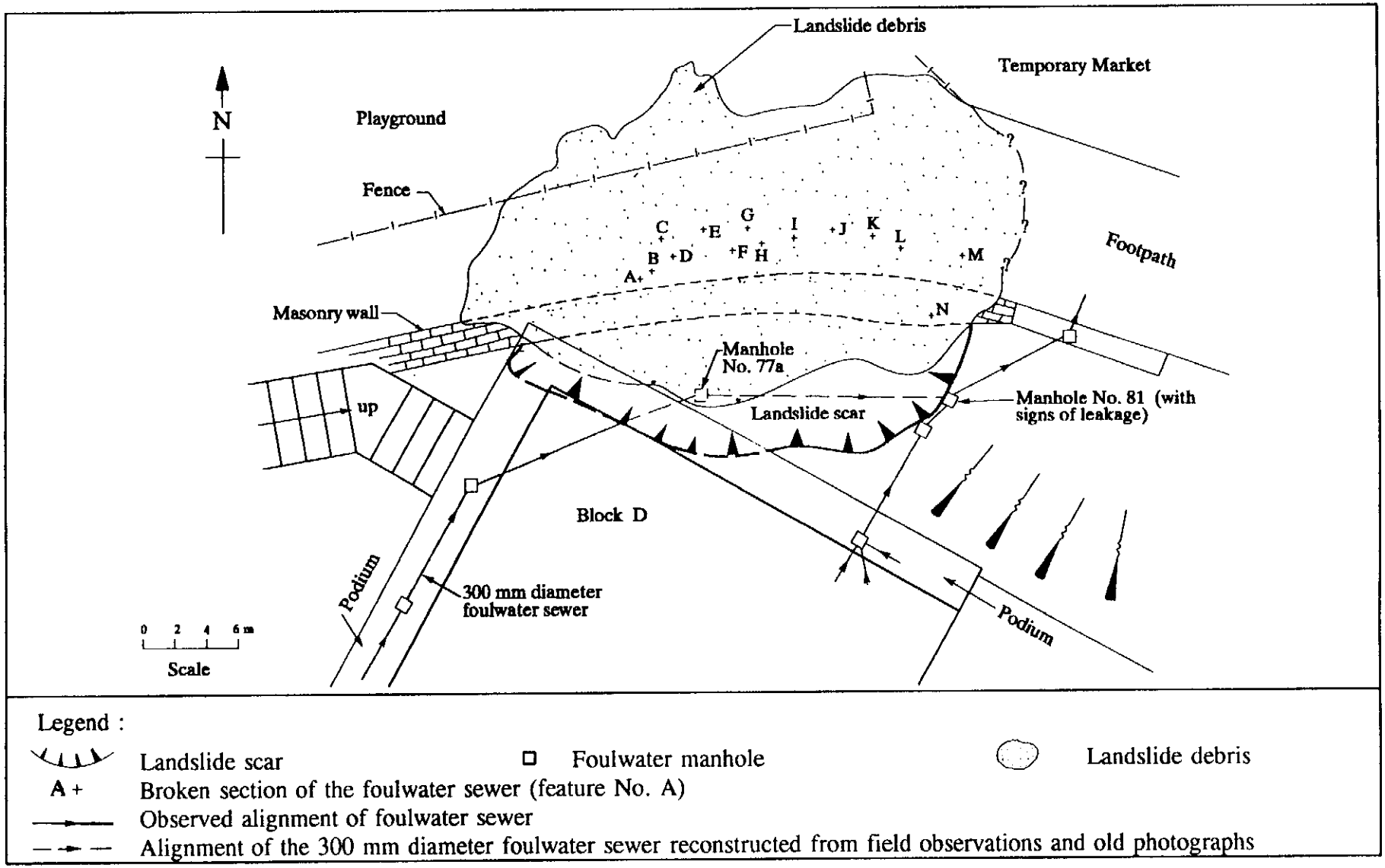

Figure K2 - Locations of Broken Sections of the Foulwater Sewer

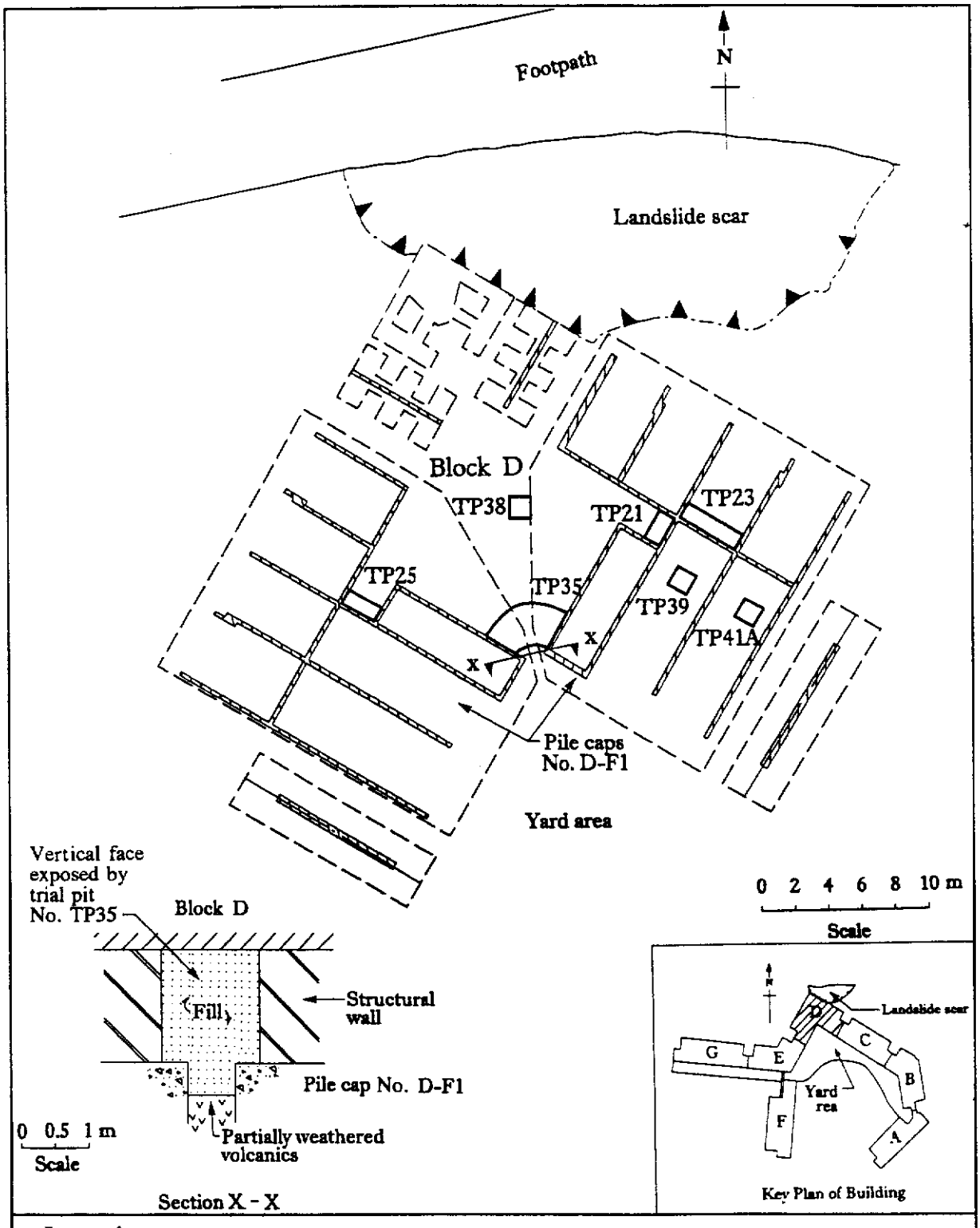

Figure K3 - Layout of the Substructure of Block D

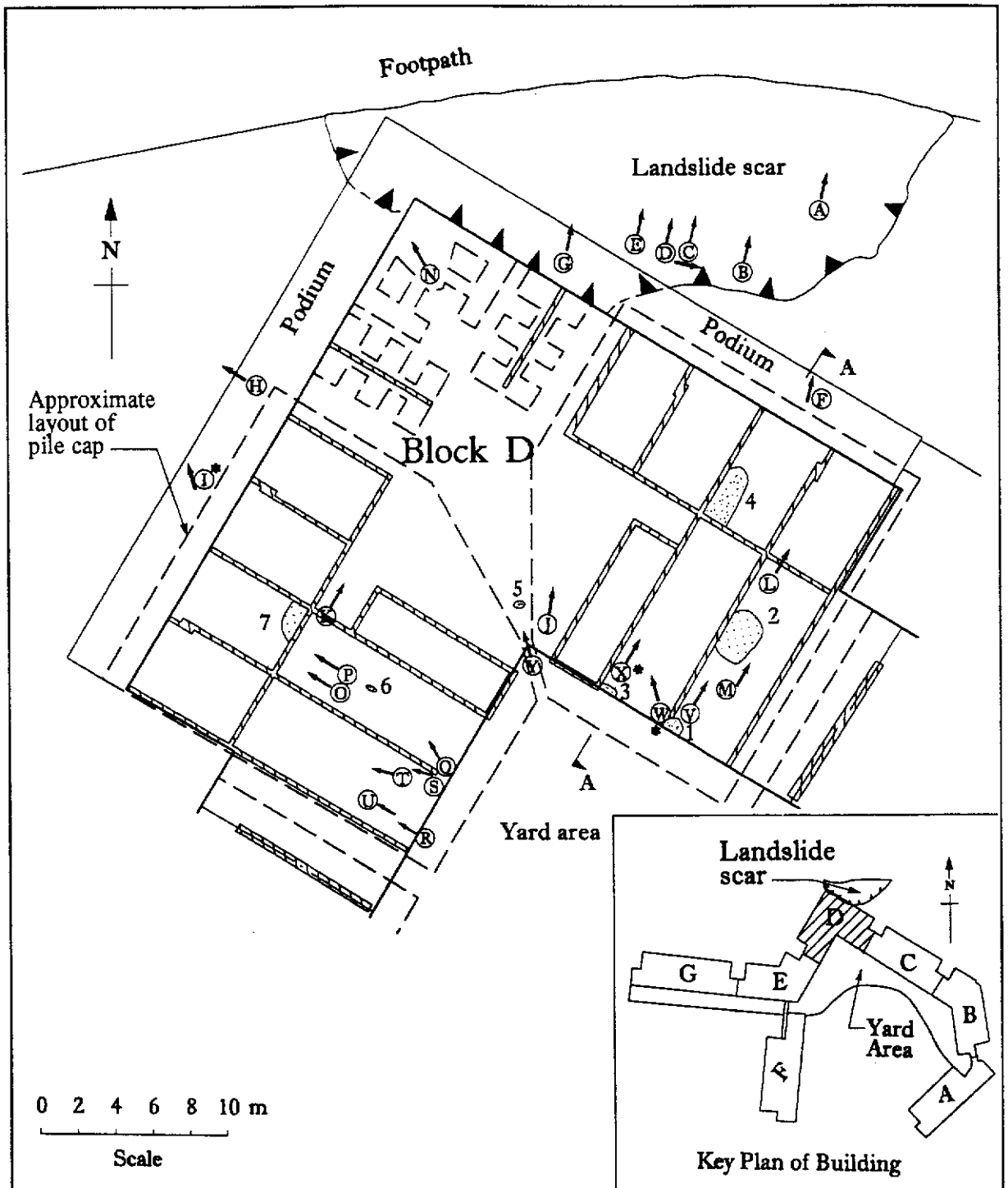

Legend :

- Structural wall on pile cap
- Seepage observed at location A
- No seepage was observed, but signs of previous seepage were noted at location W
- Void No.2

Note : See Figure K6 for Section A-A.

Figure K4 - Locations of Voids and Seepages underneath Block D

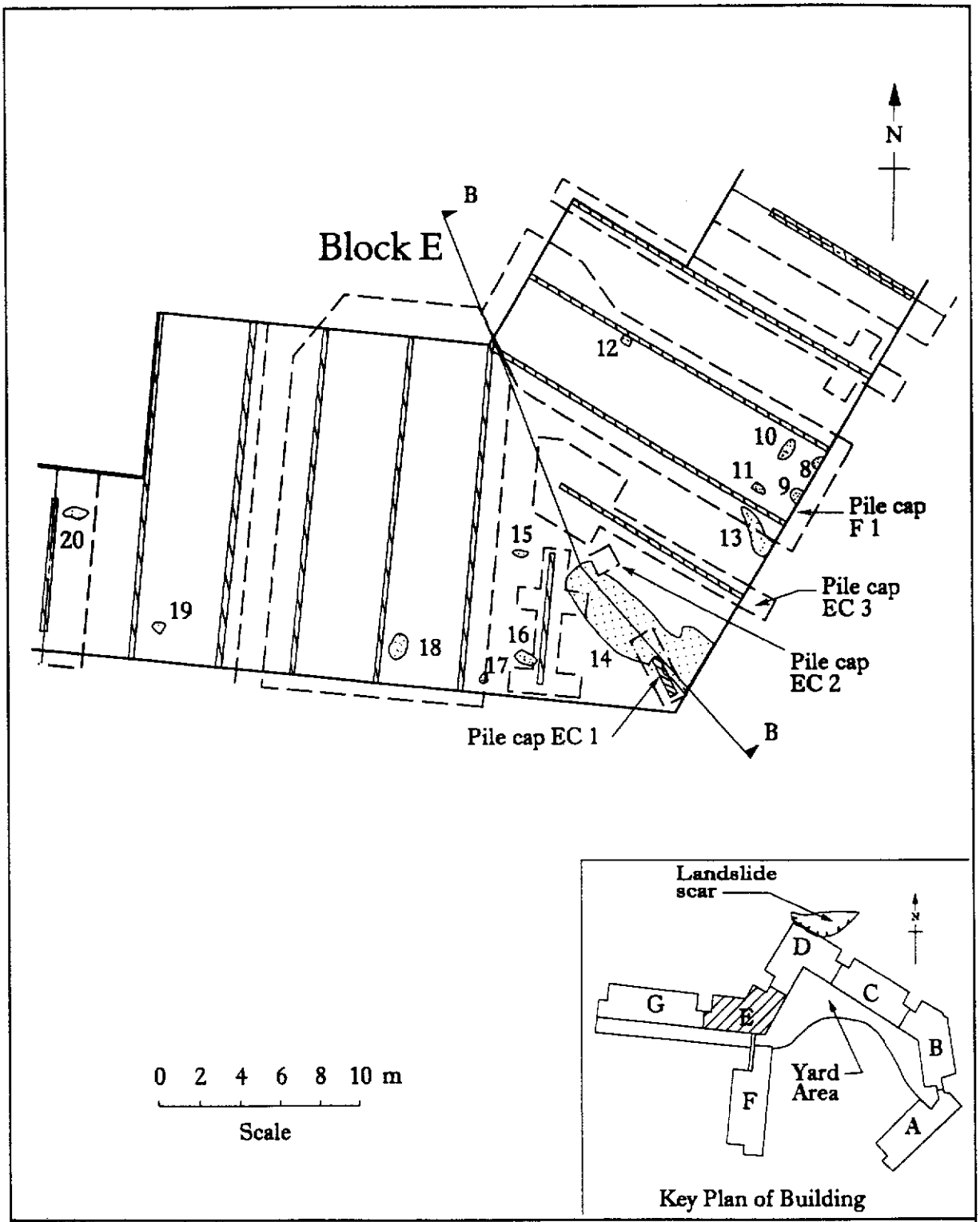

Legend :

10 Void No.10

Structural wall on pile cap

F1 Pile cap No.F1

Note : See Figure K7 for Section B-B.

Figure K5 - Locations of Voids underneath Block E

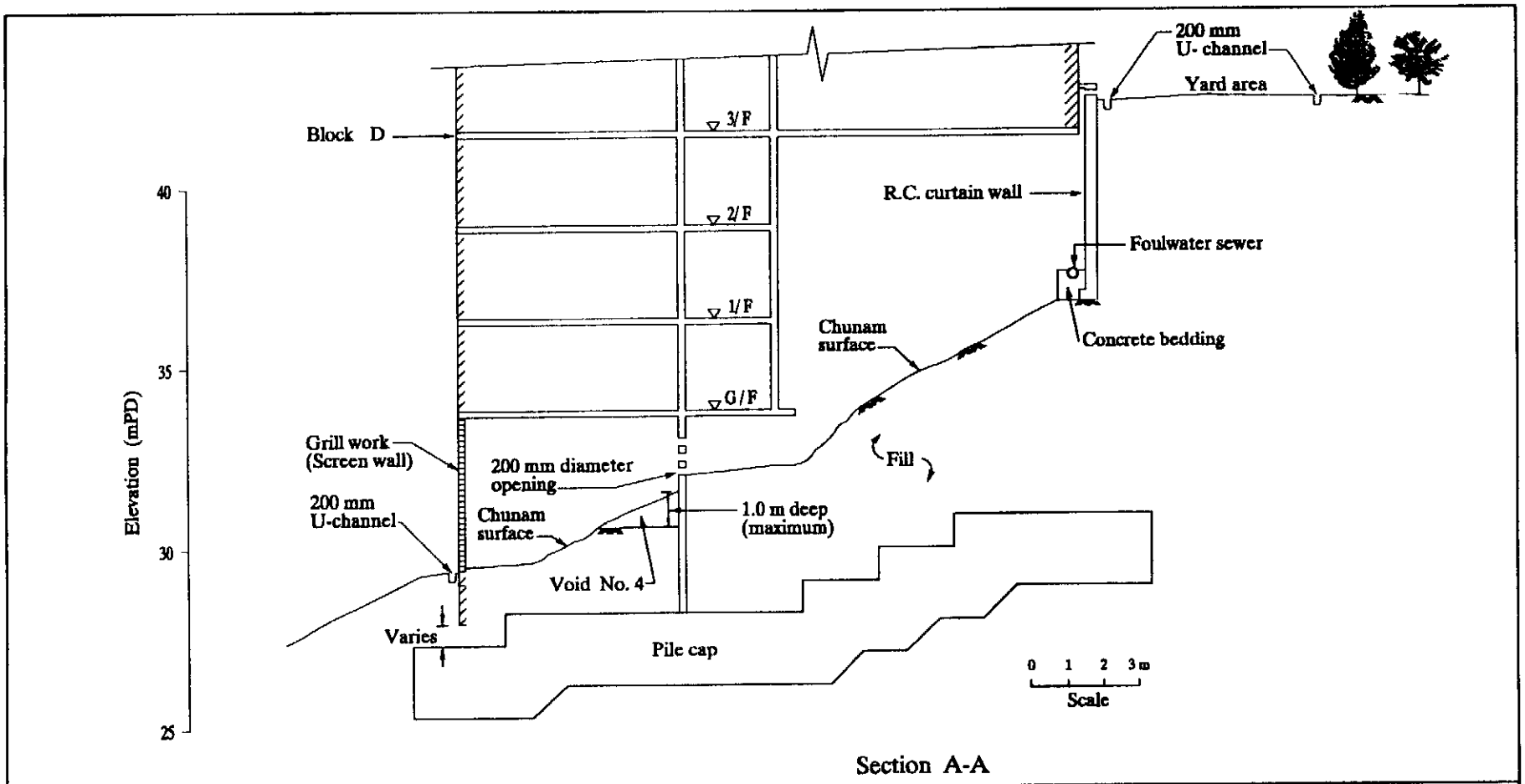

Notes : (1) Ground profile is based on survey drawing No. GCS 2411/VI.
(2) Pile cap layout is based on drawings numbered 427-64-P4A, DD1 & DD4 approved by the BOO on 15 May 1965.
(3) Piles are not shown for clarity.
(4) See Figure K4 for location of section.

Figure K6 - Section A-A through Block D

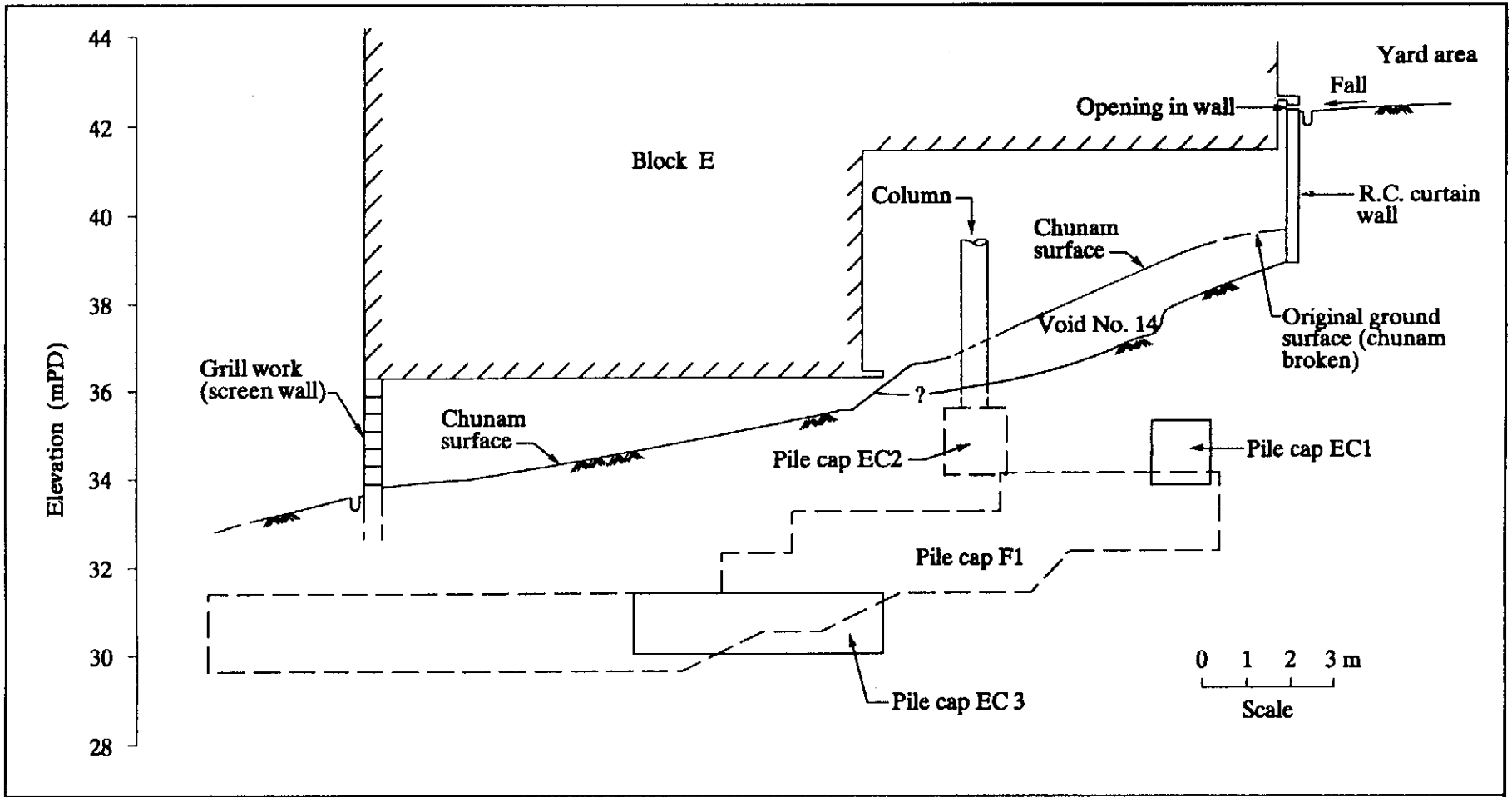

Notes :
(1) Ground profile is based on survey drawing No. GCS 2411/VI.
(2) Pile cap layout is based on drawings numbered 427-64-P5A, ED1, ED4 & ED5 approved by the BOO on 15 May 1965.
(3) Piles are not shown for clarity.
(4) See Figure K5 for location of section.

Figure K7 - Section B-B through Block E

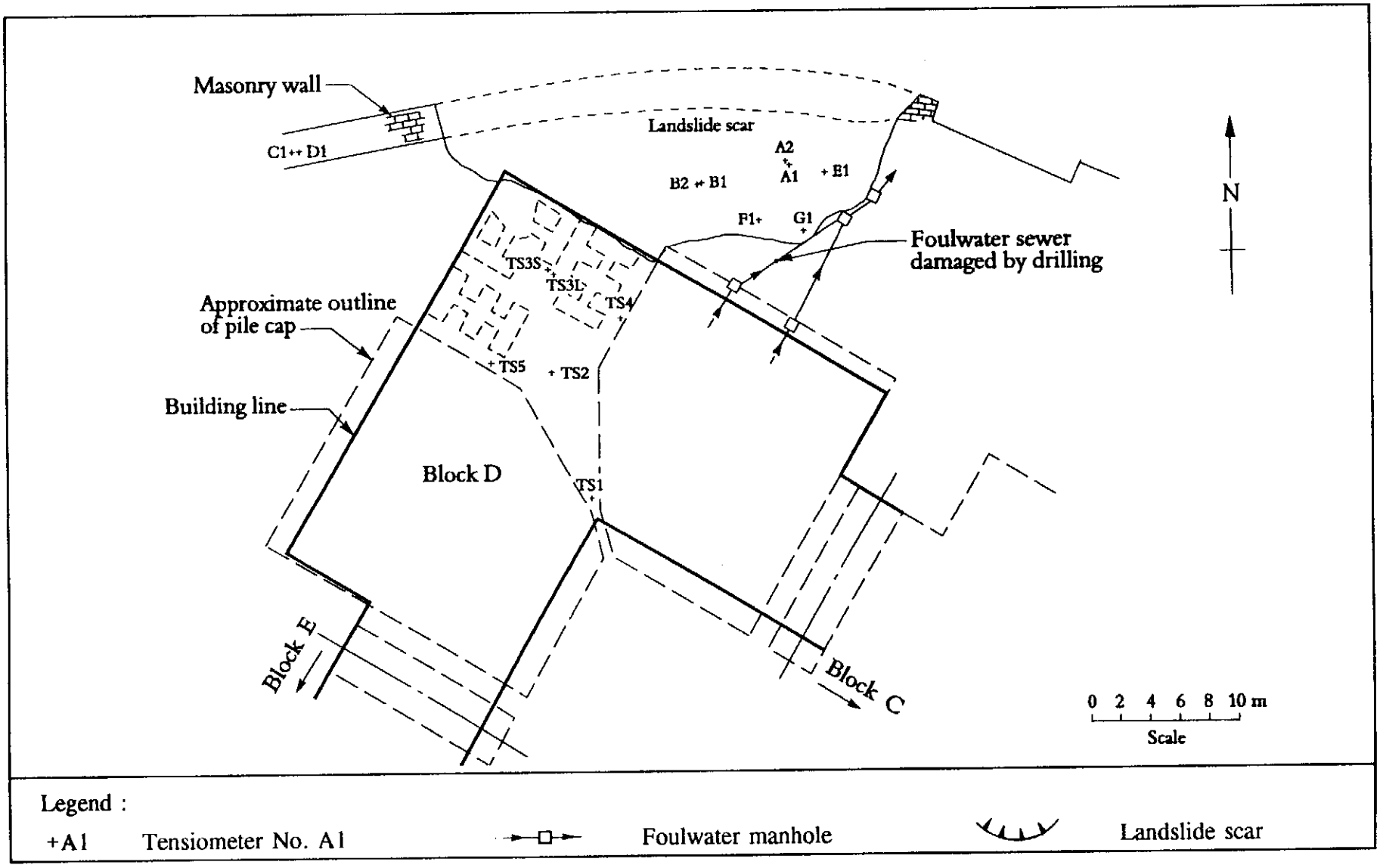

Figure K8 - Locations of Tensiometers Installed after the Landslide

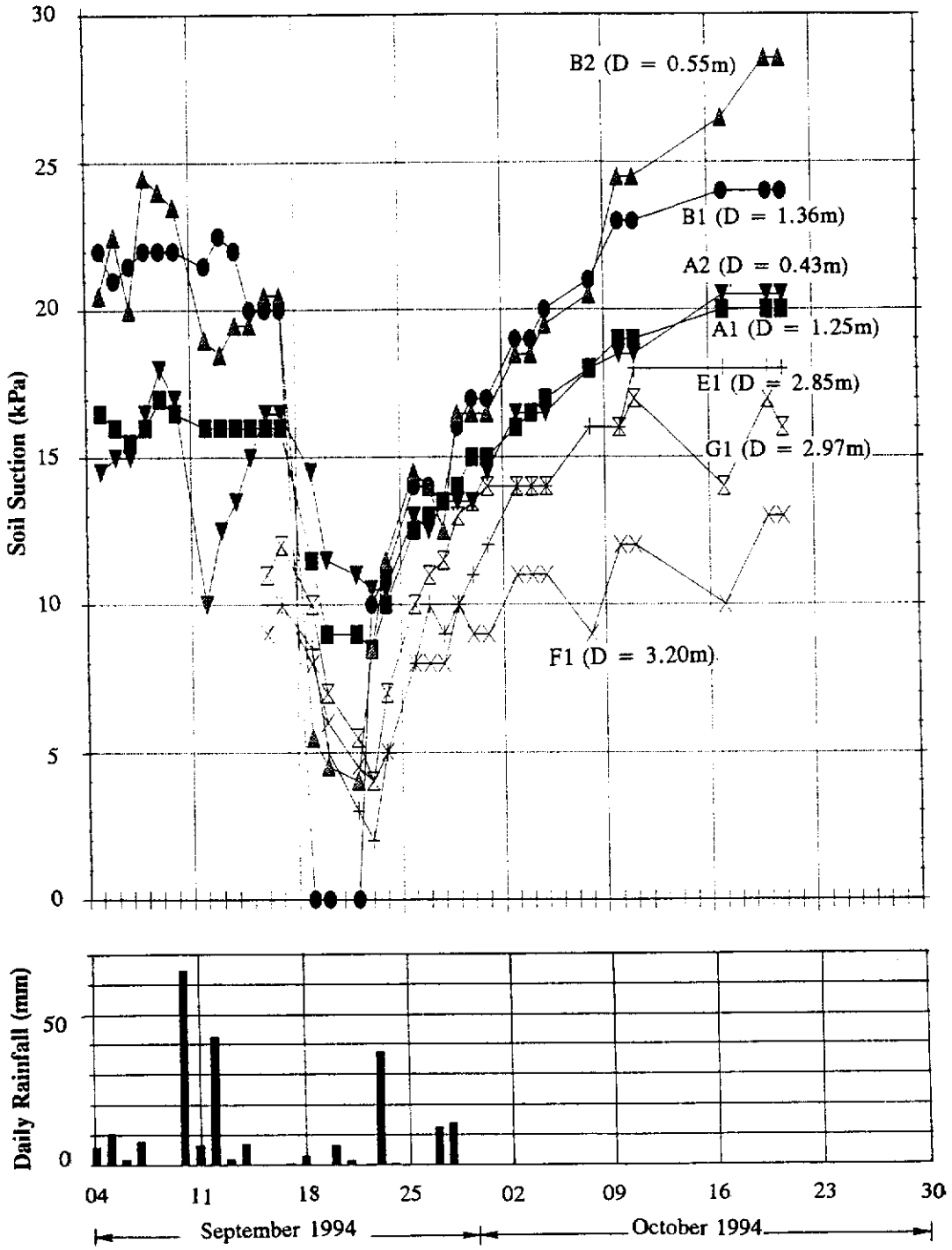

Notes : (1) D denotes depth of the tensiometer below ground level.
(2) The tensiometers were installed vertically into the ground.
(3) See Figure K8 for locations of tensiometers.

Figure K9 - Results of Soil Suction Monitoring in the Ground underneath the Landslide Scar

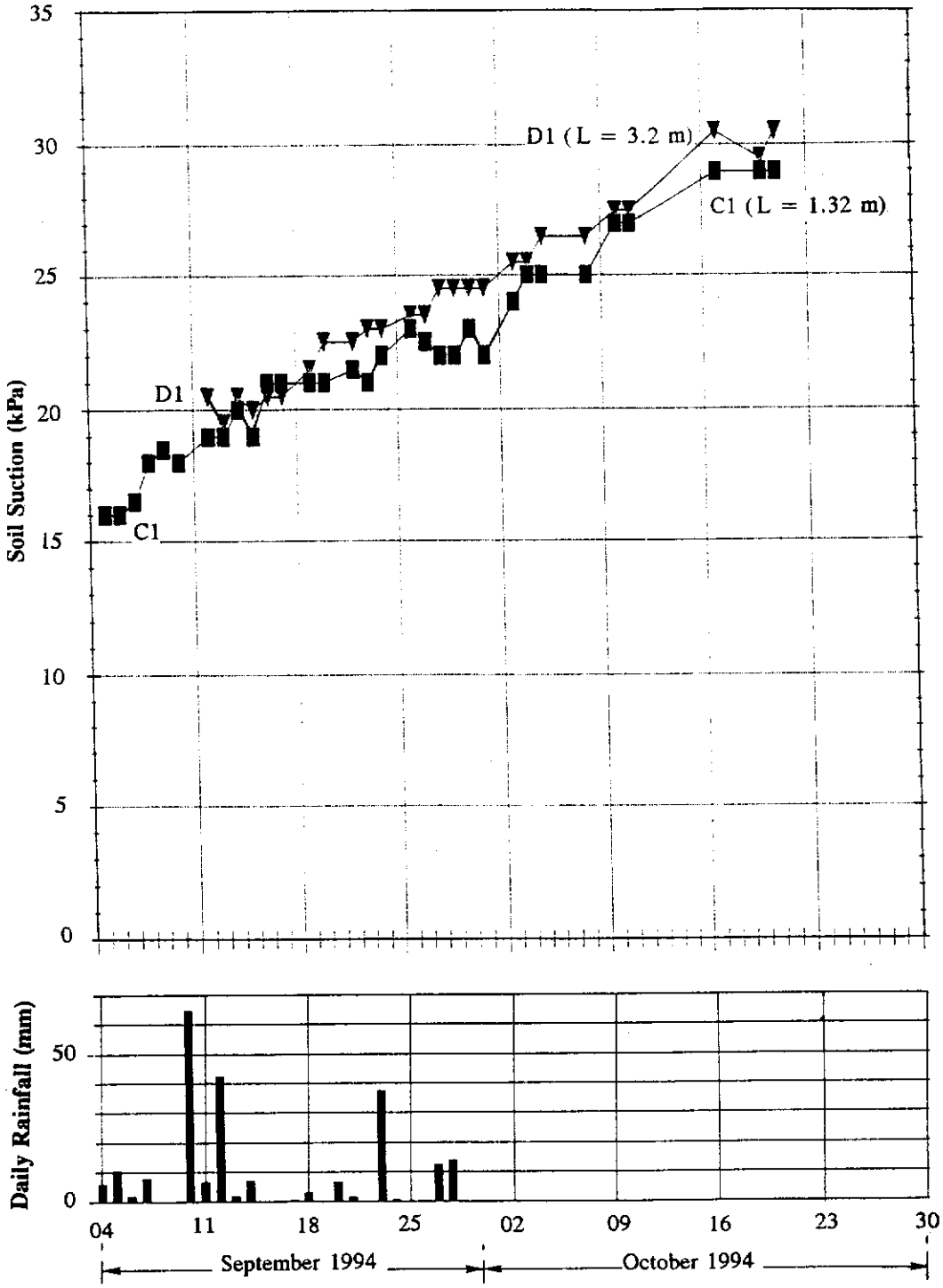

Notes :
(1) L denotes length of the tensiometer installed in the ground behind the masonry wall.
(2) Tensiometers C1 & D1 were installed at an inclination of about 20° to the horizontal.
(3) See Figure K8 for locations of tensiometers.

Figure K10 - Results of Soil Suction Monitoring in the Ground behind the Masonry Wall

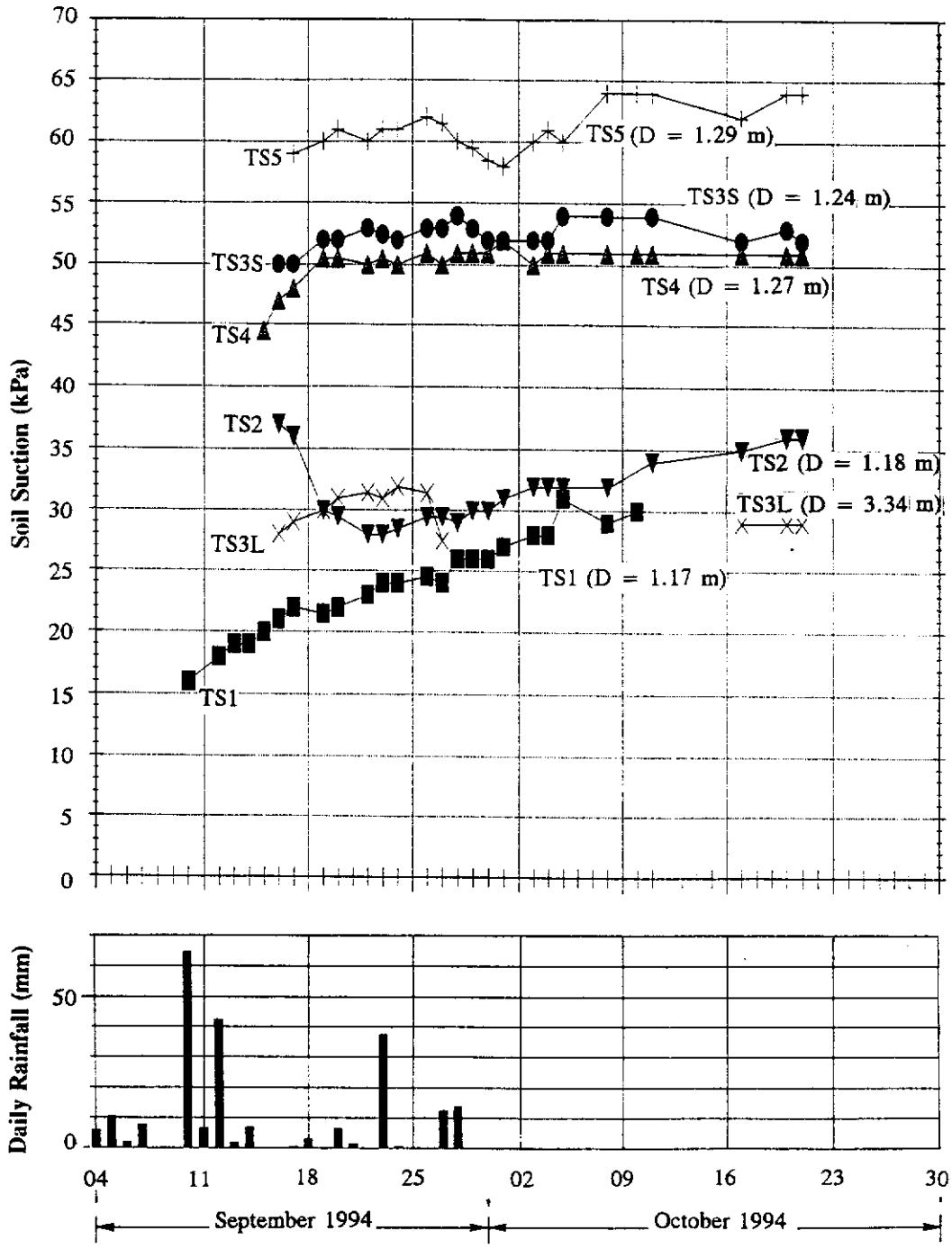

Notes : (1) D denotes depth of the tensiometer below ground level.
(2) The tensiometers were installed vertically into the ground.
(3) See Figure K8 for locations of tensiometers.

Figure K11 - Results of Soil Suction Monitoring in the Ground underneath Block D

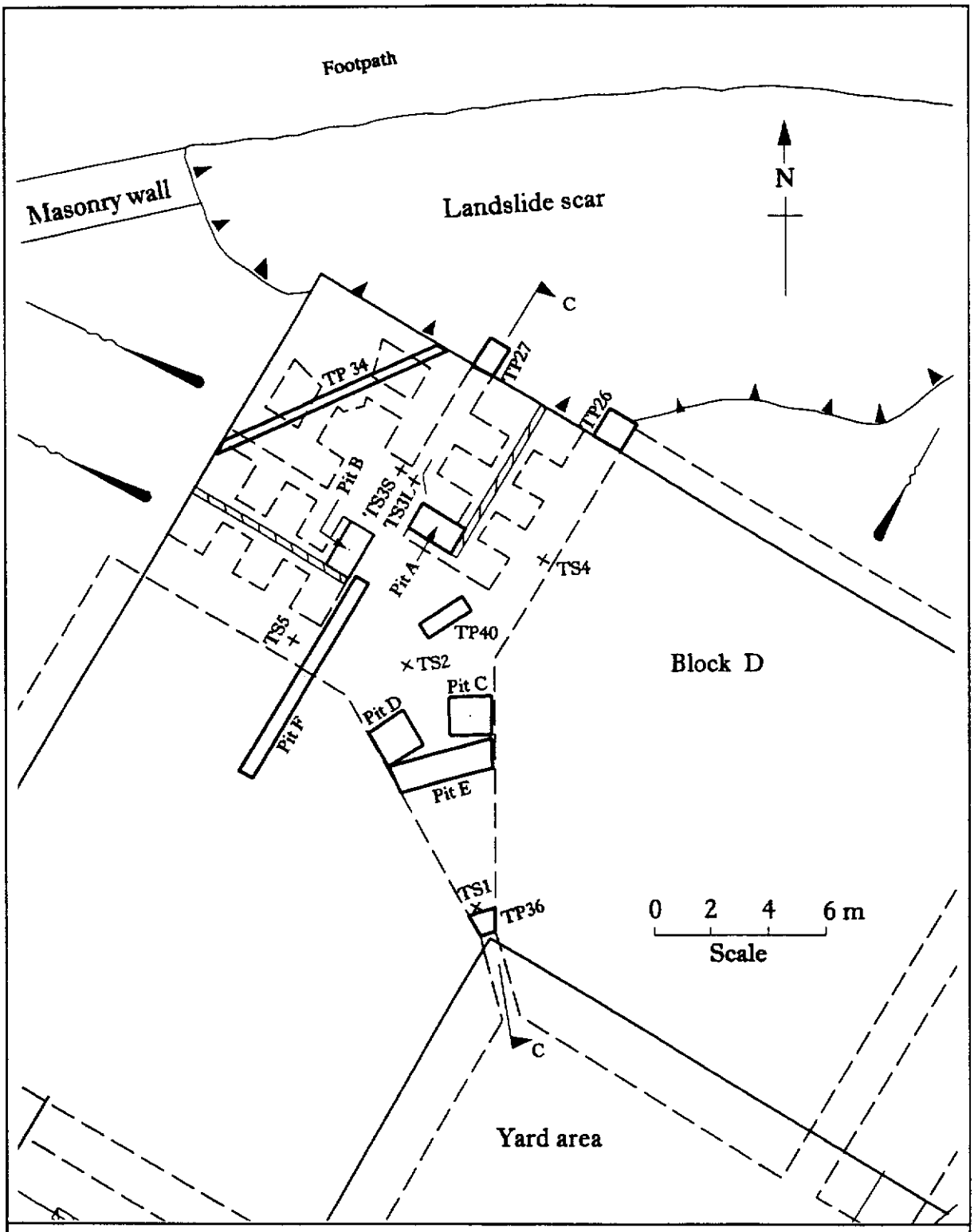

Figure K12 - Locations of Trial Pits for Water Tests underneath Block D

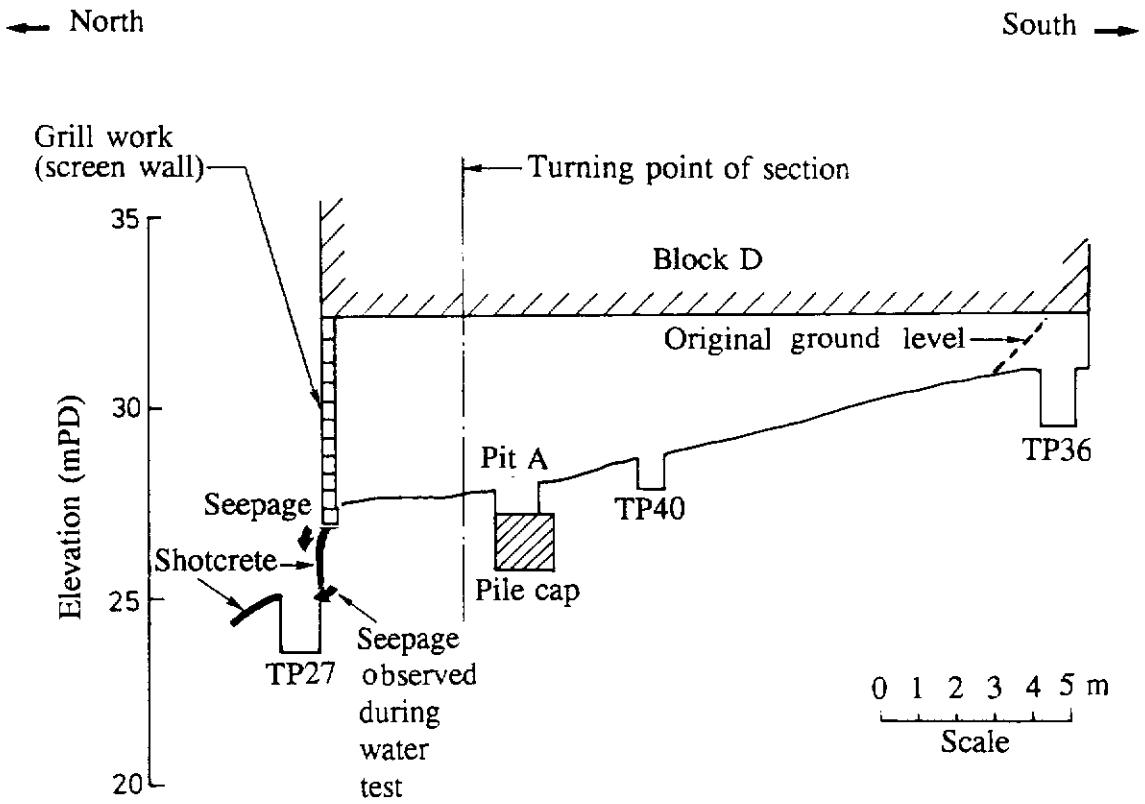

(a) Section C-C

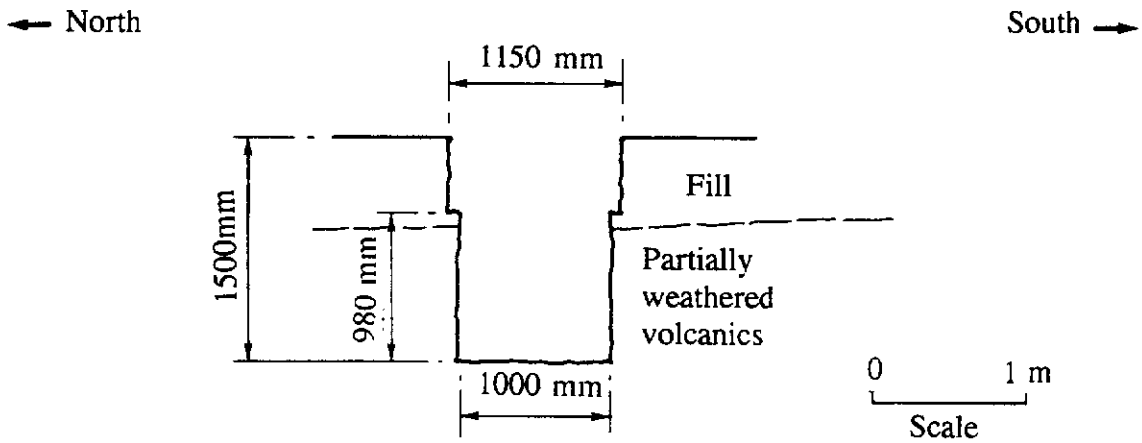

(b) Section across Trial Pit No. TP36

Note: See Figure K12 for location of Section C-C.

Figure K13 - Sections through Trial Pits for Water Tests

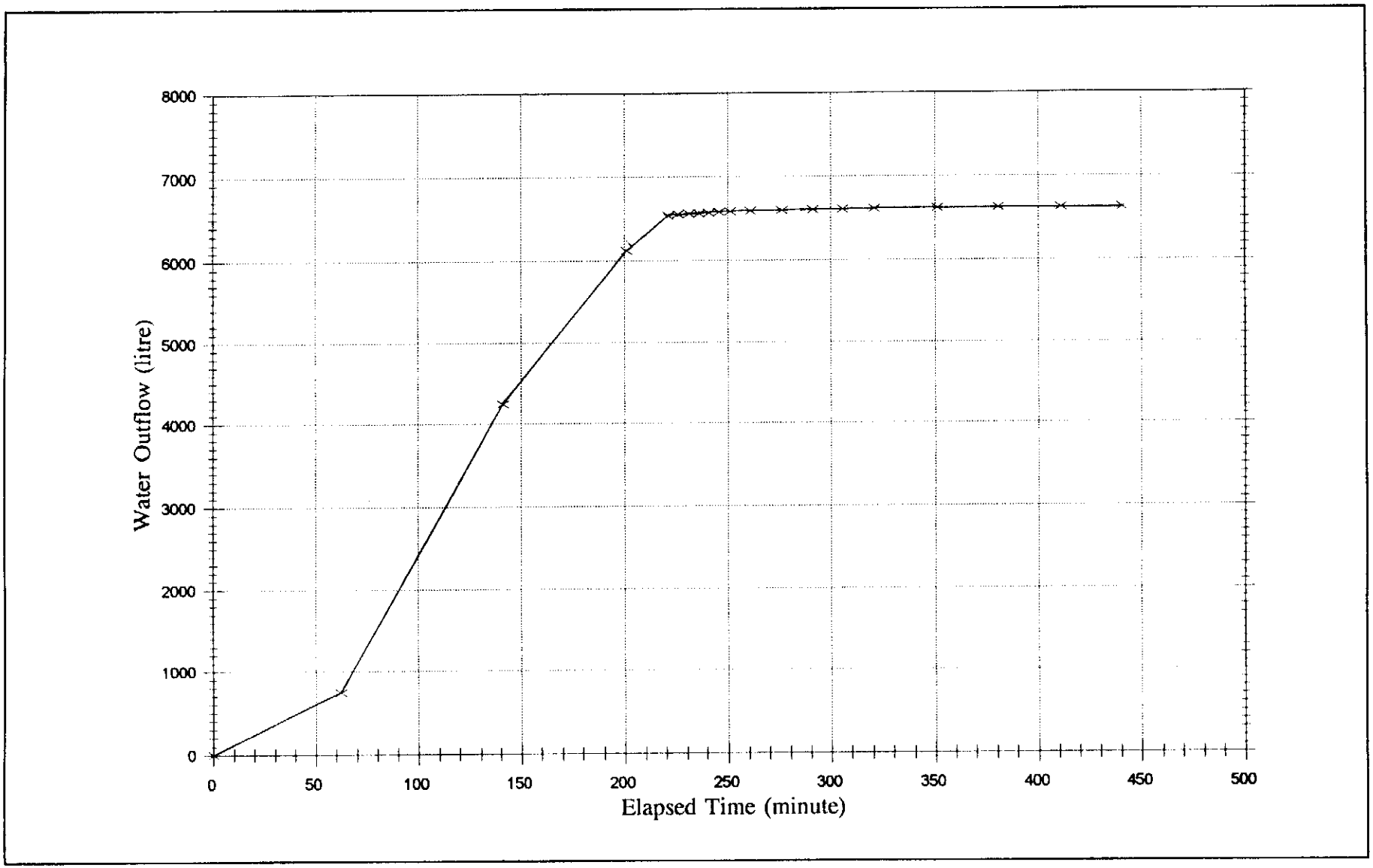

Figure K14 - Water Outflow at Different Times during the Water Test in Trial Pit No.TP40

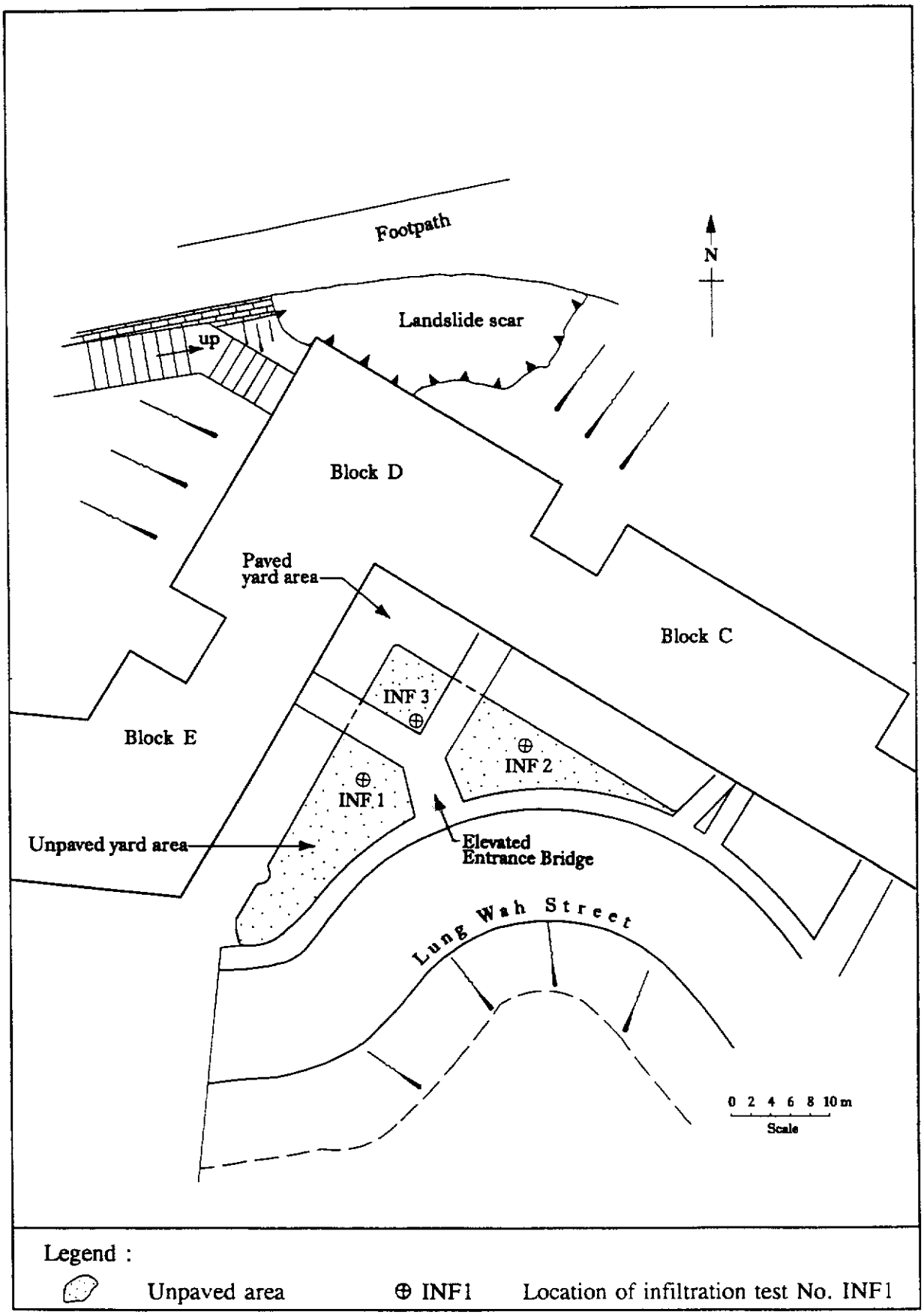

Figure K15 - Locations of Infiltration Tests

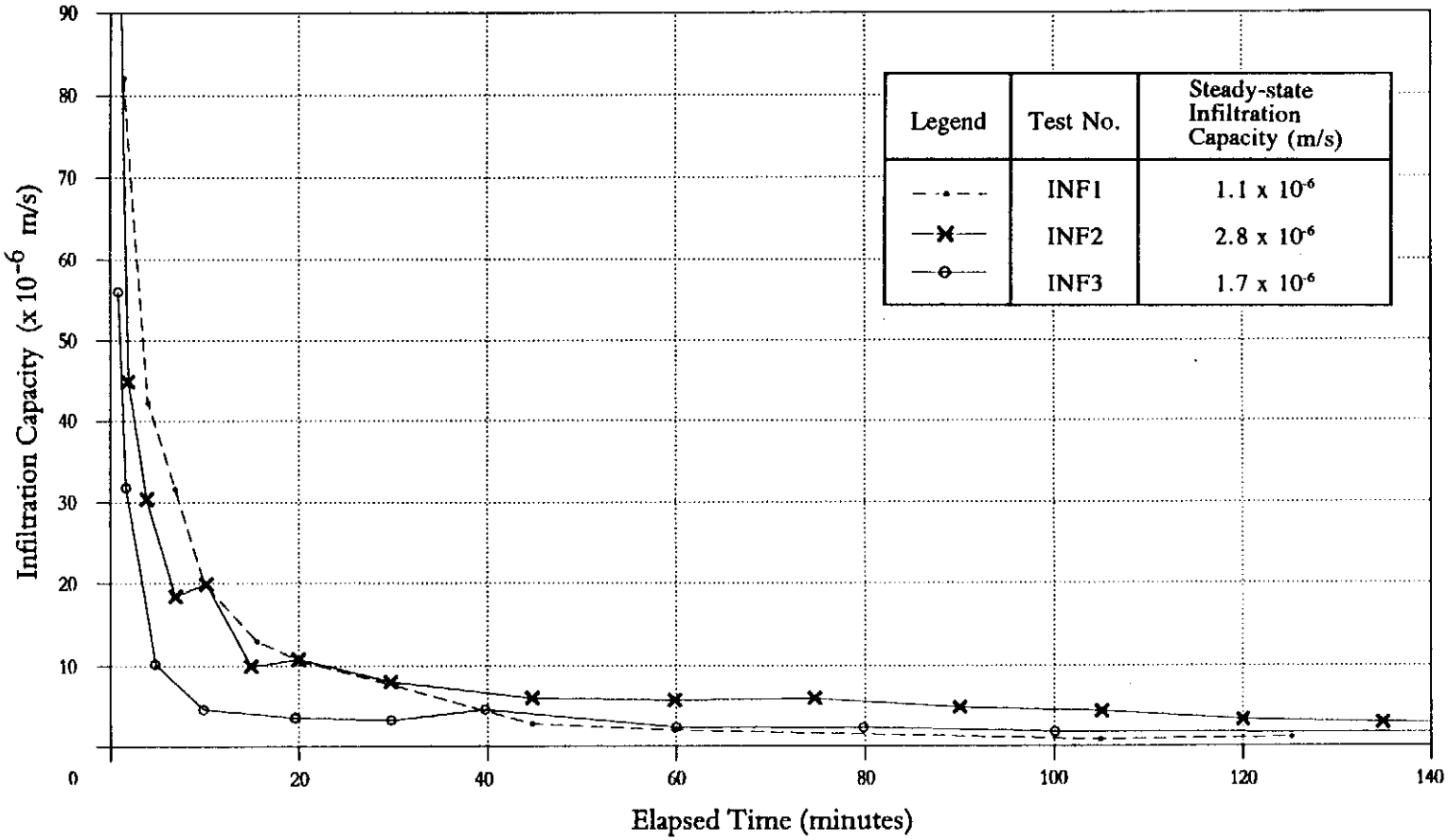

Note : See Figure K15 for test locations.

Figure K16 - Results of Infiltration Tests

APPENDIX L

ENGINEERING ANALYSES RELATED TO THE LANDSLIDE

CONTENTS

L.1 INTRODUCTION

Engineering analyses were carried out to assist in the diagnosis of the failure mechanism of the landslide. These included :

(a) limit equilibrium slope stability analyses,

(b) limit equilibrium retaining wall stability analyses,

(c) numerical analyses of the stability of the masonry wall and the slope above, and

(d) seepage analyses.

Information obtained from the post-failure ground investigation (Appendix H), laboratory tests (Appendix I), and site observations and measurements (Appendix K) was used in the analyses. Parametric studies were performed, where appropriate, to examine the effects of the different engineering parameters on the stability and mode of failure of the wall and the slope above.

The results of the analyses, together with a discussion on the main findings, are presented in this Appendix.

L.2 LIMIT EQUILIBRIUM SLOPE STABILITY ANALYSES

L.2.1 General

Limit equilibrium slope stability analyses were carried out to assess the overall stability of the masonry wall and the slope above. In the analyses, the factor of safety against shear failure along the observed landslide surface was calculated by the method of slices, using the rigorous solution given by Morgenstern & Price (1965). The computer program PCSLOPE, which was supplied by GEO-SLOPE International Ltd, was used to perform the analyses.

Three cross-sections, viz A-A, B-B & C-C, through the landslide site (Figure L1) were analysed. The sections are shown in Figures L2 to L4. Both the 1994 and 1924 ground profiles were considered. The 1994 ground profile represents the pre-failure geometry. The 1924 ground profile corresponds to the situation prior to the construction of Kwun Lung Lau, when a platform was present behind the wall, as observed in the 1924 aerial photographs.

The main ground water level was well below the landslide surface, and there was no evidence of a perched water level. Therefore, no positive pore water pressure was considered in the analyses.

The input parameters for the analyses are shown in Figures L2 to L4. An apparent cohesion, c', ranging from 0 to 200 kPa for the mortar between the masonry blocks (referred to as mortar joints in this Appendix), and c' ranging from 0 to 10 kPa for the partially weathered volcanics (PWV), were considered.

Field inspections and laboratory test results showed that the surfaces of the masonry blocks were rough and that the mortar was of good quality. The c' value of the mortar joints could be as high as 200 kPa if the joints were intact. However, tensile failure might have occurred along the joints as a result of overturning (see Section L.3) and bulging (see Section L.4) of the wall. This would damage the mortar and reduce its c'. When a mortar joint has completely failed in tension, the c' would reduce to zero.

The following two cases of ϕ' values for mortar joints were considered in the analyses :

(a) Case 1 - an angle of shearing resistance, ϕ', of 45° was adopted for the mortar joints; this value is considered representative, since the joints were rough.

(b) Case 2 - a more conservative ϕ' value of 40° was adopted to assess the effects of reduced joint roughness.

The c' value for fill, and the ϕ' values for fill and PWV, adopted in the analyses were based on the laboratory test results (Appendix I). The results of the laboratory tests on samples of CDV and C/HDV obtained from the PWV stratum suggest that c' is limited to 2 kPa if the material is fully saturated.

L.2.2 Results of the Analyses

Results of the analyses are shown in Figures L5 to L7. The calculated factors of safety for Section A-A shown in Figure L5 may be taken to be representative of the landslide. The following can be seen :

(a) For Case 1, assuming c' of the mortar joints reduces to zero, overall slope failure occurs (i.e. the factor of safety is below unity) for the 1994 ground profile, but the 1924 profile is stable if c' of the PWV is in the range of 4 kPa to 9 kPa. Assuming a c' of 2 kPa for the PWV, overall slope failure occurs for the 1994 ground profile, but the 1924 profile is stable if c' of the mortar joints is between 10 kPa and 40 kPa.

(b) For Case 2, the corresponding c' values are slightly higher to maintain equilibrium, but the results of the analyses are not very sensitive to the ϕ' value of the mortar joints.

L.2.3 Discussion

If the soil behind the wall was unsaturated, with a suction of about 15 kPa to 30 kPa as recorded during the post-failure ground investigation, c' value of the unsaturated PWV would be about 20 kPa, assuming a ϕ_b value of 39° as determined in laboratory tests (see Appendix I; ϕ^b is the angle indicating the rate of variation in shear strength relative to

changes in matric suction). In this case, the wall and slope are stable with respect to the overall slope failure mode, even if c' of the mortar joints is zero.

If the ground attained a high degree of saturation, resulting in a reduction of the c' value of the PWV to about its saturated value, overall slope failure occurs for the 1994 ground profile if there is additionally a substantial drop in the c' value of the mortar joints. Such a drop in the c' value of the mortar joints was possible if the joints were damaged as a result of the occurrence of other modes of wall instability.

The analyses also indicated that the wall is stable if there is no surcharge on the wall from the fill (i.e. with the 1924 ground profile), even if the soil behind the wall were fully saturated.

L.3 LIMIT EQUILIBRIUM WALL STABILITY ANALYSES

L.3.1 General

In the retaining wall stability analyses, the masonry wall was analysed as a monolithic structure under the action of active earth pressure. The active earth pressure was calculated using Coulomb's equation (GEO, 1993). No positive pore water pressure was assumed. The factors of safety of the wall against sliding instability and overturning instability were calculated with the aid of the spreadsheet computer program Lotus-123 (Release 3.1). No signs of bearing instability were observed in the actual landslide, and this is probably due to the fact that the masonry wall was founded on level ground comprising less weathered material. Hence, the factor of safety against bearing instability was not assessed in the analyses.

As for the slope stability analyses, Sections A-A, B-B & C-C were analysed. For the purpose of the analyses, the geometries of the sections were simplified, as shown in Figure L8. The height and back-slope angle of the sections adopted, together with the assumed material properties and interface friction parameters, are summarised in the Figure. In order to evaluate the effect of interface friction on the stability of the wall, the two cases shown in Figure L8 were analysed.

L.3.2 Results of the Analyses

The results of the analyses are plotted in Figures L9 to L12. The wall heights corresponding to Sections A-A, B-B & C-C are marked in the Figures for ease of reference. It can be seen that, with a wall friction angle of 2/3 ϕ' and a base friction angle of ϕ' (Case 1 in Figure L8), which are representative parameters (GEO, 1993), the factors of safety against sliding for all three cross-sections are marginally greater than unity. The factors of safety against overturning, however, are less than unity unless c' of the PWV is greater than about 6 kPa. If the more conservative interface friction parameters are assumed (Case 2 in Figure L8), the factors of safety against sliding and overturning are all less than unity unless c' exceeds about 12 kPa and 7 kPa respectively.

The analyses showed that the factor of safety of the wall is very much dependent on

the apparent cohesion of the PWV. The wall required some minimum apparent cohesion in the PWV for the factor of safety against overturning to be greater than unity. Figure L13 shows the minimum c' required for stability and the influence of wall friction. The minimum c' was found to be not too sensitive to the assumed wall friction. Even with the most favourable assumption for wall friction (i.e. full ϕ'), a minimum c' for the PWV of about 3 kPa is required for the factor of safety to be greater than unity.

L.3.3 Discussion

The analyses indicate that overturning is a critical mode of wall instability. Although the calculated factor of safety against sliding can be less than unity for smaller wall base friction values, sliding instability is not considered critical because the base friction is likely to be on the high side. Some previous laboratory investigations carried out by the GEO (Pun & Shen, 1993) have shown that the friction that can be generated at the base of a retaining wall is very close to the shear strength of the founding material.

The retaining wall is stable when the c' value of the PWV is high as a result of suction forces in an unsaturated soil. However, if the soil becomes substantially saturated, with the c' value reducing towards its saturated value of 2 kPa, the retaining wall becomes unstable in overturning.

L.4. NUMERICAL ANALYSES OF THE STABILITY OF THE WALL AND SLOPE

L.4.1 General

In the slope and retaining wall limit equilibrium stability analyses described above, the factors of safety against individual prescribed failure mechanisms, such as sliding along a slip surface or the wall overturning as a monolithic structure, were assessed. However, the actual failure of the wall could have involved a much more complex mode involving a combination of different mechanisms.

Numerical analyses were carried out to examine the failure mechanism of the wall and to assess the operating shear strength parameters. The analyses modelled the response of the masonry wall and the retained ground when the soil shear strength was reduced upon saturation, without any prior assumptions having been made about the mode of the failure.

The analyses were carried out with the use of the finite difference computer program Universal Distinct Element Code (UDEC), supplied by ITASCA Consulting Group, Inc. UDEC is a two-dimensional numerical analysis program based on the distinct element method for solving problems involving a discontinuum, with provisions for modelling a continuum. In the analyses, the masonry wall was modelled as a discontinuum, and was represented as an assembly of discrete blocks with mortar in between. Large displacements along the mortar joints and rotation of the blocks were allowed in the program. The retained ground was modelled as a continuum, which was subdivided into a mesh of finite difference elements (Figure L14), and each element was given its own stress-strain properties.

L.4.2 Modelling Procedures

As illustrated in Figure L15, the modelling procedures involved the following three stages :

(a) Stage 1 - level ground consolidation under a uniform insitu stress ratio (Ko).

(b) Stage 2 - excavation of the ground in front of the wall, with high shear strength parameters being adopted for the fill and PWV strata to simulate unsaturated soil conditions.

(c) Stage 3 - soil saturation, which is simulated by a reduction of the shear strength of the soils from the unsaturated values to the saturated values.

L.4.3 Material Properties

The material and joint properties assumed in the analyses are summarised in Table L1. The PWV stratum was subdivided into two layers. The upper layer was denoted PWV_U, which covered the PWV above the observed landslide surface, whereas PWV_L referred to the PWV below the landslide surface.

Typical material stiffness parameters (K & G) were adopted for the fill, PWV_U and PWV_L, and appropriate joint stiffness parameters (JKN & JKS) were adopted for the interface elements. The material stiffness parameter of the masonry blocks was assumed to be higher than those of the soils by two orders of magnitude. The results of the analyses were not sensitive to the material and joint stiffness parameters since the analyses were aimed at assessing the behaviour at failure.

The actual stiffness of the masonry blocks may be even higher. However, the use of a higher stiffness in the analyses is not warranted because this would have little effect on the results and would have significantly increased the running time of the program.

The strength parameters c' and ϕ' for the mortar joints were representative values for intact joints (Section L.2.1). The constitutive model adopted in the analyses for the joints simulated the effect of damage to the joints due to tensile or shear failure, with the c' of the failed portion of the joints assumed to be zero.

The values of c' and ϕ' for saturated fill, and ϕ' for saturated PWV_U and PWV_L, were best-estimate values based on the laboratory test results. A range of value of c' from 0 kPa to 10 kPa was considered for saturated PWV_U in the analyses. The unsaturated c' of fill and PWV_U was taken to be 20 kPa, which corresponds to the range of soil suction (15 to 30 kPa) recorded by tensiometers installed after the landslide.

The c' value of the PWV_L was taken to be 20 kPa, which is realistic in view of the recorded soil suctions and the possible presence of less weathered material in the stratum. In effect, this limited the failure area to the ground above the observed failure surface.

The ratio of insitu horizontal stress to vertical stress (Ko) in the ground was taken to be 0.5. This value is considered representative, and is commonly adopted in analyses of retaining walls in Hong Kong.

L.4.4 Types of Analysis

The following three batches of analyses were carried out :

(a) Batch No. 1 - the full height of the retained soil was assumed to be saturated in the Stage 3 analysis; this was to examine the wall stability and the failure mode for different c' values of saturated PWV_U.

(b) Batch No. 2 - a c' of 8 kPa (based on the results of the Batch 1 analyses) was adopted for saturated PWV_U; this was to assess the wall stability and the failure mode for different depths of soil saturation.

(c) Batch No. 3 - this was a parametric study to examine the sensitivity of the effect of using different stiffnesses for PWV_L, different c' and t' values (Table L1) for the mortar joints, a higher Ko value (= 1.0) and a higher stiffness value for the masonry blocks.

L.4.5 Results of the Analyses

The results of the analyses are summarised in Table L2.

The Batch No. 1 analyses enable the following conclusions to be drawn :

(a) Failure occurs if c' of the PWV is less than 9 kPa for Section C-C, and less than 7 kPa for Section A-A.

(b) The wall fails in a complex mode, as illustrated in Figures L16 & L17. These Figures show the results of the UDEC analyses for the 1994 Section C-C upon soil saturation, and they depict the mode of wall deformation and slope movement during the landslide. The wall is found to bulge initially at about mid-height, accompanied by overturning of the portion of the wall below this level. These deformation modes combine to lead to tensile failure and, hence, reduction of the shear strength of the mortar joints. Wall bulging and overturning continue, resulting in brittle fracture of the wall at about mid-height (Figure L16(d)). The ground behind the wall loses support and slides forward. The analyses suggest that the upper part of the masonry wall rotates backward as a result of the

displacement of the sliding mass, and is predicted to come to rest on the surface of the debris, with the front face of the wall facing upward. The lower portion of the masonry wall is predicted to disintegrate and become buried by the debris.

(c) The results of the analyses indicate that, once instability is initiated, the wall deforms rapidly and failure develops in an uncontrolled manner.

(d) The results of the analyses on the stability of the wall before the construction of Kwun Lung Lau are shown in Figure L18. The wall is stable under the 1924 ground profile, even if the PWV_U is fully saturated. The resulting deformation of the wall is small, with a maximum horizontal displacement of about 40 mm.

The Batch No. 2 analyses enable the following conclusions to be drawn for the 1994 ground profile :

(a) If the extent of soil wetting is small, say confined to the upper 6 m of the retained ground, the wall and slope are stable (Figures L19 to L21). However, the wall is unstable when the depth of wetting of the PWV_U extends to 8 m (Table L2).

(b) The maximum horizontal displacements of the wall for a depth of wetting of 2 m, 4 m and 6 m are about 1 mm, 3 mm and 11 mm respectively (Figures L19 to L21).

The Batch No. 3 analyses indicate that the results are not sensitive to the stiffness of the PWV_L, the value of Ko, or the apparent cohesion and tensile strength of the mortar joints.

L.4.6 Discussion

The UDEC analyses show that the operating c' of the PWV_U for the 1994 landslide is about 6 kPa to 8 kPa. These are considered best estimates of the c' value of the PWV_U, because representative values were adopted for the other parameters in the analyses, and a realistic failure mode is predicted.

For the 1924 ground profile (i.e. before the construction of Kwun Lung Lau), the analysis shows the wall to be stable, even if the ground behind the wall is fully saturated.

For the 1994 ground profile (i.e. after the construction of Kwun Lung Lau), the analysis shows that the wall remains stable with relatively small deformations if the depth of saturation is not extensive. This is consistent with the fact that no significant signs of distress were observed in the wall over the years. The stability of the wall was undoubtedly derived from the contribution of soil suction to the unsaturated shear strength.

Laboratory test results (Appendix I) indicate that the saturated c' value of the CDV and C/HDV is no higher than 2 kPa, and the analyses show that failure occurs if the ground above the observed landslide surface (i.e. the PWV_U) is substantially saturated. Failure still occurs even if c' value is a few kPa higher, which might be the case for the insitu PWV_U, because of the presence of less weathered material in the stratum and bonding which may not be readily detectable in conventional triaxial and shear box tests.

The UDEC analyses have predicted that the wall would fail according to a complex mechanism, involving a combination of bulging and overturning modes followed by total collapse of the ground. The failure has been predicted to be brittle and, once initiated, to develop in an uncontrolled manner. The results of the analyses are consistent with the observed mode of failure and the disposition of the collapsed masonry wall within the debris.

L.5 SEEPAGE ANALYSES

L.5.1 General

The purposes of the seepage analyses were :

(a) to estimate the amount of water that could have flowed from the yard through the ground underneath Block D to the landslide area, and

(b) to assess the extent of the ground behind the masonry wall that could have become substantially saturated.

The analyses considered the 50-hour period between the commencement of the rainstorm and the time of the landslide.

The analyses inevitably involved an idealisation of the ground properties. Given that soil can be very heterogeneous with regard to hydraulic parameters, the principal aim of the analyses was to provide a basis for assessing the relative importance of the various sources of water in triggering the landslide, rather than to give a precise prediction of the pattern of water flow.

The analyses were carried out using the finite element computer program SEEP/W supplied by GEO-SLOPE International Ltd. A plan section and a vertical section of the ground underneath Block D were analysed. The locations of the sections are shown in Figure L22.

L.5.2 Types of Analysis

The following four cases were analysed :

(a) Case 1 - a parametric study for the plan section to assess the amount of water that could flow through the ground underneath Block D under different water heads in the yard

area to the south.

(b) Case 2 - a parametric study for the plan section to check the time required to achieve steady-state flow in Case 1, given different permeabilities and initial degrees of saturation of the fill.

(c) Case 3 - a seepage analysis of the vertical section to evaluate the relative contribution of water from infiltration through the unpaved yard area and leakage from the defective stormwater drains in the yard area. The presence of a very permeable layer in the fill to simulate the presence of preferential flow channels was considered.

(d) Case 4 - a seepage analysis similar to Case 3, but leakage from the foulwater sewer was also considered to evaluate the relative contribution of water from various sources.

The plan and vertical sections, together with the assumed finite element meshes and input parameters for the analyses, are shown in Figures L23 & L24. The analyses were two-dimensional, but the three-dimensional nature of the problem was taken into account approximately by adjusting the thickness of each element.

L.5.3 Assumptions Made in the Analyses

For Cases 1 and 2, the fill permeability, initial degree of soil saturation and water head in the fill in the yard area were varied to examine the general characteristics of the water flow through the ground.

For the vertical section analyses, representative parameters were adopted (Figure L24). The permeability of PWV was taken to be 2×10^{-6} m/s, based on the results of the post-failure ground investigation (Appendix H) and of the water tests carried out in the ground underneath Block D (Appendix K).

The water tests also revealed that preferential flow channels were present in the upper part of the fill stratum, with an equivalent permeability of 5×10^{-2} m/s. In the lower part of the fill layer, where there were no noticeable preferential flow channels, the permeability was 10^{-5} m/s.

In the Case 3 and Case 4 analyses, the fill was subdivided into two layers, and the above permeabilities were adopted. The rate of water infiltration in the unpaved yard area was taken to be 2×10^{-6} m/s, as determined from infiltration tests (Appendix K).

The amount of water collected by the two defective stormwater drains in the yard area depended on the catchment (assessed to be about 240 m^2) and the rainfall pattern, as recorded by raingauge No. H02 within the 50-hour period before the landslide. However, the amount of leakage from the drains would have been a function of the extent of the defects. In both the Case 3 and Case 4 analyses, it was assumed that the amount of water that leaked into the

ground was 50% of the water collected by the drains.

In the Case 4 analyses, the leakage from the foulwater sewer was assumed to occur under a head of 2.5 m. The corresponding amount of leakage was about 20% of the flow recorded in the post-failure flow monitoring (Appendix J). Leakage from the foulwater sewer was assumed to commence upon substantial saturation of the fill stratum in the slope below Block D by subsurface seepage flow from the yard area.

L.5.4 Results of the Analyses

The results of the Case 1 analyses are shown in Figure L25 as a plot of the steady-state flow rate through the ground underneath Block D under different water heads in the yard. It can be seen that the flow rate is not very sensitive to the water head in the yard, but it is very sensitive to the fill permeability. For a fill permeability of 10^{-4} m/s, the steady-state flow rate is calculated to be about 2 m^3/hr.

Figure L26 shows the time required to achieve the above steady-state flow. As expected, the time required is very sensitive to the permeability and the initial degree of saturation of the fill. For a fill permeability of 10^{-4} m/s, it is predicted that 10 to 100 hours are required, depending on the initial degree of saturation of the fill.

The results of the Case 3 analyses are shown in Figures L27 & L28. The relative contributions of water from leakage of the stormwater drains and from infiltration through the unpaved yard area, for different assumptions of the degree of leakage from the drains, are shown in Figure L27. It is clear that leakage from stormwater drains is far more significant than water infiltration via the unpaved yard area.

The extent of the wetted zone at different times as a result of stormwater leakage is shown in Figure L28. It can be seen that only a relatively small part of the PWV is saturated in 50 hours, even though the fill is substantially saturated in about one day.

The results of the Case 4 analyses are shown in Figure L29. With leakage from the foulwater sewer after the fill is substantially saturated by subsurface seepage flow from the yard area in about one day, a large part of the PWV becomes saturated in the following day.

L.5.5 Discussion

The analyses show that water infiltration via the unpaved yard area is of secondary importance in comparison with leakages from the stormwater drains and from the foulwater sewer.

The analyses indicate that it was possible for the fill stratum behind the masonry wall to become substantially saturated due to leakage from the stormwater drains. The analyses also show that substantial saturation of the fill would have occurred about one day before the landslide. With major leakage from the foulwater sewer following wetting of the fill stratum, the PWV could have become substantially saturated by the time of the landslide.

L.6 REFERENCES

Geotechnical Engineering Office (1993). Guide to Retaining Wall Design (Geoguide 1). (Second edition). Geotechnical Engineering Office, Hong Kong, 267 p.

ITASCA (1991). Universal Distinct Element Code (UDEC) Version ICG 1.7 User's Manual. ITASCA Consulting Group, Inc, USA.

Morgenstern, N.R. & Price, V.E. (1965). The analysis of the stability of general slip surfaces. Géotechnique, vol. 15, pp 79-93.

Pun, W.K. & Shen, J.M. (1993). Laboratory investigation of skin friction of remoulded saprolitic soils. Geotechnical Engineering Office, Hong Kong, Special Project Report no. 6/93, 73 p. (Unpublished).

LIST OF TABLES

Table L1 - Material and Joint Properties Adopted in Batches No.1 & 2 of the UDEC Analyses

(a) Material Properties

Material	Properties					
	K (Pa)	G (Pa)	c' (kPa)	ϕ' (degree)	γ (kN/m^3)	CONS
Unsaturated fill	1.33×10^7	1×10^7	5	35	18	3
Saturated fill	1.33×10^7	1×10^7	0	35	18	3
Unsaturated PWV_U	1.33×10^7	1×10^7	20	38.5	19	3
Saturated PWV_U	1.33×10^7	1×10^7	Varies	38.5	19	3
PWV_L	4×10^7	3×10^7	20	38.5	19	3
Masonry block	1.33×10^9	1×10^9	Elastic		22	1

(b) Joint Properties

Interface between	Properties					
	JKS (Pa/m)	JNS (Pa/m)	c' (kPa)	ϕ' (degree)	t' (kPa)	JCONS
Masonry blocks (i.e. mortar joints)	1×10^9	1×10^9	200	45	20	2 (Stages 1&2) 5 (Stage 3)
Masonry blocks and unsaturated/saturated fill	1×10^9	1×10^9	0	35	0	2
Masonry blocks and unsaturated PWV_U	1×10^9	1×10^9	20	38.5	0	2
Masonry blocks and saturated PWV_U	1×10^9	1×10^9	c' of saturated PWV_U	38.5	0	2
Masonry blocks and and PWV_L (i.e. wall base)	1×10^9	1×10^9	20	38.5	0	2
Any two unsaturated soils	1×10^9	1×10^9	20	38.5	0	2
Saturated fill and any other soil and HWV	1×10^9	1×10^9	0	35	0	2
Saturated PWV_U and PWV_L	1×10^9	1×10^9	c' of saturated PWV_U	38.5	0	2

Legend :

c'	Apparent cohesion	G	Shear modulus	PWV_U	Partially weathered volcanics above the landslide surface
ϕ'	Angle of shearing resistance	K	Bulk modulus	PWU_L	Partially weathered volcanics below the landslide surface
γ	Unit weight	CONS	Material constitutive model		
t'	Tensile strength	JCONS	Joint constitutive model		
		JNS	Joint normal stiffness		
		JKS	Joint shear stiffness		

Notes :

(1) CONS=3 refers to the use of the Mohr-Coulomb plasticity model (ITASCA, 1991), i.e. shear failure of the material occurs at the Mohr-Coulomb failure envelope.

(2) CONS=1 refers to the use of an elastic and isotropic model (ITASCA, 1991).

(3) JCONS=2 refers to the use of the Coulomb slip joint model (ITASCA, 1991), i.e. shear failure of the joint occurs at the Mohr-coulomb failure envelope.

(4) JCONS=5 refers to the use of the Coulomb slip with displacement-weakening joint model (ITASCA, 1991), i.e. similar to JCONS=2 except that the joint is fractured when its tensile or shear strength is exceeded. If a joint is fractured, the tensile strength (t') and apparent cohesion (c') of the joint are ignored in all subsequent calculations.

Table L2 - Summary of Cases Analysed by UDEC

Case No.	Batch No.	Ground Profile (Year)	Section No.	c' of PWV_u (kPa)	K of PWV_L (Pa)	Ko	c' of Mortar Joints (kPa)	Depth of Saturation from Wall Top (m)	Results of Analysis
KC-1	1 & 2	1994	C-C	5	4×10^7	0.5	200	Full	Bulging failure
KC-1B	1	1994	C-C	7	4×10^7	0.5	200	Full	Bulging failure
KC-1C	1	1994	C-C	8	4×10^7	0.5	200	Full	Bulging failure
KC-1E	1	1994	C-C	9	4×10^7	0.5	200	Full	Stable (max. xdisp = 25 mm)
KC-1A	1	1994	C-C	10	4×10^7	0.5	200	Full	Stable (max. xdisp = 3 mm)
KA-1	1	1994	A-A	5	4×10^7	0.5	200	Full	Bulging failure
KA-1F	1	1994	A-A	6	4×10^7	0.5	200	Full	Bulging failure
KA-1B	1	1994	A-A	7	4×10^7	0.5	200	Full	Stable (max. xdisp = 50 mm)
PC-1	1	1924	C-C	5	4×10^7	0.5	200	Full	Stable (max. xdisp = 2 mm)
PC-1D	1	1924	C-C	2	4×10^7	0.5	200	Full	Stable (max. xdisp = 40 mm)
PA-1	1	1924	A-A	5	4×10^7	0.5	200	Full	Stable (max. xdisp = 3 mm)
KC-4C	2	1994	C-C	8	4×10^7	0.5	200	2 m	Stable (max. xdisp = 1 mm)
KC-5C	2	1994	C-C	8	4×10^7	0.5	200	4 m	Stable (max. xdisp = 3 mm)
KC-6C	2	1994	C-C	8	4×10^7	0.5	200	6 m	Stable (max. xdisp = 11 mm)
KC-7C	2	1994	C-C	8	4×10^7	0.5	200	8 m	Bulging failure
KC-2	3	1994	C-C	5	1×10^8	0.5	200	Full	Bulging failure
KC-3	3	1994	C-C	5	4×10^7	1.0	200	Full	Bulging failure
KC-8	3	1994	C-C	5	1.3×10^7	0.5	200	Full	Bulging failure
KC-8A	3	1994	C-C	10	1.3×10^7	0.5	200	Full	Stable (max. xdisp = 8 mm)
PC-9D	3	1924	C-C	2	4×10^7	0.5	100	Full	Stable (max. xdisp = 40 mm)
KC-X	3	1994	C-C	5	4×10^7	0.5	400	Full	Bulging failure
KC-Y(5)	3	1994	C-C	5	4×10^7	0.5	200	Full	Bulging failure

Notes:
(1) For legend of c', K, PWV_u, $PWVL_L$ and t', refer to Table L1.
(2) Poisson's ratio, ν, for PWV_L is 0.2.
(3) t' of mortar joints is one-tenth of c' of the joints.
(4) max. xdisp refers to the maximum horizontal displacement which occurs as a result of soil saturation.
(5) K of masonry blocks = 1.33×10^{10} Pa ; $\nu = 0.2$

LIST OF FIGURES

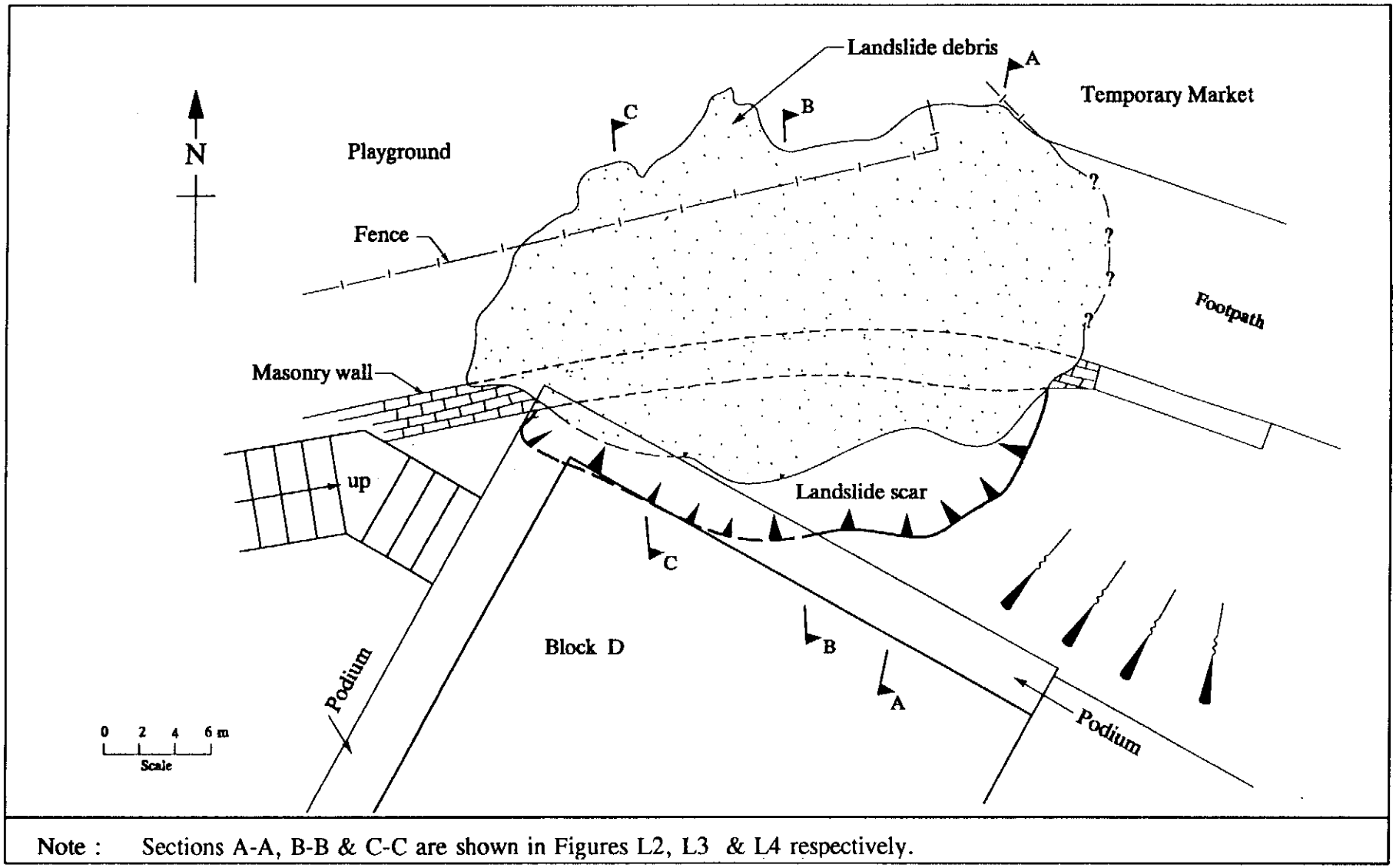

Note : Sections A-A, B-B & C-C are shown in Figures L2, L3 & L4 respectively.

Figure L1 - Location Plan

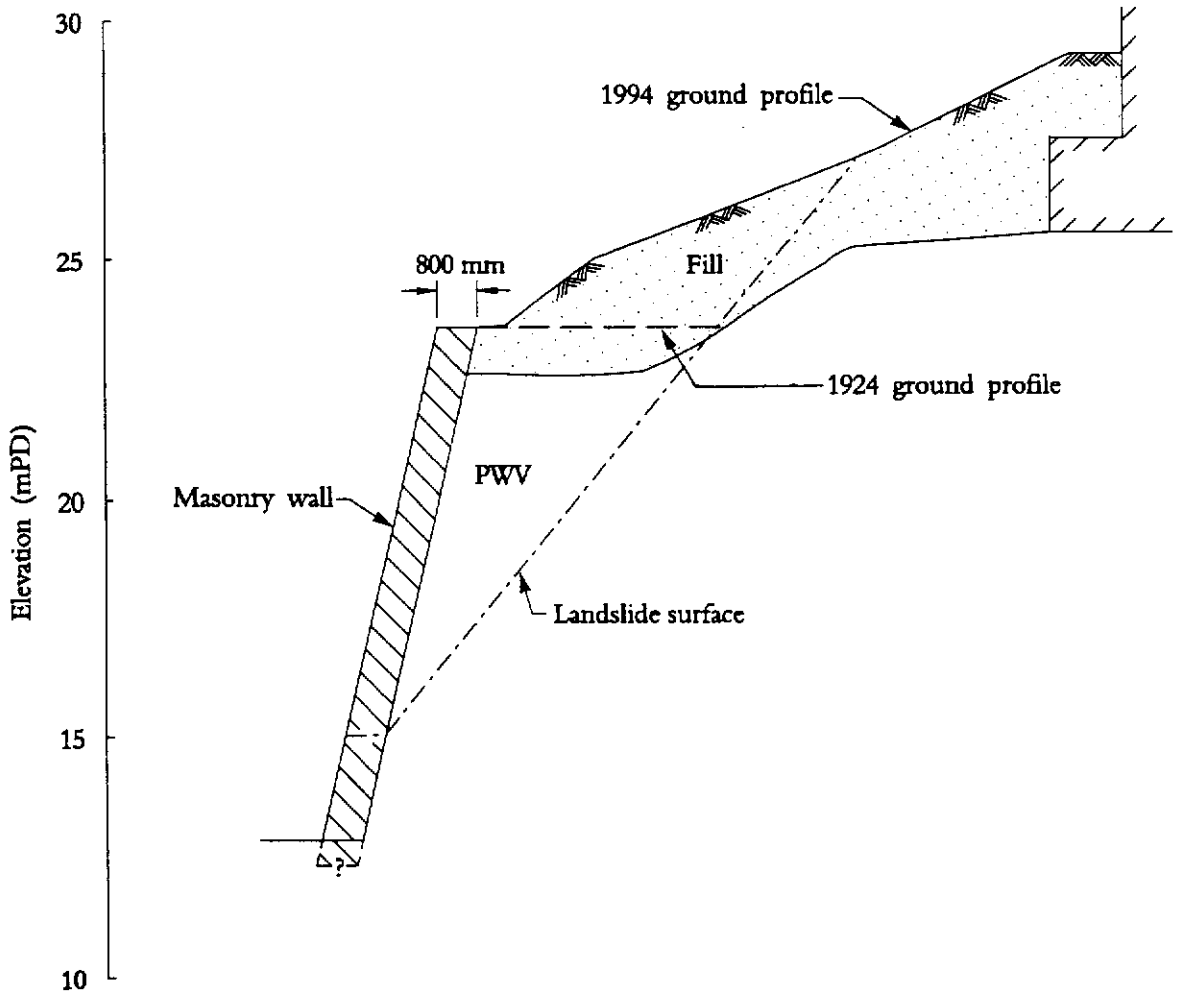

Material	Parameters		
	Apparent Cohesion c' (kPa)	Angle of Shearing Resistance ϕ'	Unit Weight (kN/m^3)
Fill	0	35°	18
PWV	Varies	38.5°	19
Wall mortar joints	Varies	45° (case 1) 40° (case 2)	22 (wall)

Notes : (1) For location of the section, see Figure L1.
(2) PWV denotes the partially weathered volcanics stratum comprising CDV and C/HDV.

Figure L2 - Section A-A for Slope Stability Analyses

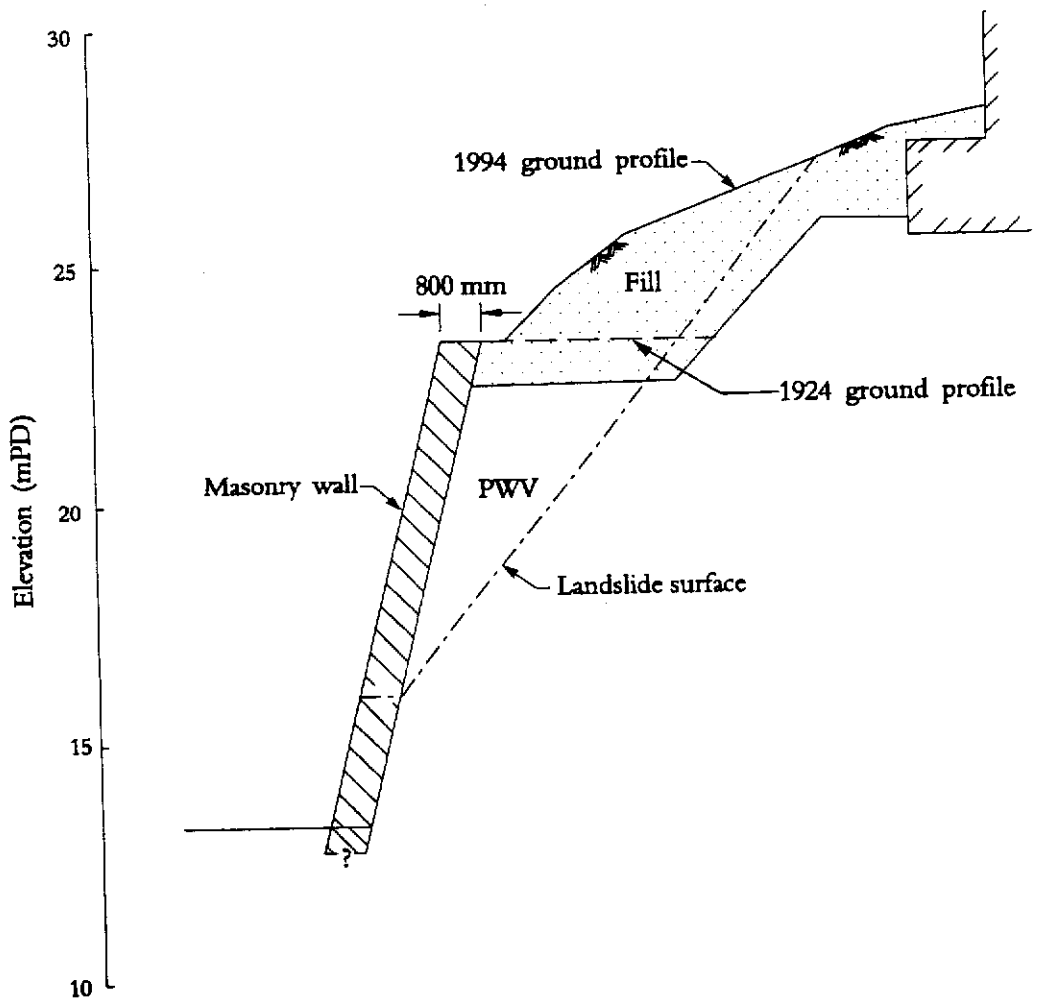

Material	Parameters		
	Apparent Cohesion c' (kPa)	Angle of Shearing Resistance ϕ'	Unit Weight (kN/m^3)
Fill	0	35°	18
PWV	Varies	38.5°	19
Wall mortar joints	Varies	45° (case 1) 40° (case 2)	22 (wall)

Notes : (1) For location of the section, see Figure L1.
(2) PWV denotes the partially weathered volcanics stratum comprising CDV and C/HDV.

Figure L3 - Section B-B for Slope Stability Analyses

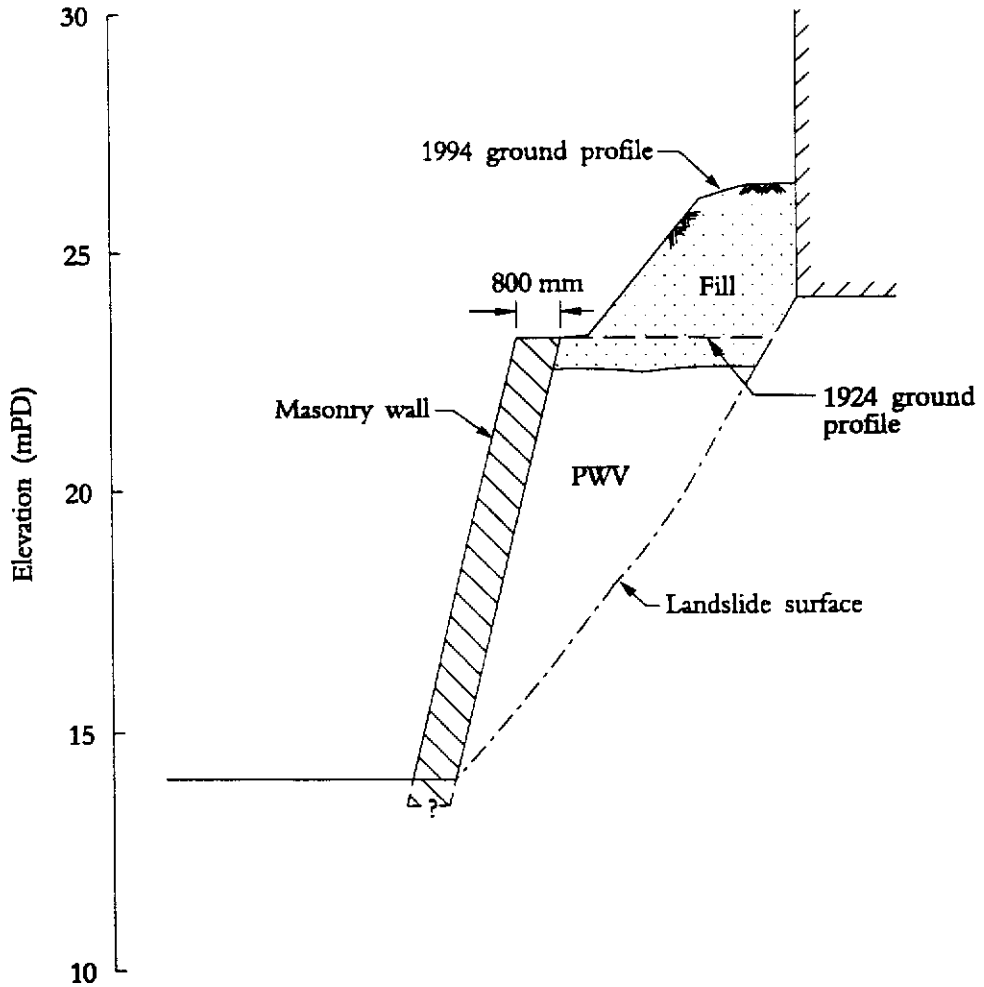

Material	Parameters		
	Apparent Cohesion c' (kPa)	Angle of Shearing Resistance ϕ'	Unit Weight (kN/m^3)
Fill	0	35°	18
PWV	Varies	38.5°	19
Wall mortar joints	Varies	45° (case 1) 40° (case 2)	22 (wall)

Notes : (1) For location of the section, see Figure L1.
(2) PWV denotes the partially weathered volcanics stratum comprising CDV and C/HDV.

Figure L4 - Section C-C for Slope Stability Analyses

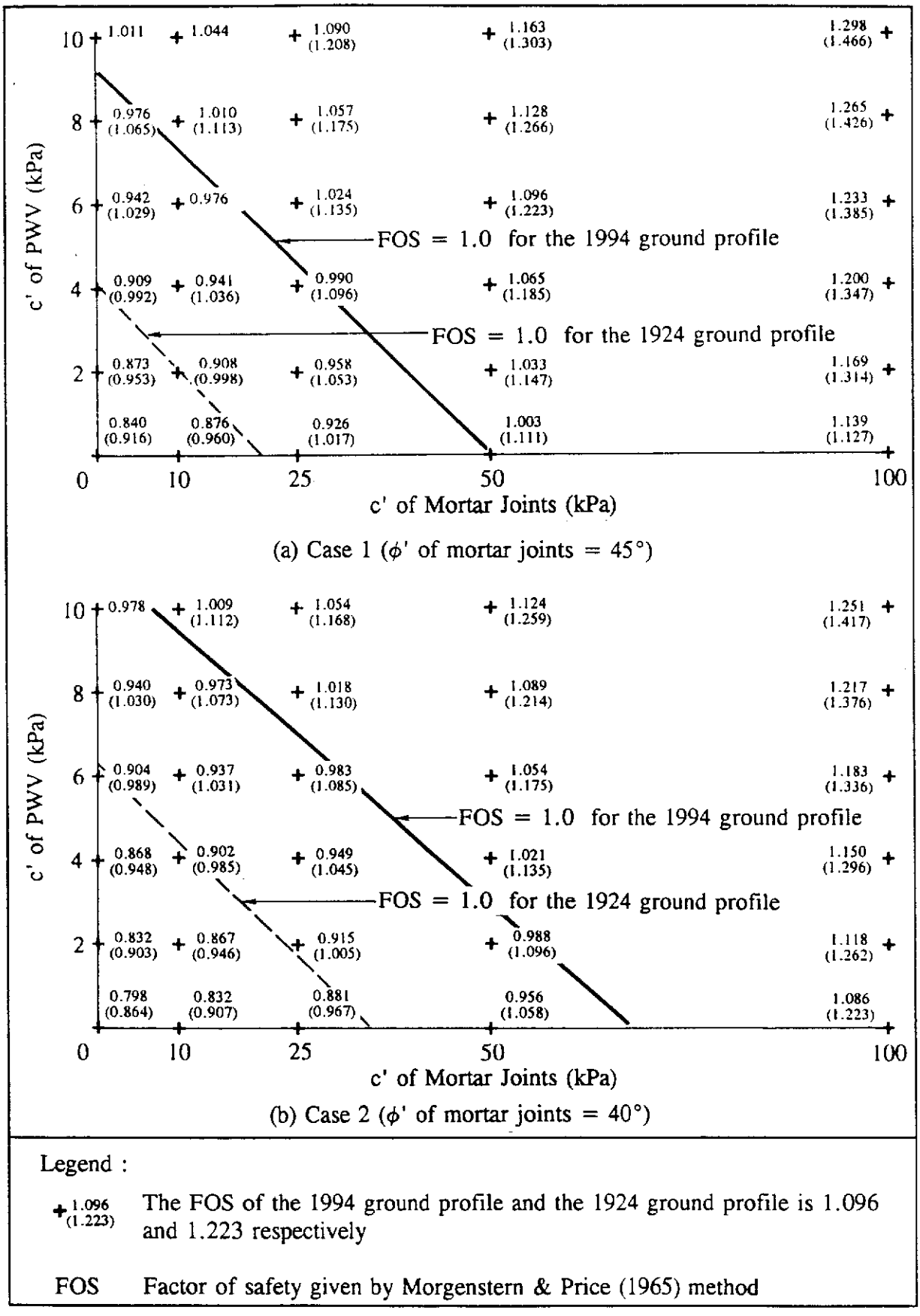

Legend :

+ 1.096 (1.223) The FOS of the 1994 ground profile and the 1924 ground profile is 1.096 and 1.223 respectively

FOS Factor of safety given by Morgenstern & Price (1965) method

Figure L5 - Results of Slope Stability Analyses for Section A-A

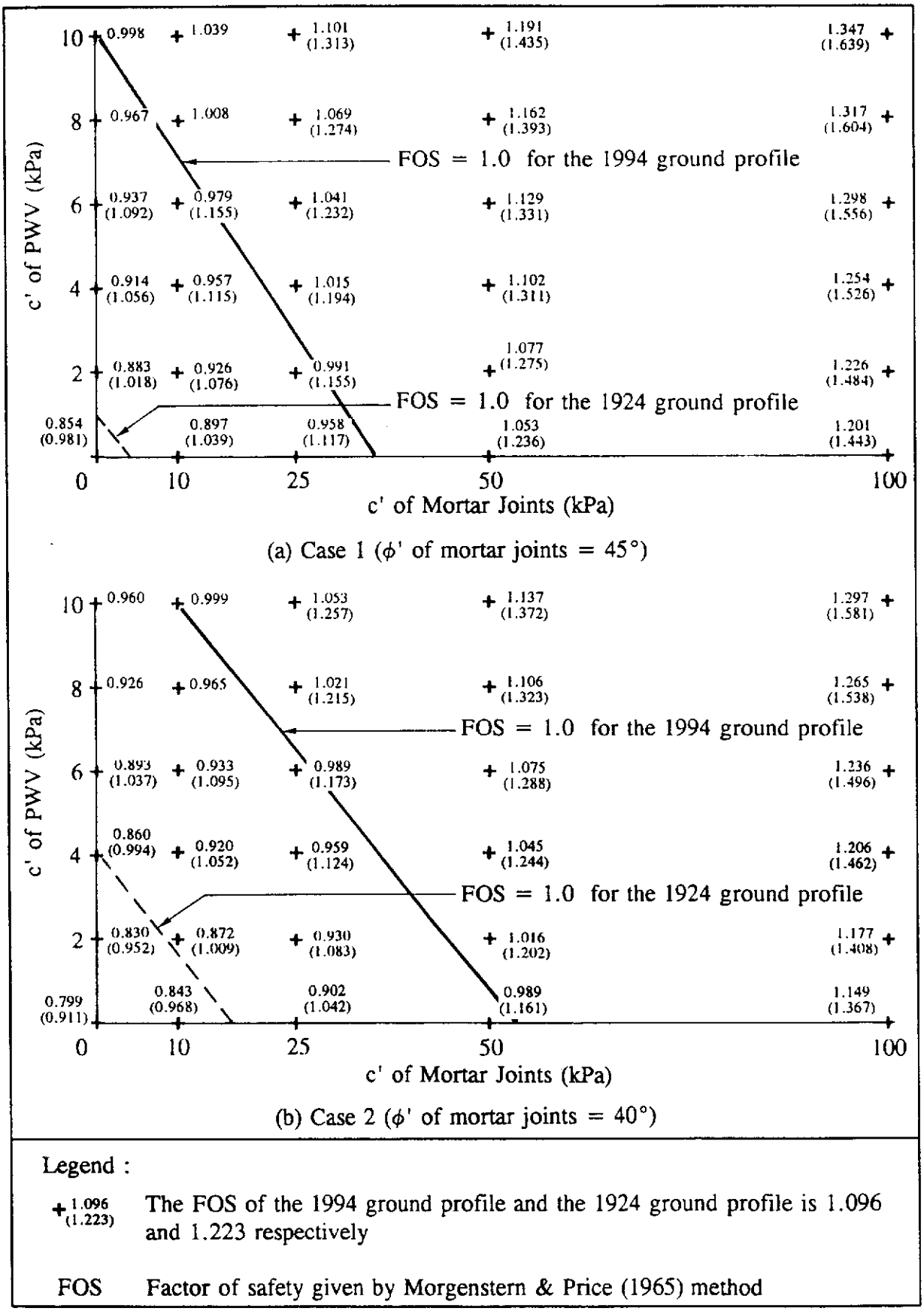

(a) Case 1 (ϕ' of mortar joints = 45°)

(b) Case 2 (ϕ' of mortar joints = 40°)

Legend :

+ 1.096 (1.223) The FOS of the 1994 ground profile and the 1924 ground profile is 1.096 and 1.223 respectively

FOS Factor of safety given by Morgenstern & Price (1965) method

Figure L6 - Results of Slope Stability Analyses for Section B-B

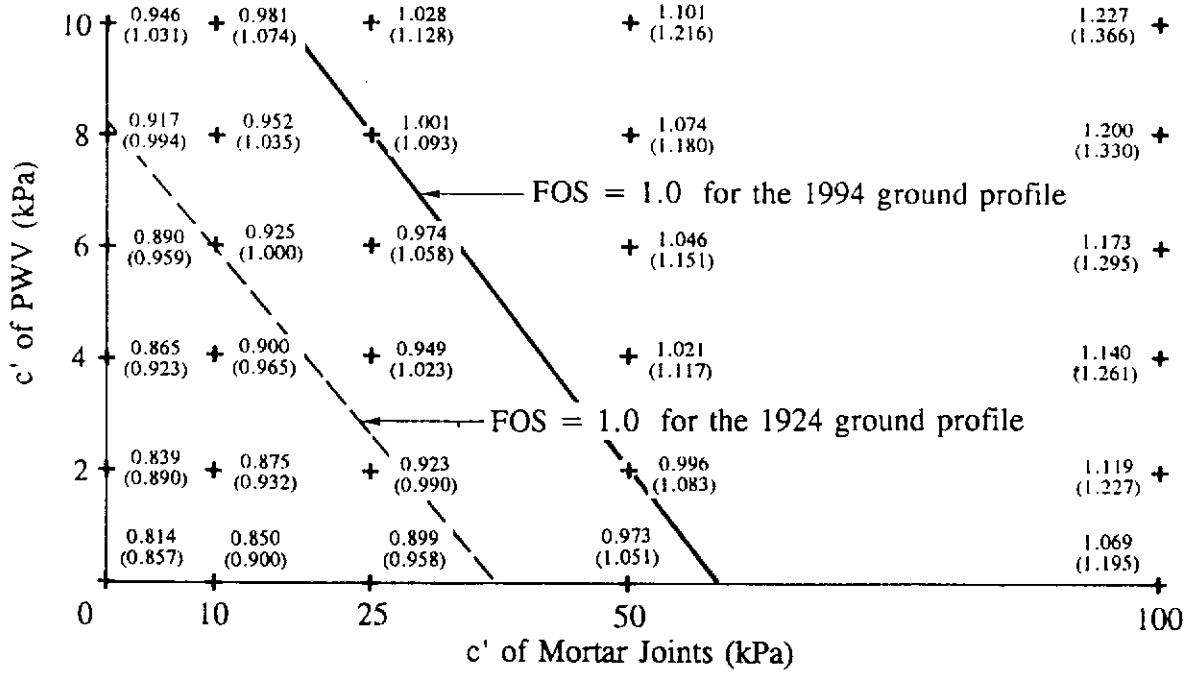

(a) Case 1 (ϕ' of mortar joints = 45°)

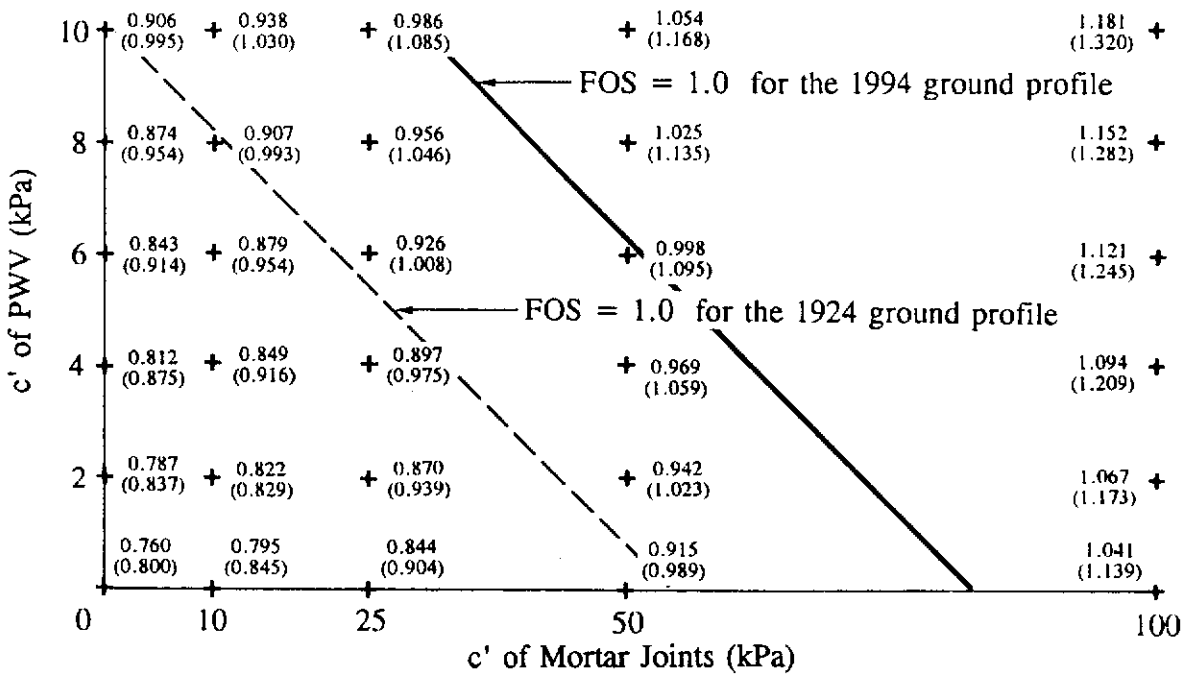

(b) Case 2 (ϕ' of mortar joints = 40°)

Legend :

+ 1.096 (1.223) The FOS of the 1994 ground profile and the 1924 ground profile is 1.096 and 1.223 respectively

FOS Factor of safety given by Morgenstern & Price (1965) method

Figure L7 - Results of Slope Stability Analyses for Section C-C

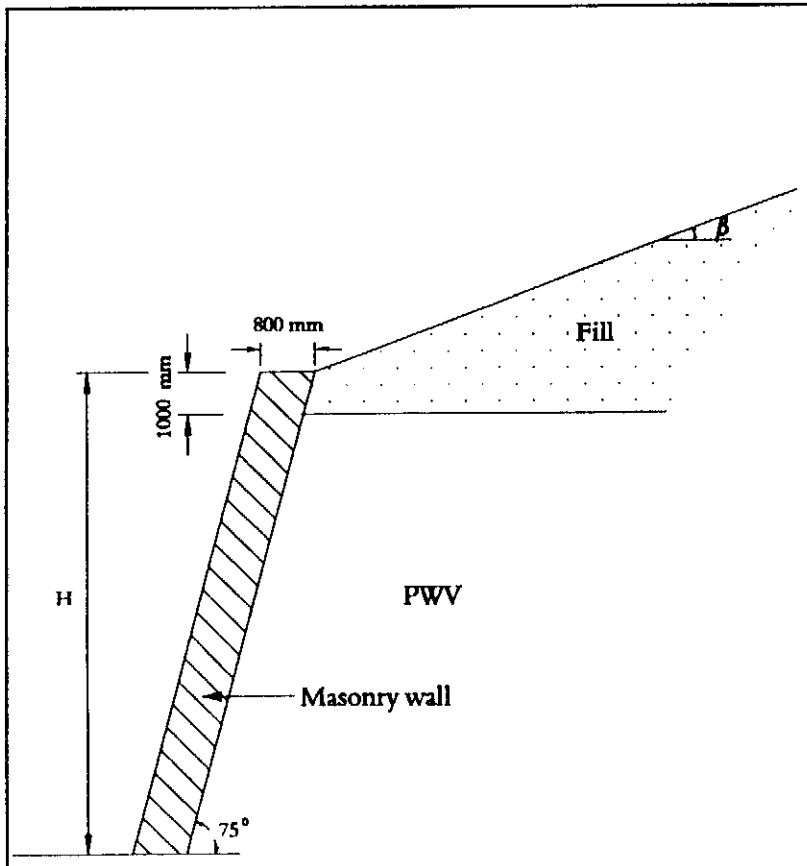

Assumptions for Limit Equilibrium Retaining Wall Stability Analyses			
Parameters	Values		
Geometry	Section A - A	Section B - B	Section C - C
Height of wall, H (m)	10.6	10.0	9.3
Back-slope angle, β	25°	25°	30°
Material properties			
Shear strength parameters of fill Apparent cohesion c' Angle of shearing resistance ϕ'	0 35°		
Shear strength parameters of PWV Apparent cohesion c' Angle of shearing resistance ϕ'	Varies from 2 to 10 kPa 38.5°		
Unit weight of fill	18 kN/m³		
Unit weight of PWV	19 kN/m³		
Unit weight of masonry wall	22 kN/m³		
Tensile strength of mortar joints	20 kPa		
Interface friction	Case 1	Case 2	
Wall friction	$\frac{2}{3}\phi'$	$\frac{1}{2}\phi'$	
Base friction	ϕ'	$\frac{2}{3}\phi'$	

Legend :
PWV Partially weathered volcanics

Figure L8 - Geometry and Material Properties Adopted in Retaining Wall Stability Analyses

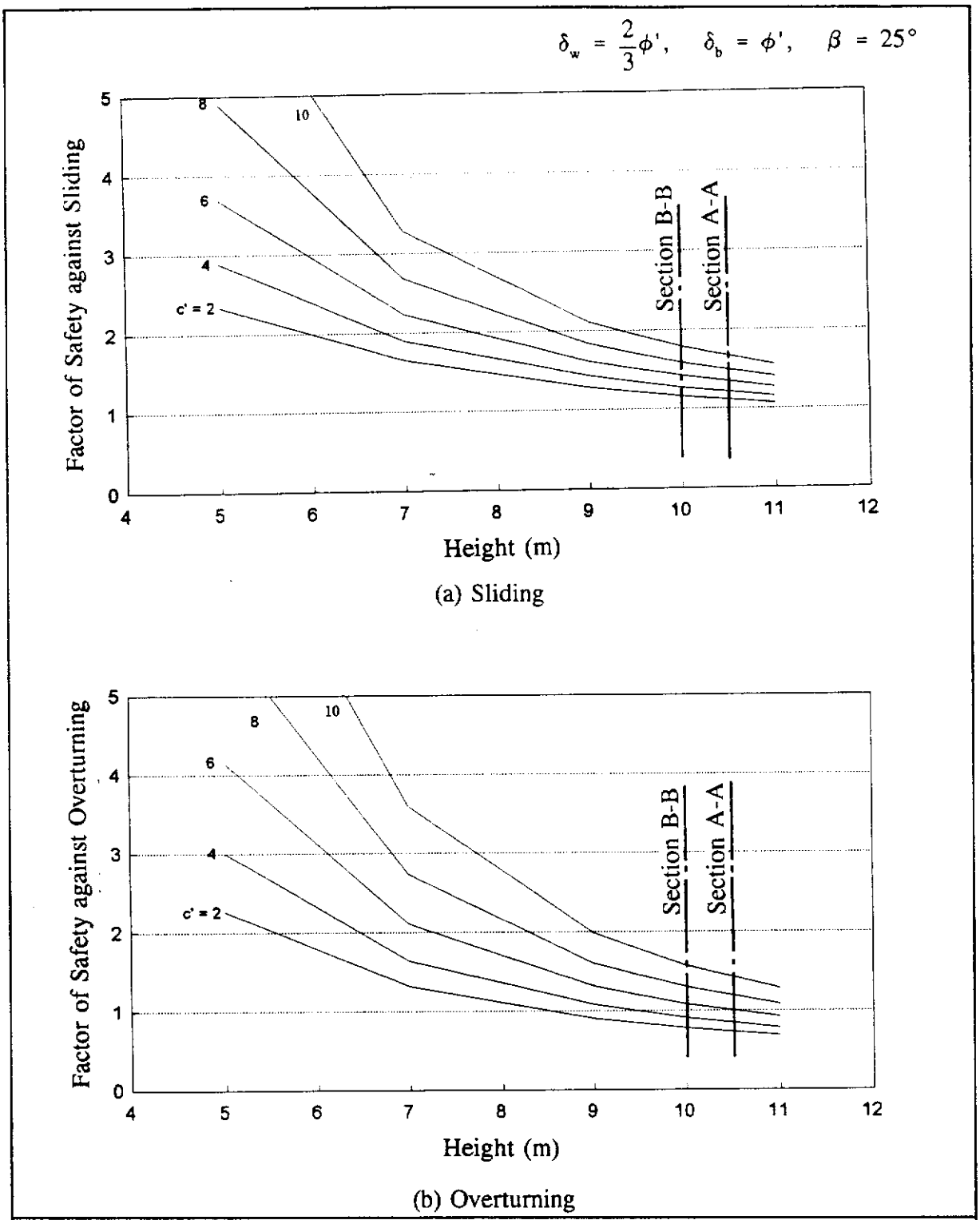

Legend :

c'	Apparent cohesion (kPa)	δ_w	Wall friction angle
ϕ'	Angle of shearing resistance	δ_b	Base friction angle
β	Back-slope angle behind retaining wall		

Figure L9 - Results of Retaining Wall Analyses for $\beta=25°$ with Representative Interface Friction Parameters

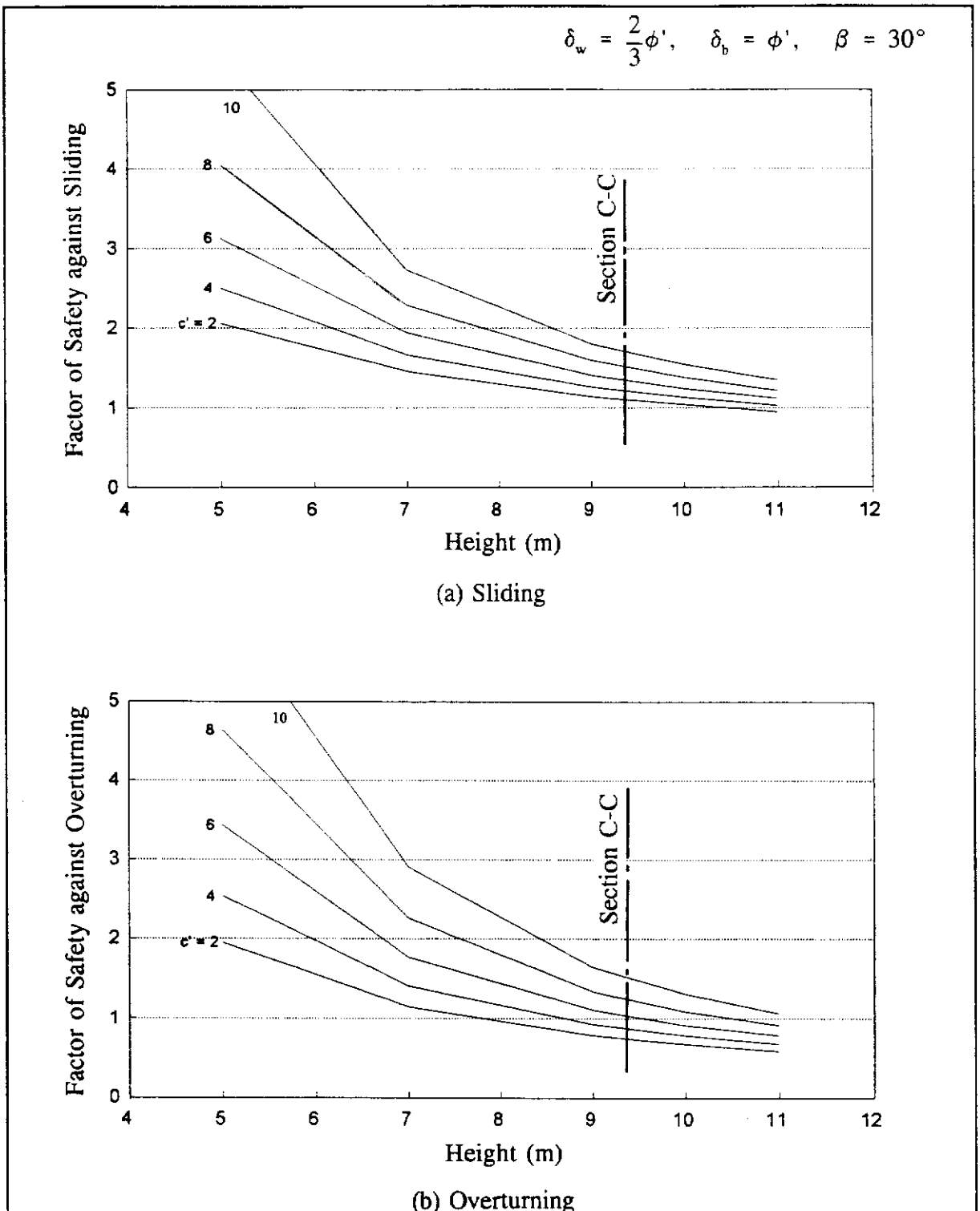

Figure L10 - Results of Retaining Wall Analyses for $\beta = 30°$ with Representative Interface Friction Parameters

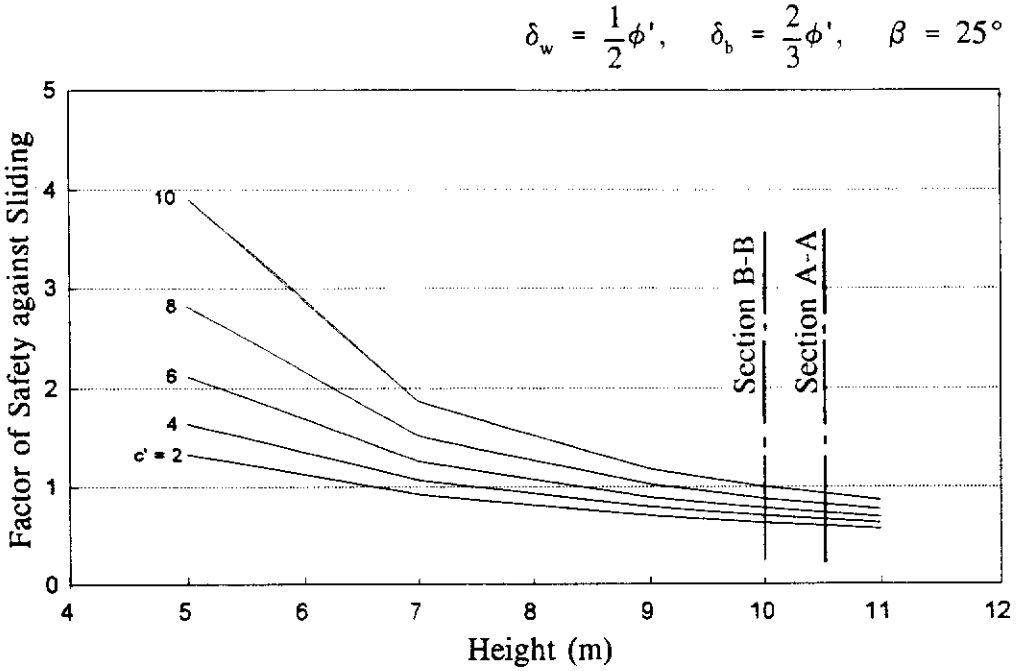

(a) Sliding

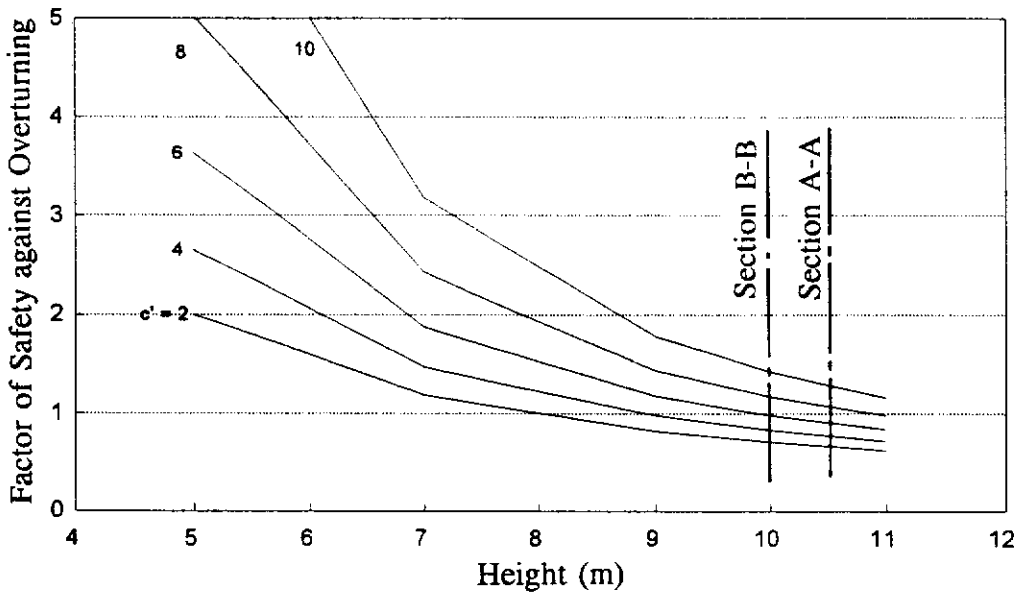

(b) Overturning

Legend :

c'	Apparent cohesion (kPa)	δ_w	Wall friction angle
ϕ'	Angle of shearing resistance	δ_b	Base friction angle
β	Back-slope angle behind retaining wall		

Figure L11 - Results of Retaining Wall Analyses for $\beta=25°$ with Conservative Interface Friction Parameters

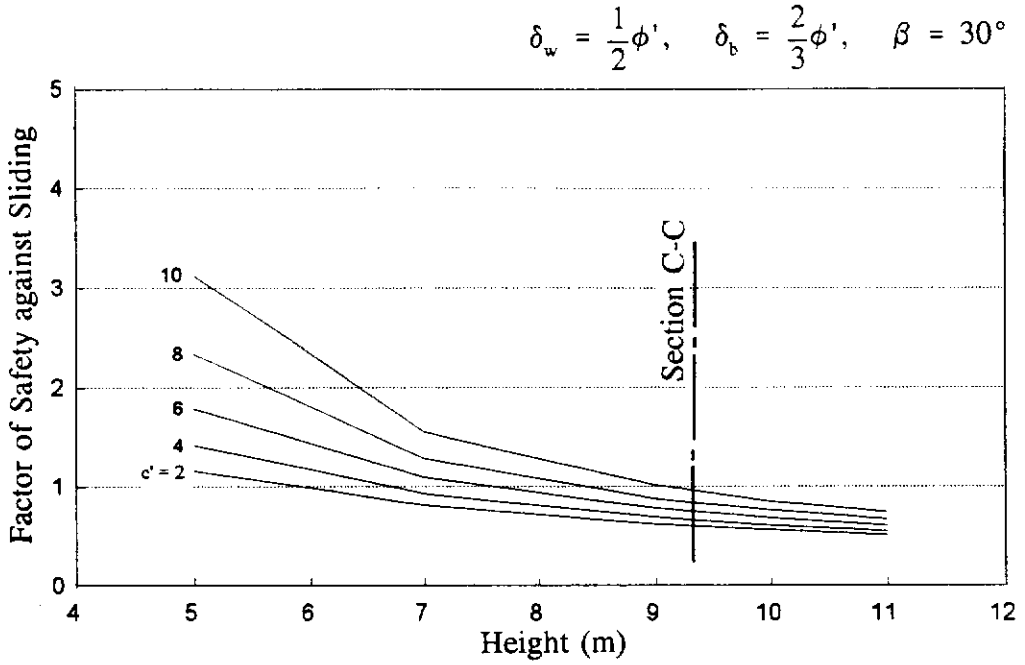

(a) Sliding

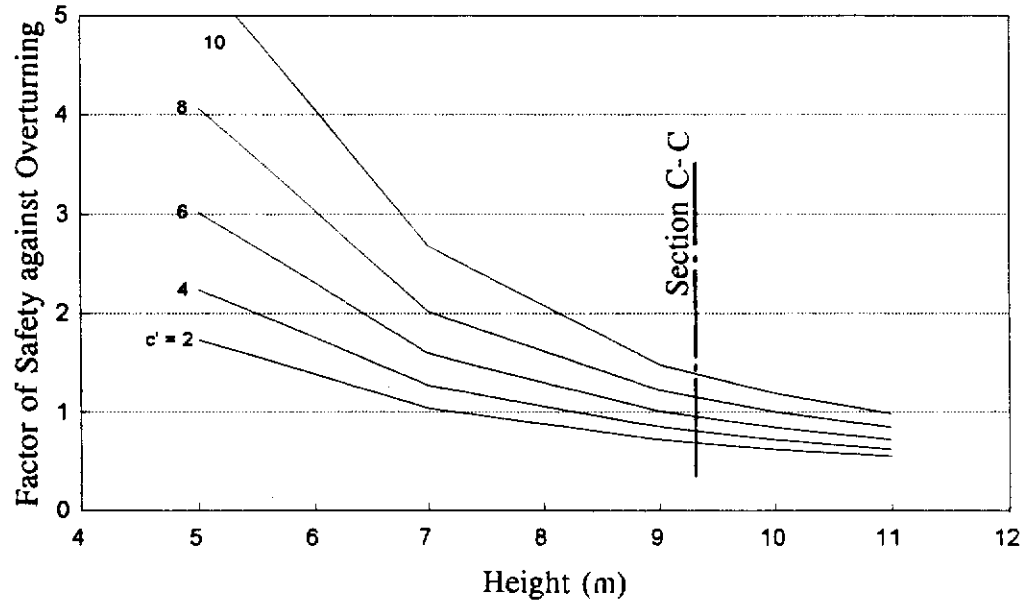

(b) Overturning

Legend :

c'	Apparent cohesion (kPa)	δ_w	Wall friction angle
ϕ'	Angle of shearing resistance	δ_b	Base friction angle
β	Back-slope angle behind retaining wall		

Figure L12 - Results of Retaining Wall Analyses for $\beta = 30°$ with Conservative Interface Friction Parameters

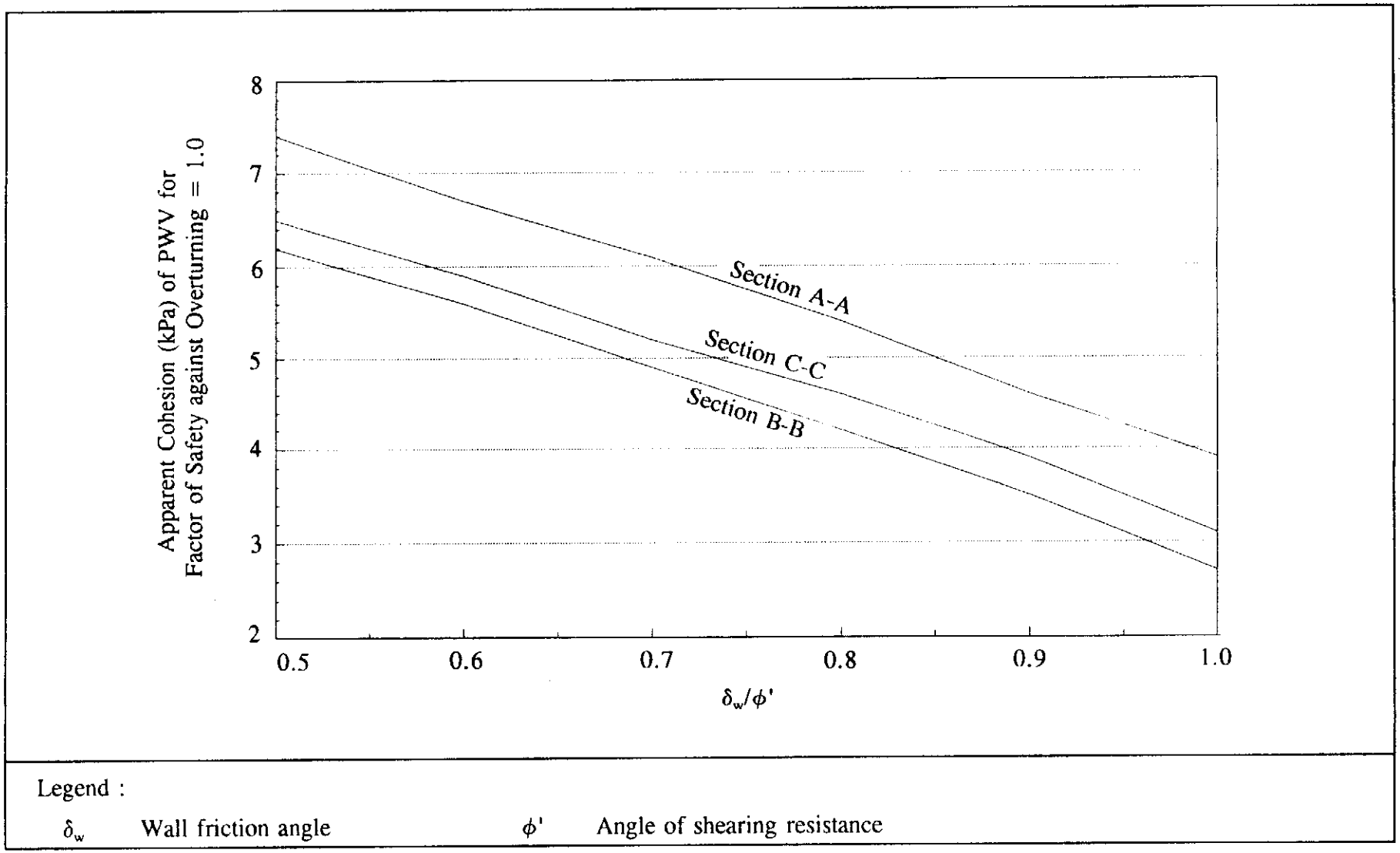

Legend :

δ_w Wall friction angle ϕ' Angle of shearing resistance

Figure L13 - Minimum Apparent Cohesion Required for Wall Stability against Overturning Failure

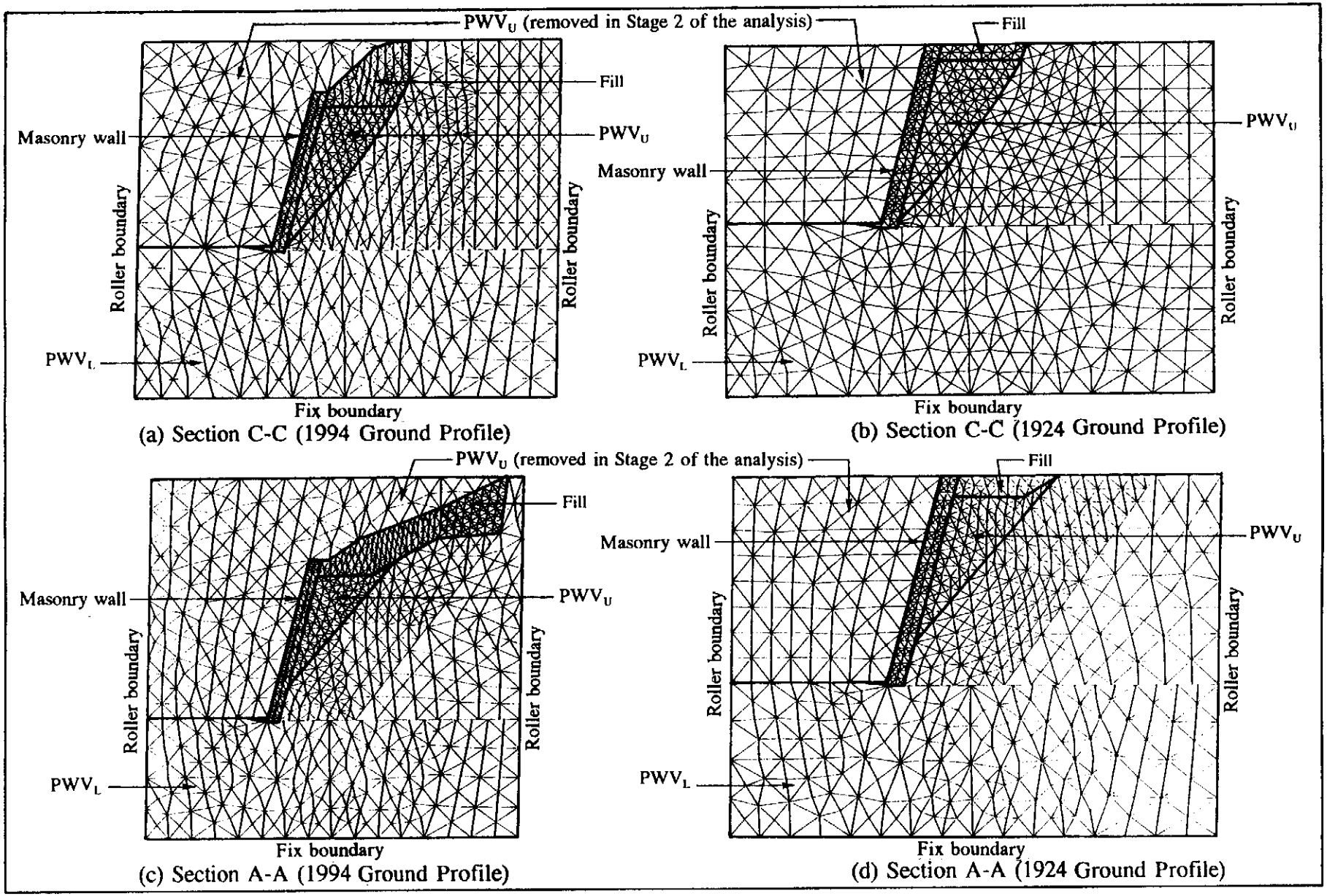

Figure L14 - Finite Difference Mesh for UDEC Analyses

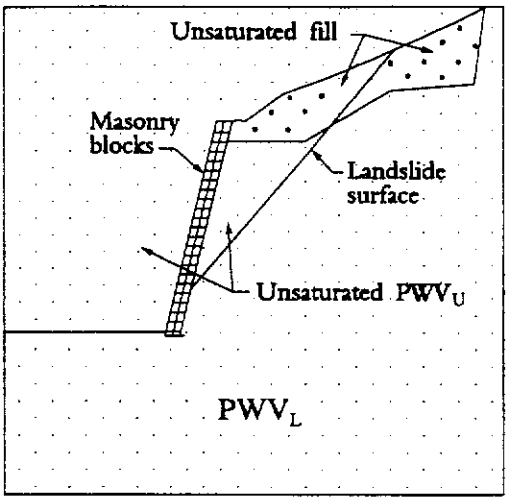

(a) Stage 1 - Level Ground Consolidation under K_o Insitu Stress

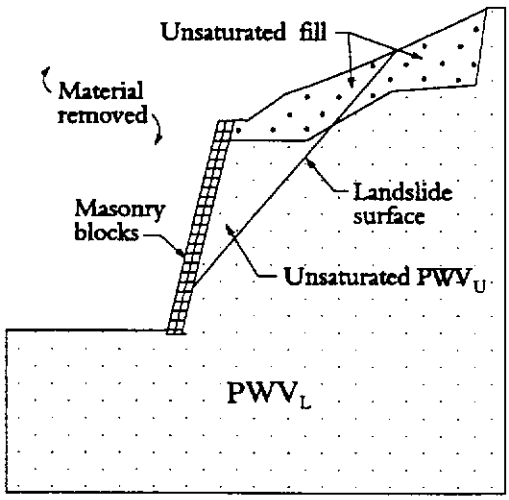

(b) Stage 2 - Excavation under Unsaturated Soil Condition

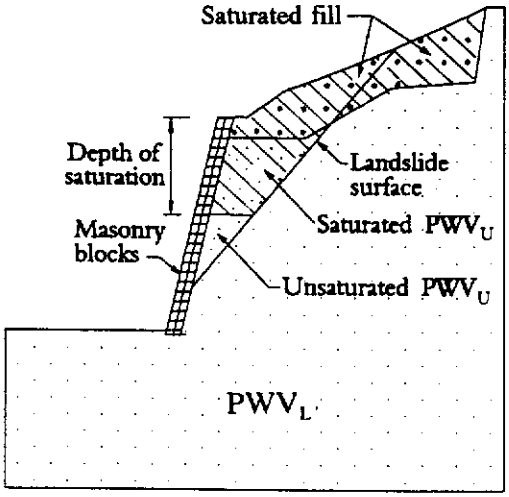

(c) Stage 3 - Soil Saturation

Figure L15 - Stages of UDEC Analysis

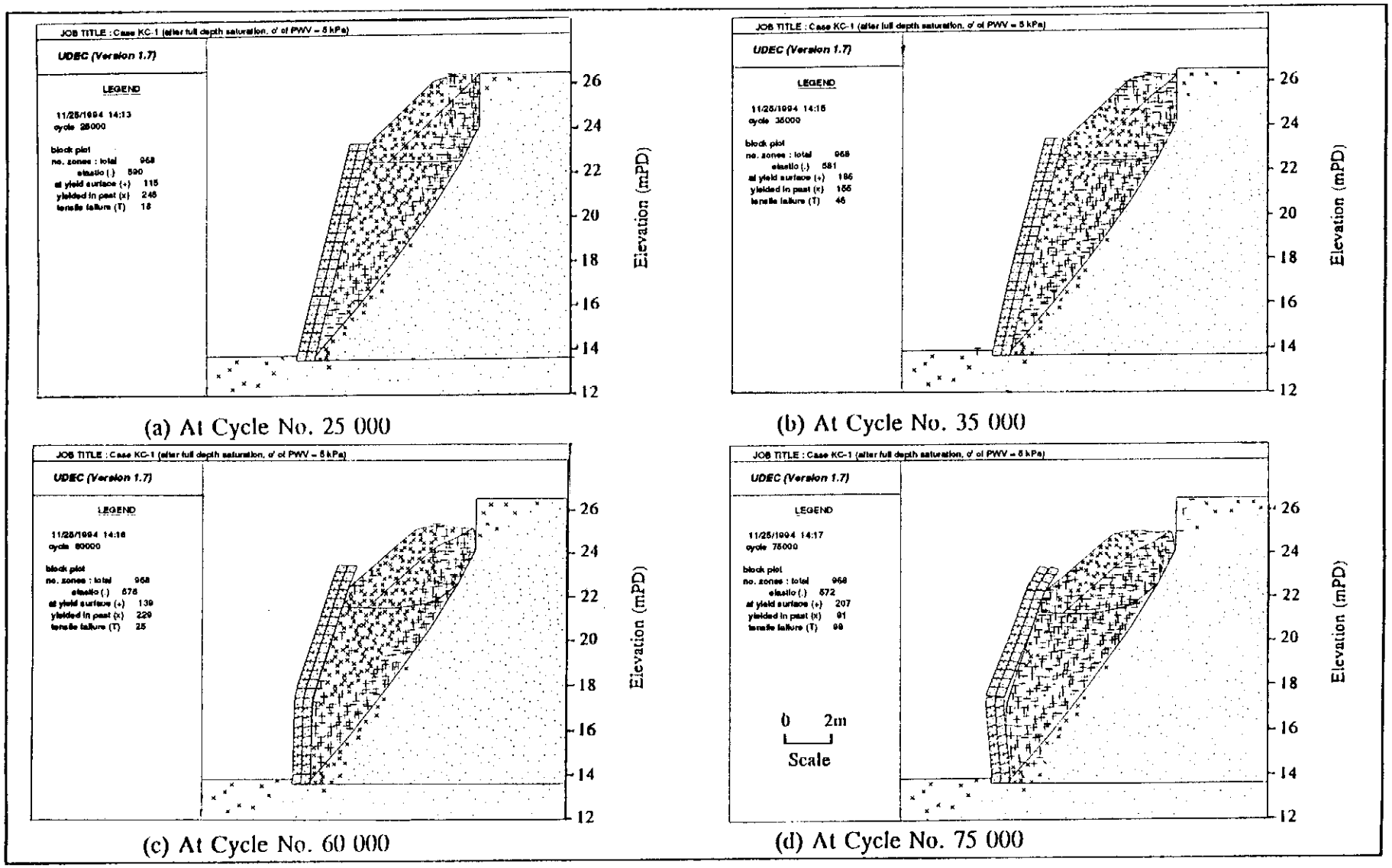

Figure L16 - Results of UDEC Analyses (Wall Condition and Stress State of Case KC-1 during Bulging Failure)

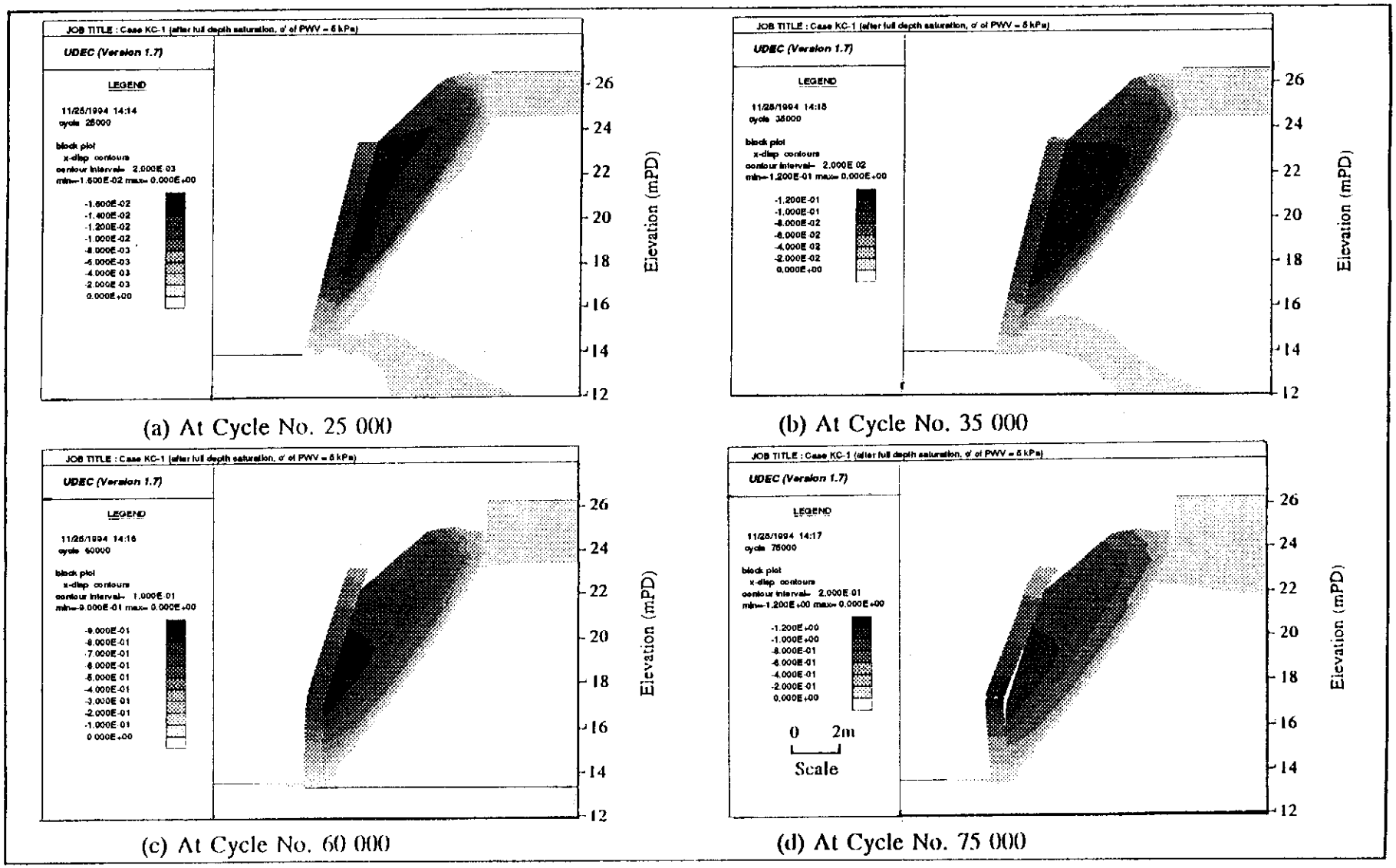

Figure L17 - Results of UDEC Analyses (Horizontal Displacement (m) of Case KC-1 during Bulging Failure)

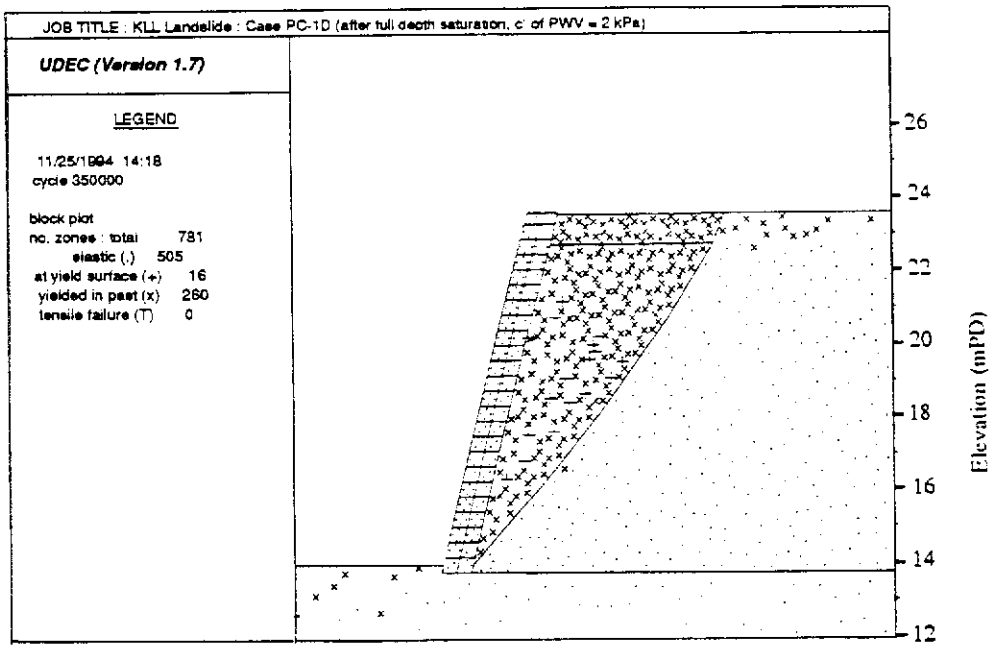

(a) Wall Condition and Stress State

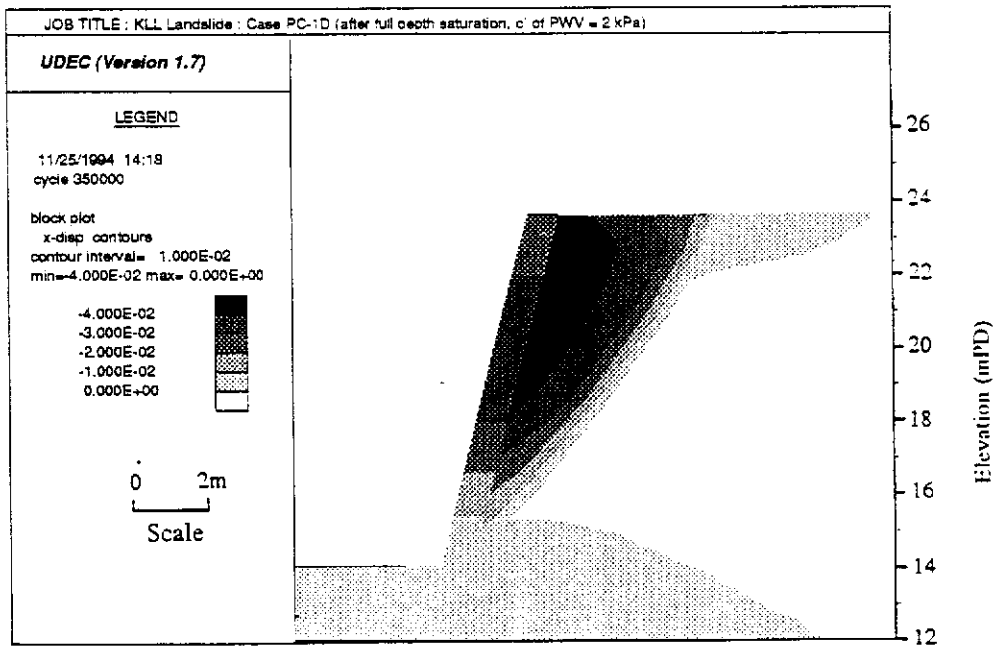

(b) Horizontal Displacement (m)

Notes : (1) Section C-C with the 1924 ground profile was analysed.
(2) The analyses show that the wall is stable. The stress state and horizontal displacement at the equilibrium condition are shown in this Figure.

Figure L18 - Results of UDEC Analyses for Case PC-1D

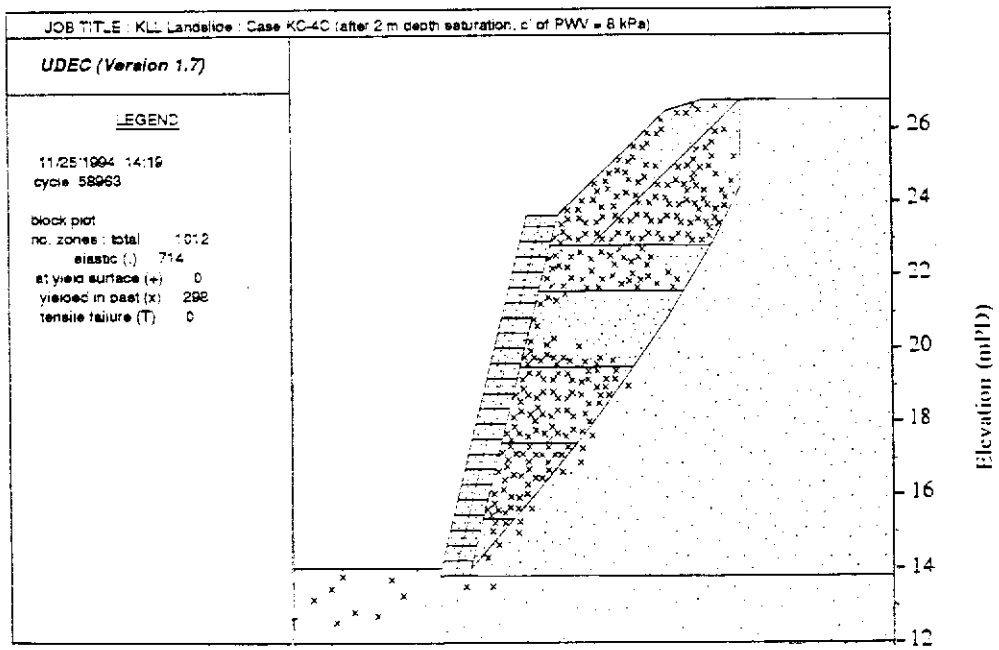

(a) Wall Condition and Stress State

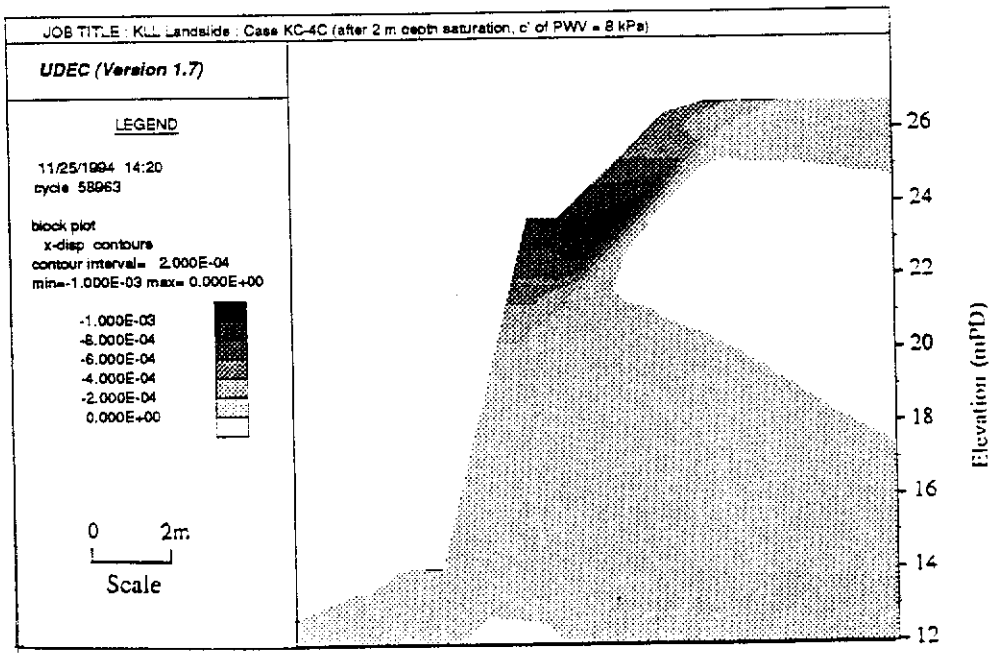

(b) Horizontal Displacement (m)

Note : The analyses show that the wall is stable. The stress state and horizontal displacement at the equilibrium condition are shown in this Figure.

Figure L19 - Results of UDEC Analyses for Case KC-4C (Depth of Saturation = 2m)

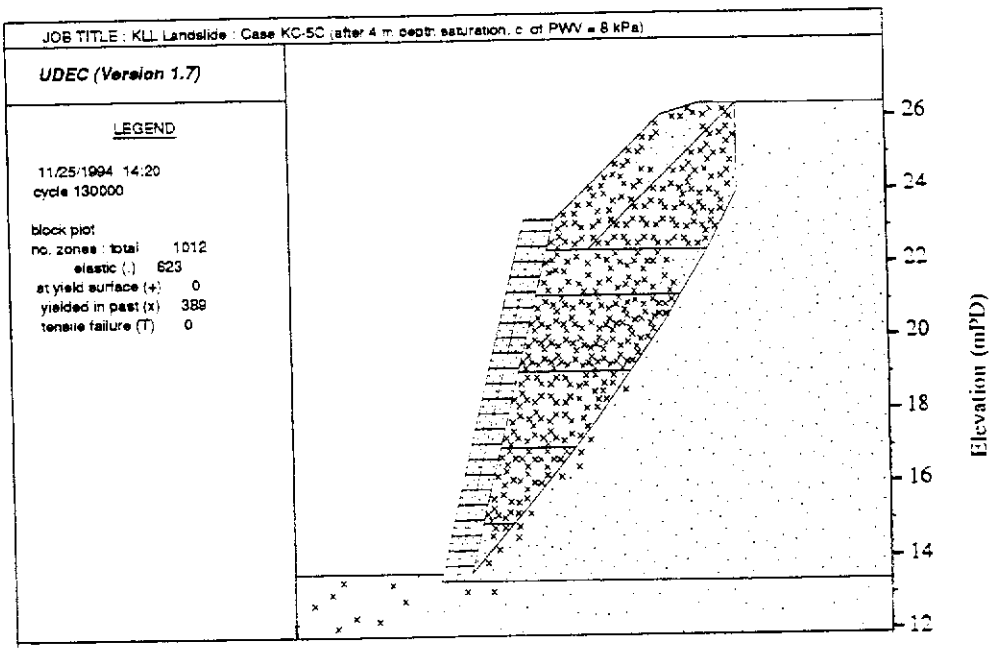

(a) Wall Condition and Stress State

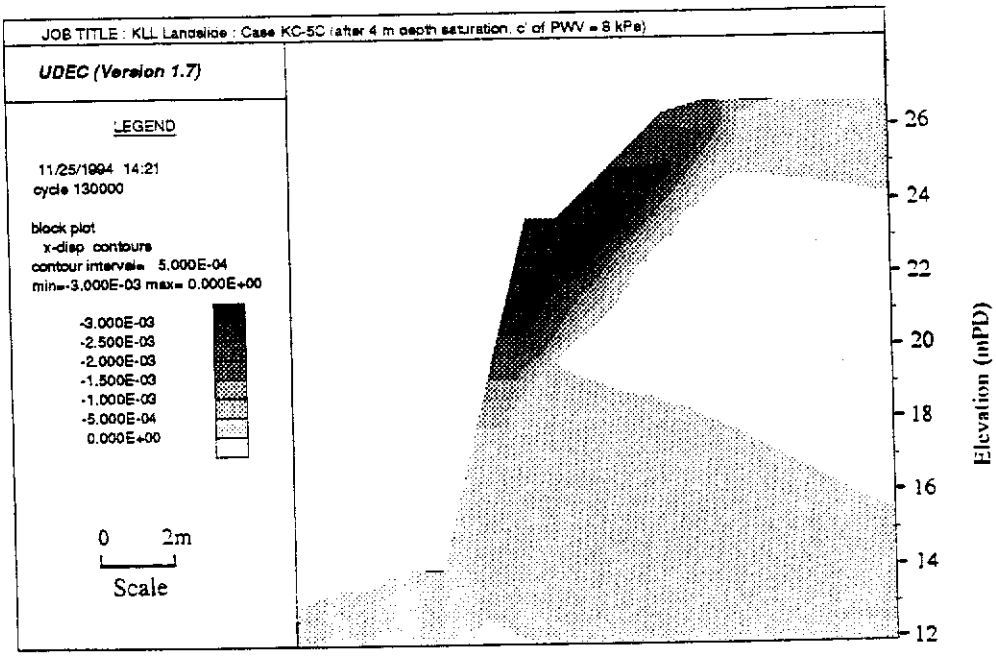

(b) Horizontal Displacement (m)

Note : The analyses show that the wall is stable. The stress state and horizontal displacement at the equilibrium condition are shown in this Figure.

Figure L20 - Results of UDEC Analyses for Case KC-5C (Depth of Saturation = 4m)

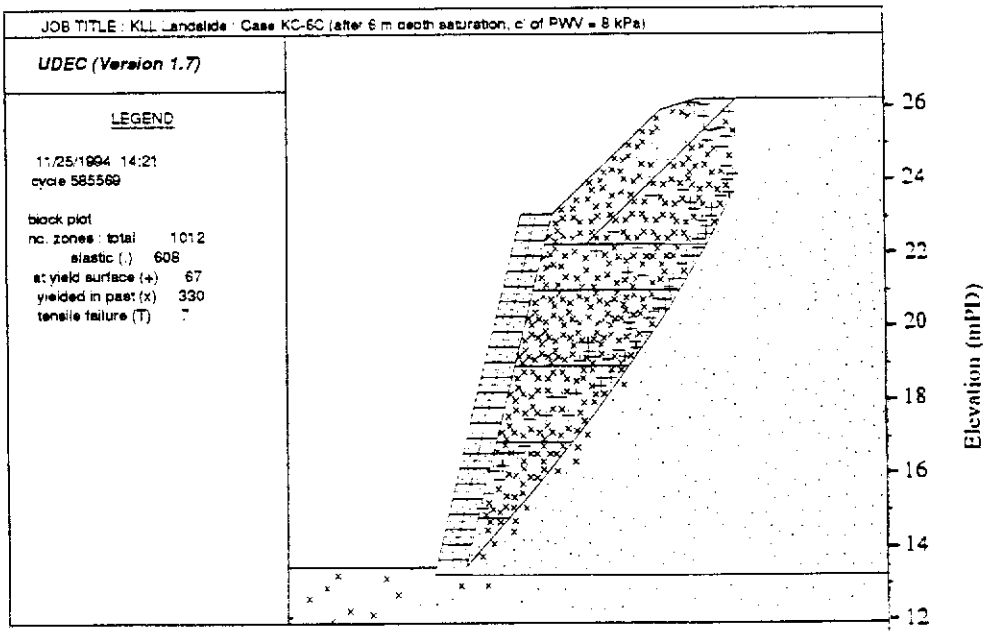

(a) Wall Condition and Stress State

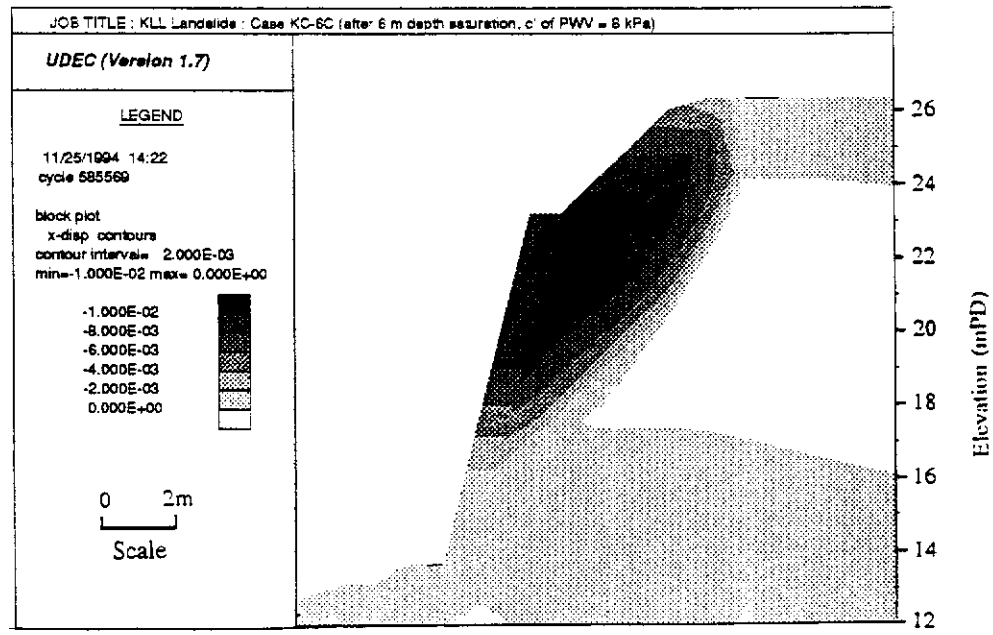

(b) Horizontal Displacement (m)

Note : The analyses show that the wall is stable. The stress state and horizontal displacement at the equilibrium condition are shown in this Figure.

Figure L21 - Results of UDEC Analyses Case KC-6C (Depth of Saturation = 6m)

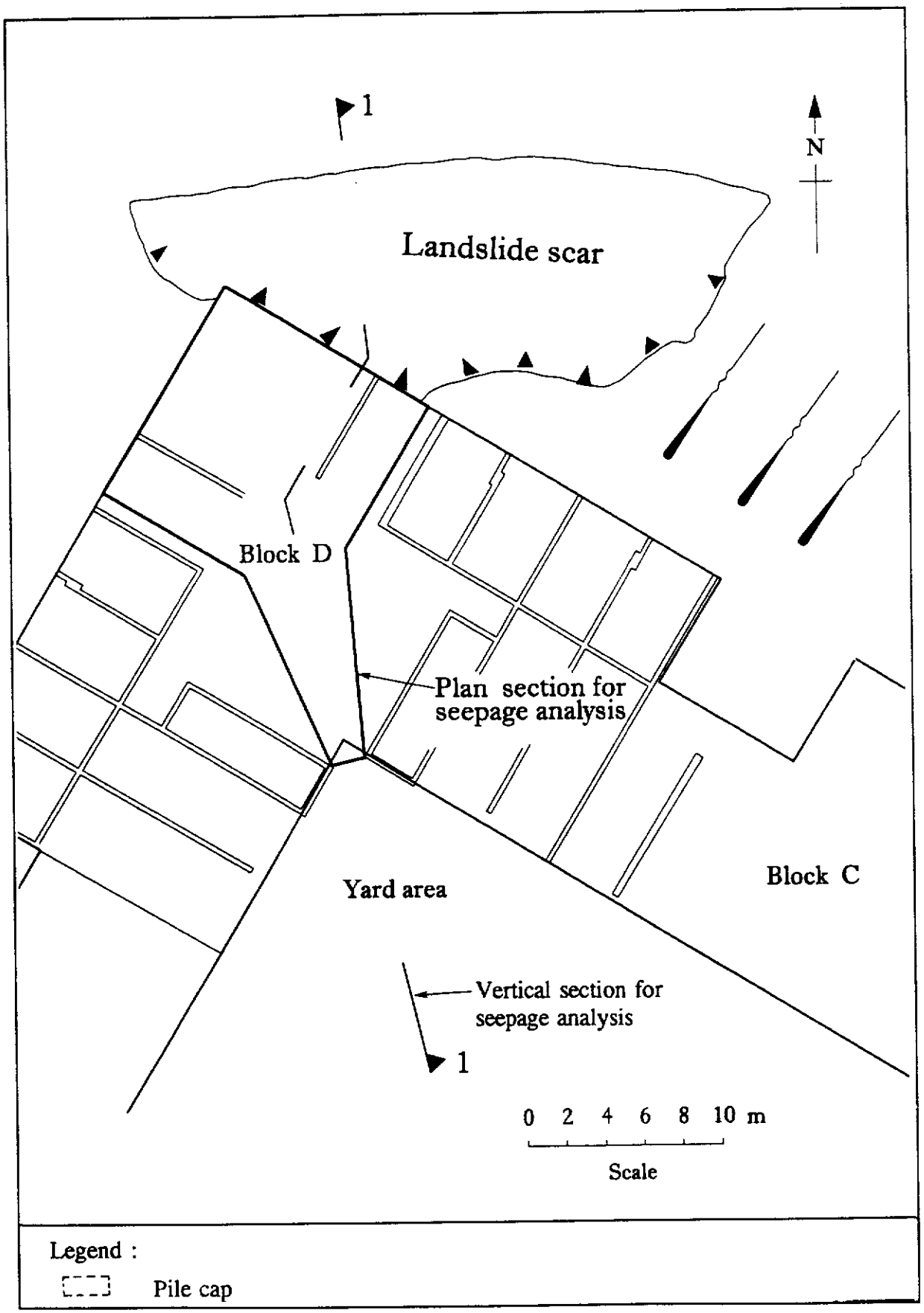

Figure L22 - Location of Plan and Section Used for Seepage Analyses

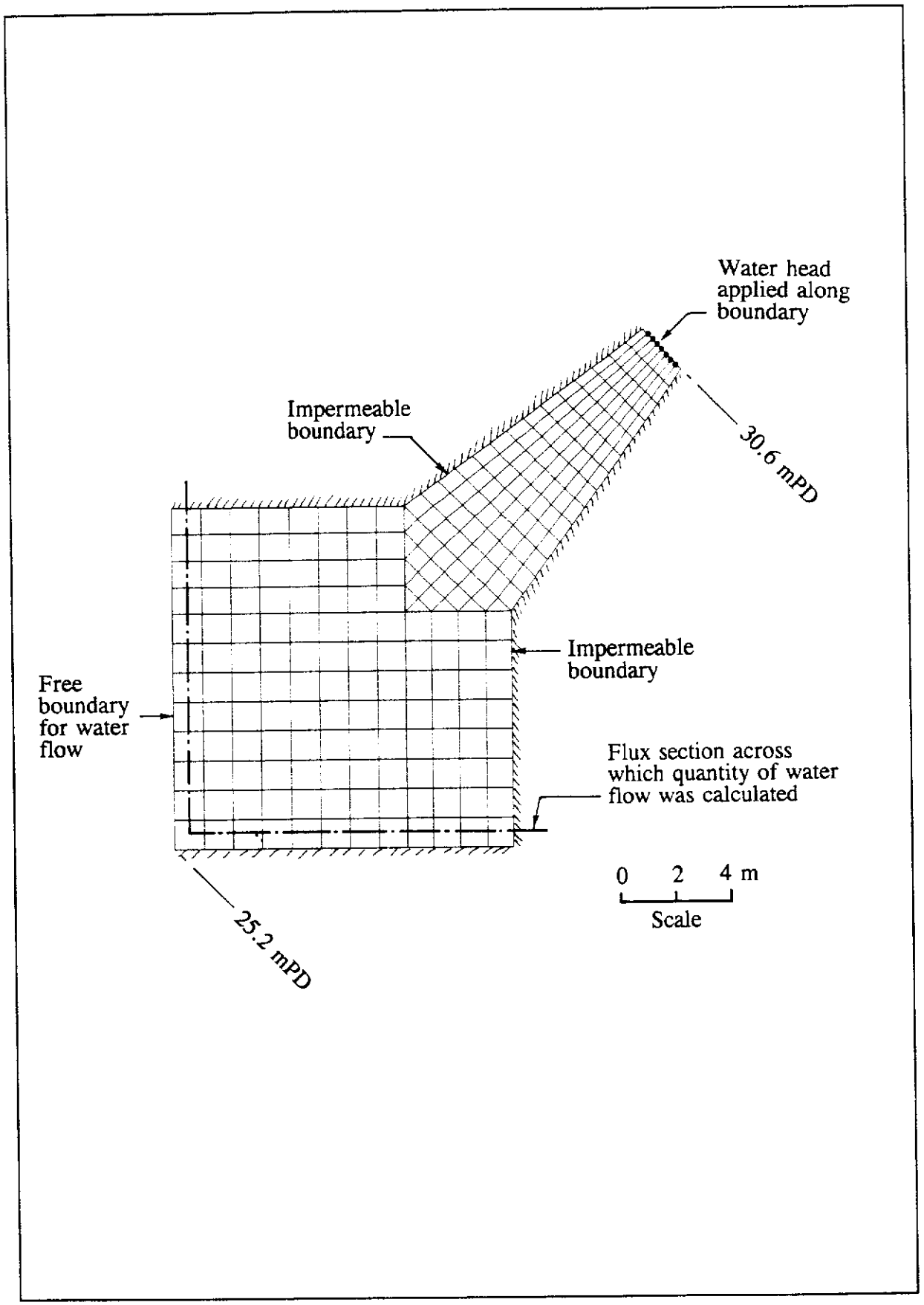

Figure L23 - Finite Element Mesh Used for Seepage Analyses of Plan Section (Cases 1 & 2)

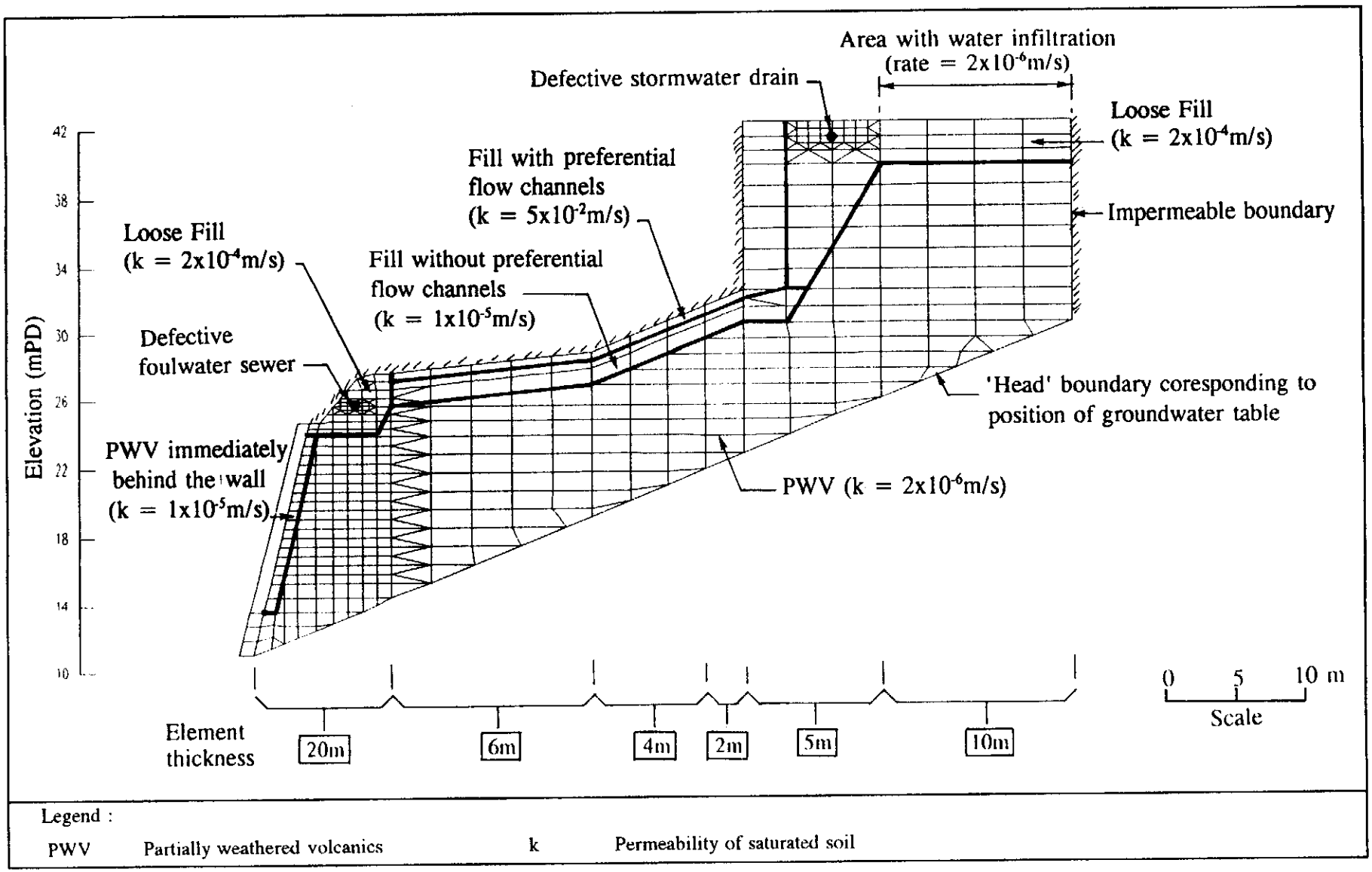

Figure L24 - Finite Element Mesh and Assumptions for Seepage Analyses of Vertical Section (Cases 3 & 4)

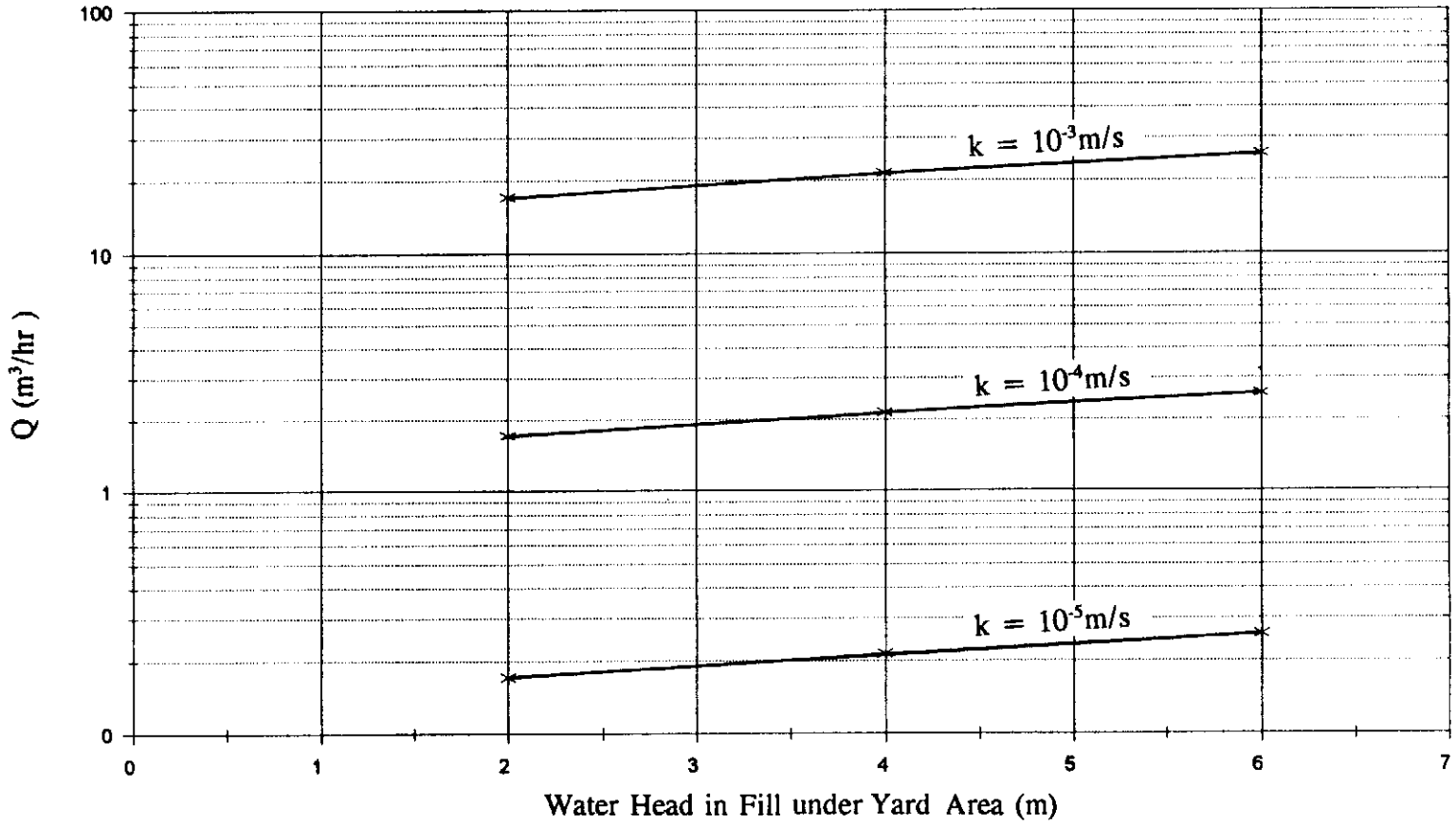

Legend :

k	Permeability of saturated fill
Q	Rate of water flowing out from the ground underneath Block D

Figure L25 - Results of Seepage Analyses (Case 1)

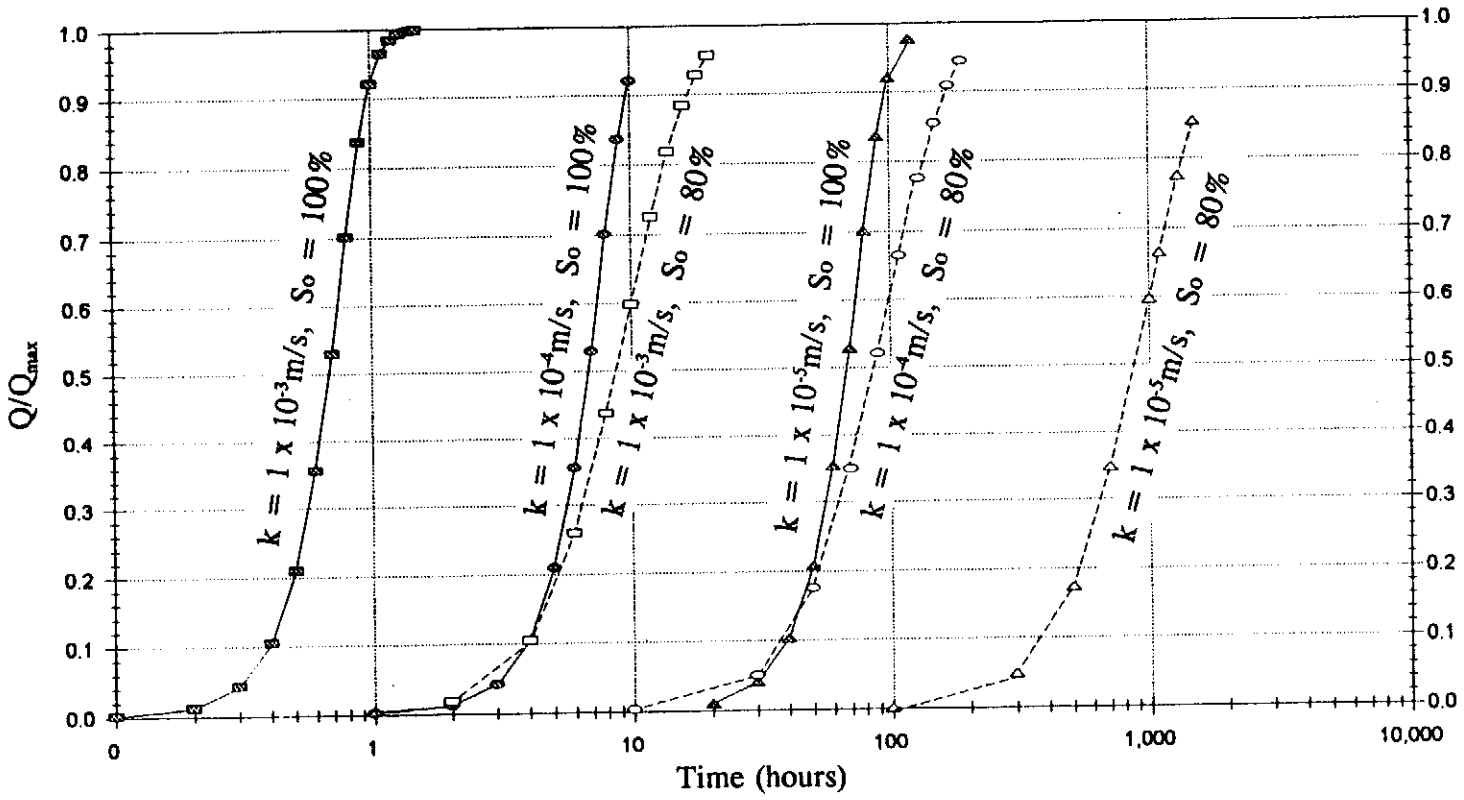

Legend :

k	Permeability of fill	So	Initial degree of saturation
Q	Rate of water flowing out from the ground beneath Block D at time t		
Q_{max}	Rate of water flowing out from the ground beneath Block D at steady-state		

Figure L26 - Results of Seepage Analyses (Case 2)

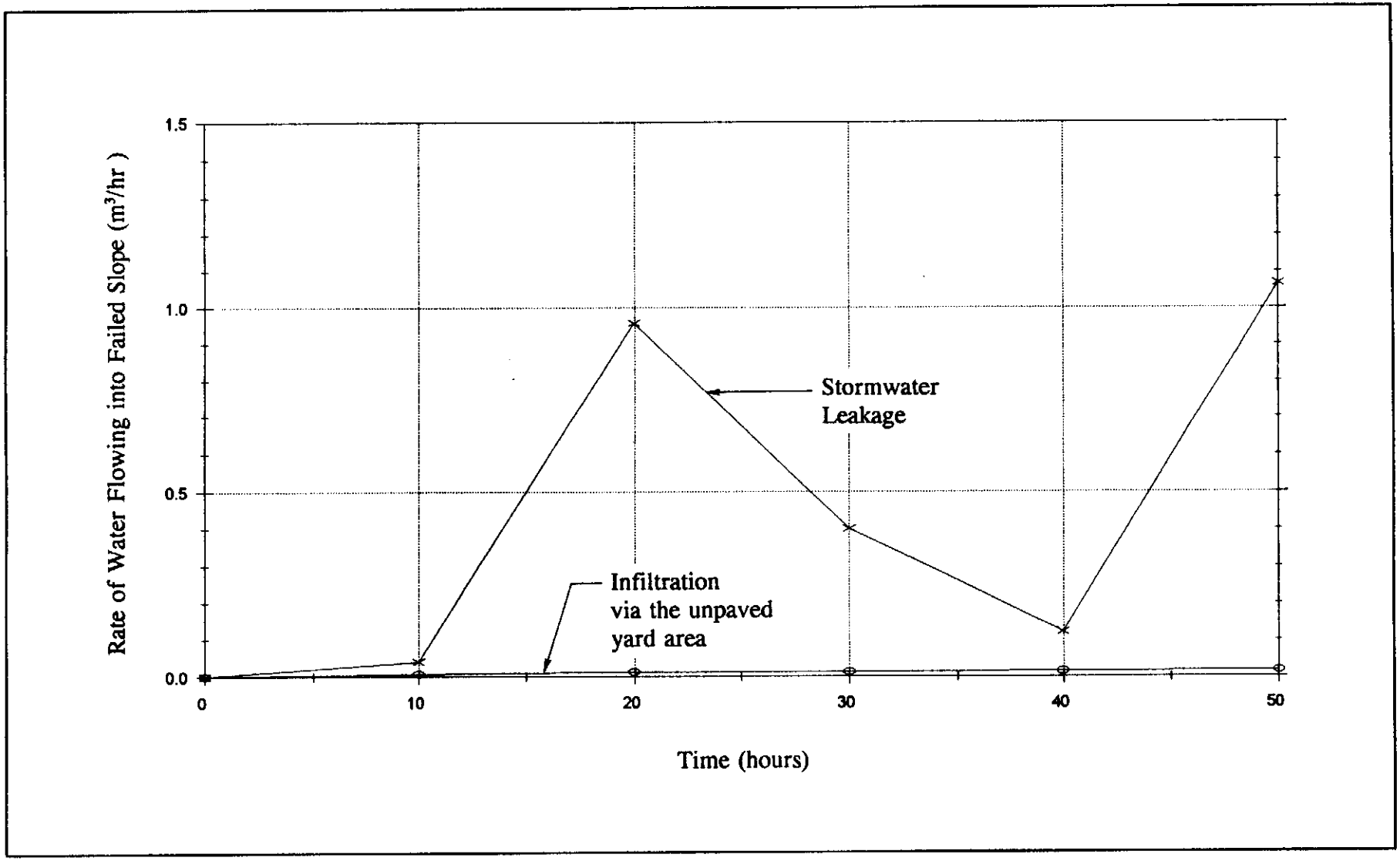

Figure L27 - Rate of Water Flow into the Failed Slope (Case 3 Seepage Analyses)

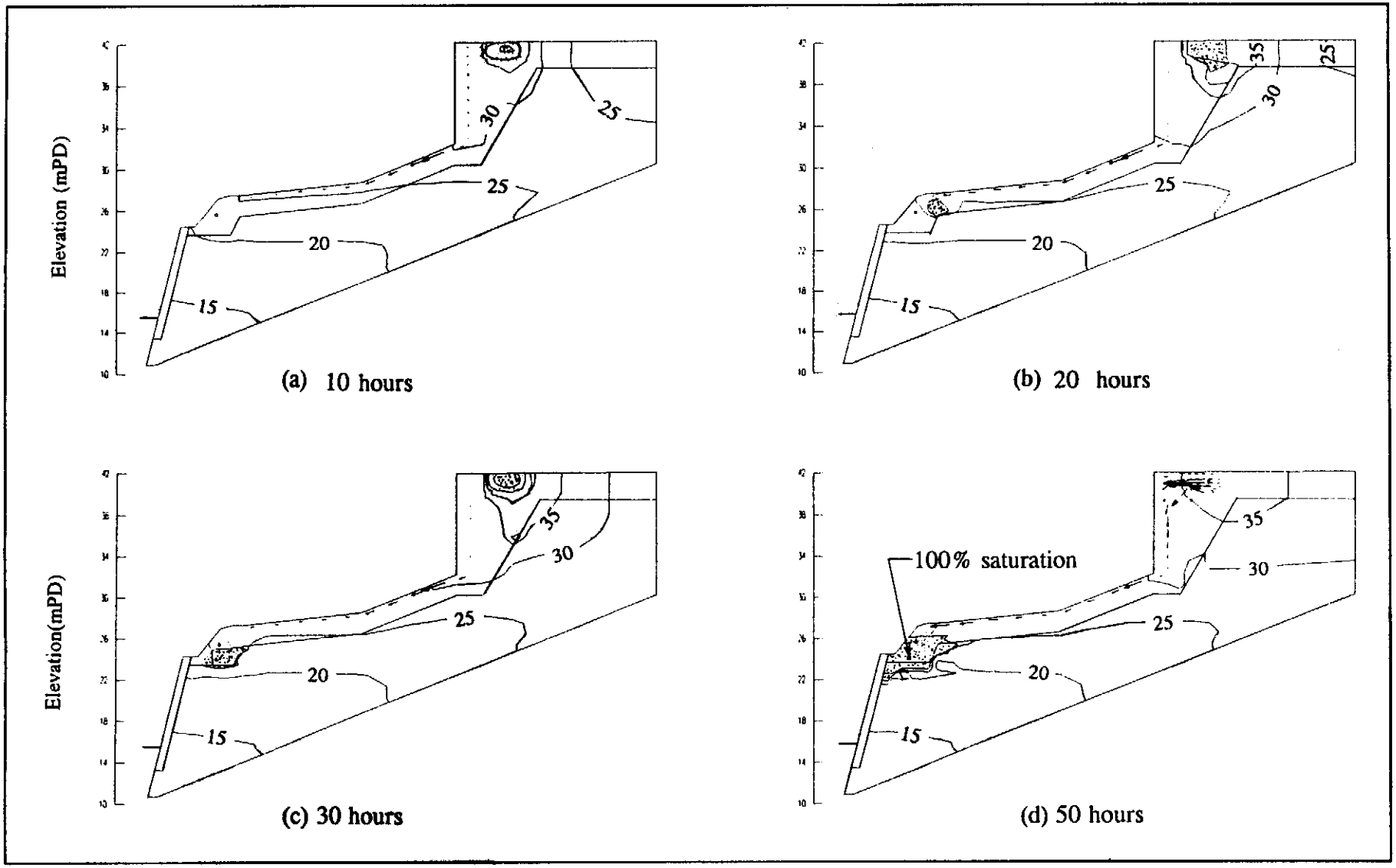

Figure L28 - Extent of Wetted Zone at Different Times due to Stormwater Leakage

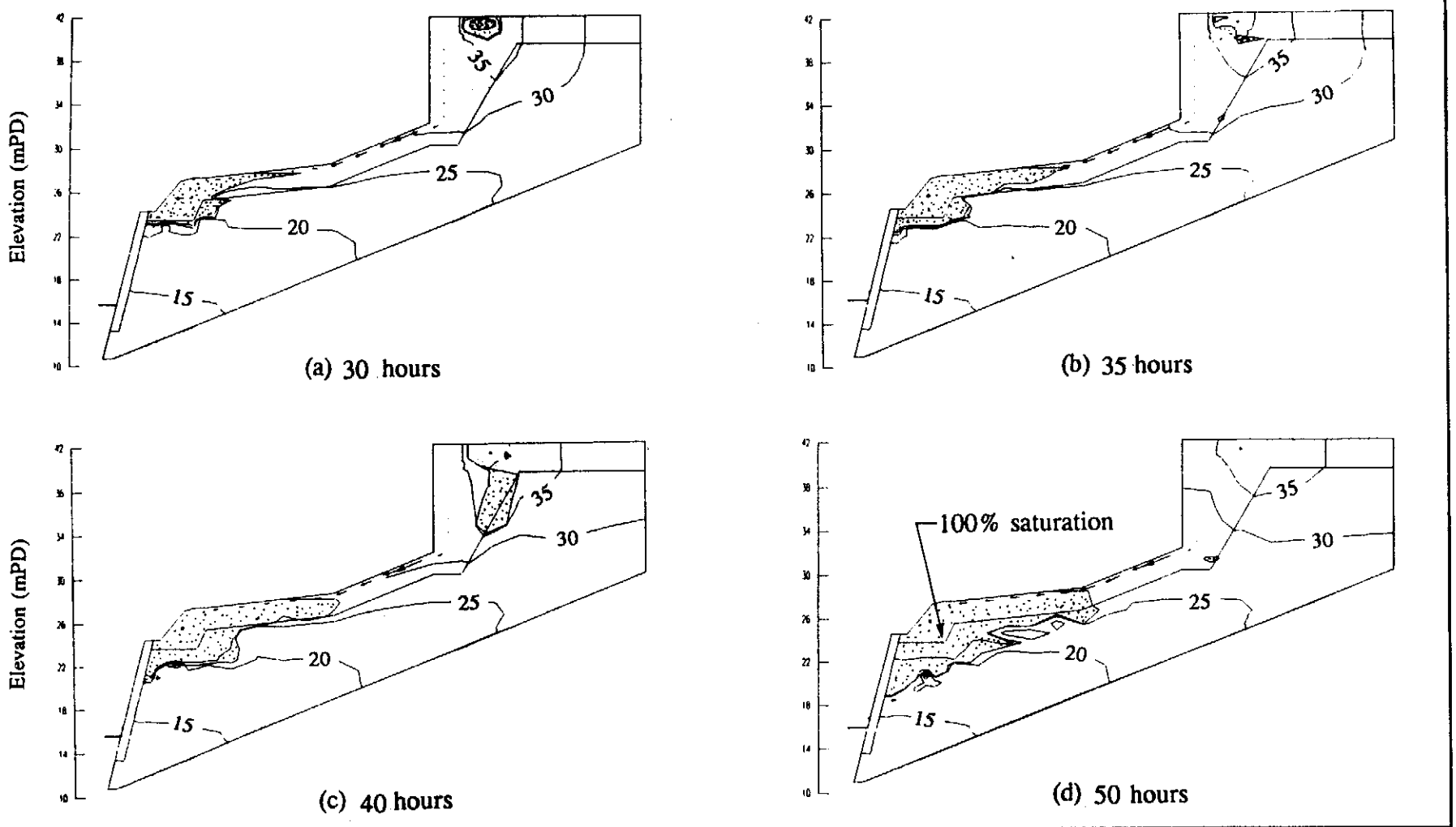

Note : See Figure L28 for the extent of wetted zone before 30 hours

Figure L29 - Extent of Wetted Zone at Different Times due to Stormwater and Foulwater Leakages

APPENDIX M

PHOTOGRAPHS

CONTENTS

M.1 PHOTOGRAPHS TAKEN BEFORE AND AFTER THE LANDSLIDE

The condition of the masonry wall and the slope above before the landslide is illustrated by photographs taken in July 1987, January 1991 and June 1994 (Plates M1 to M4).

The condition of the site after the landslide, together with various key features identified during the post-failure investigation, is shown in Plates M5 to M17.

The photographs shown in Plates M3 & M4 were provided to the Geotechnical Engineering Office by the Hong Kong Housing Society (HKHS).

LIST OF PLATES

Plate M1 - Masonry Wall No. 11SW-A/R309 in July 1987

Plate M2 - Slope above Masonry Wall No. 11SW-A/R309 in July 1987

Plate M3 - Masonry Wall No. 11SW-A/R309 in January 1991

Plate M4 - Slope between Masonry Wall No. 11SW-A/R309 and Block D in June 1994

Plate M5 - View of the Landslide on 24 July 1994

Plate M6 - View of the Landslide after Removal of Landslide Debris on 28 July 1994

Plate M7 - View of the Landslide after Shotcreting on 29 July 1994

Plate M8 - View of the Landslide after Completion of Emergency Repair Works and during Ground Investigation (Photograph taken on 13 August 1994)

Plate M9 - Unfailed Part of the Masonry Wall Immediately to the West of the Landslide Area Photograph taken on 25 July 1994)

Plate M10 - Broken Section of the Foulwater Sewer with Black-stained Soil Recovered from the Landslide Debris (Photograph taken on 27 July 1994)

Plate M11 - Part of the Foulwater Sewer with Minor Leakage between Manhole No. 77 and the Landslide Scar (Photograph taken on 5 September 1994)

Plate M12 - Foulwater Manhole No. 34 with a Crack near the Base (Photograph taken on 18 August 1994)

Plate M13 - Part of the Defective Stormwater Drain between Gully No. GT15a and Manhole No. 15 in the Yard Area (Photograph taken on 23 August 1994)

Plate M14 - The Ground underneath Block D Adjoining the Yard Area, with Signs of Seepage through the Weepholes, before Excavation of Trial Pit No. TP 35 (Photograph taken on 10 August 1994)

Plate M15 - The Ground below the Yard Area Exposed after Exposed after Excavation of Trial Pit No. TP 35 (Part of the ground collapsed when a field permeability test was carried out in drillhole No. BH12 sunk in the yard area. Photograph taken on 28 October 1994)

Plate M16 - Loose Fill near the Surface of the Ground underneath Block D
(Photograph taken on 5 September 1994)

Plate M17 - Subsurface Seepage Flow into Trial Pit No. TP26 at the Crest of the Landslide Scar during the Water Test underneath Block D
(Photograph taken on 29 October 1994)